Optimal Design and Planning of Energy Microgrids

Di Zhang

Department of Chemical Engineering

University College London

A thesis submitted in fulfilment to University College London for the degree of Doctor of Philosophy

September 2013

Declaration

I, Di Zhang, confirm that the work presented in this thesis is my own. Where information has been derived from other sources, I confirm that this has been indicated in the thesis.

Signature:_____

Date:_____

Acknowledgements

I would like to express my deepest gratitude to all the people who help and support me for this thesis.

Firstly, I want to thank my supervisors Prof. Lazaros G. Papageorgiou and Dr. Dan J.L. Brett, especially for the discussion, guidance, support and motivation from Prof. Lazaros G. Papageorgiou. I have learned a lot through my PhD studies.

I also wish to thank my colleague Dr. Songsong Liu for his kind help in various ways, expertise in GAMS, logics and paper proof reading through the last four years.

I am grateful to all my collaborators, who are Prof. Nilay Shah, Prof. Eric Fraga, Dr. Nouri J. Samsatli and Dr. Adam D. Hawkes. I enjoyed our collaboration and have obtained benefits from different aspects of research.

I would like to express my thanks to my present and past colleagues, Ozlem for her company and pressure sharing through our studies, Laura for abstract proof reading and viva presentation rehearsal, and Eria, Mozhdeh, Shirin, Maria, Melanie, Mithila, Lingjian, Han and Qi for all the quality time spent together.

I want to acknowledge my financial sponsors, Schlumberger Foundation and Centre for Process System Engineering, without whom I may struggle a lot during my studies.

感谢我的父母张凤洪先生和张玉环女士多年来精神和物质上的关爱，同时对他们近几年因为我而受到的各方面的压力深表歉意。我能够坚持到现在离不开朋友们的支持，特此感谢一直一线鼓励我并听我牢骚的好友们：潘艺嘉，高红波，徐万丽，田越，刘博特和曹德壮以及始终关注我成长的郭萍女士。我在大家的关心中完成了学业，感谢所有关心我爱护我的家人和朋友！

Abstract

Microgrids are local energy providers which reduce energy expense and gas emissions by utilising distributed energy resources (DERs) and are considered to be promising alternatives to existing centralised systems. However, currently, problems exist concerning their design and utilisation. This thesis investigates the optimal design and planning of microgrids using mathematical programming methods.

First, a fair economic settlement scheme is considered for the participants of a microgrid. A mathematical programming formulation is proposed involving the fair electricity transfer price and unit capacity selection based on the Game-theory Nash bargaining approach. The problem is first formulated as a mixed integer non-linear programming (MINLP) model, and is then reformulated as a mixed integer linear programming (MILP) model.

Second, an MILP model is formulated for the optimal scheduling of energy consumption of smart homes. DER operation and electricity consumption tasks are scheduled based on real-time electricity pricing, electricity task time windows and forecasted renewable energy output. A peak charge scheme is also adopted to reduce the peak demand from the grid.

Next, an MILP model is proposed to optimise the respective costs among multiple customers in a smart building. It is based on the minimisation/maximisation optimisation approach for the lexicographic minimax/maximin method, which guarantees a Pareto-optimal solution. Consequently each customer will pay a fair energy cost based on their respective energy consumption.

Finally, optimum electric vehicle (EV) battery operation scheduling and its related degradation are addressed within smart homes. EV batteries can be used as electricity storage for domestic appliances and provide vehicle to grid (V2G) services. However, they increase the battery degradation and decrease the battery performance. Therefore the objective is to minimise the total electricity cost and degradation cost while maintaining the demand under the agreed threshold by scheduling the operation of EV batteries.

Table of Contents

List of Figures

List of Tables

Chapter 1 Introduction

Current energy system is dominated by centralised generation, with electricity distributed to users through a macrogrid. Due to energy demand increase and the rise of global emissions of greenhouse gases, the current centralised energy generation system is challenged and needs to be restructured to meet the world's growing electricity needs [1]. Microgrids are emerging as an integral feature of the future power systems and are considered as a promising alternative to centralised generation. As a localised energy providing system, problems arise along with the processes of design and utilisation. This thesis aims to address some key problems in the optimal design and operation planning of microgrid through mathematical programming techniques.

1.1 Microgrid

Microgrid is a relatively small-scale localised energy network, which includes loads, network control system and a set of distributed energy resources (DER), such as generators and energy storage devices. A microgrid equipped with intelligent elements from smart grids has been adopted to enable the widespread of DERs and demand response programs in distribution systems [2], which is considered as future smart grid. Microgrids can be applied for single consumer, such as sport stadium; community microgrid with multiple consumers, such as campus; and utility microgrid with supply resources on utility side with consumer interaction and utility objectives [3]. Remote off-grid systems and military microgrids are also mentioned in [4]. In this thesis, the community microgrid is addressed.

Figure 1-1 shows a microgrid example for application at community level [5]; it has a group of consumers, including residential buildings, factories and commercial building which have their own energy loads. The local DERs are a wind generator, photovoltaic (PV) panels and other generators to provide local electricity and energy storage systems for energy storage. There is also macrogrid utility connection to buy electricity when there is not enough electricity generated from local generators or to sell electricity back when there is excess electricity generated. When there is an emergency, the macrogrid can be

disconnected and the microgrid can work independently to provide electricity in the 'islanded' mode.

Figure 1-1 Microgrid example [5]

Microgrids have been developed for a number of reasons: they can provide better power quality and reliability in case of blackout or other problems on the external network and they also support voltage and reduce voltage dips [6]. They may have economic and environmental benefits when emissions credits are considered because they can utilise more low carbon energy sources such as wind and solar energy; and they are localised which implies some transmission infrastructure and associated costs may be avoided. Additionally, primary energy consumption could be reduced when combined heat and power (CHP) technology is applied [7]. Moreover, microgrids could support the macrogrid handling sensitive loads from DERs locally and integrate them for peak power consumption time which alleviate or postpone current macrogrid upgrades and also reduce the central generation reserve requirements [8, 9]. The microgrid can be designed according to

customer's respective interests, such as enhancing local reliability, reducing feeder losses and uninterruptable power supply [10]. The microgrid is also one solution for energy generation in remote areas without electricity service. Finally, microgrids also have the inherent advantages of being interconnected via a local or private network, so the participants can cooperate with each other thus increasing equipment utilisation and providing yet more benefits.

1.1.1 Microgrid Concept

The microgrid concept has been popular and researched by many experts, especially in U.S., E.U., Canada and Japan [8, 11]. It operates and fulfils the local energy demands according to its own protocols and standards [12, 13]. However, the concepts proposed vary and there is still no common concept for microgrids [14-18]. The U.S. Consortium for Electric Reliability Technology Solutions (CERTS) has published a White Book [19] where a microgrid is defined as follows:

> "*The Consortium for Electric Reliability Technology Solutions (CERTS) MicroGrid concept assumes an aggregation of loads and microsources operating as a single system providing both power and heat. The majority of the microsources must be power electronic based to provide the required flexibility to insure operation as a single aggregated system. This control flexibility allows the CERTS MicroGrid to present itself to the bulk power system as a single controlled unit that meets local needs for reliability and security*."

While the U.S. Department of Energy (DOE) [20] defines microgrids as:

> "*a group of interconnected loads and distributed energy resources (DER) with clearly defined electrical boundaries that acts as a single controllable entity with respect to the grid and can connect and disconnect from the grid to enable it to operate in both grid-connected or island mode*."

For the researchers apart from U.S., other aspects of microgrid are considered, Abu-Sharkh et al. [21] describes microgrid simply as:

> "*a small-scale power supply network that is designed to provide power for a small community.*"

In the definition provided by Hatziargyriou et al. [8]:

> "*Microgrids are defined as low voltage or in some cases, e.g. Japan, as medium voltage networks with distributed generation sources, together with storage devices and controllable loads (e.g. water heaters, air conditioning) with total installed capacity in the range of few kWs to couple of MWs.*"

Zhang et al. [22] define microgrid as:

> "*a cluster of loads and relatively small energy sources operating as a single controllable power network to supply the local energy needs.*"

Also Funabashi and Yokoyama [23] describe it as:

> "*Microgrid is a small grid in which distributed generations and electric loads are placed together and controlled efficiently in an integrated manner. It contributes to utility grid's load levelling by controlling power flow between utility grid and Microgrid according to predetermined power flow pattern. Also, it contributes to an efficient operation of distributed generations by operation planning considering grid economics and energy efficiency.*"

1.1.2 Microgrid Key Components

Microgrids usually consist of distributed energy resources, power conversion equipment, communication system, controllers and energy management system to obtain flexible energy management [24, 25]. The customer is another key component for microgrid to be promoted and implemented [21].

- DER involves distributed generator (DG) and distributed storage and provides energy to meet energy demand.
- Controllers are necessary for microgrid to apply demands to DERs and control their parameters, such as frequency, voltage and power quality [26].
- Power conversion equipment, such as voltage and current transformer, are utilised to detect the microgrid running state. Also, the DERs produce DC or AC voltage with different amplitude and frequency than grid, power electric converter interface is necessary [27].
- Communication system is a medium to convey monitoring and control information in microgrids. It is applied to interconnect different elements within the system and ensures management and control [28, 29].
- Energy management system is used for data gathering and device control, state estimate and reliability evaluation of the power system [30]. It also functions in power prediction from renewable energy, load forecasting and power planning [31]. Major vendors for energy management system are summarised by [32].
- Customers, who may also be the suppliers, will affect technique selection, load control and operation of microgrid from cost and efficiency concerns. Microgrid can be deployed in demand response driven by customers [33]. The participation of customers is the fundamental driver for smart grid [34] and strongly encourage the engagement desired from the developers [35]. The customers function in user interaction needs, behaviour change, community initiatives and resources management [36].

Figure 1-2 illustrates the key components of microgrid, the solid line represents the communication system information transfer.

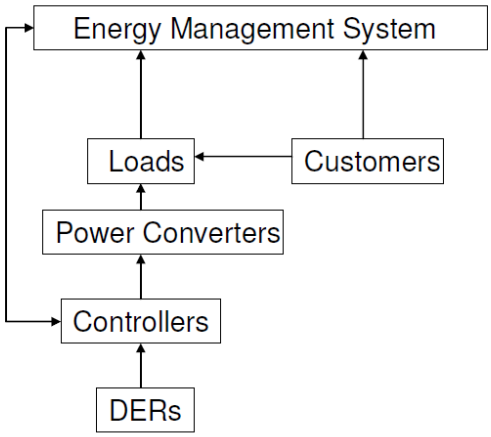

Figure 1-2 Microgrid key components

1.1.3 Microgrid and DER

A microgrid consists of a variety of distributed energy resources, such as generators, energy storage and energy demand itself. The capacity of the DER considered in microgrid is in relatively small scale, but without universal agreement. It is mentioned as smaller than 100 *kW* by Huang et al. [37], and in [38] micro-generation is considered with even smaller scale, less than 3 *kW* electrical and 30 *kW* thermal while standard EU definition of micro-generation being up to 50 *kW* based on different residential scales. While authors of [39] consider it smaller than 500 *kW*. Generally, the generators have a similar capacity size as the loads within the microgrid, and they are located close to the end users [21].

The distributed generators applicable for a microgrid comprise emerging technologies, such as CHP, wind generators, photovoltaic arrays, and also some well established generators, such as synchronous generators driven by internal combustion engines or small hydro [17, 24, 40]. The advantage of high energy efficiency of CHP results from energy cogeneration. Fossil fuel power sources CHP for microgrid are summarised in [21] and [41], which are internal combustion engine, micro-turbine, sterling engine and fuel cell.

Due to the small generators usually used, a microgrid is not able to respond to sudden load changes or disturbances rapidly. So, energy storage devices are essential for microgrid, especially under the circumstances when intermittent generators and included, limited

methods of energy generation are available or the microgrid works under islanded mode. Electrical storage devices have several forms, including gravitational potential energy with water reservoirs, batteries and flow batteries, super-capacitors, flywheels, superconducting magnetic energy storage, compressed air energy storage, fuel cell and thermal energy storage and use of traditional generation with inertia [42-44]. Among the available energy storage technologies, batteries, fly-wheels and super-capacitors are particularly suitable for microgrids [37].

Because of the characteristics of energy produced by renewable energy, the use of microgrid to integrate DERs can obtain the optimal benefit. Especially when different types of generators are available, they can compensate with each other while energy storage provides energy stability and quality [45] which enable higher penetration of many types of distributed generators [46]. Energy storage systems are also desirable to reshape the peak demand and store energy at the time of surplus and reused later [47].

1.1.4 Existing Microgrids

Microgrids have been studied worldwide and testing systems have been established for research. In the U.S., the CERTS testbed has been built near Columbus, Ohio and a battery storage is also available. University of Wisconsin-Madison has an UW microgrid testbed with a diesel driven generator [48]. There is a Smart Polygeneration Microgrid test-bed facility in the Genoa University and it is located at Savona Campus teaching & research facilities [49]. While in Canada, BC Hydro Boston Bar microgrid supplies power without energy storage unit and Hydro Quebec Senneterre substation systems serves 3000 customers with islanding attempt in 2005 [50]. In Europe, Bronsbergen Holiday Park with 208 holiday homes in Netherland has a microgrid to provide electricity from 108 roof fitted solar PVs and energy storage is also available as two battery banks [51]. A residential Am Steinweg microgrid is built in Stutensee in German, and it is a test system with CHP and PV as generators and a lead acid battery bank for energy storage. Another microgrid system in German is DeMoTec test microgrid, which has two diesel gensets, a PV generator and a wind generator and two battery units are also included [52] Italy has a CESI RICERCA DER test microgrid equipped with a fly wheel and battery banks. The Kythnos islanded

microgrid in Greece provides electricity for 12 houses with PVs, diesel generator set and battery bank while the laboratory-scale microgrid system at National Technical University of Athens consisting of two PV generators, one wind turbine and battery for energy storage [52, 53]. In the UK, University of Manchester has a laboratory microgrid with a synchronous generator and an induction motor coupled together as micro-source and a flywheel as energy storage [54]. Microgrid projects are more popular in Japan, under Energy and Industrial Technology Development Organisation (NEDO), Aichi microgrid, Kyoto eco-energy project and Hachinohe project are established. Fuel cells, PV and sodium-sulfur (NaS) battery are equipped in the Aichi microgrid [55]. Kyoto eco-energy microgrid has gas engines, a molten carbonate fuel-cell (MCFC), two PV systems, a wind turbine and lead-acid battery [56]. The Hachinohe microgrid includes a gas engine, several PV systems, a wind farm and a battery storage. A test network is located at Akagi of the Central Research Institute of Electric Power Industry, and no energy storage is included [57]. One more microgrid from Japan is the Sendai microgrid with two gas engine generators, one MCFC, PV and battery storage [58]. For China, there are a testbed microgrid in Hefei University of Technology [59] and a demonstrative microgrid implemented in Caoxi implemented by Grid Corporation of Shanghai [25]. A microgrid pilot plant has been constructed in Korea Electro-technology Research Institute and it includes PV, PV and wind hybrid, two diesel generators and battery energy storage system [60].

1.2 Optimal Design and Planning for Microgrids

Studies on microgrids are generally classified into two groups: system design and operation planning[61]. They are critical for the successful realisation of microgrid in real-time applications [62]. System design is a long-term planning activity of microgrids, which involves the selection and sizing of DERs with the objective of minimum cost, environmental or energy security issues [63]. The design of DERs plays an important role in order to maintain the reliability of the power grid, level of short-circuit current, power flow and node voltage [64]. The selection technique is constrained by energy loads, technology information, operation and maintenance cost, utility tariff from different tariff schemes and weather conditions. The optimal capacity sizing tradeoffs between peak loads

satisfaction and investment costs minimisation. Since energy demand fluctuates due to uncertainty in human behaviours and ambient conditions, hourly energy demand profile representing the dynamic nature of the problem is commonly applied to the design of microgrids [65, 66].

On the other hand, with given DER capacity operation planning deals with optimal microgrid planning over the short term, such as a day or week; and the time interval can be one hour or even smaller. Microgrid planning includes the overall management of a microgrid. It targets at obtaining an economically attractive performance under uncertainty and disturbances due to the variability of renewable energy sources and the rapid change in the power/heat demand. The optimal operation of microgrid includes two main functions, supply side optimisation and demand side optimisation. For the supply side, energy management decisions include the DER operations (production output, switch on/off status or types of fuel) and electricity purchases or sales back to grid [67]. Generation scheduling is defined as the scheduling of power production from generation units over certain time horizon while satisfying technology and system constraints [68]. DER operation generation schedule results in the cost savings under operational constraints of each DER over given time periods [30]. Demand side management involves controlling the condition of the energy system through demand modification, changing the shape of the load and optimising the generation, delivery and end use processes[69, 70]. At the same time, demand side management aggregates all energy-consuming devices and flexible loads can be rescheduled. Demand side management benefits in peak reduction, load profile reshape and overall cost and emission reductions.

1.3 Smart Grids and Microgrids

The ageing current electricity power infrastructure needs to be upgraded or transformed for environmental concerns, energy conservation as well as to accommodate increasing energy demands. Future electricity distribution system will be integrated, intelligent and better known as smart grids, which include advanced digital meters, distribution automation, communication systems and DERs. Central distributed and intermittent sources will all be included [71]. Desired smart grid functionalities include self-healing, optimising asset

utilisation and minimising operations and maintenance expenses [72]. In addition, a smart grid needs to be dynamic and has constant bi-communication involving consumers' own decision on how to use energy [73]. Many national and international projects address the smart grid concept, although there is still no agreed universal concept about it [74, 75]. Bracco et al. [49] present an overview of the smart grid projects around the world.

In a smart grid, bidirectional communication between the grid and consumers is available for energy flow where smart meters and sensors are utilised [35, 76]. With the application of energy management and two-way communication functions, energy consumption load can be reshaped. There is possibility to shift the energy generation from peak demand base to real-time demand need base [77]. Residential end-users will also play a more active role as a co-provider rather than a passive role in balancing supply and demand [36].

Microgrid has various smart grid initiatives and is expected to be prototype for smart grid because of its experimentation scalability and flexibility [2]. The small scale of microgrid provides the convenience to adopt new technologies [78]. As a significant ingredient of the future smart grid, microgrid is considered to enable widespread inclusion of renewable resources, distributed storage and demand response programs in distribution [2]. Also, with the help of Information and Communication Technologies (ICT), smart microgrids can be connected to form a network to work collaboratively for the reliability and sustainability of electrical services [79]. In [80], smart grid is referred to as a network of integrated microgrids that can monitor and heal itself. Smart grids composing of several microgrids are classified in [81].

1.4 Aim and Scope of This Thesis

A microgrid equipped with intelligent elements from smart grids has been adopted and active control of small scale energy resources is included in such smart microgrid. Such control has benefited from research attention in technical aspects [14-16], however, limited studies are available for exploring the economic incentive of participants to become involved in a microgrid. Therefore, this thesis aims at addressing this gap by considering the consumer engagement and their interaction. The aim of this work is to *develop*

frameworks based on mathematical programming techniques in order to integrate request from individual customer into the optimal design and planning of microgrid.

The issues covered in this thesis and contributions of this work are: firstly, a fair economic settlement scheme for participants in a microgrid is proposed. Electricity transfer price and unit capacity selection are obtained under given customer energy demands and their accepted equivalent annual cost upper bounds. Then, efficient energy consumption and operation management of a smart building with microgrid is addressed, where customers provide their energy consumption tasks and flexible time windows to minimise their total energy cost and reduce the peak demand from grid. Thirdly, problem of fair cost distribution among multiple smart homes sharing common microgrid is considered. Each customer competes with other neighbours to obtain lowest energy bill under accepted cost limits. Finally, as a special electricity consumption task in a smart home, electric vehicle battery operation is considered. It is scheduled based on customer's living habit, such as travelling time and respective home energy demand, to optimise the battery usage while considering the degradation effects.

1.5 Outline of the Thesis

The rest of the thesis is divided in five chapters:

In Chapter 2, the problem of fair electricity transfer price and unit capacity selection for microgrid is addressed. A mixed integer non-linear programming (MINLP) model is proposed based on the Game-theory Nash bargaining solution approach. Then a separable programming approach is applied to reform the resulting mixed integer non-linear programming model as a mixed integer linear programming (MILP) model.

In Chapter 3, the optimal scheduling of smart homes' energy consumption is studied using an MILP approach. In order to minimise a one-day forecasted energy consumption cost, DER operation and electricity-consumption household tasks are scheduled based on real-time electricity pricing, electricity task time windows and forecasted renewable energy output.

In Chapter 4, a mathematical model is proposed for the fair cost distribution among smart homes with microgrid, which is based on the Lexicographic minimax method using an MILP approach. It schedules DER operation, DER output sharing among smart homes and electricity consumption household tasks.

In Chapter 5, the intensive use of battery in household and vehicle to grid (V2G) applications is studied while an MILP model is proposed to provide the charging scheduling for load shifting and cost minimisation together with minimising degradation cost. Two boundaries for demand from grid are applied to guarantee the stability of the grids.

Finally, Chapter 6 summarises the main contributions of the thesis and provides recommendations for future work.

Chapter 2 Fair Electricity Pricing and Capacity Design in a Microgrid

As a localised energy network, microgrids are proposed to alleviate current macrogrid demand burden and reduce emissions. The successful deployment of microgrids depends heavily upon the DERs combination selection, capacity sizing and operation plan. Microgrids can be considered as collaborative networks and cooperation amongst microgrid participants can provide better economic outcome than being isolated from each other with pure self interest. The participants in a microgrid can benefit from cooperation for improved design and operation. Although a number of models have been developed for cost minimisation of the whole microgrid, the cost to respective participants is usually not considered.

In this chapter, an MILP model that optimises the respective cost distribution amongst participants in a microgrid is proposed based on the game theoretical Nash method.

2.1 Introduction and Literature Review

A number of concepts have emerged in recent years in relation to deployment and control of DERs, such as smart grids and microgrids. These concepts represent a significant departure from the top-down and asset-intensive nature of current electricity systems, and capitalise on the availability of new generation equipment and ICT systems to facilitate the use of many small-scale energy resources to serve growing demands. Such technology can provide economic benefits through avoidance of investment as demonstrated in upstream infrastructure, security and reliability benefits through interconnection and coordinated control, and environmental (and additional economic) benefits by using low carbon/low pollutant generation and co-production of heat and power. The smart grid concept remains only loosely defined at present based on specific focuses [74, 75]. However, active control of small scale energy resources is most likely to be included. This work addresses the economic incentive of customers by considering a fair economic settlement scheme for participants in a microgrid.

2.1.1 Unit Capacity Selection in Microgrids

Several studies have considered how to design the capacity of a microgrid system to minimise the annual cost of meeting demand [7, 82, 83]. A computer program that optimises the equipment arrangement of each building linked to a fuel cell network and the path of the hot-water piping network under the cost minimisation objective has also been developed [84]. Another work considering the optimal DER sizing and allocation problem is given by [85]. Kumar et al. [86] propose an architecture of smart microgrid for integration of renewable energy sources, and it focuses on the design, modelling and operational analyses. Optimal plan and design of DER capacity in microgrid is also provided by [87] based on the Chinese meteorological conditions, the authors also present the allocation method of output power. Authors of [88] propose a generalised approach to design generation capacity sizing and power quality evaluation for a microgrid in islanded and grid connected modes, where PSCAD (Power System Computer Aided Design) software is used for modelling. And in [89] generation design is addressed in islanded mode along with the analysis of power reliability and voltage quality of the system. The optimal configuration of DGs at different locations is obtained by applying electromagnetism-like mechanism in [64]. Mizani and Yazdani [90] demonstrate the optimal selection of DER in a grid connected microgrid together with optimal dispatch strategies and they can reduce microgrid lifetime cost and emission on a campus. Proper CHP-based DERs are deployed in the work of [91] and optimisation is done using particle swarm optimisation (PSO) technique. Bando et al. [92] develop a methodology for the designing of DER in microgrid with steam supply from a municipal waste incinerator, and both primary energy consumption and CO_2 emissions have been reduced. A genetic algorithm (GA)-based optimal design of microgrid is investigated under pool and hybrid electricity market model in [93], and the optimal operation of the microgrid with DG unites under deregulated energy environment is also presented. Sheikhi et al. [94] propose a model to find the optimal size and operation of DERs with the consideration of electricity and gas network. In [95] a methodology using PSO is also provided for the DERs location and size selection to obtain the maximum loss reduction. Authors of [96] present a strategy to obtain the optimal location of DER and reactive power injection by applying

evolutionary optimisation methodology, where voltage stability of the system and the DG penetration level are both improved. An rrthogonal array-GA hybrid method is applied to optimise equipment capacity and the operational methods in [97]. Hawkes and Leach [65] presented a linear programming cost minimisation model for the high level system design and corresponding unit commitment of generators and storage devices within a microgrid. Sensitivity analysis of total microgrid costs to variations in energy prices has been implemented and the results indicate that a microgrid can offer a positive economic proposition. This model provides both the optimised capacities of candidate technologies as well as the optimised operating schedule. King and Morgan [98] perform a baseline analysis estimating the economic benefits of microgrids. They found that it indicates a good mix of customer types would result in better overall system efficiency and cost savings. The problem is formulated as a nonlinear mixed integer optimisation problem with evolutionary strategy. A MILP model for optimal DER design is presented in [99] at the level of a small neighbourhood, which provides the microgrid configuration together with the design of a heating pipeline network among nodes. Methodology for optimal DER selection and capacity sizing is proposed in [100] for integrated microgrids. Strategic deployment of DERs in a microgrid is presented by Basu [101] using differential evolutionary algorithm.

However, for all of these models, the objective function is to minimise the total cost of capital and operation for the whole microgrid; the costs to respective participants are not considered. This raises a problem that design and operation of the microgrid is based on the mutual interest of all participants instead of the self-interest of each participant. This cost minimisation approach could be improved, because there is the possibility that some participants will not benefit from the microgrid, whilst others do benefit. Therefore, a fair method for settlement between microgrid participants is essential.

2.1.2 Fair Settlement using Game Theory

Microgrids can be considered as collaborative networks. Microgrid participants may have their own objectives and constraints which make them compete with other participants, but they will also recognise they can be better off via cooperation. Cooperation among

microgrid participants can provide better economic outcome than being isolated from each other with pure self interest. Asset utilisation could be increased and the average capital cost for each participant could also be decreased. A number of collaborative planning schemes with different assumptions and different areas of application have been reviewed in [102].

Game theory is a powerful tool for studying strategic decision making under cooperation and conflict conditions [103]. It attempts to mathematically describe people's rational decision making behaviour under a competitive situation, where the players' benefits depend on their own choices as well as the choices of the other players. Nash [104] presents the equilibrium point of finite games, where all players adopt the strategy which gives them the best outcome given that they know their opponents' strategy. In essence, Nash equilibrium is defined as a profile of strategies such that each player's strategy is an optimal response to the other players' strategies. Game theory has been applied in diverse areas, such as anthropology, auction, biology, business, economics, management-labour arbitration, politics and sports. Yang and Sirianni [105] set up a framework for sharing regional carbon concentration under global carbon concentration cooperation. In the area of energy economics, authors of [106] proposed a decision-making model for competitive electric power generation between different subsystems in Brazil based on Nash-Cournot equilibrium with the objective of maximising regional benefits. Using an agent-based approach incorporated with game theory, Sueyoshi [107] investigates the learning speed of traders and their strategic collaboration in a dynamic electricity market. In the area of supply chain management, game theory is utilised to help understand and predict strategic operational decisions. The work of [108] deals with energy management decision making process problem with a hybrid methodology using fuzzy and game theory analytical methods, where industry and environment are the competitors. Li et al. [109] build a single-stage deterministic model based on game theory in the field of power engineering to analyze the strategic interaction between the generation enterprises and transmission enterprises. And in the work of [110], game theory is applied to model the planning of a grid-connected hybrid power system, where both non-cooperative and cooperative game-theoretic models are built. The players being considered there are wind generators, PV

panels and storage batteries. There are two recent reviews on the application of game theory in supply chain management, and both non-cooperative and cooperative games are discussed [111, 112]. Authors of [113] reviewed some applications of cooperative game theory to supply chain management with the focus on profit allocation and stability. Min et al. [114] propose a competitive generation maintenance scheduling process to obtain an optimal maintenance plan via a coordination procedure in electricity markets. Oliveira et al. [115] derive the supply chain Nash equilibriums for the general structure of the interaction between spot and futures markets, and the contract for differences and the two-part tariff. In [116] a decision making tool is built by combining the use of the game theory optimisation framework and a multi-objective optimisation MILP-based approach to optimise the supply chain planning problem under cooperative and competitive multi-objective environments. Authors of [117] propose a cooperative game approach to help the coordination issue between manufacturers and retailers in supply chain using option contracts. An option contract model is developed, taking the wholesale price mechanism as a benchmark. Leng and Parlar [111] apply both the non-cooperative Nash and Stackelberg equilibrium, and coordination with cost-sharing contracts, to achieve the maximum system-wide expected profit. Nash equilibrium approach is used to deal with multi-objective integrated process planning and scheduling in [118].

Game theory has been applied to find a 'fair' solution, although there are different measures of fairness. Mathies and Gudergan [119] suggest the definition of fairness as the reasonable, acceptable or just judgment of an outcome which the process used to arrive. The fair solution suggests that all game participants can receive an acceptable or 'fair' portion of benefits. While in [120], fairness is considered as the maximisation of the benefit of the worse-off individual. The fair solution suggests that all game participants can receive an acceptable or 'fair' portion of benefits. As Leng and Zhu [121] discussed, an appropriate side-payment[1] contract can be developed to coordinate the participants in a network. Various side-payment schemes to coordinate supply chains are reviewed, and a procedure for such contract development is provided and applied. It has the assumption that all side-payment contracts in the discussion are legally possible, while some of them could be

[1] Side-payment is defined as an additional monetary transfer to improve the chain-wide performance.

illegal and will be prohibited in practice. Rosenhal [122] presents a cooperative game that provides transfer prices for the intermediate products in the supply chain to allocate the net profit in a fair manner. It applies when the market prices for the products are known and when the values differ. In the work of [123], fairness is defined as facilities burden sharing. A benchmark is set first, then the respective participant cost is compared with this benchmark and the objective is to minimise the absolute deviation of the difference. In this way, the sum of the unfairness is minimised, but the result shows the fair solutions sacrifice one third on average in solution quality. The Nash bargaining framework from cooperative game theory has been applied for 'fair' solution in different areas. It has been applied by Yaiche et al. [124] for bandwidth allocation of services in high-speed networks. Ganji et al. [125] develop a discrete stochastic dynamic Nash game model for reservoir operation and water allocation with the assumption that the decision maker has sufficient information of the random element of the game. Gjerdrum et al. [126] propose a methodology based on the game theoretical bargaining concepts developed by Nash, which considers fair profit sharing between two coordinating enterprises. The minimum profit of each participant is achieved first, and a non-linear objective function is formed as the product of the differences from the calculated and minimum benefit values. Ideally, the two enterprises should have the same amount of benefit differences. Gjerdrum et al. [127] also presented a model framework based on game theoretical Nash, which is applied to find the fair, optimised profit distribution among participants of multi-enterprise supply chains. It is formulated as a mixed integer non-linear programming model including a non-linear Nash-type objective function. A separable programming approach is applied to convert the model to mixed-integer linear programming form. The results indicate this method can produce fairly distributed profits with low errors on solutions.

In this chapter, an MILP model is proposed to optimise the respective profits among participants in a microgrid. It is based on the framework in [65] by utilising the game theoretical Nash method regarding the fair distribution of costs [127]. A fair settlement among microgrid participants is provided in order to guarantee each participant will pay fair cost from cooperation. The problem is first formulated as an MINLP model; and it is then tackled with a separable programming approach applying logarithmic differentiation

and approximations of the variables in the objective function, thus leading to an MILP model. The key decision variables include: intra-microgrid electricity transfer price, flow of electricity transferred, unit allocation and capacities and resources utilised.

2.2 Problem Description

This work considers a general microgrid, which involves *N* different participant sites as shown in Figure 2-1. They are different types of buildings, which can be dwellings, schools and shops. The microgrid considered in this work is assumed to include an energy management system, local controllers for each energy source and communications system that can provide an optimal energy production schedule. Macrogrid is available to provide electricity to the participant in the microgrid and extra electricity can also be sold back to the macrogrid when it benefits.

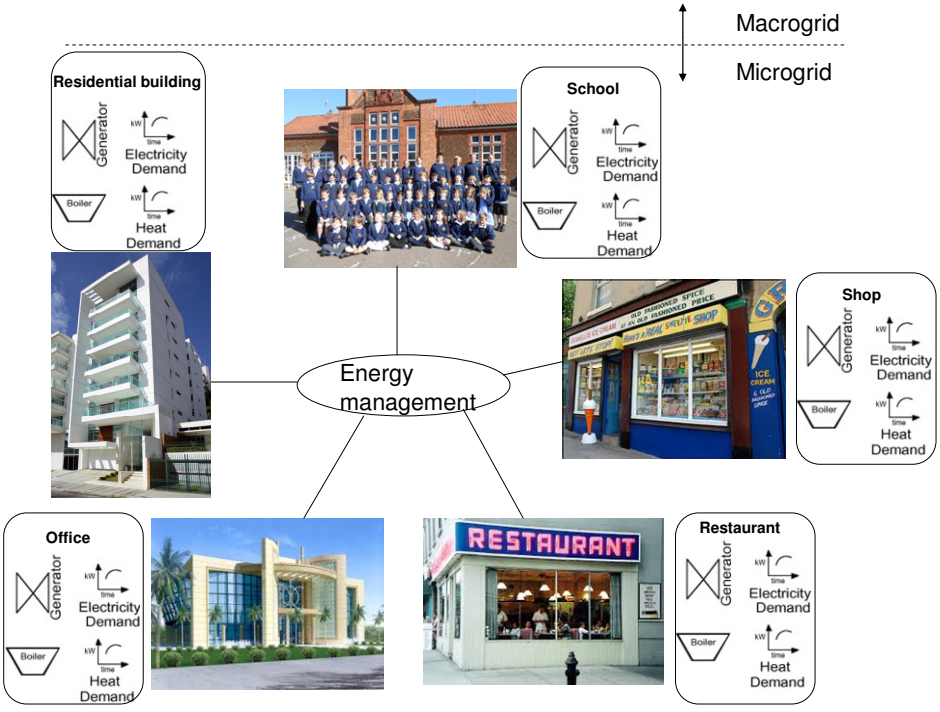

Figure 2-1 Participants of a microgrid

The candidate technologies involved in this study only include CHP generators (with different capacities and heat-to-power ratios), boilers, thermal storage and a macrogrid

power connection; while excess electricity produced by each site can possibly be transferred to other sites at a certain transfer price or sold to the macrogrid. Turn-key costs of CHP generators are based on the CHP types as well as the capacity range. Non-dispatchable generators are not considered in this study; because of the uncertainties caused by weather conditions.

Energy production is modelled on specific sample days, which are classified from seasons and weekday or weekend, weighting factors of day type are multiplied in the cost function of each participant site. The microgrid and the macrogrid are interacted and constrained through exporting or importing electricity. The assumptions made for each participant are listed below:

- up to one CHP generator;
- up to one boiler;
- up to one thermal storage;
- a grid connection (allowing import and export of electricity during parallel operating to the grid);
- no heat transfer is allowed between sites.

Administered transfer pricing is applied in the proposed model, where a 'central manager' in the microgrid decides the best solution for all participants utilising the Nash bargaining model. No other negotiations exist after that. No information sharing among participants is required while each participant must provide information to a central planner. Electricity can be transferred among sites, and the total electricity transfer cost is determined by transfer prices multiplied by the amount transferred. The cost is equal to the revenue gained by the site where the electricity is transferred from.

The system adopts two key assumptions as each participant: i) provides its information to a central planner and ii) accepts electricity transfer prices as determined by the central planner over long term. Each participant needs to provide the following information to the central planner:

- Electricity and heat loads

- Status quo point (*i.e.* cap on equivalent annual cost)
- Available distributed energy resources, such as CHP, boiler and thermal storage
- Range of allowed electricity transfer prices with the other participants.

The overall problem can be stated as follows:

Given (a) a time horizon split into a number of intervals (not necessary equal), (b) energy demand at each site for each time interval, (c) gas and electricity costs from macrogrid, (d) turn-key costs of candidate technologies, (e) efficiencies of candidate technologies, (f) heat-to-power ratio of different CHP technologies, (g) ramp limits for CHP generators, (h) charge and discharge rates for thermal storage, (i) fixed cost for microgrid components, (j) weighting factor for day type and (k) range of available electricity transfer prices.

Determine (a) the maximum acceptable equivalent annual cost, (b) the candidate technologies selected and their capacities, (c) energy resources consumed, (d) energy production plan, (e) thermal energy storage plan, (f) transfer price level and (g) transferred electricity plan.

In order to (a) find the multi-participant strategies which result in optimal, fair distribution of the equivalent annualised cost and (b) fulfil the energy demand.

2.3 Mathematical Formulation

An MINLP model is formulated first for the microgrid planning problem concerning the fair electricity transfer price and unit capacity selection and then an MILP model is obtained by transforming the MINLP model with a separable programming approach. The key decision variables included in the model are intra-microgrid electricity transfer price, flow of electricity transferred, unit capacities and resources utilised. They are determined by maximising the equivalent annualised cost (EAC) of all participants based on given EAC upper bounds, subject to equipment capacity constraints, CHP ramp limit constraints, energy demand constraints, CHP selection constraints, thermal storage constraints and transfer price level constraints.

2.3.1 Nomenclature

A list of the notation used in this model is provided as:

Indices

j	time interval
k	electricity transfer price levels available
l	CHP generator capacity level
q	interval in *EAC* linearisation
s	site
t	sample day

Parameters

a^B	lifetime of boiler (year)
a^C	lifetime of CHP (year)
a^T	lifetime of thermal storage (year)
c^{Ex}	price of exported electricity to the grid (*£/kWh*)
c^I	price of electricity imported from the grid (*£/kWh*)
c^{Ip}	peak price of electricity imported from the grid (*£/kWh*)
c^N	price of natural gas (*£/kWh*)
c^T	cost per unit output for thermal storage unit (*£/kWh*)

C_l^{CU} CHP capacity upper limit at level l (kW)

C_l^{CL} CHP capacity lower limit at level l (kW)

D^T maximum discharge rate for thermal energy storage (kW)

$\overline{e}_{ss'k}$ k available electricity transfer price levels from site s to site s' ($£/kW_e h$)

F^B capital recovery factor of the boiler

F^C capital recovery factor of CHP

F^T capital recovery factor of the thermal storage

G^T maximum charge rate for thermal energy storage (kW)

H_{tjs} heat demand of day t during time interval j at site s (kW)

L_{tjs} electrical demand of day t during time interval j at site s (kW)

m number of linearisation intervals of objective function

P_s fixed cost for microgrid components, shared by site s (£)

Q_l heat to power ratio for CHP generator at capacity level l

r interest rate

R_l ramp limit for CHP generator from capacity level l (kW)

T_j time duration of each time period j(h)

W_t weight for day t (reflection of number of days of this type per year)

$Y_{ss'}^{U}$ upper bound of electricity transferred from site s to site s' (kW)

Y_{s}^{U} upper bound of electricity sent to site s (kW)

α_l cost per kW_e installed for CHP generator of l level (£/kW_e)

β cost per kW_{th} installed for boiler (£/kW_{th})

γ cost per $kW_{th}h$ installed for thermal energy storage (£/$kW_{th}h$)

η centralised electricity generation efficiency

η_l^C electrical efficiency of the CHP generator at level l

η^B efficiency of boiler

η^T turn around efficiency of thermal energy storage

μ_{sq} parameter related to EAC_{sq} (linearised EAC values of site s at interval q (£)

κ_s agreed electricity load limit from grid for site s (kW)

ρ^G CO_2 emission factor of grid electricity

ρ^N CO_2 emission factor of natural gas

EAC_{sq} linearised EAC values of site s at interval q (£)

EAC_s^U EAC upper bound value for site s (£)

Variables

C_s^T installed capacity of thermal energy storage unit at site s ($kW_{th}h$)

C_s^B installed thermal capacity of boiler at site s (kW_{th})

C_{sl}^C installed electrical capacity of CHP from level l at site s (kW_e)

d_{tjs} dumped heat on day t at time j at site s (kW_{th})

$e_{ss'}$ electricity transfer price from site s to site s' ($£/kW_eh$)

E_{tjs} electricity exported to the grid on day t at time j from site s (kW_e)

f_{tjs} heat received from the thermal storage on day t at time j at site s (kW_{th})

g_{tjs} heat sent to the thermal storage on day t at time j at site s (kW_{th})

I_{tjs} electricity imported from the grid on day t at time j for site s (kW_e)

S_{tjs}^T heat stored in the thermal storage on day t at time j at site s ($kW_{th}h$)

u_{tjsl} output of CHP on day t at time j at site s from level l (kW_e)

x_{tjs} output of boiler on day t at time j at site s (kW_{th})

$y_{tjss'}$ electricity transferred on day t at time j from site s to site s' (kW_e)

$\overline{Y}_{tjss'k}$ linearised electricity transferred amount, during day t, time j from site s to site s', at k transfer price level (kW_e)

ϕ objective value (£)

λ_{sq} linearisation factor, these are SOS2 (Special Order Sets of Type 2) special ordered variables [128], where only two adjacent λ_{sq} can be non-zero.

ξ_{tjs} extra electricity load from grid over the agreed threshold for day t time interval j at site s

ACC_s annual capital cost of site s (£)

CE total CO_2 emissions (kg)

EAC_s equivalent annual cost of site s (£)

EC_s electricity cost of site s(£)

OPC_s operation cost of site s(£)

PR total primary energy resources (kWh)

TEC_s transferred electricity cost of site s (£)

Binary variables

X^I_{tjs} 1 if electricity is imported from the grid or bought from other sites, on day t at time j, at site s, 0 otherwise

$X_{ss'k}$ 1 if between site s and site s', transfer price level k is selected, 0 otherwise

X^C_{sl} 1 if for site s CHP capacity level l is selected; 0 otherwise

2.3.2 Objective Function

Common approach of optimising the design of a microgrid is simply to minimise the total cost of all participants as shown in Eq.2-1.

$$\tilde{\phi} = \sum_s EAC_s \qquad \textbf{Eq. 2-1}$$

where EAC_s is the equivalent annual cost of site *s*, which includes the annualised capital cost and operation cost of each candidate technology, cost from transferred electricity within the microgrid, electricity cost from macrogrid and fixed cost for microgrid components. EAC_s^U is the upper bound of EAC for site *s*, which is obtained based on the macrogrid scenario when there is no local DER, and all electricity is bought from grid and all heat is obtained from boilers. No electricity transfer among sites is allowed. The formula for EAC_s is:

$$\begin{aligned} EAC_s = {} & ACC_s^{CHP} + ACC_s^{B} + ACC_s^{THS} \\ & + OPC_s^{CHP} + OPC_s^{B} + OPC_s^{THS} \qquad \forall s \\ & + TEC_s + EC_s + P_s \end{aligned} \qquad \textbf{Eq. 2-2}$$

where P_s is the fixed cost for microgrid components from each site *s*. Details of each term is provided in Table 2-1.

Table 2-1 Description of EAC_s components

Respective term calculation	Description
$ACC_s^{CHP} = \sum_l (\alpha_l F^C C_{sl}^C)$	Annual capital cost of CHP generator
$ACC_s^B = \beta F^B C_s^B$	Annual capital cost of boiler
$ACC_s^{THS} = \gamma F^T C_s^T$	Annual capital cost of thermal storage
$OPC_s^{CHP} = \sum_{t,s,l} c^N W_t T_j u_{tjsl} / \eta_l^C$	Operation cost of CHP generator
$OPC_s^B = \sum_{t,j} c^N W_t T_j x_{tjs} / \eta^B$	Operation cost of boiler
$OPC_s^{THS} = \sum_{t,j} c^T W_t T_j g_{tjs}$	Operation cost of thermal storage
$TEC_s = \sum_{t,j,s'} W_t T_j e_{s's} y_{tjs's} - \sum_{t,j,s'} W_t T_j e_{ss'} y_{tjss'}$	Transferred electricity cost within microgrid
$EC_s = \sum_{t,j} c^I W_t T_j I_{tjs} - \sum_{t,j} c^{Ex} W_t T_j E_{tjs}$	Electricity cost from macrogrid

However, the total cost minimisation approach may result in an unfair cost distribution among participants. It would be possible to ultimately undermine the microgrid concept because it does not attract some participants to join the microgrid. Each single participant requires their own minimum EAC_s and they will bargain for their own benefits. The performance of the whole microgrid is desired while the respective reward among participants is still guaranteed. It requires an approach that produces a fair costs distribution subject to similar overall performance. Game theory provides a tool for fair sharing among players. The Nash bargaining solution [104] is applied, which maximises the product of the deviations of the given *EAC* upper bound of each participant by the status quo cost levels. The objective function is given as Eq. 2-3. It obtains a Pareto optimal (within a pre-specified margin) solution for all participating partners [127]. Each EAC_s yields minimum value while trying to achieve the maximum objective value in Eq. 2-3, which guarantees both individual benefits and overall performance.

$$\text{Max}\,\phi = \prod_{s} (EAC_s^U - EAC_s) \qquad \textbf{Eq. 2-3}$$

2.3.3 Capacity Constraints

The output from the CHP generators and boilers over any period on any day at each participant site cannot exceed their installed unit capacities:

$$u_{tjsl} - C_{sl}^C \le 0 \qquad \forall t, j, s, l \qquad \textbf{Eq. 2-4}$$

$$x_{tjs} - C_s^B \le 0 \qquad \forall t, j, s \qquad \textbf{Eq. 2-5}$$

At any time on any day at each participant site, heat stored in the thermal storage cannot exceed the installed capacity of the thermal storage unit.

$$S_{tjs}^T \le C_s^T \qquad \forall t, j, s \qquad \textbf{Eq. 2-6}$$

2.3.4 Ramp Limit Constraints

Degradation of CHP performance with time can affect significantly the economics of ownership [129, 130]. In order to avoid generator damage and unit degradation, CHP generator outputs between two adjacent time intervals are constraint to change within a range. These 'ramp limits' for each CHP generator capacity level are given as:

$$-R_l \le u_{t,j+1,s,l} - u_{tjsl} \le R_l \qquad \forall t, j, s, l \qquad \textbf{Eq. 2-7}$$

Thermal storage charge and discharge rates are the rates at which heat is added to or removed from thermal storage. It depends on the characteristics of specific thermal storage equipment, the charge and discharge rates are limited by constraints Eq. 2-8 and 2-9:

Thermal storage:

$$f_{tjs} \le D^Y \qquad \forall t, j, s \qquad \textbf{Eq. 2-8}$$

$$g_{tjs} \le G^T \qquad \forall t, j, s \qquad \textbf{Eq. 2-9}$$

2.3.5 Energy Demand Constraints

For each time interval, electricity demand equals the sum of electricity outputs of the CHP generator, electricity transferred from other sites and electricity imported from the grid minus the electricity transferred to other sites and electricity exported to the macrogrid.

$$\sum_l u_{tjsl} + \sum_{s'} y_{tjs's} - \sum_{s'} y_{tjss'} + I_{tjs} - E_{tjs} = L_{tjs} \qquad \forall t, j, s \qquad \textbf{Eq. 2-10}$$

Since heat transfer between sites is not allowed, the heat demand equals the sum of heat output of the CHP generators, boilers and heat discharged from the thermal storage minus the heat sent to the thermal storage. The heat generated from CHP generators is calculated by multiplying the electricity output with the heat-to-power ratio Q_i of each type of CHP generator. The heat balance is:

$$\sum_l Q_l u_{tjsl} + f_{tjs} - g_{tjs} + x_{tjs} = H_{tjs} \qquad \forall t, j, s \qquad \textbf{Eq. 2-11}$$

It should be noted that in some models, heat venting is not allowed because of environmental concerns or specifics of the site and engineering options. However, if heat dumping is unconstraint, Eq. 2-11 can simply be modified to:

$$\sum_l Q_l u_{tjsl} + f_{tjs} - g_{tjs} + x_{tjs} = H_{tjs} + d_{tjs} \qquad \forall t, j, s \qquad \textbf{Eq. 2-11a}$$

2.3.6 CHP Constraints

As assumed, for each site at most one CHP generator can be selected from different capacity levels.

$$\sum_l X_{sl}^C \le 1 \qquad \forall s \qquad \textbf{Eq. 2-12}$$

Turn-key cost of CHP generator depends on the capacity size which has different heat-to-power ratio, so the turn-key cost per *kW* is considered as the same under certain capacity range. If a CHP generator is selected for one site, its capacity should be within the capacity range for the selected capacity interval; otherwise it has a capacity of 0, which means it is not selected.

$$C_l^{CL} X_{sl}^{C} \le C_{sl} \le C_l^{CU} X_{sl}^{C} \qquad \forall s,l \qquad \textbf{Eq. 2-13}$$

2.3.7 Thermal Storage Constraints

For each site at each time interval, energy stored in the thermal storage is the sum of the energy stored from the previous time period and the energy charged into the storage minus the energy discharged from the storage. Heat would be lost with efficiency during the charging and discharging processes. For example with thermal storage turn-around efficiency η^T, during any period when amount of heat $T_j v_{tjs}$ is sent to the thermal storage, only $T_j \eta^T v_{tjs}$ will be charged, and the rest being lost. On the other hand during the discharging process, in order to send $T_j z_{tjs}$ of heat to the site, $T_j / \eta^T z_{tjs}$ of heat is sent.

$$S_{tjs}^T = S_{t,j-1,s}^T + T_j \eta^T g_{tjs} - T_j / \eta^T f_{tjs} \qquad \forall t, j, s \qquad \textbf{Eq. 2-14}$$

In order to guarantee no heat is accumulated day to day, the thermal storage has an initial storage state at the beginning of each sample day, and at the end of day, the thermal storage must return to its initial value.

$$S_{t,0,s}^T = S_{t-1,J,s}^T \qquad \forall t, s \qquad \textbf{Eq. 2-15}$$

2.3.8 Transfer Price Levels

There is a non-linear term in the electricity transfer cost, TEC_s, given in Table 2-1. In order to convert the non-linear model to an exact linear equivalent, the following formulation is applied. There are k discrete transfer price levels available for electricity transferred

between sites, defined via the parameter $\bar{e}_{ss'k}$. To determine the price level $e_{ss'}$, the binary decision variable $X_{ss'k}$ is multiplied by $\bar{e}_{ss'k}$ and summed over all transfer price levels:

$$e_{ss'} = \sum_k \bar{e}_{ss'k} X_{ss'k} \qquad \forall s, s' \qquad \textbf{Eq. 2-16}$$

At most one transfer price level can be chosen:

$$\sum_k X_{ss'k} \le 1 \qquad \forall s, s' \qquad \textbf{Eq. 2-17}$$

The same electricity transfer prices of each pair of sites are assumed between the two transfer directions.

$$X_{ss'k} = X_{s'sk} \qquad \forall s, s' \qquad \textbf{Eq. 2-18}$$

2.3.9 Electricity Transfer Amount

The amount of electricity transferred $y_{tjss'}$ is the sum of amounts transferred at each transfer price level *k*:

$$y_{tjss'} = \sum_k \bar{Y}_{tjss'k} \qquad \forall t, j, s, s' \qquad \textbf{Eq. 2-19}$$

The upper bound for the amount of electricity transferred from site *s* to site *s'* is introduced, which guarantees $\bar{Y}_{tjss'k}$ cannot be more than $Y^U_{ss'}$. No electricity can be transferred at that level if the transfer price level *k* is not selected, as $\bar{Y}_{tjss'k} = 0$.

$$\bar{Y}_{tjss'k} \le Y^U_{ss'} X_{ss'k} \qquad \forall t, j, s, s', k \qquad \textbf{Eq. 2-20}$$

Electricity is forbidden to be sold from one site to another site or the macrogrid before it fulfils its own demand. Equally, any site cannot buy electricity from other sites and sell it to the grid simultaneously. The binary variable X^I_{tjs} is introduced in order to ensure that the

above two conditions are satisfied by using the two constraints below, where Y_s^U is the upper bound of electricity sent to site s .

$$\sum_{s'} y_{tjs's} + I_{tjs} \le Y_s^U X^I{}_{tjs} \qquad \forall t, j, s \qquad \textbf{Eq. 2-21}$$

$$\sum_{s'} y_{tjss'} + E_{tjs} \le Y_s^U (1 - X^I{}_{tjs}) \qquad \forall t, j, s \qquad \textbf{Eq. 2-22}$$

Term $e_{ss'} y_{tjss'}$ in transferred electricity cost TEC_s is formulated as $\sum_k \overline{e}_{ss'k} \overline{Y}_{tjss'k}$, which is linear.

2.3.10 A Separable Programming Approach

The objective function Eq. 2-3 is non-linear and a separable programming approach is applied to tackle the non-linear problem. The non-linear objective function can be expressed as a sum of functions involving only one variable via the separable programming approach.

The separable technique is briefly described as: a continuous strictly convex function in one variable, *f(x)*, can be approximated over an interval as a piecewise linear function $f(x_q)$ using m grid points, the approximation is given by Eq. 2-23 to 2-25. Variables λ_q are special ordered variables, and only two adjacent λ_q can be non-zero. Constraints 2-24, 2-25 and the convexity requirement guarantee that two adjacent nodes take non-zero values.

$$\bar{f}(x) = \sum_{q=1}^{m} \lambda_q f(x_q) \qquad \textbf{Eq. 2-23}$$

$$\sum_{q=1}^{m} \lambda_q = 1 \qquad \textbf{Eq. 2-24}$$

$$\lambda_q \ge 0 \quad \forall q \qquad \textbf{Eq. 2-25}$$

The objective function of this study, Eq. 2-3, is non-linear, being the product of the benefit over given upper bound of each site. The objective function can be rewritten via logarithmic differentiation as:

$$\ln\phi = \sum_{s} \ln(EAC_s^U - EAC_s) \qquad \textbf{Eq. 2-26}$$

Using the separable programming approach, the objective function is converted to Eq. 2-27, where EAC_{sq} is the value of EAC_s interval q. The convexity properties hold, since $\ln(EAC_s^U - EAC_{sq})$ is maximised and is strictly concave (equivalent to minimisation of a convex function) and EAC_{sq} is linear and therefore convex.

The final formulation is therefore:

$$\max \hat{\phi} = \sum_{s} \sum_{q=1}^{m} \mu_{sq} \lambda_{sq} \qquad \textbf{Eq. 2-27}$$

where $\hat{\phi} \equiv \ln\phi$

$$\begin{aligned} \sum_{q=1}^{m} EAC_{sq}\lambda_{sq} = {} & ACC_s^{CHP} + ACC_s^{B} + ACC_s^{THS} \\ & + OPC_s^{CHP} + OPC_s^{B} + OPC_s^{THS} + EC_s + P_s \qquad \forall s \quad \textbf{Eq. 2-28} \\ & + \sum_{t,j,s',k} W_t T_j \bar{e}_{s'sk} \bar{Y}_{s'stjk} - \sum_{t,j,s',k} W_t T_j \bar{e}_{ss'k} \bar{Y}_{ss'tjk} \end{aligned}$$

$$\sum_{q=1}^{m} \lambda_{sq} = 1 \qquad \forall s \qquad \textbf{Eq. 2-29}$$

$$\lambda_{sq} \geq 0 \qquad \forall s, q \qquad \textbf{Eq. 2-30}$$

where μ_{sq} are parameters given by $\mu_{sq} = \ln(EAC_s^U - EAC_{sq})$, EAC_{sq} are taken according to the upper bounds EAC_s^U and the minimum cost by minimising EAC_s of each site. Terms in Eq. 2-28, ACC, OPC and EC are given as before by Table 2-1. The mathematical

program described in Eq.2-27 through 2-30 should be solved subject to the constraints in Eq. 2-4 to2-22, Eq. 2-27 being the linear approximation to Eq. 2-3.

2.3.11 CO_2 Emissions and Primary Energy Resources

CO_2 emissions are calculated based on CO_2 emission factors of electricity from grid and natural gas consumption as in Eq. 2-31. Total CO_2 emissions are composed of emissions of electricity from grid and natural gas consumed by CHP generators and boilers.

$$CE = \sum_{t,j,s} \rho^E W_{t,j} T_j I_{tjs} + \rho^G \left(\sum_{t,j,l,s} W_t T_j u_{tjsl} / \eta_l^C + \sum_{t,j,s} W_t T_j x_{tjs} / \eta^B \right) \quad \textbf{Eq. 2-31}$$

Primary energy resource consumption is calculated according to the efficiencies of centralised electricity generation, CHP and boiler. The total primary energy consumed sums up primary energy consumption from energy generation from grid and local CHPs and boilers.

$$PR = \sum_{t,j,s} W_{t,j} T_j I_{tjs} / \eta + \sum_{t,j,l,s} W_t T_j w_{tjsl} / \eta_l^C + \sum_{t,j,s} W_t T_j x_{tjs} / \eta^B \quad \textbf{Eq. 2-32}$$

2.4 Case Study

The MILP model is implemented on a case study of a microgrid with five local sites: a school, a hotel, a restaurant, an office building and a residential building. All the buildings are built to PassiveHaus standards according to information provided by the developers of [131]. CPLEX 12.3.0.0 in GAMS 23.7 [128] on a PC with an Intel Core 2 Duo, 2.99 GHz CPU and 3.25GB of RAM is used. The model involves 7,307 equations with 5,682 continuous and 440 discrete variables. Basic technical parameters and energy demands are given first. Then microgrid is considered as a whole unit, global *EAC* savings compared with current energy providing system, macrogrid scenario, are analysed based on gas price, electricity buying price and selling prices. Under given fixed gas price and electricity buying and selling prices, *EAC* upper bounds of participants are determined based on the macrogrid scenario cost and energy demand pattern. Later, the minimised global *EAC* is

obtained under fixed transfer prices. *EAC* savings of respective participants then indicate the possibility of unfair benefits distribution. Fair microgrid settlement is achieved by applying the Game theory Nash approach and the solution includes the intra electricity transfer price and quantity, unit capacity and operation planning. Finally, peak demand charge scheme is applied in the fair settlement solution.

2.4.1 Basic Technical Parameters and Costs of Microgrid Candidate Technologies

The parameters for the candidate technologies are presented in Table 2-2, with CHP, boiler and thermal energy storage.

Table 2-2 Technical parameters and costs of microgrid candidate technologies [65]

Technology	Turn-key cost (£/*kW*)	Operating cost (£/*kW*h)	Electrical efficiency	Overall efficiency	Lifetime (year)	F
CHP	-	0.027	-	0.9 [131]	15	0.147
Boiler	40	0.027	-	0.8	15	0.147
Thermal storage	20	0.001	0.98	-	25	0.128

Turn-key costs consist of the costs from investment, installation, foundations and main connections. CHP turn-key cost and electrical efficiency vary from different the capacity sizes, while the overall efficiency (electrical and heat efficiency) is assumed as 90%. Operating costs for CHP generators and boilers are as only the fuel cost. For the fuel tariff, the gas price is 2.7 p/kWh and electricity bought from the grid is 13 p/kWh; while the microgrid can sell electricity back to the macrogrid at 1 p/kWh. The operating cost of thermal storage is the equipment maintenance cost. The capital recovery factor (F) is calculated from Eq. 2-33:

$$F = \frac{r(1+r)^a}{(1+r)^a - 1} \qquad \textbf{Eq. 2-33}$$

where a is the lifetime of given candidate equipment (see Table 2-2) and r is the interest rate. In the case study, 12% interest rate is applied. The electricity transfer prices can be selected from values between 3 p/kWh to 10 p/kWh.

The CHP capacity levels are determined from the energy demand profile and turn-key costs are given based on the different capacity levels in Table 2-3; the smallest acceptable CHP capacity is 3 kW_e. The average turn-key costs for each kW_e decrease when the CHP capacities increase. CHP generators smaller than 3 kW_e are not considered because of the relative high turn-key cost. The turn-key costs selected here are listed according to [132], while the electrical efficiency is obtained from [131].

Table 2-3 CHP turn-key cost and electrical efficiency [131, 132]

Range (kW_e)	Turn-key costs (£/kW_e)	Electrical efficiency	Heat to power ratio
3-5	1,900	0.25	2.60
6-10	1,230	0.27	2.33
11-15	1,165	0.28	2.21
16-20	1,120	0.29	2.10
21-25	1,080	0.295	2.05
26-50	1,050	0.30	2.00

2.4.2 Energy Demand Profiles

The consumption profiles have been defined with 18 different periods in total: 6 periods per day for 3 representative days per year (120 winter days, 153 mid-season days and 92 summer days in total). The periods are shown in Table 2-4 and the weighting factor W_t represents the number of days for each day type, e.g. sample day in winter, the weighting factor is 120. Basic statistics for the energy demand profiles are provided in Table 2-5.

Table 2-4 Time periods

Period	Hours in the day
1	7.00am-9.00am
2	9.00am-12.00pm
3	12.00pm-1.00.pm
4	1.00pm-6.00pm
5	6.00pm-10.00pm
6	10.00pm-7.00am

Table 2-5 Statistics of investigated energy demand profile [131]

	School	Hotel	Restaurant	Office	Residential building	Total
Annual heat demand ($kW_{th}h$)	149,000	184,000	8,460	8,220	111,000	461,000
Annual electricity demand (kW_eh)	50,000	66,000	90,000	23,400	68,000	297,400
Peak heat demand (kW_{th})	42.1	65.6	2.5	2.8	67.4	-
Peak electricity demand (kW_e)	10.7	11.6	17.7	4.1	18.6	-

Electricity and heat demand profiles for a winter day are shown in Figure 2-2 and Figure 2-3; the energy profiles present the constant energy demand density during each respective time period [131]. The five sites have different energy pattern from their respective function. The school has energy consumption hours primarily during day time; the restaurant has electricity peak hours during lunch time and dinner time; the residential building has the energy peak hour during the evening, when most people return home. The hotel and office building are commercial buildings, which have relatively flat energy consumption during the working hours. These different energy consumption patterns provide possibilities for the five sites to cooperate with each other and benefit within the microgrid.

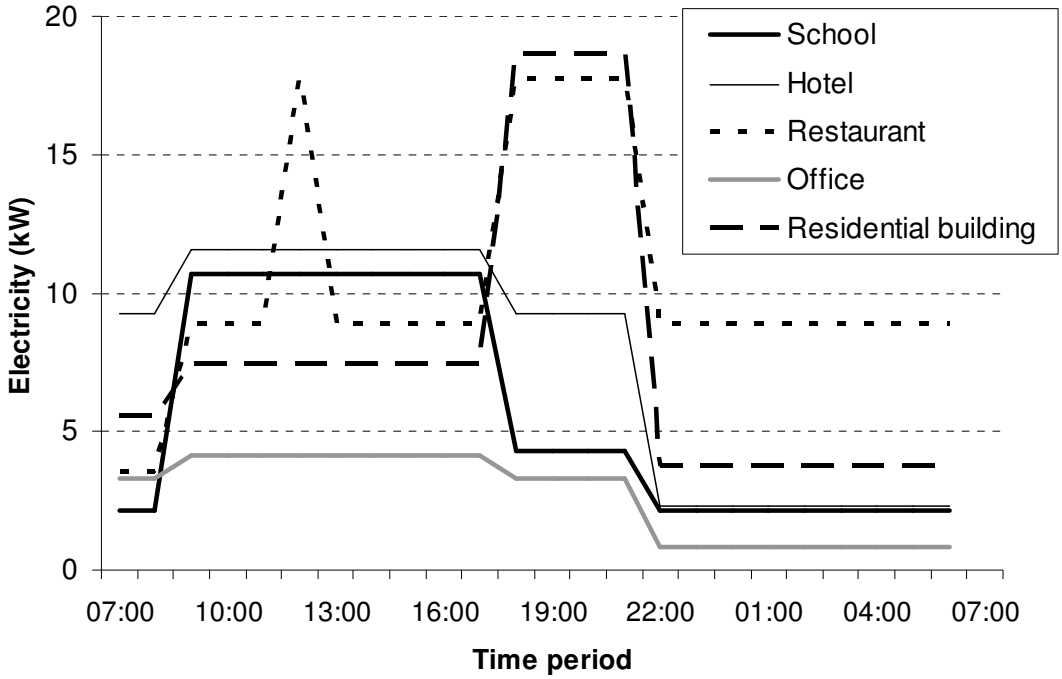

Figure 2-2 Electricity demand (winter day) [131]

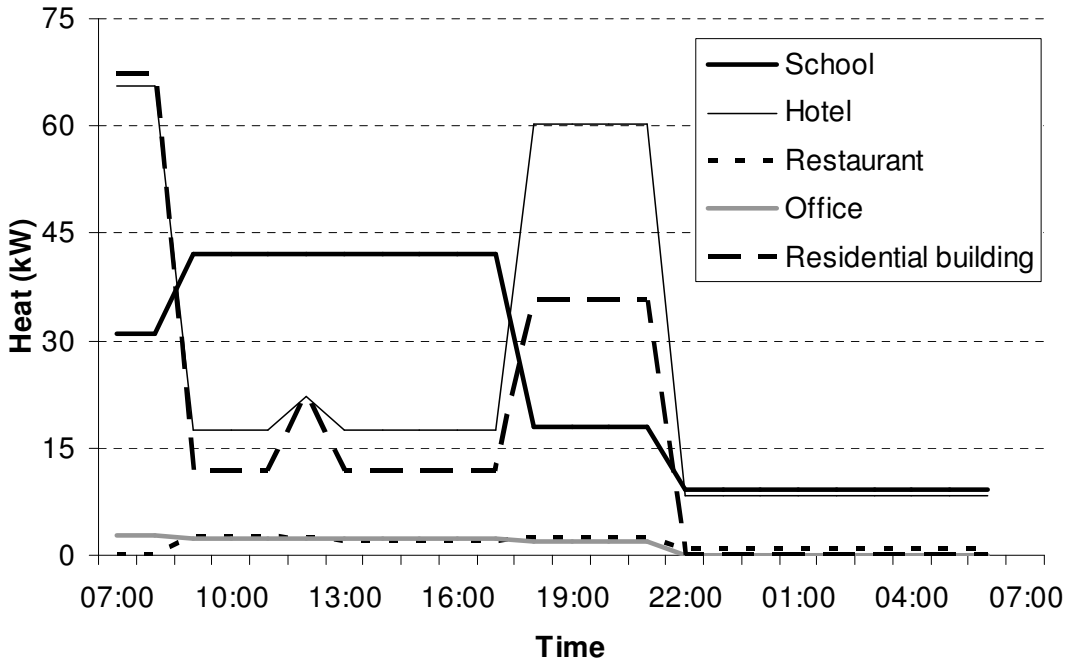

Figure 2-3 Heat demand (winter day) [131]

2.4.3 Global Microgrid EAC Savings with Gas Price, Electricity Buying and Selling Prices

Compared with macrogrid scenario, *EAC* decreases by utilising a microgrid. Effects on total *EAC* savings from gas price, electricity buying and selling prices are analysed. The objective is to minimise the total EAC of the five participants in the microgrid as Eq. 2-1. The constraints are listed in Table 2-6, where active equations for other sections in this work are also listed.

Table 2-6 Model summaries

Sections	Objective function	Constraints
4.3 Global microgrid EAC savings	2-1	2-2, 4 to 22
4.4 EAC upper bounds	2-1	2-2, 5, 10, 11
4.5 Global minimum microgrid EAC	2-1	2-2, 4 to 22
4.6 Game theory for fair settlement	2-27	2-4 to 22, 28 to 30
4.7 Fair settlement under peak demand charge	2-27	2-4 to 22, 28 to 30, 34 to 35

It is expected that as gas price increases *EAC* savings will decrease, since the electricity price difference increases between electricity generated from CHP and the electricity buying from macrogrid. When electricity buying price increases, *EAC* savings will increase because electricity generated from CHP is cheaper. While electricity selling price increases, *EAC* savings will increase and CHP will be promoted since it can produce electricity with lower expense. To analyse the impact of gas price, electricity buying and selling prices on microgrid equipment capacity selection and *EAC* savings, different combinations of these prices are implemented. Gas price varies from 2 to 10 p/kWh, electricity buying price varies from 10 to 15 p/kWh and electricity selling price varies from 1 to 10 p/kWh. These value ranges are assumed based on the case study in this chapter and common energy tariff range. The *EAC* savings compared with the macrogrid scenario are shown in Figure 2-4 based on the three prices, where X axis is gas price, Y axis is electricity buying price and Z axis is electricity selling price. No microgrid network cost is considered and the *EAC* savings are presented with coloured dots, the hot colour (red) represents high *EAC* saving values while cold colour (blue) represents low values. The highest *EAC* saving is £17,400,

when gas price is 2 p/kWh, electricity buying price is 15 p/kWh and electricity selling price is 10 p/kWh. The lowest *EAC* savings are zeros when gas price and electricity buying price are both 10 p/kWh under all electricity selling prices. As shown in Figure 2-4, the increase of electricity selling price does not influence much on the *EAC* savings, which is indicated by the colour difference and the size of the dots in the figure. *EAC* savings mainly depend on gas price and electricity buying price.

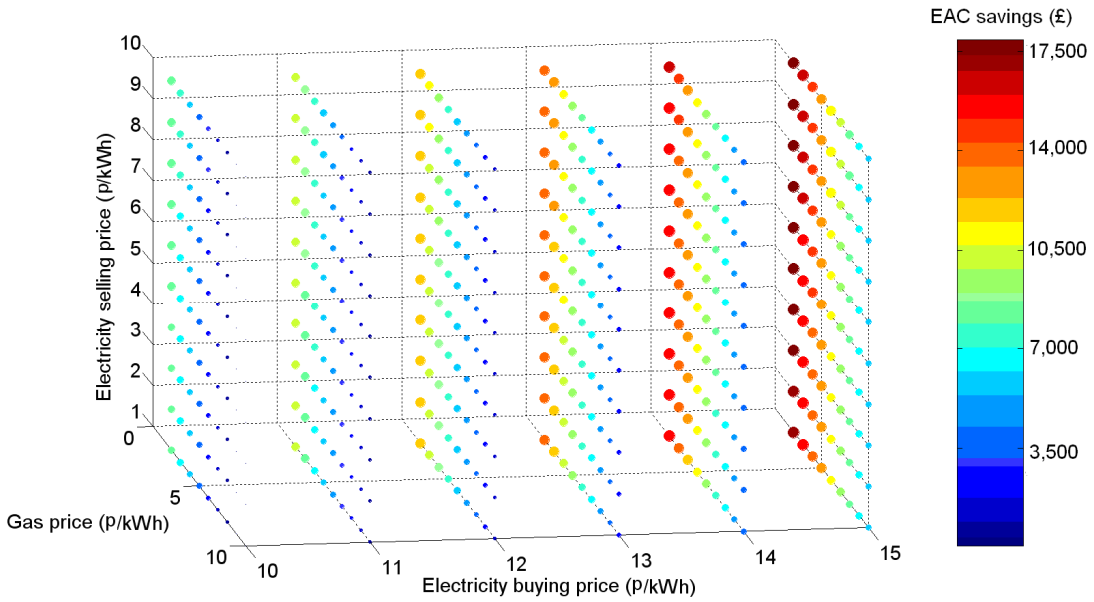

Figure 2-4 EAC savings as a function of gas, electricity buying and selling prices

To illustrate how the gas price influences the *EAC* savings, electricity buying price is bounded to 13 p/kWh which is adopted in this case study as given in 2.4.1. *EAC* savings from microgrid scenario are only influenced by gas price and electricity selling price, which is presented in Figure 2-5.

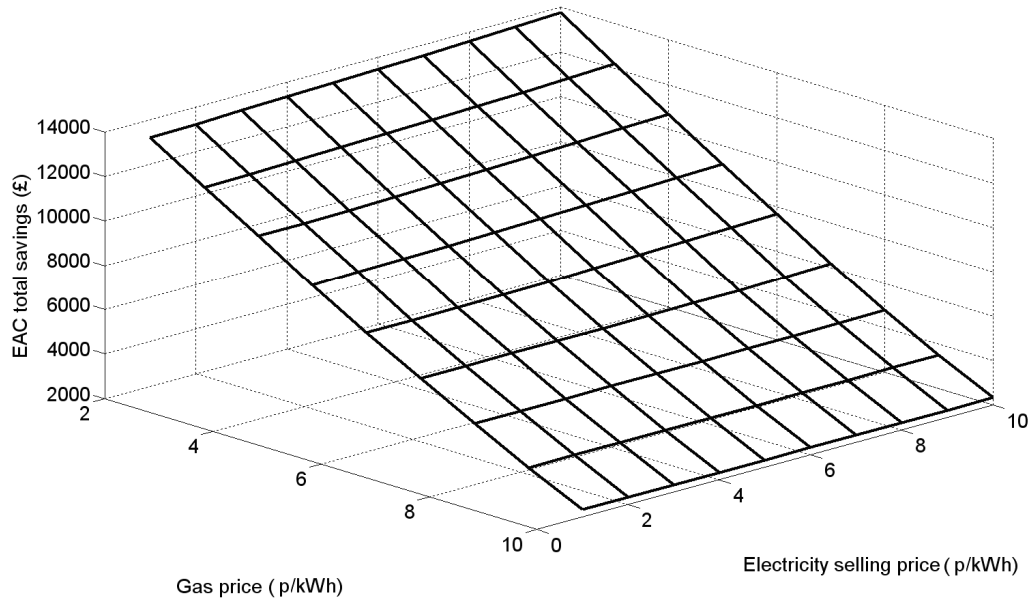

Figure 2-5 EAC savings as a function of gas and electricity selling prices to grid

No microgrid network cost is considered in the saving calculations. As shown in the figure, gas price plays an important role in *EAC* savings, as gas price increases from 2 to 10 *p/kWh*, the *EAC* savings decrease from £13,000 to £2,300. Although savings are always positive, when microgrid network or service cost is considered, negative savings would appear. Also, when the saving is not obvious over current macrogrid scenario energy providing system, it is difficult to promote the microgrid system to potential customers. For the electricity selling price, as expected there is an increasing trend for the *EAC* savings, but it does not influence *EAC* savings as much as gas price does. Although the high electricity selling price will promote the selection of local CHP due to the revenue from selling electricity to grid, two main factors constrain bigger size CHP selection and *EAC* savings. Most importantly, excess heat from each participant cannot be transferred to other sites or other heat sinks except its own local thermal storage, so CHP cannot generate more electricity to sell to grid or other participants after it reaches its own heat demand. Secondly, the capital cost of CHP is relative expensive, the selling revenue cannot cover the capital cost if bigger capacity is selected.

EAC savings as a function of electricity buying and selling prices is shown in Figure 2-6, and gas price is fixed as 3 *p/kWh* .

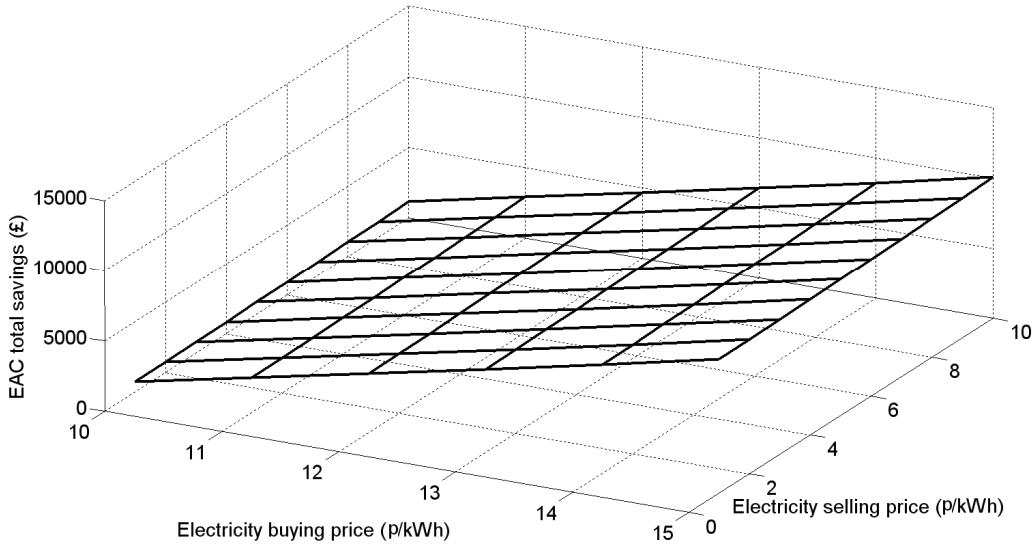

Figure 2-6 EAC savings as a function of electricity buying and selling prices

As the electricity buying prices increase from 10 *p/kWh* to 15 *p/kWh*, *EAC* savings increase from £800 to £10,000. The increase of electricity selling price to grid also tends to increase the *EAC* savings with relative minor effect. By increasing electricity selling price from 1 to 10 *p/kWh*, the *EAC* savings increase by about £500 for all electricity buying price cases.

By fixing electricity selling price at 1 *p/kWh*, *EAC* savings are shown in Figure 2-7 as a function of gas price and electricity buying price. *EAC* savings increase when gas price decreases and electricity price increases. Gas price and electricity price have similar influences on *EAC* savings. When electricity buying prices increase from 10 to 15 *p/kWh* , *EAC* savings increase by an average of £8,380 for all gas prices, which is about £1,400 for each 1 *p/kWh* electricity buying price increase. When gas price decreases from 10 to 2 *p/kWh* , *EAC* savings increase an average of £9,930 for all electricity selling price, which is about £1,100 for each 1 *p/kWh* gas price decrease. Total *EAC* savings from microgrid is heavily dependent on the prices of gas and electricity buying from grid.

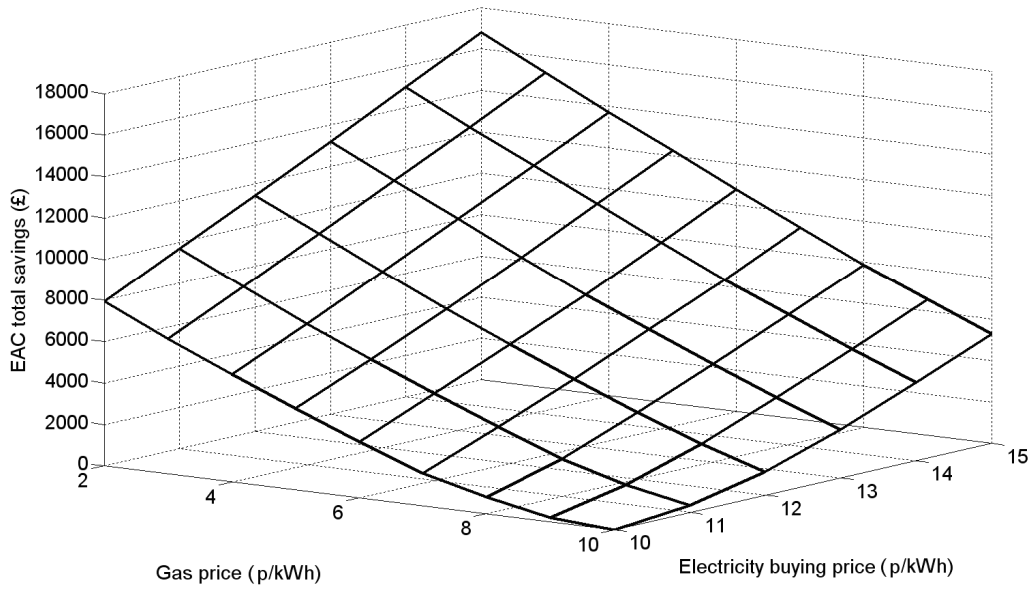

Figure 2-7 EAC savings as a function of gas and electricity buying prices

2.4.4 EAC Upper Bounds

For the case study, the gas price is 2.7 p/kWh and the price of electricity bought from the grid is 13 p/kWh; the microgrid can sell electricity back to the macrogrid at 1 p/kWh. The EAC upper bounds, EAC_s^U, are determined according to the macrogrid scenario cost of each site, electricity demand is satisfied from grid and heat demand is fulfilled only by boilers. By minimising the sum of EAC_s under the macrogrid scenario (*i.e.* minimise Eq. 2-1 subject to Eq. 2-2, 2-5, and 2-10 to 11)), the optimal results are shown in Table 2-7.

Table 2-7 Optimal results of macrogrid scenario

	School	**Hotel**	**Restaurant**	**Office**	**Residential building**	**Total**
EAC (£)	11,789	15,183	12,000	3,336	12,998	55,296
Boiler(kW_{th})	42.1	65.6	2.5	2.8	67.4	-

In order to promote the implementation of microgrids, the maximum EAC_s^U spending is assigned to each participant according to their macrogrid scenario EAC_s as well as their energy consumption style (heat to power ratio). Microgrid participants will not spend more than the assigned EAC_s^U. Compared with the restaurant and residential building, the school and hotel have higher heat-to-power ratios. Therefore, because no heat is allowed to be transferred between sites, the school and hotel could have more surplus electricity to sell to other participants. So, the upper bounds of school and hotel are assigned as 85% of their macrogrid scenario costs. Restaurant and residential building have upper bound of 90% of the macrogrid scenario costs. The office has relatively small *EAC*, so the upper bound is the same as the current macrogrid cost. For the $EAC_{s,1}$ values, they are set £1 smaller than EAC_s^U values to guarantee $EAC_s^U - EAC_{sq}$ is positive, which is required for calculating the logarithmic values. Then in the microgrid case, CHP and thermal storage are available to be selected and electricity transfer among sites is allowed. EAC_s of each site is minimised to obtain the lower bound values, with microgrid network fixed cost as £17,000 over 20 years given by [65]. The piecewise EAC_{sq} values are determined based on the range of the upper bounds and the lower bounds, differences between the two bounds are spread equally among given intervals over each site. EAC_{sq} values of upper bound and lower bound are shown in Table 2-8 and linearised values over 17 breakpoints are presented in Figure 2-8.

Table 2-8 Values of EAC_s^U, $EAC_{1,s}$ and $EAC_{q\max,s}$

	School	Hotel	Restaurant	Office	Residential building	Total
EAC_s^U (£)	10,021	12,906	10,800	3,336	11,698	48,761
$EAC_{s,1}$ (£)	10,020	12,905	10,799	3,335	11,697	48,756
$EAC_{s,q\max}$ (£)	7,570	9,370	6,060	1,560	7,650	32,210

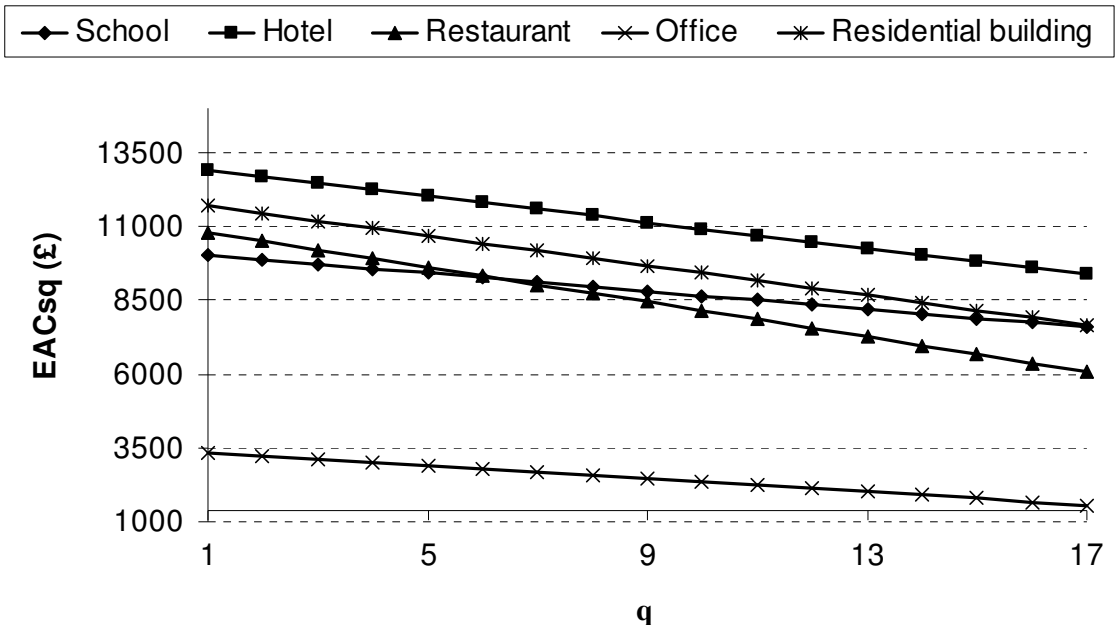

Figure 2-8 EAC_{sq} **linearised values**

2.4.5 Global Minimum Microgrid EAC

If the objective is only to minimise the total EAC of the five sites in Eq. 2-1, subject to Eq.2-4 to 2-22 and Eq. 2-28 to 2-30, there is no guarantee that all sites will benefit. Prices for electricity transfer between sites are fixed first to show how much each site can save when only the total minimum EAC is considered. Electricity transfer prices are taken as 3-10 p/kW_eh, and the optimal results are shown in Table 2-9.

Table 2-9 Optimum EAC results without Game theory

Transfer price *p/kWh*	School (£)	Hotel (£)	Restaurant (£)	Office (£)	Residential building (£)	Total (£)
3	9,620	12,039	10,148	3,035	10,834	45,675
4	9,471	11,896	11,051	3,035	10,221	45,675
5	9,306	11,600	11,466	2,639	10,664	45,675
6	9,101	11,493	11,499	2,949	10,633	45,675
7	8,975	11,254	11,458	3,206	10,782	45,675
8	8,824	10,998	11,735	3,054	11,065	45,675
9	8,661	10,794	11,878	3,389	10,954	45,675
10	8,480	10,654	11,983	3,439	11,120	45,675

In an integrated microgrid system, the intra electricity transfer price does not affect the total *EAC*, because within the microgrid, revenue from selling electricity to one participant means cost of buying electricity for the other participant. However, electricity transferred amount and transfer prices influence *EAC* of respective participant. The savings compared with given upper bounds are shown in Figure 2-9.

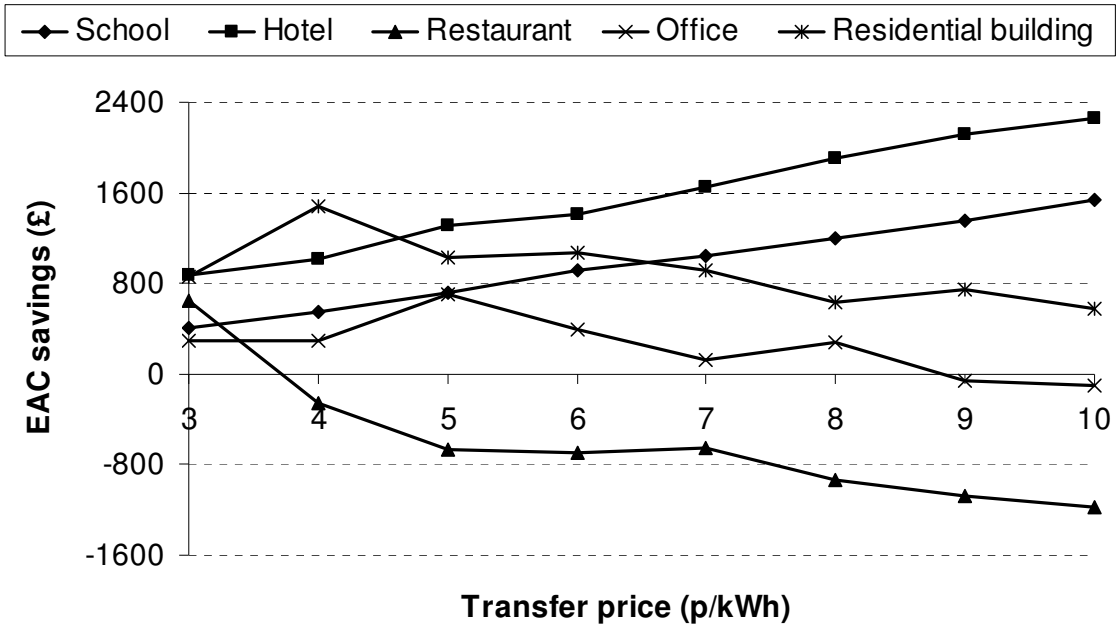

Figure 2-9 EAC savings of each microgrid participant without Game theory

The total saving through microgrid of the five sites is £3,086 and it is about 6.33% of the upper bounds. However, for each participant the saving is not distributed fairly. The benefits of each participant would vary quite differently on the fixed electricity transfer price cases, although the total saving of the whole microgrid is the same. For the restaurant, it almost always sacrifices and receives negative savings which happens to the office for two transfer price cases as well. That is because the objective is to minimise the total EAC, respective benefit is not considered, there is possibility that some participants could sacrifice their benefits to achieve the mutual benefit. The negative values come from the microgrid network sharing. The restaurant and office have relative low heat demand and high electricity demand and the capital cost for small CHP is high, they constrain the two sites from selecting CHP generator and they can only buy electricity from the grid or other sites and generate heat from their own boilers. Their benefits depend on the electricity transfer price and transferred amount. When electricity transfer price is high, the restaurant or office may not benefit from participating the microgrid scheme if only the total EAC is minimised. A fair settlement system among microgrid participants should be developed to guarantee that benefits are shared in a fair manner. This is done in the following section.

2.4.6 Application of Game Theory for Fair Settlement

When the Game theory Nash approach is applied, with the upper bounds obtained in 2.4.4, the objective function Eq. 2-27 is maximised subject to Eq.2-4 to 2-22 and Eq. 2-28 to 2-30. For the case study, when the number of linearisation pieces is over 17, the objective values stabilise. Increasing the number of linearisation pieces beyond this does not significantly affect the objective values. The optimal results from 17 linearisation pieces are shown in Table 2-10.

Table 2-10 Optimum results with Game theory

	School	Hotel	Restaurant	Office	Residential building	Total
EAC (£)	9,408	12,242	10,207	2,669	11,149	45,675
Savings (£)	613	664	593	667	549	3,086
CHP (kWe)	16.0	16.0	0	0	8.0	
Boiler (kW_{th})	8.5	32.0	2.5	2.8	48.7	
Thermal Storage ($kW_{th}h$)	0	108.6	0	0	50.1	

The total EAC is £45,675, the savings are about 17.4% compared to the macrogrid costs of £55,296. Based on the given upper bounds, the total saving through transferring electricity among the five sites is £3,086, which is 6.33% of the total cost. Values of macrogrid EAC_s, upper bound EAC_s^U and optimal EAC_s of each microgrid participant are presented in Figure 2-10. The solution implies that all microgrid participants will benefit in EAC savings by a fair amount.

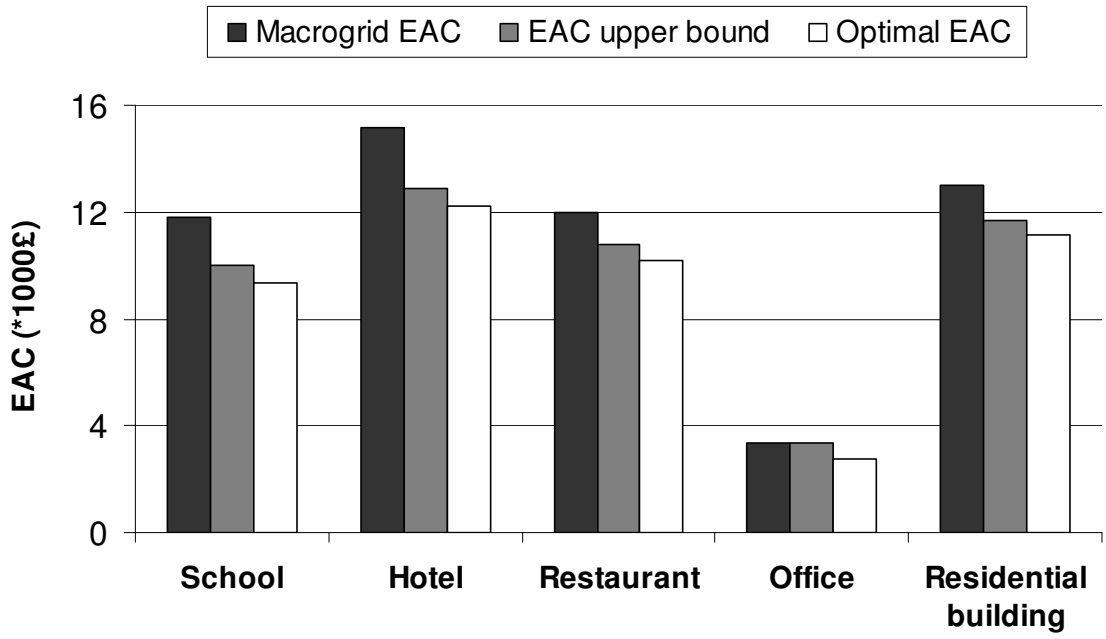

Figure 2-10 EAC values of each microgrid participant

The saving is fairly distributed by selecting appropriate technologies, their capacity, amounts of electricity transferred and transfer price. The electricity transfer prices can be selected from 3 p/kW_eh to 10 p/kW_eh. The optimal transfer prices and amount of electricity transferred during one year are shown in Table 2-11.

Table 2-11 Transfer price between sites and annual transferred amount

Sites	Transfer price (Pence/ kW_eh)	Annual transferred amount (kW_eh)
School, Restaurant	7	2,352
School, Office	3	9,308
School, Residential building	6	5,103
Hotel, Office	3	20,337
Hotel, Residential building	3	1,833
Residential building, School	6	394
Residential building, Restaurant	4	1,314
Residential building, Office	5	644

The optimal result from selecting transfer prices with game theory obtains the objective value of $\hat{\phi}$ as 32.10 and in a CPU time of 10.6*s*. There is no CHP generator selected for office and restaurant. The main reason is that their heat-to-power demand ratios and peak demands are relatively low compared to other sites, so no CHP generators can be selected which could save money. These units receive electricity from school, hotel, residential building or the macrogrid when needed. There is no electricity transferred between hotel and residential building.

To satisfy the annual microgrid electricity demand, 122.6*MWh* electricity is bought from macrogrid, which is 41.4% of the microgrid annual power demand. CHP generators provide 177.3*MWh* electricity to the microgrid, of which 2.6*MWh* electricity is sold to the macrogrid. The total amount of electricity transferred between participants is 41.3*MWh*, which is 13.9% of the total annual demand. Figure 2-11 presents these electricity flows (where 'CHP local site consumption is the electricity generated by a CHP unit while that electricity is consumed at the site where that CHP is located).

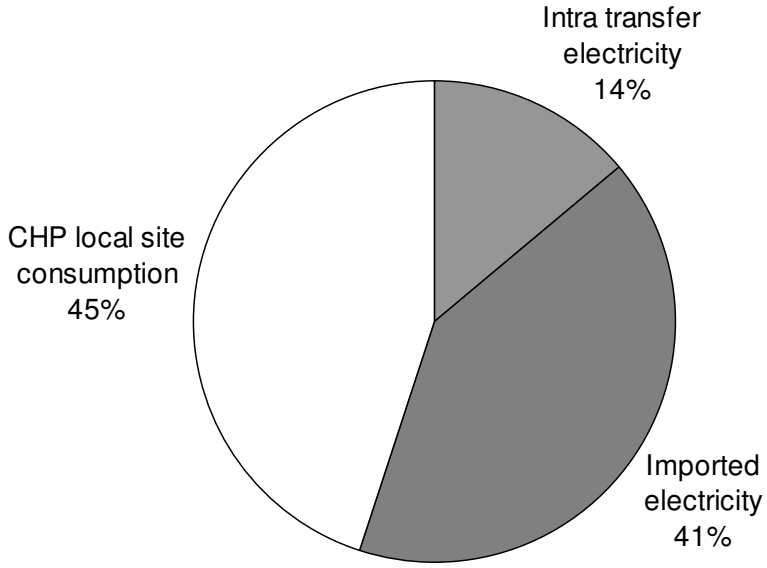

Figure 2-11 Contributions to microgrid electricity demand

Although CO_2 emissions are not considered in the objective function, they are reduced due to CHP utilisation. CO_2 emissions are calculated based on the carbon dioxide emission factors for UK energy use, which are 0.422 $kgCO_2/kWh$ and 0.194 $kgCO_2/kWh$ for electricity and gas respectively [131]. For the macrogrid scenario, the total CO_2 emissions from electricity and gas consumption is 237.4 tonnes, whereas in the microgrid scenario the total CO_2 emissions are 192.2 tonnes. There is 19.0% emission savings by utilising CHP in microgrid. Primary energy resource consumption is calculated from Eq. 2-32 based on UK centralised electricity generation efficiency of 35% [133]. Heat generation is based on an energy efficiency of 82%. Under the macrogrid scenario total primary energy consumption is 1,425MWh, while with microgrid utilisation the primary energy resources consumption is reduced to 1,067MWh, a 25.1% decrease.

Next, we study the scenario where heat dumping is allowed (*i.e.* replacing Eq. 2-11 by Eq. 2-11a). In this case the CHP capacity of the school increases to 21.0 kW_e and no boiler is required. Thermal storage of the residential building decreases slightly to 49.2 $kW_{th}h$. All the other sites have the same capacity selections as shown in Table 2-10. Overall, CHP generators produce 286.7MWh electricity, which is 61.7% more than that from the no heat

dumping scenario. Figure 2-12 presents the contributions to microgrid electricity demand, in total 95% of electricity demand is provided by CHP generators and 44% of electricity demand is fulfilled through intra electricity transfer. There is 3.7*MWh* electricity being sold back to the macrogrid. The total *EAC* of the microgrid is £41,842, which is reduced by 8.4% when compared with the case of not allowing heat waste. However, it results in high heat dumping (212.2 $MW_{th}h$), which is 46.0% of the total heat demand. It should also be noted that the primary energy consumption is 1,110.2*MWh* and CO_2 emissions are 215.5 *tonnes*, representing increase of 4.0% and 12.1%, respectively.

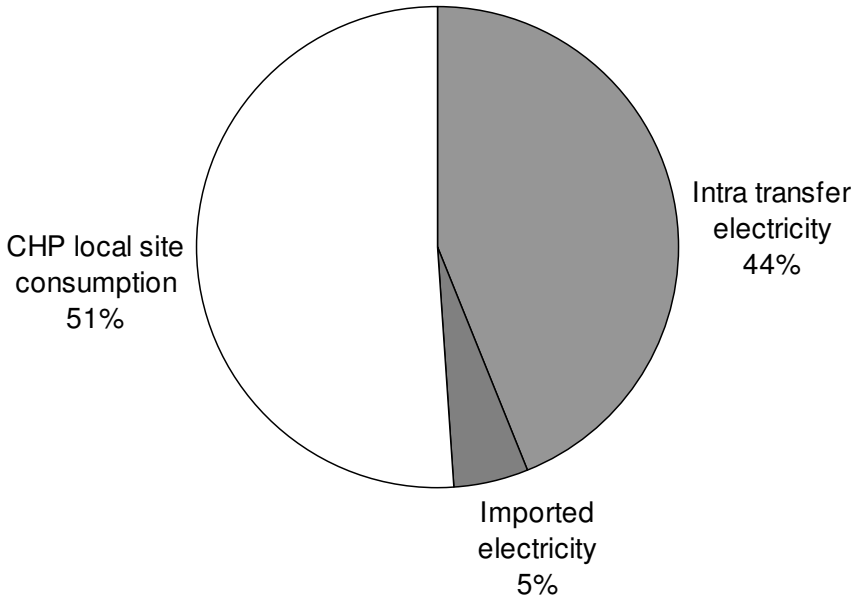

Figure 2-12 Contributions to microgrid electricity demand under heat dumping

2.4.7 Fair Settlement under Peak Demand Charge

Macrogrid electricity consumption peak reduction is also desired to avoid the need for high capacity in the macrogrid-microgrid connection (thus avoiding charges levied by the System Operator for consumption at times of macrogrid peak). One way to achieve this is to increase the grid tariff rate for the high electricity load periods, and therefore motivate consumers to redistribute or reduce their electricity consumption [134]. In order to reflect this within our approach, additional mathematical constraints Eq. 2-34 and Eq. 2-35 have

been introduced. It is assumed that if electricity load from grid (for each time interval) is below a given threshold κ_s, then the normal electricity price will be applied. However, when electricity load from grid is over the threshold value (κ_s), then the surplus amount will be charged at a higher rate. Electricity cost term, EC_s, should be redefined as follows:

$$\xi_{tjs} \geq I_{tjs} - \kappa_s \qquad \forall t, j, s \qquad \textbf{(Eq. 2-34)}$$

$$EC_s = \sum_{t,j} c^I W_t T_j I_{tjs} + \sum_{t,j} (c^{Ip} - c^I) W_t T_j \xi_{tjs} - \sum_{t,j} c^{Ex} W_t T_j E_{tjs} \qquad \forall s \qquad \textbf{(Eq. 2-35)}$$

Below the threshold, the electricity price is still 13 *p/kWh* while the peak demand charge is nearly 50% more expensive (here, 20 *p/kWh*). The electricity threshold load from the grid is set to 5 *kW* for all sites involved. Under this peak charge scheme, the macrogrid scenario costs are higher than that from the constant price case. The game theory Nash approach is applied under the new EAC_s^U values[2]. The corresponding EAC_s values together with capacities selected for CHPs, boilers and thermal storages are given in Table 2-12.

Table 2-12 Peak demand charge scheme with game theory

	School	**Hotel**	**Restaurant**	**Office**	**Residential building**	**Total**
Macrogrid EAC	13,100	17,354	15,309	3,336	14,975	64,074
EAC_s^U (£)	11,135	14,751	13,013	3,336	12,729	54,963
EAC_s (£)	9,578	13,069	11,289	2,413	11,143	47,492
EAC_s savings (£)	1,557	1,682	1,724	923	1,586	7,471
κ_s (kW)	5	5	5	5	5	-
CHP (kW_e)	21.0	21.0	0	0	11.0	-
Boiler(kW_{th})	0	22.6	2.5	2.8	43.1	-
Thermal Storage ($kW_{th}h$)	70.4	70.0	0	0	46.8	-

[2] The upper bounds are still set as 85% macrogrid costs for school and hotel, 90% macrogrid costs for restaurant and residential building, and 100% macrogrid costs for the office.

When there is demand charge for the peak load, the *EAC* values and microgrid operations are quite different compared with those of the 'constant' case (shown in Table 2-10). More specifically, due to the higher upper bounds being used, higher CHP capacities are finally selected for school, hotel and residential building. Overall, the savings achieved are 25.9% when compared with the macrogrid scenario. Figure 2-13 presents the electricity demands of the five sites under the macrogrid and microgrid scenarios when peak demand charge is applied. It should be mentioned that the grey bars represent the annual grid electricity supply within the given threshold $5\,kW$, while the white bars show the annual grid electricity provision over the $5\,kW$ threshold value.

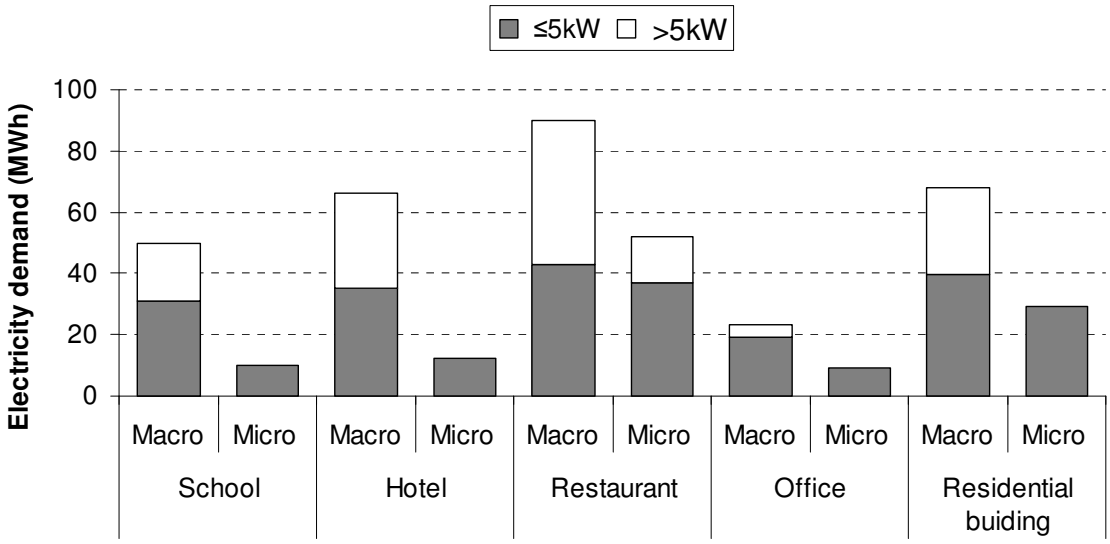

Figure 2-13 Grid electricity supply under macrogrid and microgrid case under peak demand charge

In the macrogrid scenario, all electricity is bought from the grid and the total imported electricity is 297.4*MWh*, while in the microgrid scenario it can be noted that 112.3*MWh* is imported from the grid. This reduction on grid electricity supply is achieved by increased CHP electricity generation within the microgrid thus avoiding or reducing significantly peak demand charge for many sites. More specifically, the annual grid electricity supplies charged at peak price for macrogrid and microgrids scenarios is 129.7*MWh* and 15.0*MWh*, respectively. This indicates that the electricity peak charge scheme will promote the

application of microgrid and increase CHP capacity selection and operation in the microgrid.

2.4.8 Fair Settlement with lower CHP overall efficiency

In this case study presented, the overall efficiency of CHP is considered as 90% according the assumption given in [131]. However, the overall efficiency of CHP is presented as 80% in [65]. In order to analyze the effect of the overall efficiency over the fair settlement of a microgrid, the presented model applied in 2.4.6 is implemented with 80% overall efficiency of CHP while the electrical efficiencies keep the same as given in Table 2-3. The optimal design under this assumption is provided in Table 2-13.

Table 2-13 Optimal design with 80% CHP overall efficiency

	School	**Hotel**	**Restaurant**	**Office**	**Residential building**	**Total**
EAC_s^U (£)	10,021	12,906	10,800	3,336	11,698	48,761
$EAC_{s,q\max}$ (£)	7,841	10,103	7,790	1,520	8,795	36,049
EAC_s (£)	9,439	12,260	10,198	2,730	11,109	45,736
EAC_s savings (£)	582	646	602	606	589	3,025
CHP (kW_e)	16.9	16.0	0	0	11.0	-
Boiler(kW_{th})	12.4	37.5	2.5	2.8	46.9	-
Thermal Storage ($kW_{th}h$)	0	104.8	0	0	49.0	-

Compared with the optimum results presented in Table 2-9 and Table 2-10, the EAC_s^U values keep the same while the lower bounds are higher except office based on this lower CHP overall efficiency. Since the electrical efficiencies keep the same while the heat efficiencies drops, CHP capacities are increased for school, hotel and residential building because of their relative high heat demands. Also boiler capacities of school and hotel are bigger to cover the heat supply loss caused by the lower CHP heat efficiency. However, the total *EAC* savings are almost the same, which is only 2% decrease. Again the *EAC* costs of the five participants are fairly distributed based on the given upper bounds. So the overall

efficiency decrease affects the fair settlement of a microgrid but has minor effect on the *EAC* savings.

2.4.9 Fair Settlement with Alternative CHP Specs

In the proposed model, it assumes that only one CHP technology is available while the capital cost decreases with the capacity size. Without modifying current equations, the model can be applied for selecting from multiple alternative CHP technologies, such as internal combustion engine (ICE), Stirling engine (SE), solid oxide fuel cell (SOFC) and proton exchange membrane fuel cell (PEMFC). The above four different micro-CHP technologies are considered. Basic technical characteristics and specific capital cost of each of these candidate technologies are described in Table 2-14.

Table 2-14 Specifications of CHP candidate technologies [135]

Technology	Range (*kWe*)	Turn-key costs (£/*kWe*)	Electrical efficiency	Heat to power ratio	Lifetime (Year)
SE	5-10	1,980	0.25	2.80	15
PEM	0-5	2,981	0.45	1.11	25
SOFC	0-5	5,520	0.50	0.9	25
ICE	10-50	866	0.40	1.25	15

By replacing the candidate technology with the capacity level, the optimum results are presented in Table 2-15.With candidate CHP technologies, ICEs are selected for school, hotel and residential building because of its low capital cost among others. PEM is assigned to restaurant as it is cheaper than SOFC within the same capacity range. Although PEM is expensive, it is still beneficial than buying electricity from other participants and macrogrid and generating heat solely from its own boiler. Since ICE has much lower capital cost than given in Table 2-3, *EAC* savings are much higher while they are still fairly distributed. More candidate CHP technologies or technologies with more capacity ranges can be easily added to the model.

Table 2-15 Optimal design with candidate CHP technologies

	School	Hotel	Restaurant	Office	Residential building	Total
EAC_s^U (£)	10,021	12,906	10,800	3,336	11,698	48,761
$EAC_{s,q\max}$ (£)	4,969	6,668	4,613	1,495	6,408	24,153
EAC_s (£)	7,724	10,826	8,738	1,495	9,576	38,359
EAC_s savings (£)	2,297	2,080	2,062	1,841	2,122	10,402
CHP (kW_e)	ICE 14.4	ICE 20.0	PEM 0.6	-	ICE 16.1	-
Boiler(kW_{th})	24.1	40.7	1.6	2.8	47.2	-
Thermal Storage ($kW_{th}h$)	0	117.8	1.12	0	33.8	-

2.5 Conclusions

An MINLP model has been developed to provide a fair settlement system among microgrid participants with the Game theory Nash approach. It has been solved in MILP form based on a separable programming approach. The costs of all participants are minimised by determining the fair intra-microgrid electricity transfer price, flow of electricity between sites, unit capacities and unit commitment.

The proposed model has been implemented on a case study with five local sites: a school, a hotel, a restaurant, an office building and a residential building. Total *EAC* savings as a function of gas price, electricity buying and selling price is analysed and total *EAC* savings is heavily dependent on gas price and electricity selling price. Electricity selling price influences on the total *EAC* savings with minor effect because heat cannot be transferred to other participants and thermal sinks except its own thermal storage. The result of the case study has indicated that the method proposed provides a promising approach to microgrid planning with fairly distributed benefits. The participants' cooperative action provides better economic outcome for the microgrid, with 17.4% savings compared with the 'no microgrid' case. Also, the costs of installing a microgrid have been fairly distributed among participants. CHP has been selected in the case study for three microgrid participants, and

these systems provide the majority of the microgrid's electricity needs. Furthermore, CO_2 emissions and primary energy consumption has been decreased by 19% and 25% respectively through CHP utilisation. While a peak demand charge scheme is included, CHP capacity in the microgrid has been increased and microgrid is promoted. CHP technologies play an important role in promoting microgrid and primary energy saving because of their high efficiency. However, their high capital costs are obstacles to be adopted by participants with relative low energy demands.

When there are more participants in the microgrid, the total and individual savings could be increased, but this depends on the energy consumption patterns of the participants in the microgrid group. There would be more benefits if the energy consumption patterns (heat-to-power ratio) and peak hours of each participant are very different from each other. And the participants can obtain higher income by selling electricity to other participants than selling to the grid. Game theory provides the necessary tool to carry out the fair settlement among participants, although the total saving in the fairly distributed case could be smaller.

Chapter 3 Optimal Energy Consumption Scheduling and Operation Management of Smart Homes Microgrid

In the previous chapter, optimal microgrid design and operation are obtained for the fair cost distribution amongst participants in a microgrid over long term consideration. In this chapter, it addressed the scheduling and overall management of smart homes with a common microgrid over short term under given microgrid design. Most energy-consuming household tasks are not enforced to be performed at specific times but rather within a preferred time period. If these flexible tasks can be coordinated among multiple homes so that they do not all occur at the same time yet still satisfy customers' requirements, the energy cost and power peak demand could be reduced.

In this chapter, we aim to develop an MILP model to minimise the total one-day-ahead expense of a smart building's energy consumption, including operation and energy costs. Both electricity load and DERs operation are scheduled. Peak demand charge scheme is also adopted to reduce the peak demand from grid.

3.1 Introduction and Literature Review

In this section, work related to operation planning of microgrids and energy consumption in smart buildings is reviewed.

3.1.1 Operation Planning in Microgrid

As mentioned in Chapter 2, the optimal planning of microgrids has attracted much attention over the last few years. Besides the microgrid design, microgrid operation planning over the short term is another branch addressed by many researchers. Bagherian and Tafreshi [136] present energy management systems and optimal scheduling of microgrid. The optimal decisions, including the use of generators for power and heat production, storage system scheduling, proper load management and local grid power selling and purchasing for next day, are determined by maximising the profit. A generalised formulation to determine the optimal strategy and cost optimisation scheme for a microgrid is shown in

[137], accounting for emission cost, start-up costs, operation cost and maintenance costs. Optimal economic operation scheduling of a microgrid in an isolated load area is obtained by MILP model in [138], and a Virtual Power Producer (VPP) is used to operate the generation units optimally and the methodology is applied to a real microgrid case study. A short-term DER management methodology in smart grids is presented by [139], which involves as short as five minutes ahead scheduling and the previously obtained schedule is rescheduled accordingly. GA approach is used for optimisation. Obara et al. [140] investigate the operational planning of an independent microgrid with tidal power generators, solid oxide fuel cells (SOFCs) and PV. That microgrid supplies heat and electricity to the surrounding towns and harbour facilities. A probabilistic energy management system is proposed by Mohammadi et al. [141] to optimise the operation of the microgrid based on an efficient Point Estimate Method. The authors in [142] propose an intelligent energy management system to optimise the operation of DERs in a CHP-based microgrid over a 24-hour time interval with a modified bacterial foraging optimisation algorithm. Both operation cost and emissions are minimised. Local energy management is provided by [143] for a building integrated microgrid, which considers grid time-of-use tariffs, grid access limits, storage capacity, load and PV power shedding. An optimal operation of a CHP-based microgrid is presented in the work of [144], where DER resource scheduling with demand response programs over a day-head period is determined by minimising the total cost and emissions. Baziar and Kavousi-Fard [145] investigate the optimal operation management of DER in a renewable microgrid for a 24-hour time interval, and it considers the uncertainties from load demand forecasting error, grid bid changes and non-dispatchable generator output power variations. Marzband et al. [146] propose an operational architecture for real time operation of an islanded microgrid, and day ahead scheduling and real time scheduling are both considered. Chaotic quantum genetic algorithm is applied for the environmental economic dispatch problem for DERs in a smart microgrid [147]. Operation planning of an independent microgrid is obtained from the genetic algorithm, where solar cell, heat pumps, fuel cells and water electrolysers are applied. An MILP framework is presented for the energy production planning problem to minimise the total cost, and heat interchange within subgroups of overall microgrid is also proposed in [148].

3.1.2 Energy Consumption in Smart Buildings

The energy consumption by buildings represents 30-40% of the world's primary energy consumption [149], and the proportion of energy use in building is 39% in the UK [150]. Smart planning of energy supply to buildings is important to conserve energy and protect the environment. Basic actions to improve energy efficiency in commercial buildings in operation are presented in [151]. Domestic energy consumption depends on the dwelling physical properties, such as location, design and construction, as well as appliances' efficiency and occupants' behaviour. By changing the living behaviour itself, there can be 10-30% energy consumption reduction [152]. More importantly, the liberalisation of electricity markets results in electricity hourly or half-hourly prices and real-time electricity prices encourage consumers to get involved in searching for optimal power consumption patterns to reduce their energy costs [153].

The work of this chapter considers a smart residential building with its own microgrid, DER and automation system. Smart building is becoming more attractive and viable in the building industry while meeting both desires of comfort and energy savings. The idea of the smart home originated from the concept of home automation, which provides some common benefits to the end users, including lower energy costs, provision of comfort, security and home-based health care and assistance to elderly or disabled users [154]. Smart homes with automation operations are becoming capable along with the technology development, where heating or lighting can be controlled according to the presence of customers [155]. PSO algorithm is applied to the load balancing problem in smart homes in [77], where the optimal distribution of energy resources is determined by an adapted version of the Binary PSO. A method based on LP techniques is proposed for economic evaluation of microgrids from the consumer's point of view in [156]. Operation of distributed generators and energy storage systems are optimised and power interruption costs together with additional expenses to construct the microgrid itself are involved. Some work has also been done to achieve the energy conservation and management perspectives. A multi-agent system for energy resource scheduling of an islanded power system with microgrid is proposed by [157], with an objective to manage the resources efficiently and obtain the minimum operation cost while satisfying the internal demand. A dynamic

decision model is presented in [158] to optimise energy flows in a green building with a hybrid energy system, which involves different renewable energy sources. A fuzzy controller is developed and the Human Machine Interface (HMI) is integrated with building energy management systems to improve the indoor environmental conditions with minimum energy needs [159]. While in [160], an MILP model is developed for scheduling operations in microgrids connected to the national grid to analyse potential policies. A linear diversity constraint is introduced to maintain diversity in the generation of electricity from multiple resources on the production schedule. An energy management and warning system for resident has been proposed for energy saving in [161], which monitors the power usage and warns the users when the power usage is getting close to the monthly prescribed energy usage levels. The electric power dispatch optimisation problem is solved by the genetic algorithm approach by [162], the proposed model determines the optimum operation of a microgrid for residential application under environmental and economic concerns. However, these scheduling optimisation models only consider operation scheduling based on given energy profile rather than scheduling the energy demand.

Scheduling tasks subject to limited resources is a well known problem in many areas of the process industry and other fields, but there are differences when considering the scheduling of electrical appliances. Different time representations and mathematical models for process scheduling problems are summarised in [163]. Four time representations are presented with strengthened formulations which are compared in different scheduling problems. While short-term and medium-term scheduling of a large-scale industrial continuous plant is addressed in [164]. A systematic framework is proposed there and applied to an industrial continuous plant to utilise the main units efficiently. Maravelias and Sung [165] review the integration of production planning and scheduling, while key concepts and advantages/disadvantages of different modelling methods are presented. Sun and Huang [166] reviewed energy optimisation methods for energy management in smart homes, such as fuzzy logic, neural networks and evolutionary approaches. Hybrid intelligent control systems for generating control rules is recommended for further study and works considering scheduling of appliance operation time are also included. An MILP based smart residential appliance scheduling framework is proposed in [167], where

electricity is solely bought from grid and the tariff is known 24 hours in advance. Another work for scheduling the operation of smart appliances is presented by [168], where the savings from energy is maximised by shifting domestic loads with real-time pricing. A peak-load shaving online scheduling framework is proposed by [169], and the power consumption scheduling is developed in a systematic manner by introducing a generic appliance model.

Scheduling of both energy generation and loads has been studied for single smart home in recent work. The operation of an electrical demand-side management system is presented by [170], where deferrable and no-deferrable tasks commanded by the user are scheduled for one day of a house with PV generation. Kriett and Salani [171] propose a generic MILP model to minimise the operating cost of both electrical and thermal supply and demand in a residential microgrid. A home energy comfort management system is designed by [172], which helps end users to control and manage residential energy and enable the users to set savings goals. The authors of [173] propose an energy management system based on action dependent heuristic dynamic programming in a smart home. Muratori et al. [174] present a model to simulate the electricity demand of a single household, and total consumption from cold appliances, heating, ventilation, air condition and other activities is considered. A real-time price-based demand response management application is presented by [175] for residential appliances in a single house to determine the optimal operation in the next 5-minute time interval by considering future electricity price uncertainties, stochastic optimisation and robust optimisation approaches have been applied. An optimal and automatic residential load commitment framework is proposed by [176] to minimise household payment, which determines on/off status of appliances, charging/discharging of battery storage and plug-in hybrid electric vehicles. Derin and Ferrante [177] develop a model that considers both operation scheduling and electricity consumption tasks order scheduling. But their results indicate relatively high computation time, over 35 minutes, to schedule only three electricity consumption tasks. And Finn et al. [178] investigate the demand side management when renewable energy is applied by shifting the timing of a domestic dishwasher electrical demand in response to pricing and wind availability.

This chapter extends the scope of single smart home energy management by considering a smart building composed of multiple smart homes. An MILP model is proposed to minimise the total one-day-ahead expense of a smart building's energy consumption, including operation and energy costs. Both the operations of the DERs and the domestic appliances with their specific energy consumption profiles are scheduled. The scheduling is based on real-time electricity prices at each time interval, renewable energy output forecast, subject to the constraints at the earliest starting time and latest ending time for each appliance provided by the consumers. Peak demand charge scheme is also applied to reduce the peak electricity demand from grid.

3.2 Problem Description

In this work, a smart building with a number of smart homes is considered. Example of such smart building is shown in Figure 3-1.

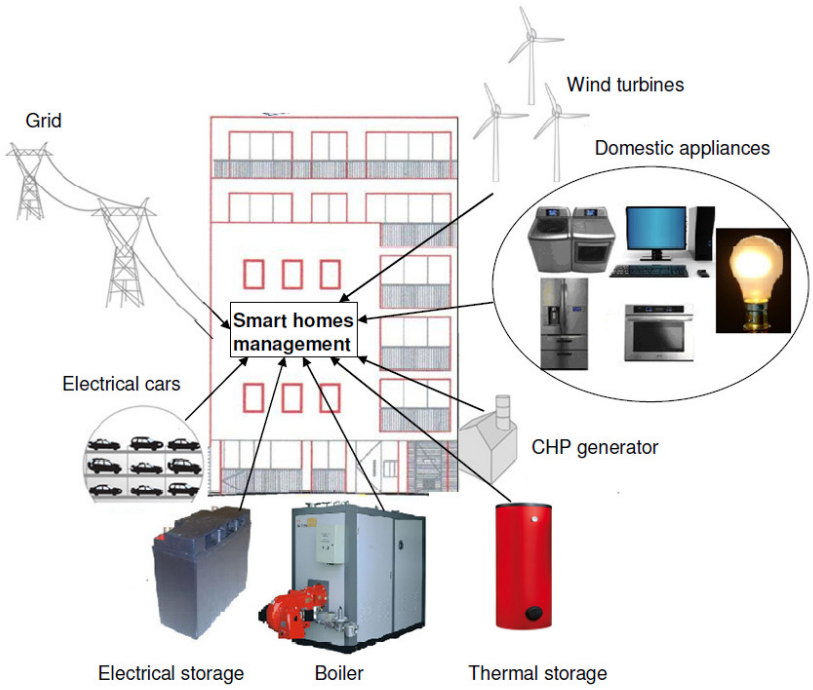

Figure 3-1 Example of smart building

It is assumed to have its own microgrid to provide energy locally, which includes some DERs, such as CHP generator, boiler, wind generator, thermal storage and electrical storage. All homes in the building share common microgrid DERs. It also has a grid connection to obtain electricity during power demand peak hours or sell electricity to the grid when there is surplus electricity generation. The building is assumed to have an energy management system, local controllers for each DER and communication system to distribute the energy consumption scheme. Since the model presented in this work only provides the optimal scheduling for one day, equipment capacity selection is not considered here, and all the equipment capacities are given. The real-time electricity price profile from the grid is known and varies within a day. Peak demand charge for the over consumed electricity from the grid is given. It is also assumed that weather forecast can provide 24 hour wind speed data. Heat demand of the whole building is given while the electricity demand depends on the operation of domestic appliances.

Generally, each home has a number of domestic appliances, such as dishwasher, washing machine and oven. They are flexible under different time window, earliest starting time and latest finishing time, such as shown in Table 3-1. If their operations can be scheduled based on their time windows, both energy cost and peak demand from grid can be reduced.

Table 3-1 Electricity consumption for different electrical tasks [179]

Task	Power (kW)	Earliest starting time (hour)	Latest finishing time (hour)	Time window length (hour)	Duration (hour)
Dishwasher	-	9	17	8	2
Washing machine	-	9	12	3	1.5
Spin dryer	2.5	13	18	5	1
Cooker hob	3	8	9	1	0.5
Cooker oven	5	18	19	1	0.5
Microwave	1.7	8	9	1	0.5
Interior lighting	0.84	18	24	6	6
Laptop	0.1	18	24	6	2
Desktop	0.3	18	24	6	3
Vacuum cleaner	1.2	9	17	8	0.5
Fridge	0.3	0	24	-	24
Electrical car	3.5	18	8	14	3

The overall problem can be stated as follows:

Given (a) a time horizon split into a number of equal intervals, (b) heat demand of the whole building, (c) equipment capacities, (d) efficiencies of technologies, (e) maintenance cost of all equipment, (f) heat-to-power ratio of CHP generator, (g) charge and discharge limit rates for thermal/electrical storage, (h) gas price, real-time electricity prices from grid and peak demand charge price for any over-threshold amount, (i) peak demand threshold from grid, (j) wind speed, (k) earliest starting and latest finishing times, (l) task capacity profiles, (m) task duration.

Determine (a) energy production plan, (b) task starting time, (c) thermal/electrical storage plan, (d) electricity bought from grid, (e) electricity sold to grid.

So as to minimise daily operation and energy cost.

3.3 Mathematical Formulation

The smart homes power consumption scheduling problem is formulated as an MILP model. The daily power consumption tasks are scheduled based on their given operation time windows, which is defined as the time period between the earliest starting time and latest finishing time of each task. The objective is to minimise the daily power cost and reduce the power consumption peak from grid. The time domain is modelled in a discrete form with intervals of equal length. The key model decision variables include equipment operation, resources utilised and task starting time. These are determined by minimising the daily energy and operation cost of all homes subject to equipment capacity constraints, energy demand constraints, electrical/thermal storage constraints and task operation time window.

3.3.1 Nomenclature

The notation used in the MILP model is given below, the superscript is used to indicate equipment and the subscript is used for indices:

Indices

i task

j home in the smart building

t time interval

θ task operation period

Parameters

A wind generator blade area (m^2)

c^E cost per unit input (maintenance) for electrical storage unit (£/kWh_e)

c_t^I electricity buying price from grid at time interval t (£/kWh_e)

c^W wind generator maintenance cost (£/kWh_e)

C_i constant power consumption capacity of task i (kW_e)

$C_{i\theta}$ power consumption capacity of task i at operation period θ (kW_e)

C^B boiler capacity (kW_{th})

C^C CHP generator capacity (kW_e)

C^E electrical storage capacity (kWh_e)

C^T thermal storage capacity (kWh_{th})

C^W wind generator capacity (kW_e)

D^E electrical storage discharge limit (kW_e)

G^E electrical storage charge limit (kW_e)

H_t heat demand at time interval t (kW_{th})

p difference between peak and base electricity demand price from grid (£/kWh_e)

P_{ji} processing time of task i of home j

Q CHP heat-to-power ratio

T_{ji}^F latest finishing time of task i of home j

T_{ji}^S earliest starting time of task i of home j

v_t wind speed at time interval t (m/s)

V^{nom} nominal wind speed (m/s)

V^{cut-in} cut-in wind speed (m/s)

$V^{cut-out}$ cut-out wind speed (m/s)

w_t output from wind generator at time interval t (kW_e)

δ time interval duration ($hour$)

ρ air density (kg/m^3)

η^C CHP generator electrical efficiency

η^E electrical storage charge/discharge efficiency

η^W wind generator power coefficient

κ agreed electricity peak demand threshold from grid (kW_e)

Variables

E_t electricity exported to the grid at time interval t (kW_e)

f_t thermal storage discharge rate at time interval t (kW_{th})

g_t thermal storage charge rate at time interval t (kW_{th})

I_t electricity imported from the grid at time interval t (kW_e)

S^{IE} initial state of electrical storage (kWh_e)

S^{IT} initial state of thermal storage (kWh_{th})

S_t^E electricity in storage at time interval t (kWh_e)

S_t^T heat in storage at time interval t (kWh_{th})

u_t electricity output from CHP generator at time interval t (kW_e)

x_t heat output from boiler at time interval t (kW_{th})

y_t electrical storage discharge rate at time interval t (kW_e)

z_t electrical storage charge rate at time interval t (kW_e)

ϕ daily electricity cost of a home (£)

ξ_t extra electricity load from grid over the agreed threshold κ at time interal t (kW_e)

Binary Variables

X_{jit} 1 if task i of home j starts at time interval t, 0 otherwise

3.3.2 Capacity Constraints

The output from each equipment should not exceed its designed capacity,

CHP generator:

$$u_t \le C^C \qquad \forall t \qquad \textbf{Eq. 3-1}$$

Boiler:

$$x_t \le C^B \qquad \forall t \qquad \textbf{Eq. 3-2}$$

Electrical storage:

$$S_t^E \le C^E \qquad \forall t \qquad \textbf{Eq. 3-3}$$

Thermal storage:

$$S_t^T \le C^T \qquad \forall t \qquad \textbf{Eq. 3-4}$$

3.3.3 Energy Storage Constraints

Electricity stored in the electrical storage at time t is equal to the amount stored at t –1 plus the electricity charged minus the electricity discharged. Electricity would be lost during the charging and discharging process, for example during any period when amount of electricity δz_t is sent to the electrical storage, only $\delta \eta^E z_t$ will be charged, and the rest being lost, where η^E is turn-around efficiency of electrical storage. Meanwhile, during the discharging process, in order to send δy_t of electricity to the user, $\delta y_t / \eta^E$ of electricity is needed.

$$S_t^E = S_{t-1}^E + \delta \eta^E z_t - \delta y_t / \eta^E \qquad \forall t \qquad \textbf{Eq. 3-5}$$

The electrical storage has an initial storage state at the beginning of each sample day. At the end of each day, the electrical storage must return to its initial value, so as to avoid net accumulation. The initial storage state value is optimised through the model to decide the best initial state for one day utilisation. Otherwise, the initial state can be obtained from the previous day and at the end of the day, the electrical storage must return to be over certain lower limit to protect the equipment.

$$S_0^E = S_T^E = S^{IE} \qquad \textbf{Eq. 3-6}$$

The rates of discharge or charge of electricity cannot exceed the electrical storage discharge and charge limits defined by the battery manufacturer, in order to prevent excessive discharge/charge rates that would damage the battery or reduce its capacity:

$$y_t \le D^E \qquad \forall t \qquad \textbf{Eq. 3-7}$$

$$z_t \le C^E \qquad \forall t \qquad \textbf{Eq. 3-8}$$

Heat stored in the thermal storage at time t is equal to the amount stored at $t-1$ plus the heat charged minus the heat discharged. The heat loss during the heat storage process is represented in the same way as shown for the electrical storage.

$$S_t^T = S_{t-1}^T + \delta\eta^T g_t - \delta f_t / \eta^T \qquad \forall t \qquad \textbf{Eq. 3-9}$$

Stored heat must return to the initial state at the end of the day so that no heat is accumulated over one day. The initial storage state value is also optimised through the model.

$$S_0^T = S_T^T = S^{IT} \qquad \textbf{Eq. 3-10}$$

The rates of discharge and charge of heat cannot exceed the thermal storage discharge and charge limits based on the type of storage medium, mass and latent heat of the material:

$$f_t \le D^T \qquad \forall t \qquad \textbf{Eq. 3-11}$$

$$g_t \le G^T \qquad \forall t \qquad \textbf{Eq. 3-12}$$

3.3.4 Wind Generator Output

The electricity output from the wind generators is calculated from the wind power generation equation, based on the wind blade area, wind speed and wind generator efficiency. The power output is constrained by both cut-in speed and cut-out speed in the model. The cut-in speed is the minimum wind speed at which the wind turbine will generate its designated rated power. While the cut-out speed is wind speed at which the wind generator would be shut down for the safety reasons in order to protect the wind turbine from damage [180].

$$w_t = \begin{cases} 0.5\rho A\eta^W \min(v_t, V^{nom})^3 & \forall t:\ V^{cut-in} \le v_t \le V^{cut-out} \\ 0 & \forall t:\ v_t \le V^{cut-in} \quad and \quad v_t \ge V^{cut-out} \end{cases} \qquad \textbf{Eq. 3-13}$$

3.3.5 Energy Balances

In each time interval, the total electricity consumption is the sum of the power consumption capacities from all tasks of all homes. The electricity consumed during each time period is supplied by the wind generator, CHP generator, electricity received from the electrical storage and grid, minus electricity sent to the electrical storage and grid. If the power consumption capacity of task *i* is constant, then the electricity balance can be represented as Eq. 3-14. But the power consumption capacity of some tasks varies over the operation time intervals, e.g. washing machine has different capacity profiles over washing and spinning processes. Eq. 3-14a is more appropriate for such case, in which the electricity consumption is summed over the task operation periods θ.

$$\sum_j \sum_i C_i X_{jit} = w_t + u_t + y_t + I_t - z_t - R_t \qquad \forall t \qquad \textbf{Eq. 3-14}$$

$$\sum_j \sum_i \sum_{\theta=0}^{P_{ji}-1} C_{i\theta} X_{ji,t-\theta} = w_t + u_t + y_t + I_t - z_t - E_t \qquad \forall t \qquad \textbf{Eq. 3-14a}$$

The heat consumed during each time period is equal to heat supplied by the CHP generator, boiler, heat received from the thermal storage, minus heat sent to the thermal storage.

$$H_t = Qu_t + x_t + f_t - g_t \qquad \forall t \qquad \textbf{Eq. 3-15}$$

3.3.6 Starting Time and Finishing Time

The operation time of each task must be within the given time window. The starting time of each task cannot be earlier than the given earliest starting time, and must finish before the latest finishing time. For each task from each home, it has to be started once.

$$\sum_{T_{ji}^S \le t \le T_{ji}^F - P_{ji}} X_{jit} = 1 \qquad \forall j,i \qquad \textbf{Eq. 3-16}$$

3.3.7 Peak Demand Charge

There is also a desire to reduce the electricity peak demand from the grid to avoid the need for high capacity in the macrogrid-microgrid connection (and to avoid charges levied by the System Operator for consumption at times of macrogrid peak). One way to achieve this is to increase the grid tariff rate for the high electricity load periods, and thus motivating consumers to redistribute or reduce their electricity consumption [134]. In order to reflect this, in our approach, an extra constraint, Eq. 3-17, is introduced in the model. For each time interval, when electricity load from grid is below the agreed threshold κ, the normal electricity price is applied. But when electricity load from grid is over the agreed threshold κ, the additional amount, γ_t over threshold value, is charged with an extra rate.

$$\xi_t \geq I_t - \kappa \qquad \forall t \qquad \textbf{Eq. 3-17}$$

3.3.8 Objective Function

The objective function is to minimise the total daily electricity cost, which includes: the operation and maintenance cost of the CHP generator, wind generator, boiler, electrical storage and thermal storage; the cost of electricity purchased from the grid; the revenue from electricity sold to the grid. Since the equipment capacities are fixed, their capital costs are independent of the schedule and are therefore not considered. If only the real-time pricing is applied, the total cost is calculated as in Eq. 3-18a.

$$\phi = \sum_t \delta w u_t / \eta^C \quad \text{CHP operation cost}$$

$$+ \sum_t \delta c^W w_t \quad \text{wind turbine maintenance cost}$$

$$+ \sum_t \delta c^N x_t / \eta^B \quad \text{boiler operation cost}$$

$$+ \sum_t \delta c^E y_t \quad \text{electrical storage maintenance cost} \qquad \textbf{Eq. 3-18a}$$

$$+ \sum_t \delta c^T f_t \quad \text{thermal storage maintenance cost}$$

$$+ \sum_t \delta c_t^I I_t \quad \text{electricity buying cost from grid}$$

$$- \sum_t \delta c^{Ex} R_t \quad \text{revenue from electricity selling to grid}$$

When peak demand charge scheme is applied, the total daily cost is calculated as in Eq. 3-18b. Below the threshold, the electricity price follows the real-time electricity price but when the demand is over the threshold extra cost is assigned to the additional electricity amount.

$$\phi = \sum_t \delta m u_t / \eta^C \quad \text{CHP operation cost}$$

$$+ \sum_t \delta c^W w_t \quad \text{wind turbine maintenance cost}$$

$$+ \sum_t \delta c^N x_t / \eta^B \quad \text{boiler operation cost}$$

$$+ \sum_t \delta c^E y_t \quad \text{electrical storage maintenance cost} \qquad \textbf{Eq. 3-18b}$$

$$+ \sum_t \delta c^T f_t \quad \text{thermal storage maintenance cost}$$

$$+ \sum_t \delta c_t^I I_t \quad \text{electricity buying cost from grid}$$

$$+ \sum_t \delta p \gamma_t \quad \text{peak demand extra charge from grid}$$

$$- \sum_t \delta c^{Ex} R_t \quad \text{revenue from electricity selling to grid}$$

3.4 Illustrative Examples

In this work, the proposed MILP model for energy consumption scheduling is applied to two numerical examples: (i) a smart building of 30 homes with same living habits and (ii) a smart building of 90 homes with different living habits.

3.4.1 Example 1: Smart Building of 30 Homes with Same Living Habits

Example 1 considers a smart building system with 30 homes with the following DERs, and their capacities are obtained according to the total energy demand while the technical parameters and costs are obtained from [65].

- one CHP generator with a capacity of 20 kW_e and electrical efficiency of 35%. Heat to power ratio is assumed to be equal to 1.3, and natural gas cost is 2.7 *p/kWh*;
- one wind farm with a capacity of 10 kW_e and a maintenance cost of 0.5 p/kWh_e;
- one boiler with capacity of 120 kW_{th} and natural gas cost is 2.7 *p/kWh*;
- one electrical storage unit with a capacity of 10 kW_eh, charge/discharge efficiency of 95%, discharge limit and charge limit are both 10 kW_e, and the maintenance cost is 0.5 p/kWh_e;
- one thermal storage unit with a capacity of 20 $kW_{th}h$; charge/discharge efficiency of 98%, discharge limit and charge limit are both 20 kW_{th}, and the maintenance cost is 0.1 p/kWh_{th};
- a grid connection (allowing import and export of electricity when operating parallel to grid); the real-time electricity price at different times is collected from Balancing Mechanism Reporting System [181] as shown in Figure 3-2. When electricity demand from grid is over 30 kW_e, an extra cost of 5 p/kWh_e is charged to the additional electricity. Electricity may also be sold to the grid with 1 p/kWh_e;

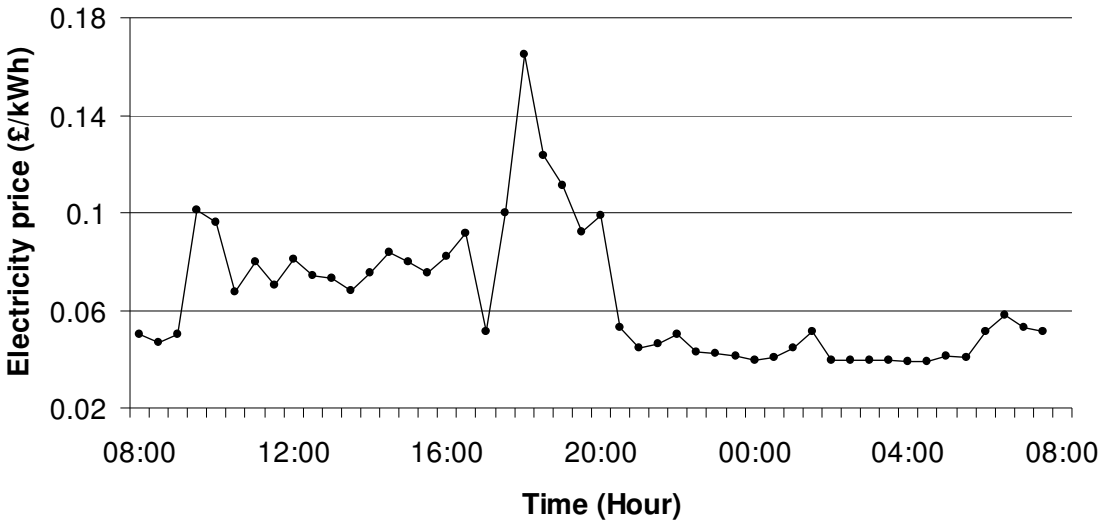

Figure 3-2 Electricity tariff (3rd March, 2011) [181]

Each time interval considered is half an hour. So, there are 48 time intervals in total for a single day. The total heat demand profile is generated for a building with floor area of

2,500m^2 on a sample winter day using CHP Sizer Version 2 Software [182]. For the electricity demand, each home has 12 basic tasks that consume electricity as shown in Table 3-1. These tasks are available to be scheduled according to the given earliest starting time, latest finishing time, their respective duration and power requirements [179]. All tasks, except the dishwasher and washing machine, have constant power consumption rates given in the table. The electrical profiles for dish washer and washing machine are shown in Figure 3-3. Also it is assumed that all homes have the same living habits and every task has to be performed once a day.

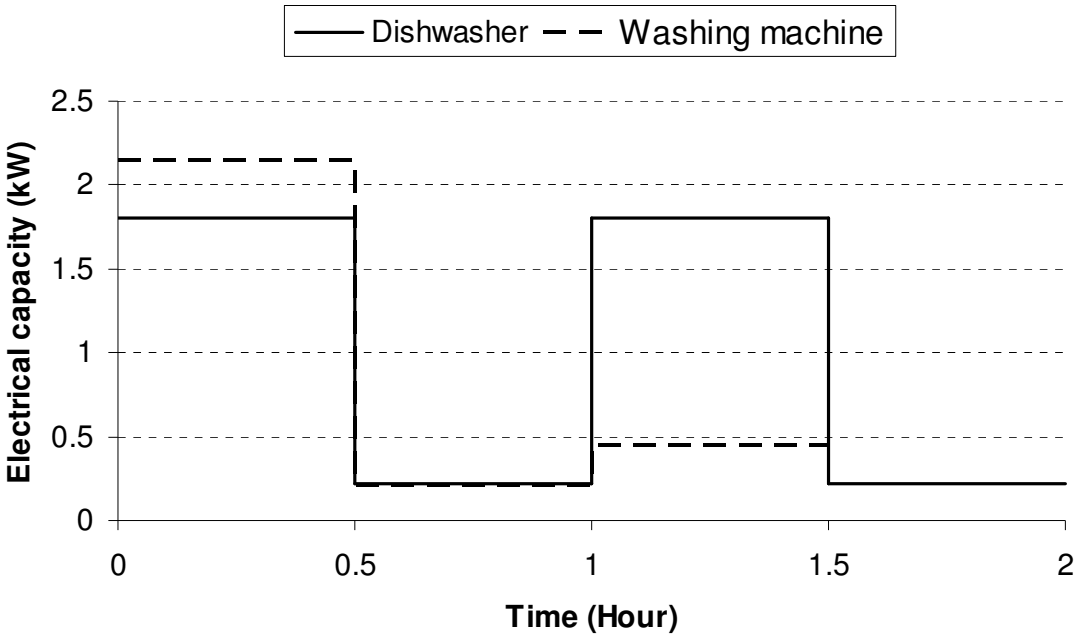

Figure 3-3 Electricity utilisation profiles of dishwasher and washing machine

There are 10 identical wind generators in the wind farm, with a power coefficient of 45% [180]. The blade diameter is 1.6 *m* and the wind speed is generated from a Weibull distribution using MATLAB with a mean velocity of 7 *m/s*. The cut-in and cut-out wind speeds are assumed to be 5 *m/s* and 25 *m/s*, respectively, and the nominal wind speed is taken as 12 *m/s*. The wind generators do not produce any power when the wind speed is under the cut-in speed or above the cut-out speed. When the wind speed is above the nominal wind speed, the power output is at the maximum output, which is equal to the

output produced at the nominal wind speed. Between cut-in and cut-out nominal wind speed, the wind generator power output varies according to Eq. 3-13.

3.4.2 Example 2: Smart Building of 90 Homes with Different Living Habits

Example 2 considers a smart building with 90 homes and it has the same distributed energy resources as those in Example 1, but with tripled equipment capacities, and heat demand and peak demand threshold from grid are also tripled. There are still 12 electrical tasks for each home, and task processing duration, time window length and power consumption rate are the same as those in Example 1. The main difference is that the 90 homes have different living habits. The earliest starting time for each task of each home is generated randomly based on the modified hourly operation probability distribution as given in [183]. Only the operation hours with a probability higher than 5% are selected and then the hourly operation possibility is redistributed accordingly. The modified earliest starting time hourly probability distribution for the 12 electrical consumption tasks is presented in Figure 3-4, where y axis represents the probability percentage. Some tasks have the same hourly probability distribution, so only one distribution plot is presented for each type of tasks.

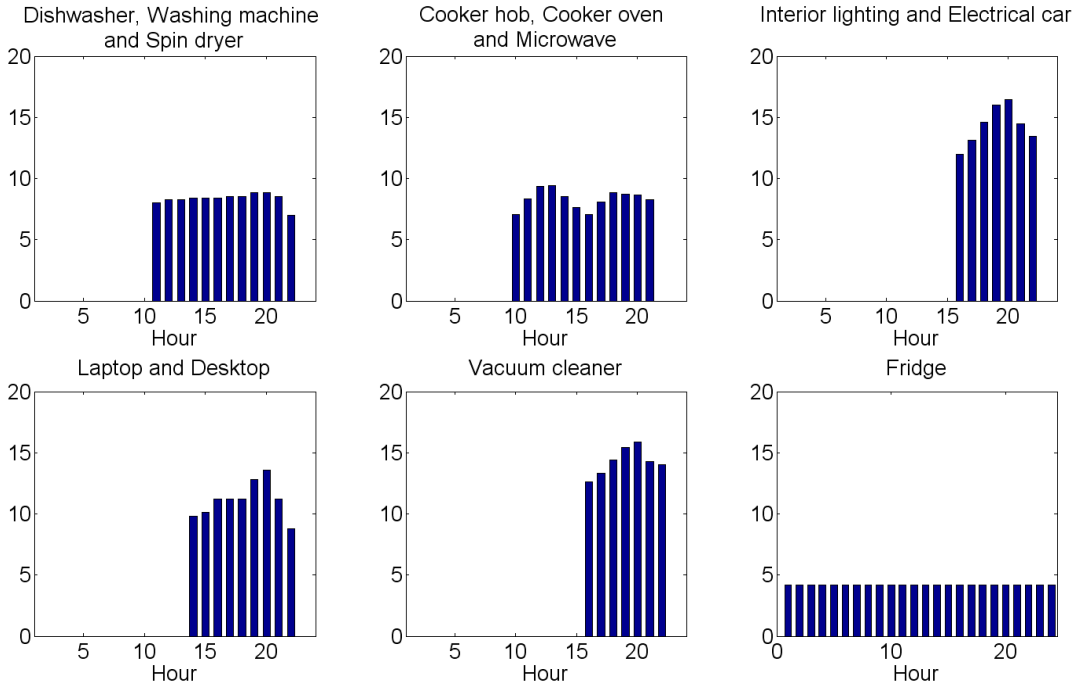

Figure 3-4 Earliest starting time hourly probability distribution for electrical consumption tasks [183]

3.5 Computational Results

Two pricing schemes have been applied for both examples above, which are real-time price scheme and peak demand price schemes. For the real-time price scheme, the objective is to minimise the total daily cost under real-time electricity prices as shown in Eq. 3-18a, subject to Eq. 3-1 to 3-13, Eq. 3-14a to 16. While for the peak demand price scheme, the objective is to minimise the total daily cost together with the extra cost charged for over consumed electricity from the grid as described by Eq. 3-18b, subject to Eq. 3-1 to 3-13, 3-14a to 3-17.

For each pricing scheme, four scenarios are considered, which are (a) macrogrid earliest starting time, (b) macrogrid optimised scheduling, (c) microgrid earliest starting time and (d) microgrid optimised scheduling. Abbreviations are used to indicate the combinations of

pricing scheme and scenario, e.g. RMO[3] is short for real-time price scheme macrogrid optimised scheduling scenario while PmE represents peak demand price scheme microgrid earliest starting time scenario.

In the macrogrid scenarios (a, b), electricity is solely bought from grid and heat is produced only by boiler. There is no other DER to provide electricity or heat to the building. For the microgrid scenarios (c, d), DERs are available to provide local electricity and heat. The earliest starting scenario (a scheduling heuristic) means all the domestic electricity appliances are turned on at their given earliest starting time, which is similar to common living habits. For example, the washing machine would be turned on as soon as people want to do some washing, most likely when leaving home for work in the morning. When task operation within time window is allowed in the optimised scheduling scenario, the domestic tasks operation order as well as the equipment operation time could be scheduled in order to minimise the total cost (Eq. 3-18a or 18b). Tasks, such as interior lighting and fridge, have fixed electricity consumption time period and have no other alternatives. Tasks with flexible operation time can be scattered as much as possible to avoid electricity consumption peak and utilise electricity generated from local generators as much as possible. Also, when electricity is cheaper from grid, it will be imported from the grid instead of being generated from generators which could also be stored in the battery for later use.

The developed MILP model is implemented using CPLEX 12.4.0.1 in GAMS 23.9[4][128] on a PC with an Intel Core 2 Duo, 2.99 GHz CPU and 3.25GB of RAM. The model statistics of the microgrid optimised scheduling scenarios under the two pricing schemes are presented in Table 3-2 for both examples, where numbers of continuous equations, continuous and discrete variables and CPU time taken are presented. With an optimality gap as 0.1%, even in Example 2, scheduling scenarios RmO and PmO require 0.8 CUP *s*

[3] Format ‘xyz’ is used for abbreviation, where ‘x’ represents real-time price scheme (R) or peak demand price scheme (P); ‘y’ represents macrogrid (M) or microgrid (m) and ‘z’ represents earliest starting time (E) or optimised scheduling (O).

[4] www.gams.com

and 1.3 CPU *s* , respectively, for the scheduling. It is evident that the proposed MILP model is able to offer significant cost savings and peak demand savings with very modest computational difficulties for smart buildings with the same living habit or different ones.

Table 3-2 Model statistics

Example	Scenario	Continuous equations	Continuous variables	Discrete variables	CPU (s)
1	RmO	1,178	17,814	17,280	0.2
	PmO	1,226	17,862	17,280	0.3
2	RmO	1,898	52,374	51,840	0.8
	PmO	1,946	52,422	51,840	1.3

3.5.1 Example 1:Real-Time Price and Peak Demand Price Schemes

The planning horizon for both examples is from 8 am in a day to 8 am on the next morning. The optimal electricity balance and total daily cost resulting from Example 1 under the real-time price scheme is shown in Figure 3-5 and Figure 3-6. Under the RMO scenario, the tasks are scheduled based on the real-time electricity pricing. Tasks are preferred to be performed when electricity price is low, e.g. during night time. The total cost is reduced from £154 in the RME scenario to £137 in the RMO scenario. The electricity demand from the grid is scattered while the peak demand from the grid is decreased from 301 *kW* in RME scenario to 186 *kW* in the RMO scenario. Under the real-time price scheme for the RmE and RmO scenarios, the electrical storage is used to store electricity when there is an excess; it is mainly for utilising the wind generator output more efficiently. There is no excess electricity sold to the utility grid in Example 1. The total cost is reduced to £123 in the RmO scenario. With the earliest starting time scenarios, the peak hours are mainly during the evening when occupants are back from work. In the RmO scenario, the peak demand from the grid is decreased from 270 *kW* in the RmE scenario to 153 *kW* in the RmO scenario, and the electricity demand is flatter in RmO than RmE. During the day, about 30% of the total electricity and 18% of total heat are produced from the CHP in the RmE scenario and 45% of electricity and 27% of heat are produced from the CHP in the RmO scenario.

(a) RME (£154)

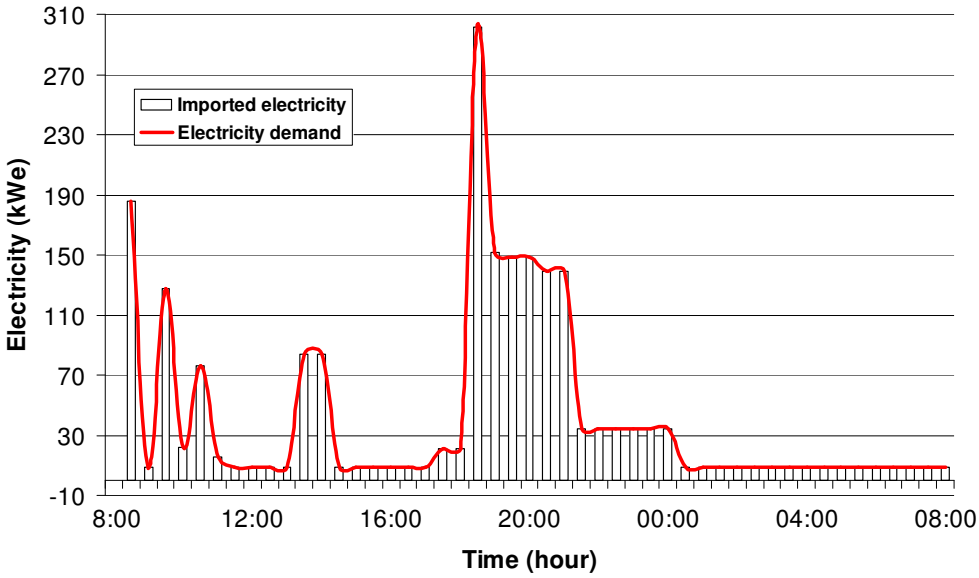

(b) RMO (£137)

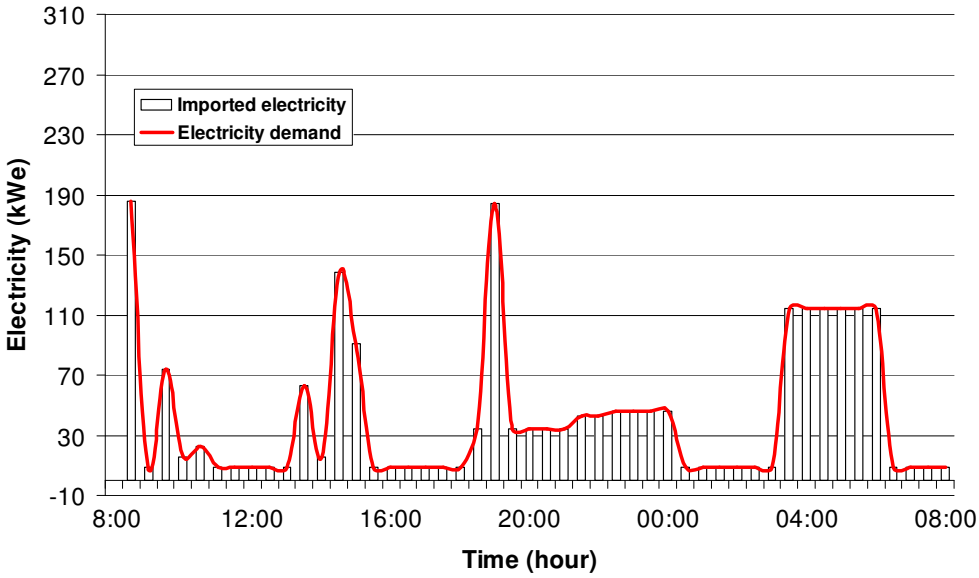

Figure 3-5 30 homes: Macrogrid electricity balance and total cost under real-time price scheme

(c) RmE (£142)

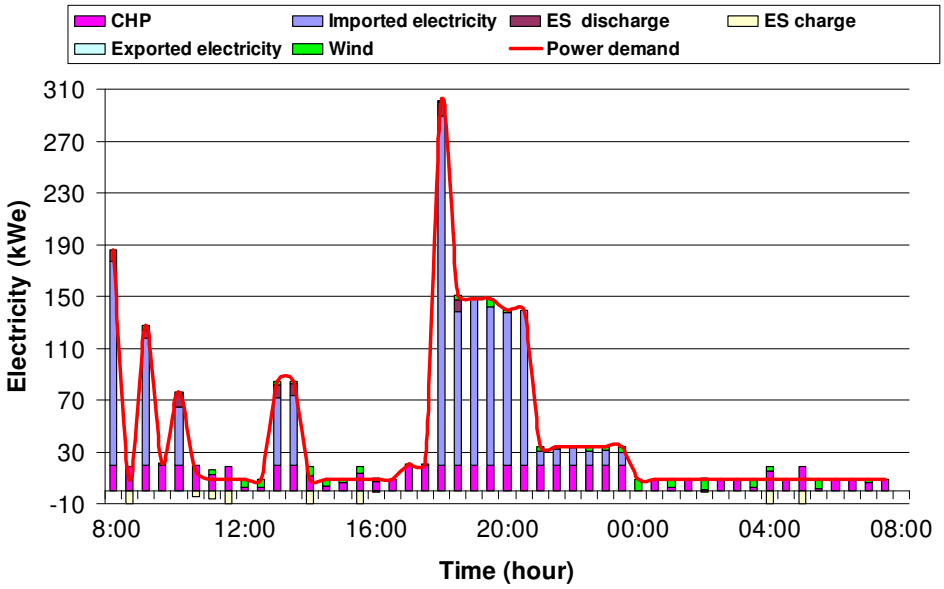

(d) RmO (£123)

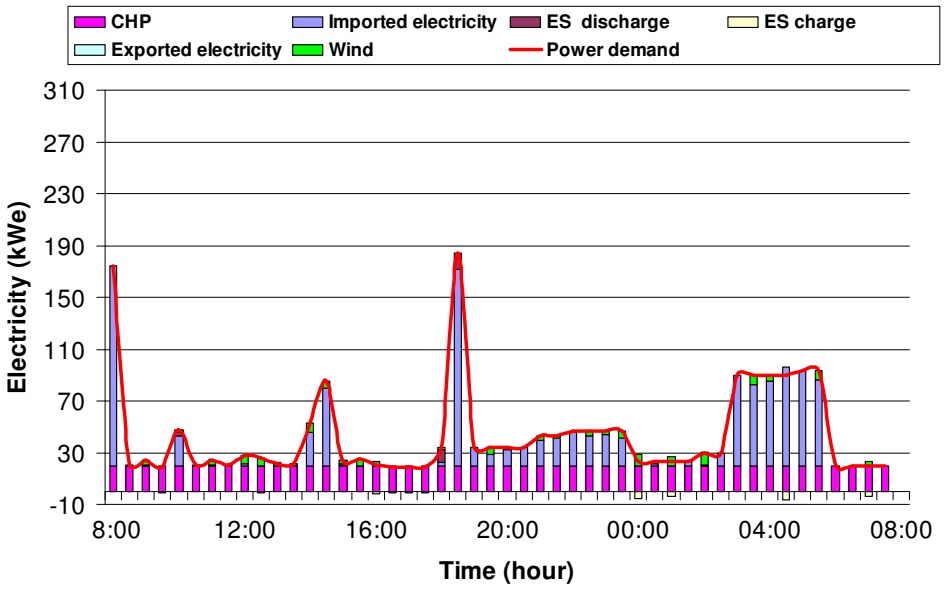

Figure 3-6 30 homes: Microgrid electricity balance and total cost under real-time price scheme

The optimal electricity balance and total one day cost resulting from Example 1 under peak demand price scheme is shown in Figure 3-7 and Figure 3-8. When extra cost is charged for the over consumed electricity from grid, the peak demand is reduced through optimisation.

Under the PMO scenario, the tasks are scattered according to real-time prices and peak demand extra charge. The total cost for PME scenario is £186 while it decreases to £157 when optimised scheduling is applied in the PMO scenario. The peak demand from grid is reduced to 184 kW. There are still peaks in the early morning and evening which cannot be avoided, mainly because of the inflexible time window requirement for specific tasks. It happens even in the PmO scenario although the demand pattern is smoother. Under microgrid scenarios, the total cost is £165 in the PmE scenario, which is further reduced to £127 in the PmO scenario. The peak demand from the grid is reduced from 270 kW in the PmE scenario to 121 kW in the PmO scenario. The demand pattern in the PmO scenario is smoother than that in the PmE scenario.

(a) PME (£186)

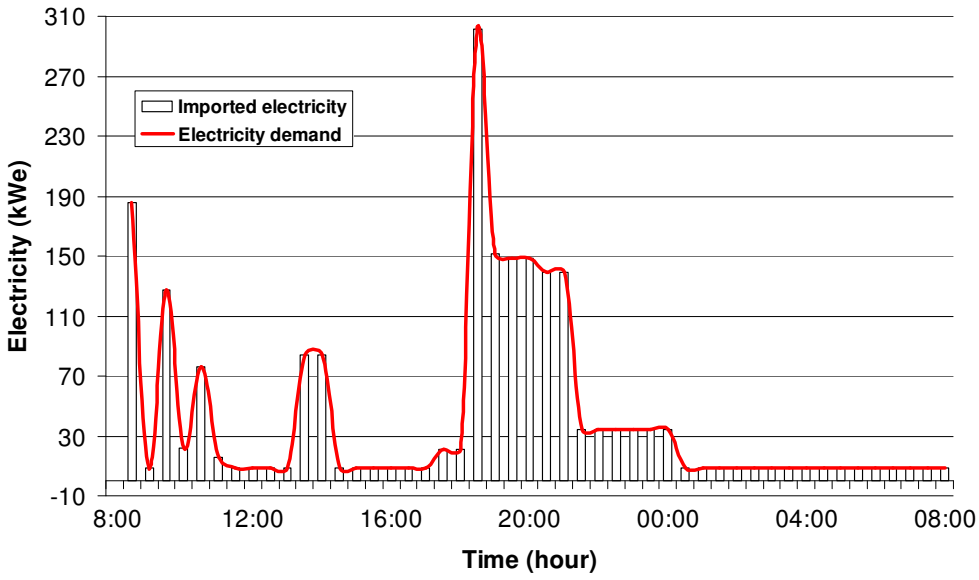

(b) PMO (£157)

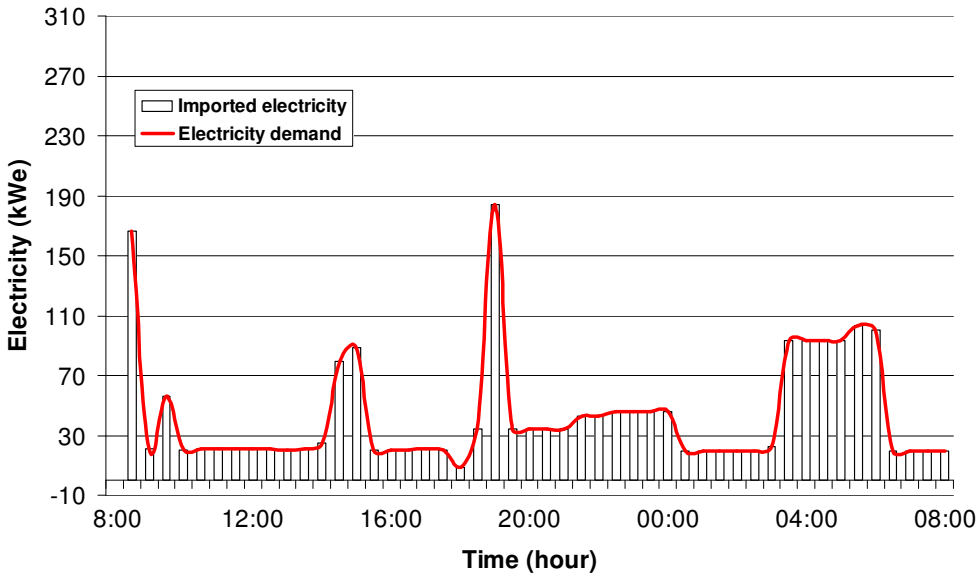

Figure 3-7 30 homes: Macrogrid electricity balance and total cost under peak demand price scheme

(c) PmE (£165)

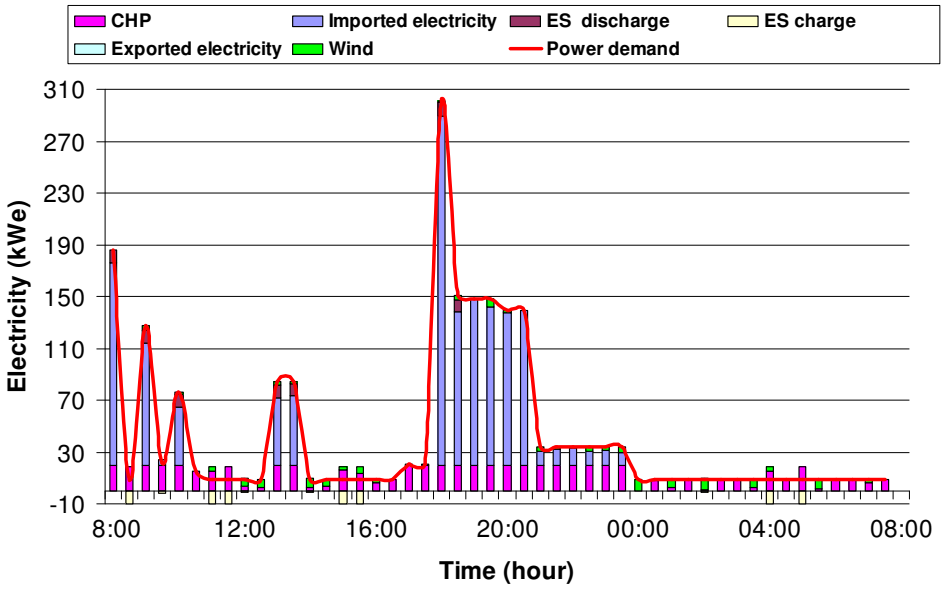

(d) PmO(£127)

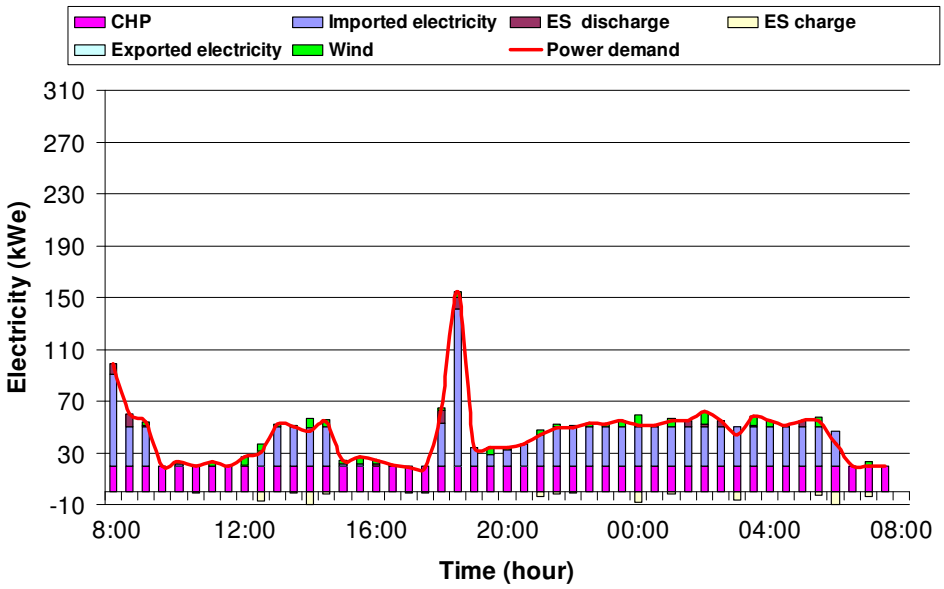

Figure 3-8 30 homes: Microgrid electricity balance and total cost under peak demand price scheme

The comparison between the real-time price scheme and peak demand price scheme of Example 1 is presented in Table 3-3. It is clearly shown that by applying the optimised

scheduling scenarios, the total cost is always lower than that of the earliest starting time scenarios. When peak demand extra cost is considered, although the total cost under each scenario is higher than that of the real-time price scheme, the total peak demand over the whole day is quite different. It can be seen from Figure 3-5(b) and Figure 3-7(b), the electricity demand over the day is flatter in Figure 3-7(b). The total peak demand over the threshold has been reduced from 586 *kWh* in RMO scenario to 350 *kWh* in PMO scenario, satisfying the aim of the peak demand schemes to reduce the peak demand from the grid. It indicates that even without microgrid, the task starting time scheduling can help in peak demand reduction and cost savings. When microgrid is applied, more savings can be achieved and peak demand from grid can be reduced further by obtaining electricity from local DERs. By utilising microgrid and the peak demand price scheme, the total cost is the lowest while highest peak demand from the grid is reduced to 121 *kW* in PmO scenario (which is 153 *kW* in the RmO scenario). The total peak demand over the threshold of 30 *kW* in PmO scenario is 67 *kWh*, which represents about 6% of the total electricity demand (1,056 *kWh*).

Table 3-3 Results of Example 1 under two pricing schemes

	Total cost (£)	**Peak demand from grid (*kW*)**	**Total peak demand (*kWh*)**	**CHP production (*kWh*)**	**Peak demand over total demand**
RME	154	301	640	0	61%
RMO	137	186	586	0	55%
RmE	142	270	475	322	45%
RmO	123	153	252	480	24%
PME	186	301	640	0	61%
PMO	157	184	350	0	33%
PmE	165	270	473	322	45%
PmO	127	121	67	480	6%

The heat balances for microgrid scenarios are shown in Figure 3-9 and Figure 3-10. Since all the heat in the macrogrid scenarios is provided by the boiler and heat demand profile is the same under all scenarios, the heat balance for those macrogrid scenarios are not presented. Under the microgrid earliest starting time scenarios, the heat output from CHP

varies, while under the microgrid optimal scheduling scenarios, the heat output from CHP is constant and CHP operates at its full capacity.

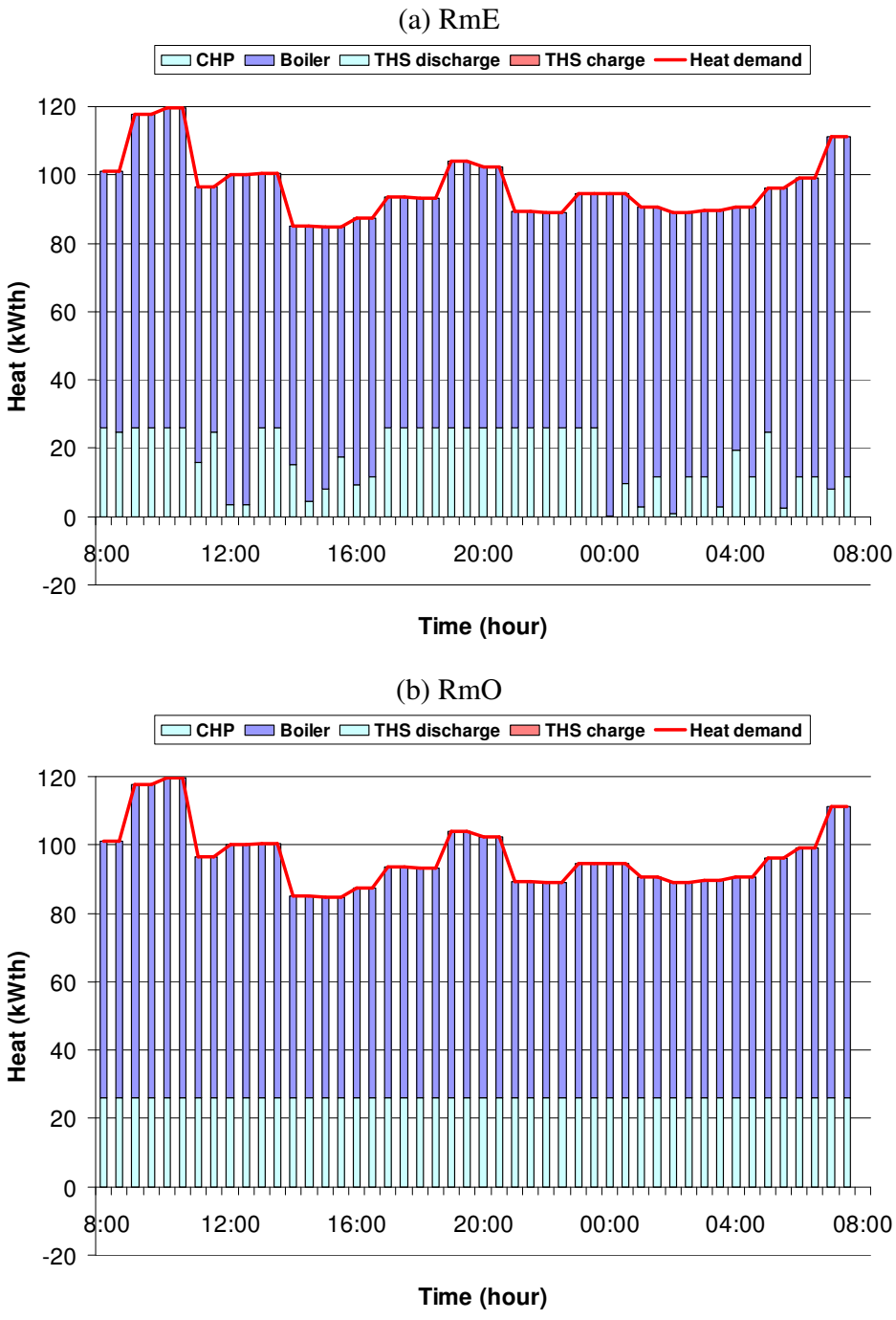

Figure 3-9 30 homes: heat balance for microgrid real-time price scenarios

(c) PmE

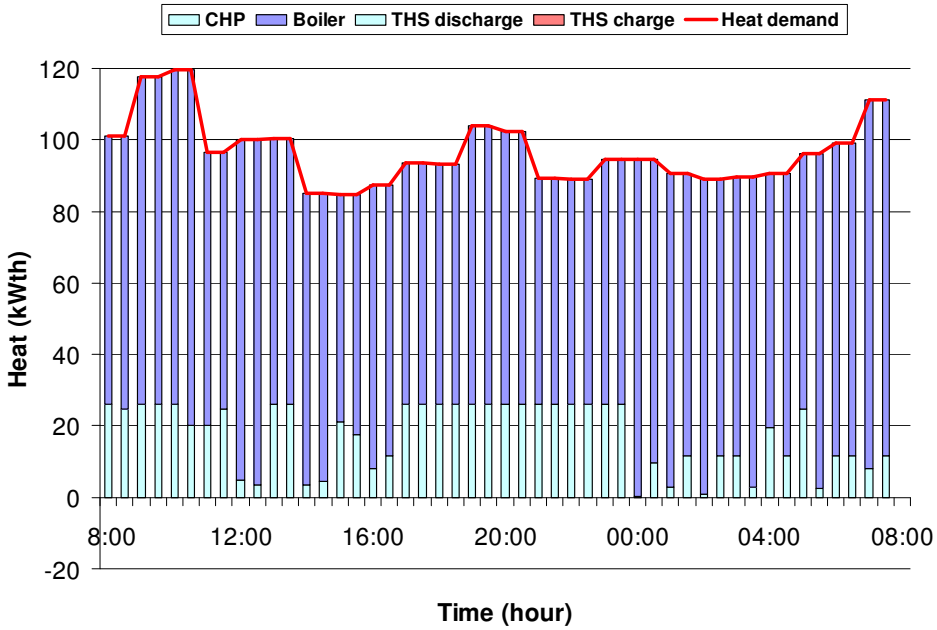

(d) PmO

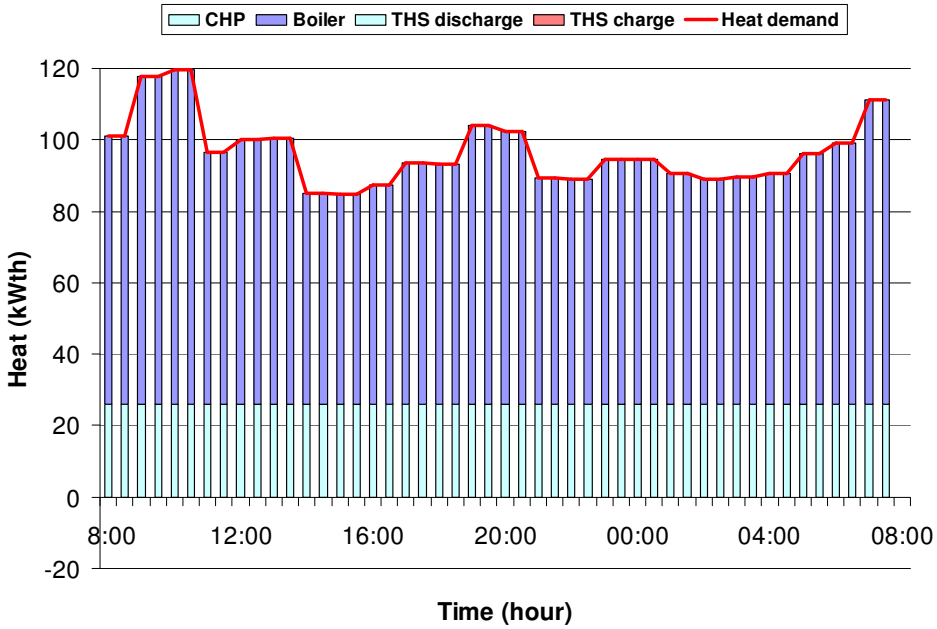

Figure 3-10 30 homes: heat balance for microgrid peak demand price scenarios

3.5.2 Example 2:Real-Time Price and Peak Demand Price Schemes

The optimal electricity balance and total daily day cost resulting from Example 2 under real-time price scheme are shown in Figure 3-11 and Figure 3-12. Under the RMO scenario, all tasks are scheduled based on the real-time electricity price to obtain minimum daily energy cost. The total cost is reduced to £409 in the RMO scenario, which is 12% cost savings. As shown in Figure 3-11(b), task starting times are shifted to mid-night when electricity price is low. The electricity demand from the grid is scattered and the peak demand is decreased from 424 *kW* in the RME scenario to 363 *kW* in the RMO scenario. Under the RmE and RmO scenarios, equipment operation time from each technique is scheduled accordingly to minimise the total operation cost. When time window is allowed, tasks with flexible operation time are scattered as much as possible as in Example 1. The power consumption peak periods are shifted to the early morning when the electricity buying price is cheaper. The total cost is £354 in the RmO scenario. The electrical storage is used to store electricity. There is no excess electricity sold to the utility grid in Example 2. This is mainly due to the small CHP capacity and cannot provide extra electricity. Also, the electricity selling price to the grid is relative low. The boiler capacity can fulfil the peak heat demand, but when the heat demand is over the boiler capacity and the electricity demand is low, it is possible to sell electricity to grid from the microgrid. In that case, CHP generator has to provide more electricity than needed to cover the increased heat demand. The excess electricity can be stored in battery for later use or sold to the grid. However, when electrical storage is full, export to the grid is the only option although the selling price is low. In the RmE and RmO scenarios, the total costs are £409 and £354, respectively. The electricity peak demand from the grid is decreased from 358 *kW* in the RmE scenario to 283 *kW* in the RmO scenario. During the day, about 37% of the total electricity and 22% of total heat are produced from the CHP in the RmE scenario and 44% of electricity and 26% of total heat are produced from the CHP in the RmO scenario. The total electricity demand of the smart building is 3,169 *kWh*.

(a) RME (£464)

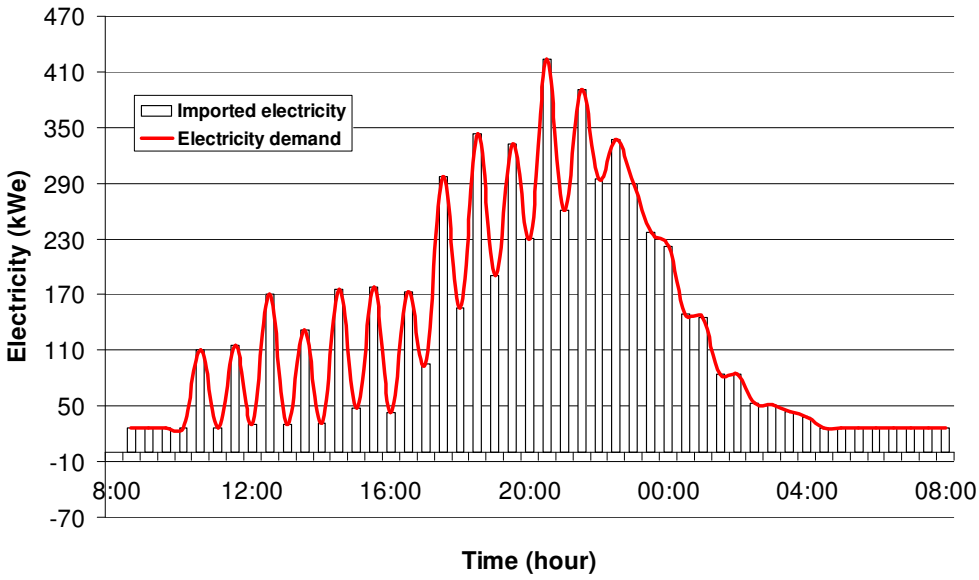

(b) RMO (£409)

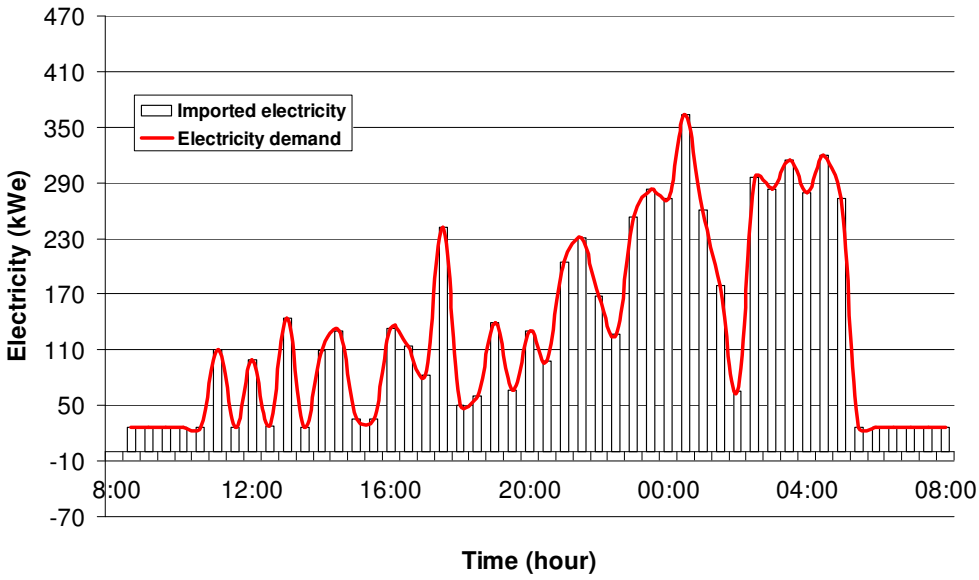

Figure 3-11 90 homes: Macrogrid electricity balance and total cost under real-time price scheme

(c) RmE (£409)

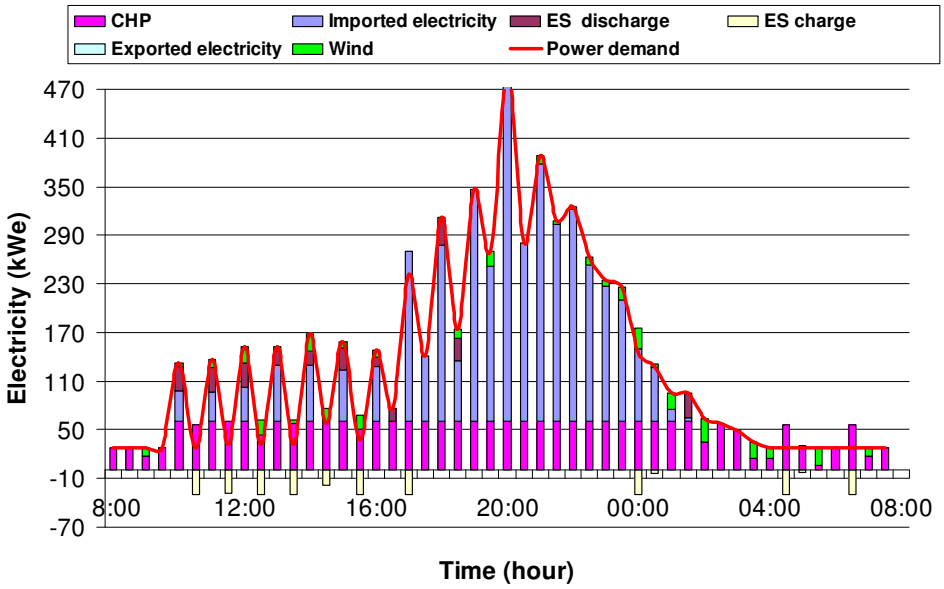

(d) RmO (£354)

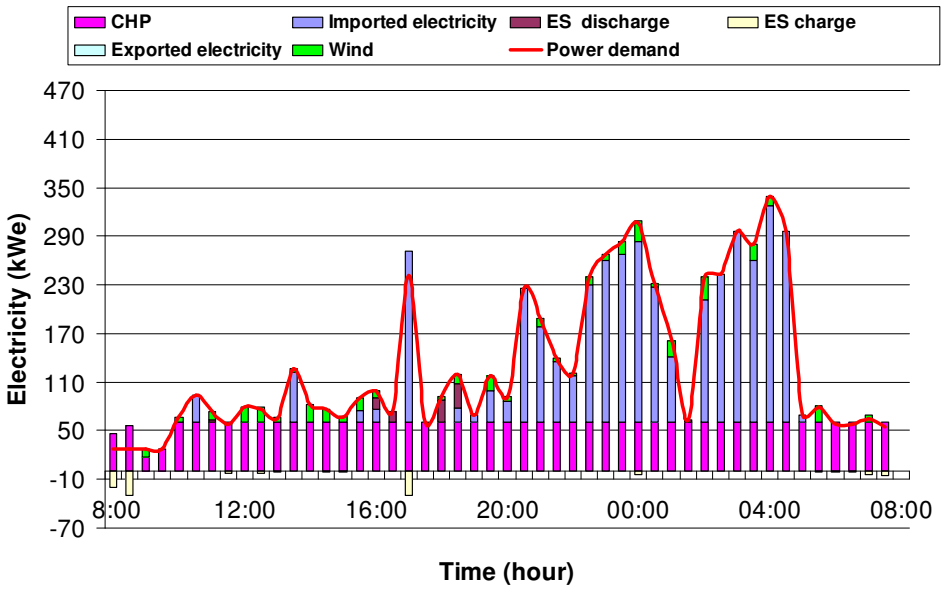

Figure 3-12 90 homes: Microgrid electricity balance and total cost under real-time price scheme

The optimal electricity balance and total daily cost resulting from Example 2 under the peak demand price scheme are shown in Figure 3-13 and Figure 3-14. When the extra cost is charged for the over consumed electricity from the grid, the peak demand is reduced through task scheduling. The total costs are £546 and £474 for the PME scenario and PMO scenario. Under the PMO scenario, the peak demand from grid is reduced to 340 kW compared to the PME scenario. The energy consumption peaks are in the mid-night instead of the evening in this scenario. Since there is no DER to provide electricity, the tasks are scattered as much as possible to reduce the peak demand extra charge over the threshold at 90 kW. Under microgrid scenarios, PmE scenario and PmO scenario, the total costs are both lower than that from the macrogrid scenarios, which are £454 and £378, respectively. Also the peak demand from grid is reduced from 358 kW in the PmE scenario to 250 kW in the PmO scenario. The PmO scenario has the flattest electricity demand.

(a) PME (£456)

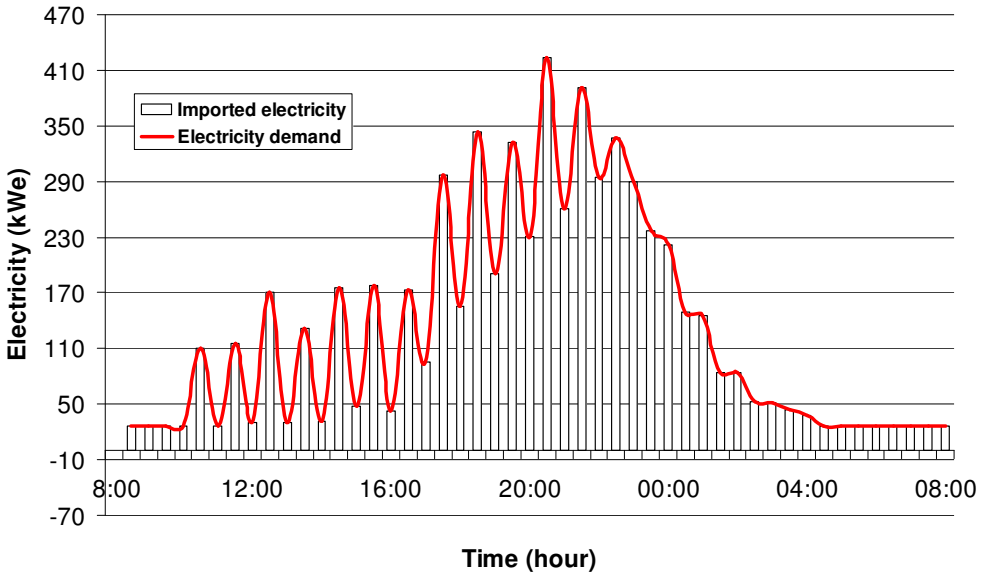

(b) PMO (£474)

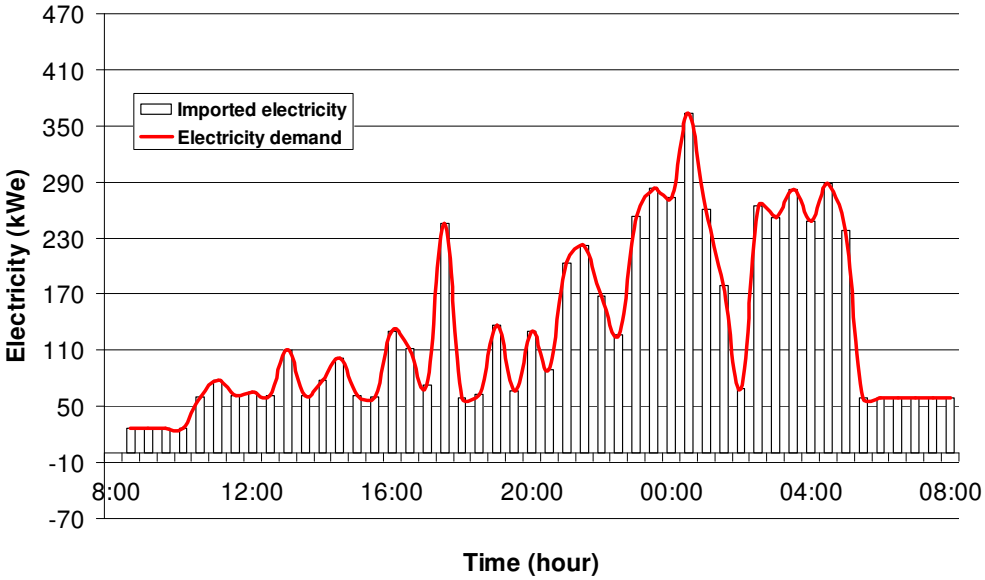

Figure 3-13 90 homes: Macrogrid electricity balance and total cost under peak demand price scheme

(a) PmE (£454)

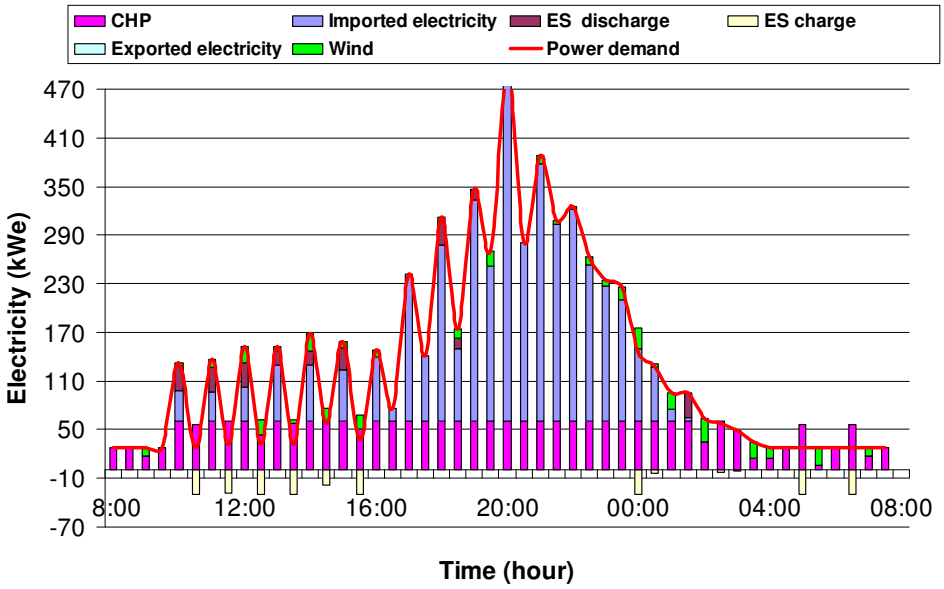

(b) PmO (£378)

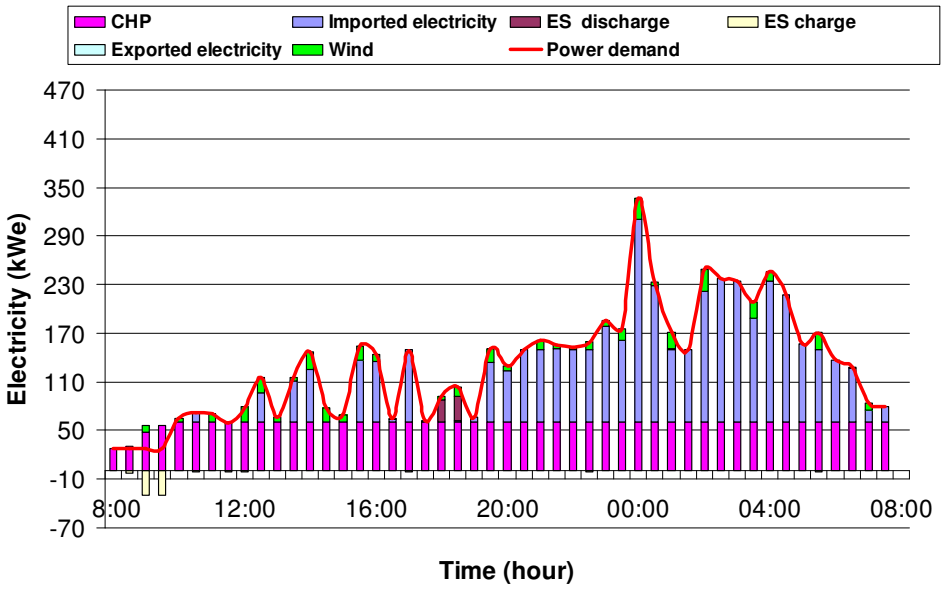

Figure 3-14 90 homes: Microgrid electricity balance and total cost under peak demand price scheme

The comparison between the real-time and peak demand price schemes of Example 2 is presented in Table 3-4. Similarly to Example 1, the total cost is always lower for the optimised scheduling scenarios than that of the earliest starting time scenarios. The total cost under each scenario from peak price scheme is higher than that of the real-time price scheme. As expected, the peak demand schemes reduce the peak demand from the grid. The highest peak demand in the PMO scenario is smaller than that from the RMO scenario, and the total daily peak demand has also been reduced. The electricity demand over the day in Figure 3-13(b) is flatter than that shown in Figure 3-11(b). The total peak demand over the threshold has been reduced from 1,566 *kWh* in the RMO scenario to 1,191 *kWh* in the PMO scenario. The task starting time optimal scheduling can reduce peak demand and achieve higher cost savings. Microgrid provides local electricity by utilising DERs, which further reduce the peak demand from the grid and obtain more savings. By applying microgrid and the peak demand price scheme in the PmO scenario, the total cost is the lowest and the peak demand from the grid is reduced to 250 *kW* (from 283 *kW* in the RmO scenario). Total peak demand from the grid over the threshold 90 *kW* in the PmO scenario is reduced to 360 *kWh*, which is 11% of the total electricity demand.

Table 3-4 Results of Example 2 under two pricing scheme

	Total cost (£)	**Peak demand from grid (*kW*)**	**Total peak demand (*kWh*)**	**CHP production (*kWh*)**	**Peak demand over total demand**
RME	464	424	1,646	0	52%
RMO	409	363	1,566	0	49%
RmE	409	358	902	1,183	28%
RmO	354	283	738	1,393	23%
PME	546	424	1,646	0	52%
PMO	474	340	1,191	0	38%
PmE	454	358	880	1,183	28%
PmO	378	250	360	1,401	11%

The heat balances for microgrid scenarios are shown in Figure 3-15 and Figure 3-16. Under the earliest starting time scenarios, the heat output from CHP varies, while under the

optimal scheduling scenarios, the heat output from CHP is constant except from the beginning of the day and CHP almost operates at its full capacity.

(a) RmE

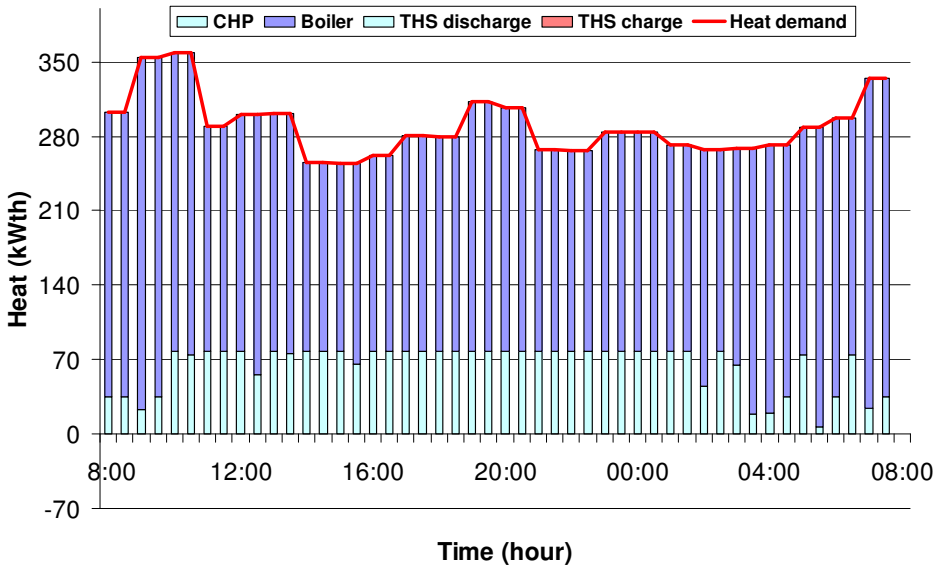

(b) RmO

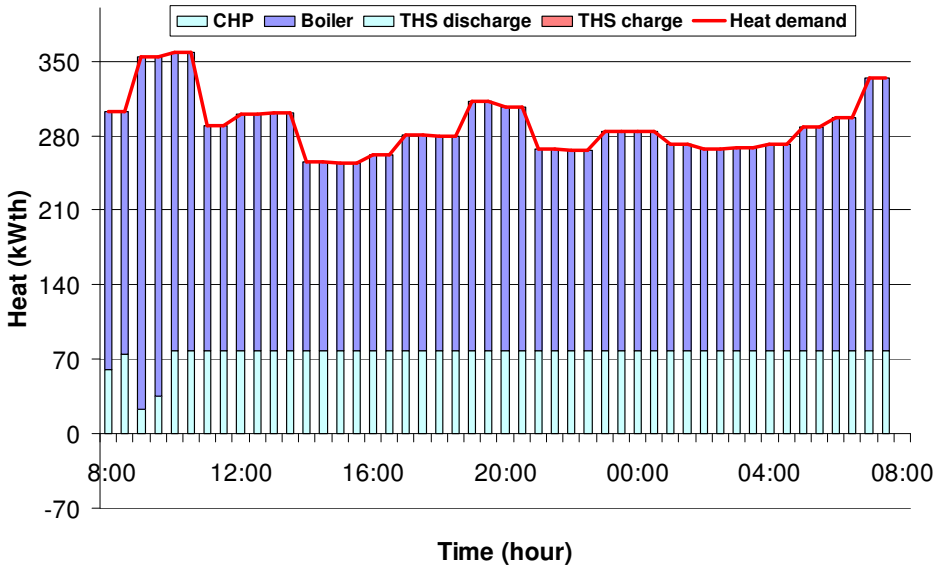

Figure 3-15 90 homes: heat balance for microgrid real-time price scenarios

(c)PmE

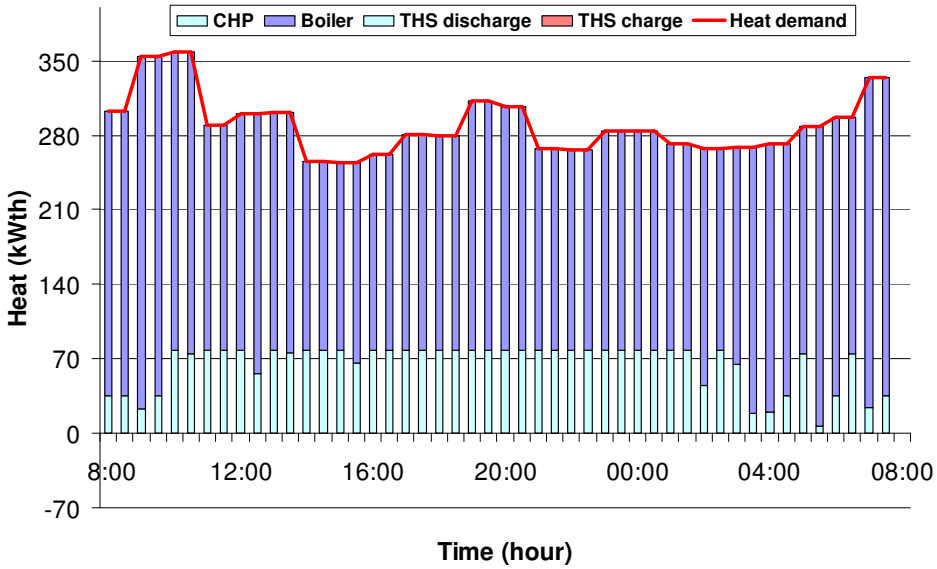

(d) PmO

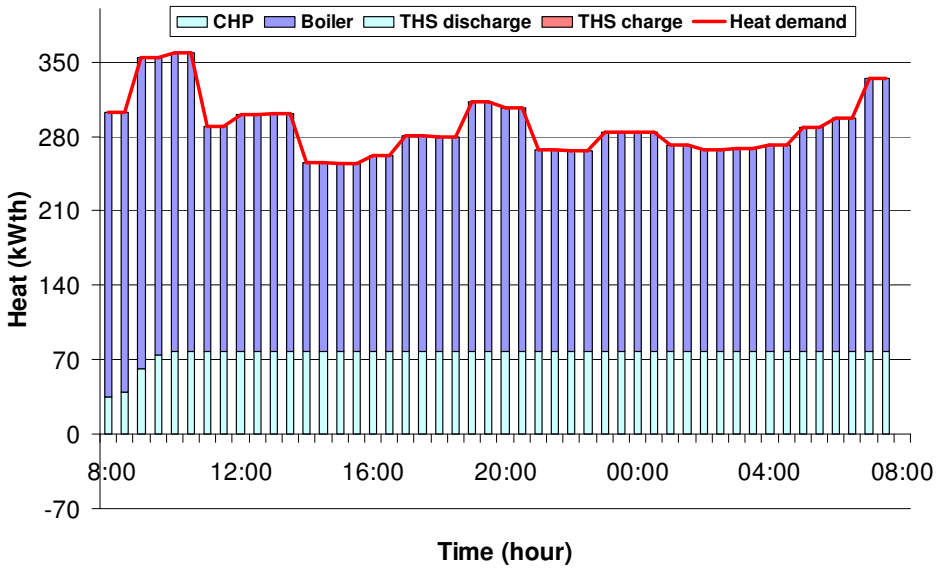

Figure 3-16 90 homes: heat balance for microgrid peak demand price scenarios

3.5.3 Comparison between Example 1 and Example 2

By comparing with the scenarios where all tasks start at their earliest possible starting time, there are obvious savings through task starting time scheduling in both examples under the two pricing schemes. Compared with the earliest starting time scenarios, the cost savings and total peak demand savings from the grid between earliest starting scenario by scheduling task starting time are presented in Table 3-5 under different scenarios. With the real-time price scheme, both examples have similar cost savings, while under the peak demand scheme, Example 1 demonstrates more cost savings. Example 2 considers 90 homes with different living habits and with different earliest starting time for flexible tasks. So as expected, its average power peak is lower than that from the same living habits assumed in Example 1, since the tasks are scattered even without scheduling. As shown in Table 3-5, under all scenarios Example 1 has higher peak demand savings percentage from the grid. In both examples, when microgrid is utilised, the lowest cost saving is 13% while the lowest peak demand saving is 18%. Microgrid application is an important alternative solution for cost and peak demand reductions. There are peak demand savings even only real-time price scheme is applied as shown in Table 3-5. However, the peak demands are accidentally reduced there resulting from task starting time optimised scheduling based on electricity real-time price. When peak demand price scheme is applied, the total peak demands from grid are minimised from objective function, which are reduced by 86% and 59% in the peak demand price scheme microgrid scenarios for Examples 1 and 2, respectively.

Table 3-5 Comparison between earliest starting time and optimised scheduling scenarios

Example	Scenario	Cost savings	Total peak demand savings
1	RM(E-O)	11%	9%
	Rm(E-O)	13%	47%
	PM(E-O)	16%	45%
	Pm(E-O)	23%	86%
2	RM(E-O)	12%	5%
	Rm(E-O)	13%	18%
	PM(E-O)	13%	28%
	Pm(E-O)	17%	59%

3.5.4 Scheduling with summer electricity tariff and heat demand

Heat demand of a winter day is considered in the case study to illustrate the scheduling of domestic electrical tasks and DER operations for smart homes. However, the scheduling would vary if it is a summer day with different electricity tariff profile. In this subsection, the same domestic tasks in the two examples are scheduled with summer heat demand and electricity tariff. The selected summer electricity price is presented in Figure 3-17 and heat demands for the two examples are shown in Figure 3-18.

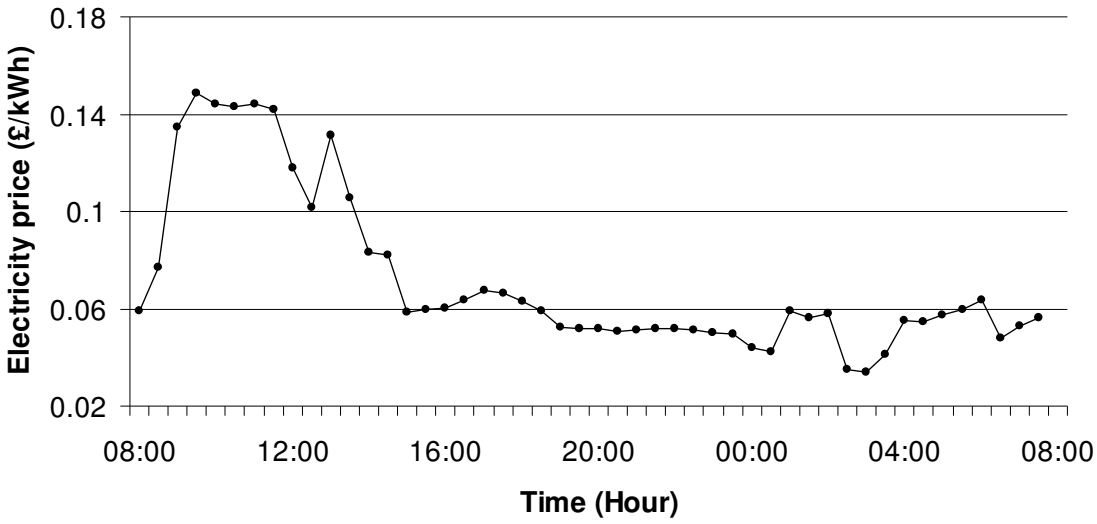

Figure 3-17 Electricity tariff (25th July, 2013) [181]

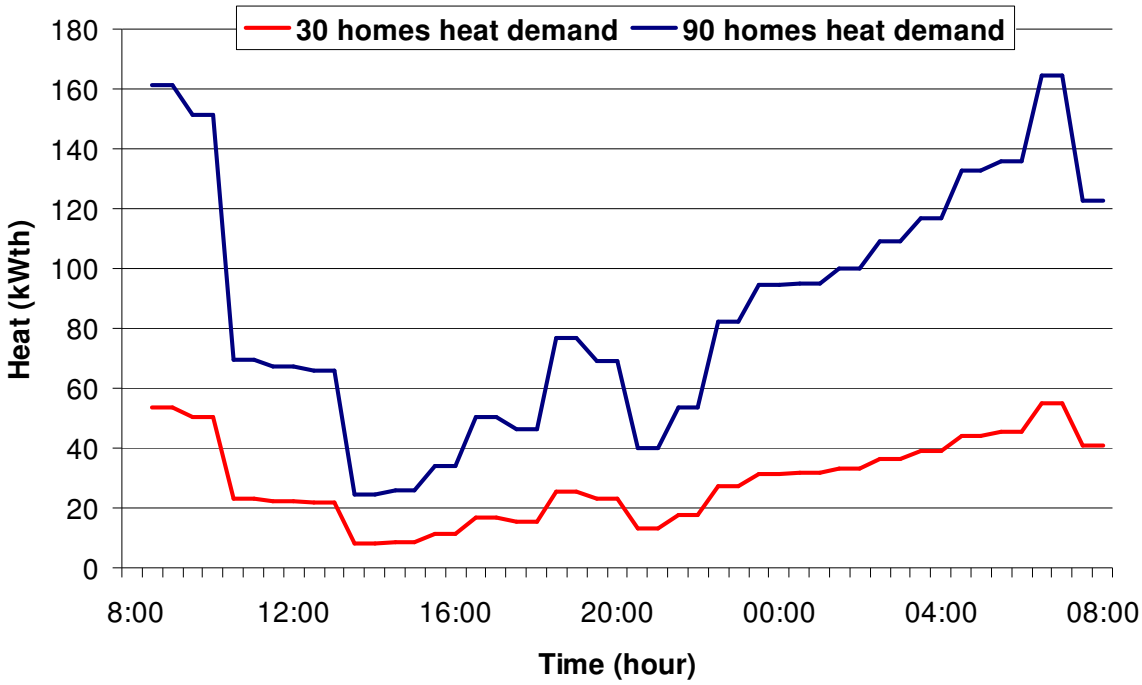

Figure 3-18 Heat demands of 30 and 90 homes in a summer day [182]

The results of Example 1 and Example 2 under summer electricity tariff and heat demand are presented in Table 3-6 and Table 3-7. Compared with Table 3-3 and Table 3-4, the total costs in the two examples are both lower under each scenario as the heat demand in summer is lower. But there are still obvious cost savings and peak demand reductions by optimising the starting times of domestic electric tasks and DER operation over flexible time window. Less electricity is produced from CHP in summer since its corresponding heat generation cannot be fully consumed by smart homes with lower heat demand.

Table 3-6 Results of Example 1 under summer electricity tariff and heat demand

	Total cost (£)	Peak demand from grid (kW)	Total peak demand (kWh)	CHP production (kWh)	Peak demand over total demand
RME	99	301	640	0	61%
RMO	87	184	586	0	55%
RmE	82	301	491	300	47%
RmO	69	174	290	415	27%
PME	131	301	640	0	61%
PMO	109	184	381	0	36%
PmE	106	301	473	301	45%
PmO	75	154	77	415	7%

Table 3-7 Results of Example 2 under summer electricity tariff and heat demand

	Total cost (£)	Peak demand from grid (kW)	Total peak demand (kWh)	CHP production (kWh)	Peak demand over total demand
RME	273	424	1646	0	52%
RMO	255	407	1533	0	48%
RmE	220	424	1044	1004	33%
RmO	199	369	794	1207	25%
PME	355	424	1646	0	52%
PMO	319	340	1227	0	39%
PmE	269	424	953	1005	30%
PmO	219	296	251	1206	8%

Table 3-8 presents the comparison between the earliest starting time and optimised scheduling scenarios. Compared with Table 3-5, cost savings and peak demand reductions of Example 1 are still higher than those of Example 2. In Example 1, cost savings are slightly higher while peak demand savings are slight lower for the sample summer day than the sample winter day. In Example 2, the cost savings are lower except scenario Pm(E-O), while the total peak demand savings are higher except scenario PM(E-O) for the sample summer day than the sample winter day.

Table 3-8 Comparison between earliest starting time and optimised scheduling scenarios with summer electricity tariff and heat demand

Example	Scenario	Cost savings	Total peak demand savings
1	RM(E-O)	12%	8%
	Rm(E-O)	16%	41%
	PM(E-O)	17%	40%
	Pm(E-O)	29%	84%
2	RM(E-O)	7%	7%
	Rm(E-O)	10%	24%
	PM(E-O)	10%	25%
	Pm(E-O)	19%	74%

3.5.5 Scheduling with wider time window

Domestic electrical tasks in Table 3-1 are scheduled within the earliest starting time and the latest finishing time. If this time window could be wider, higher cost savings and peak demand reductions can be obtained. In this subsection, the latest finishing time is extended by 2 hours where applicable in the two examples to analyse its impact on the optimal results. The results of the two examples with 2 hours wider time window are shown in Table 3-9 and Table 3-10. As expected, total costs have been reduced further in the optimal results in the two examples. However, total peak demand reductions are not reduced further simultaneously. Since peak demand reduction is not included in the objective function in real-time pricing scheme scenarios, the peak demands are just accidentally reduced resulting from task scheduling with real-time electricity price as shown in Table 3-3 and Table 3-4. Although the time window has been extended by 2 hours, peak demand reductions are lower in the two examples compared with those without time window extension. On the other hand, peak demand reductions are involved under the peak demand price scheme scenarios by charging peak demand penalty. However, peak demand reduction only happens under the PmO scenario in Example 1. So although time window has been extended, the cost saving objective overcomes the peak demand reduction aspect by moving peak demand to the time periods with lower real-time prices (even with the penalty). CHP productions are the same under all microgrid scenarios in both examples.

Table 3-9 Results of Example 1 with 2 hours wider time window

	Total cost (£)	Peak demand from grid (kW)	Total peak demand (kWh)	CHP production (kWh)	Peak demand over total demand
RME	154	301	640	0	61%
RMO	129	186	589	0	56%
RmE	142	301	475	322	45%
RmO	117	174	271	480	26%
PME	186	301	640	0	61%
PMO	150	165	382	0	36%
PmE	165	301	473	322	45%
PmO	119	64	6	480	1%

Table 3-10 Results of Example 2 with 2 hours wider time window

	Total cost (£)	Peak demand from grid (kW)	Total peak demand (kWh)	CHP production (kWh)	Peak demand over total demand
RME	464	424	1646	0	52%
RMO	394	467	1779	0	56%
RmE	409	424	902	1183	29%
RmO	348	405	928	1400	29%
PME	546	424	1646	0	52%
PMO	467	386	1291	0	41%
PmE	454	424	880	1183	28%
PmO	375	358	380	1401	12%

The comparison between the two examples is shown in Table 3-11. Both cost savings and peak demand reductions of Example 1 are still higher than those of Example 2 as shown in Table 3-5. Compared with the earliest starting time scenarios, more cost savings have been obtained. Example 1 always has higher peak demand savings than Example 2 while there are even negative peak demand savings under real-time price scenarios.

Table 3-11 Comparison between earliest starting time and optimised scheduling scenarios with 2 hours wider time window

Example	Scenario	Cost savings	Total peak demand savings
1	RM(E-O)	16%	8%
	Rm(E-O)	18%	43%
	PM(E-O)	19%	40%
	Pm(E-O)	28%	99%
2	RM(E-O)	15%	-8%
	Rm(E-O)	15%	-3%
	PM(E-O)	14%	22%
	Pm(E-O)	17%	57%

3.6 Concluding Remarks

An MILP model has been proposed for energy consumption and operation management in a smart building with multiple smart homes. It has been applied to two examples, 30 homes with same living habit and 90 homes with different living habits for a winter day. Twelve domestic electrical tasks and equipment operations have been scheduled based on given time windows, real-time half-hourly grid electricity prices and peak demand extra charge to minimise the total energy cost and electricity peak demand from grid. Significant cost savings and peak demand reduction have been achieved in both examples. The proposed model has also been applied with summer electricity tariff and heat demand, obvious cost savings and peak demand reduction can still be obtained. With more flexible time window, it could reduce total cost further while peak demand saving would not be reduced simultaneously.

The power output from the wind generator varies according to the weather conditions. The proposed MILP scheduling model has used the power generated by wind generators when available, providing further savings for the customers. Under the optimised scheduling scenario, the CHP generator has been used more efficiently and provided heat more steadily than under the earliest starting time scenario. When the peak demand price scheme is applied, the highest peak demand from the grid and total peak demand over the threshold has been significantly reduced. This power demand reduction has the benefit of releasing

the burden on the central grid and reducing the expense of upgrading the current grid infrastructure to fulfil increasing energy demand.

In Chapter 4, this proposed model is extended to deal with the respective cost minimisation among multiple homes sharing common DERs.

Chapter 4 Cost Distribution among Multiple Smart Homes

The total daily cost of a smart building with several smart homes is minimised by scheduling electricity demand and DERs operation as described in chapter 3. However, when local DERs cannot fulfil the whole demand, in order to determine their respective lowest cost, smart homes will compete with each other to obtain energy from local DERs.

In this chapter, a mathematical programming formulation is presented for the cost distribution among multiple smart homes with microgrid. The model is based on the lexicographic minimax method using an MILP approach. The forecasted daily expense for each smart home is minimised on fairness. Besides the scheduling of electricity demand and DERs operation, DERs output sharing among smart homes is also planned.

4.1 Introduction and Literature Review

All energy management work mentioned in Chapter 3 considers either single smart home or a number of smart homes as a whole customer, where only the total energy cost is considered in the objective functions. Practically, DERs are located in a building and shared by all the residents within the building [184]. Due to the different living habits of residents and domestic appliances in homes, the energy tasks and task operation times vary from home to home. Each smart home pays its own energy bill according to their respective energy consumption. There is a desire for them to achieve their own benefits by scheduling their energy task operation time. However, the DERs, which provide cheaper energy, cannot fully supply the demand for each home all the time. In essence, the smart homes will compete with other homes for the cheaper energy generated from DERs during peak demand hours. So the concern of this chapter is how to distribute the costs fairly among multiple smart homes with common DERs in microgrid under competition situation.

Smart homes sharing the common DERs in a building can be considered as collaborative networks. Each smart home has its own cost concern and competes with other participants for energy resources, but they can achieve more benefits via cooperation. Concept of

fairness and fair settlement with Game theory have been reviewed in section 2.1.2. In this chapter, lexicographic minimax method is applied for the fair cost distribution of the smart homes with microgrid. Every player is treated equally and impartially. The fairness concept is a refinement of the Pareto optimality in the lexicographic minimax method which has been investigated and applied in several areas, such as, bandwidth allocation in computer networks, facility location problems and resource allocation.

Lexicographic minimax originates from the subset selection of optimal strategies from the optimal minimax strategy through the exploit of the opponent optimality mistakes [185] and Erkut et al. [186] stated that lexicographic minimax solution is known in the game theory as the nucleolus of a matrix game. Klein et al. [187] develop a lexicographic minimax algorithm to deal with multi-period resource allocation problem. The location problem is addressed in [188] and the distribution of travel distances among the service recipients is considered as an important issue. He develops a concept of the lexicographic minimax solution, which is a refinement of the standard minimax approach. The lexicographic minimax solution concept for fair allocation is applied to locate water rights for the demand sites in the Aral Sea region in the work of [189] and the problem is solved by an iterative algorithm. Wang et al. [190] adopt the lexicographic minimax fairness concept and develop the lexicographic minimax water shortage ratios approach for modelling water allocation under public water rights regime. Lexicographic minimax algorithm is applied for a sensor nodes placement technique by the authors of [185]. Erkut et al. [186] apply the lexicographic minimax approach to find a fair non-dominated solution to the location allocation problem for municipal solid waste management at the regional level in North Greece. The lexicographic minimax method is used in [191] to tackle the multi-objective optimisation problem of global supply chains in the process industry.

In this chapter, an MILP model is proposed to obtain fair cost distribution amongst participants in a smart building. It is based on the minimisation optimisation approach for the lexicographic minimax method proposed by Erkut et al. [186] which guarantees a Pareto-optimal solution. A fair cost distribution amongst smart homes is provided and each participant will pay a fair energy cost based on their respective energy consumption. The

key decision variables include: DER operation plan, equipment output sharing plan, task starting time, and energy resources utilisation.

4.2 Problem Description

In the work of this chapter, multiple homes in a smart building are considered rather than considering total energy demand presented in Chapter 3. There is a microgrid to provide local energy to the smart homes. DERs, such as CHP generator, boiler, thermal or electrical storage, are shared by the smart homes. Grid connection is available all the time to provide electricity when there is no sufficient energy generated from local DERs. Surplus electricity generated over the local demand can be sold back to the grid. Each smart home has its own energy (heat and electricity) demands, which depend on the household types and living habits. Heat demand for each home is given based on types of household. While the electricity demand of each home depends on its own daily domestic appliance tasks, which are assumed to be flexible. Typical flexible tasks include dishwasher, washing machine and spin dryer. Thus, the electricity demand profile depends on the operation time of domestic appliances. It is assumed that the smart building has local controllers for each DER and communication system to distribute the energy consumption scheme. In this work, equipment capacities are all given and only operation or maintenance costs are considered. Electricity real-time price is forecasted and given one day in advance. The energy cost for each smart home is calculated based on their respective energy consumption rate. Since energy with lower price provided by DER cannot fulfil demands for all smart homes all the time, the smart homes need to compete with each other for the energy generated from DERs to minimise their own energy cost. Also since electricity tariff varies over time, the electrical tasks tend to be operated in low tariff periods within the given task operation time window.

The overall problem can be stated as follows:

Given are (a) a time horizon split into a number of equal intervals, (b) heat demand of each smart home, (c) equipment capacities, (d) efficiencies of technologies, (e) maintenance cost of all equipment, (f) heat-to-power ratio of CHP generator, (g) charge and discharge limit

rates for thermal/electrical storage, (h) gas price, real-time electricity prices from grid, (i) earliest starting and latest finishing times, (j) task capacity profiles, (k) task duration,

Determine (a) energy production plan, (b) equipment output sharing plan, (c) task starting time, (d) thermal/electrical storage plan, (e) electricity bought from grid, (f) electricity sold to grid,

So as to find the multi-participant strategies which result in optimal fair cost distribution among smart homes.

4.3 Mathematical Formulation

The smart homes power consumption scheduling problem is formulated as an MILP model. The daily power consumption tasks are scheduled based on their given operation time windows, which is defined as the time period between the earliest starting time and latest finishing time of each task. The objective is to minimise the daily power cost of each home. The time domain is modelled in a discrete form with intervals of equal length. The key model decision variables include equipment operation, equipment output sharing, resources utilised and task starting time. These are determined by minimising the daily energy cost of each home subject to equipment capacity constraints, energy demand constraints, electrical/thermal storage constraints and task operation time window.

4.3.1 Nomenclature

Most notations in Chapter 3 are used in this chapter as well, while modified and new notations are given below, the superscript is used to indicate equipment and the subscript is used for indices:

Indices

j smart home in the smart building

Parameters

H_{jt} heat demand of smart home j at time t (kW_{th})

P_{ji} processing time of task i of home j

T_{ji}^{F} latest finishing time of task i of home j

T_{ji}^{S} earliest starting time of task i of home j

Continuous Variables

E_{jt} electricity exported to the grid of smart home j at time t (kW_e)

f_{jt} thermal storage discharge rate of smart home j at time t (kW_{th})

g_{jt} thermal storage charge rate of smart home j at time t (kW_{th})

I_{jt} electricity imported from the grid of smart home j at time t (kW_e)

S_t^{ET} total electricity in electrical storage at time t (kWh_e)

S_{jt}^{E} electricity in electrical storage of smart home j at time t (kWh_e)

S_t^{TT} total heat in thermal storage at time t (kWh_{th})

S_{jt}^{T} heat in thermal storage of smart home j at time t (kWh_{th})

u_{jt} electricity output from CHP generator of smart home j at time t (kW_e)

x_{jt} heat output from boiler of smart home j at time t (kW_{th})

y_{jt} electrical storage discharge rate of smart home *j* at time *t* (kW_e)

z_{jt} electrical storage charge rate of smart home *j* at time *t* (kW_e)

Binary Variables

X_{jit} 1 if task *i* of home *j* starts at time *t*, 0 otherwise

X_{jt}^{G} 1 if electricity is bought from grid by home *j* at time *t*, 0 otherwise

X_{jt}^{E} 1 if electrical storage is charged by home *j* at time *t*, 0 otherwise

X_{jt}^{T} 1 if thermal storage is charged by home *j* at time *t*, 0 otherwise

Next, the constraints involved in the proposed mathematical model are described:

4.3.2 Capacity Constraint

The output from each equipment should not exceed its designed capacity. Since all the equipments are shared by the customers, the outputs utilised by all customer are summarised.

CHP generator:

$$\sum_{j} u_{jt} \le C^{C} \qquad \forall t \qquad \textbf{Eq. 4-1}$$

Boiler:

$$\sum_{j} x_{jt} \le C^{B} \qquad \forall t \qquad \textbf{Eq. 4-2}$$

Electrical storage:

$$\sum_j S_{jt}^E \le C^E \qquad \forall t \qquad \textbf{Eq. 4-3}$$

Thermal storage:

$$\sum_j S_{jt}^T \le C^T \qquad \forall t \qquad \textbf{Eq. 4-4}$$

4.3.3 Energy Storage Constraints

There is a central electrical storage for the whole building. Each home can send or receive electricity/heat from the battery, but the charging or discharging amount from battery for each home is recorded. No electricity can be obtained from the battery unless electricity has been stored before from that home. It can be considered as each home has its own sub-battery, but the capacity for each home is flexible and the total capacity of the battery for the whole building is provided. Electricity stored in the electrical storage at time t is equal to the amount stored at $t-1$ plus the electricity charged minus the electricity discharged. Electricity would be lost during the charging and discharging process, for example during any period when amount of electricity δz_{jt} is sent to the electrical storage, only $\delta\eta^E z_{jt}$ will be charged, and the rest being lost, where η^E is turn-around efficiency of electrical storage. Meanwhile, during the discharging process, in order to send δy_{jt} of electricity to the user, $\delta y_{jt}/\eta^E$ of electricity is needed.

$$S_{jt}^E = S_{j,t-1}^E + \delta\eta^E z_{jt} - \delta y_{jt}/\eta^E \qquad \forall j,t \qquad \textbf{Eq. 4-5}$$

The discharged amount cannot exceed the storage amount from the previous time interval.

$$S_{j,t-1}^E \ge \delta y_{jt}/\eta^E \qquad \forall j,t \qquad \textbf{Eq. 4-6}$$

Charge and discharge of electricity cannot happen at the same time for each home:

$$z_{jt} \le MX_{jt}^{E} \qquad \forall j,t \qquad \textbf{Eq. 4-7}$$

$$y_{jt} \le M(1 - X_{jt}^{E}) \qquad \forall j,t \qquad \textbf{Eq. 4-8}$$

At each time interval, the electrical storage is the total storage amount over all sub-batteries in the building.

$$S_t^{ET} = \sum_j S_{jt}^{E} \qquad \forall t \qquad \textbf{Eq. 4-9}$$

The electrical storage has an initial storage state at the beginning of each sample day. At the end of each day, the electrical storage must return to its initial value, so as to avoid net accumulation. The initial storage state value is optimised through the model to decide the best initial state for one day utilisation. Otherwise, the initial state can be obtained from the previous day and at the end of the day, the electrical storage must return to be over certain lower limit to protect the equipment.

$$S_0^{ET} = S_T^{ET} = S^{IE} \qquad \textbf{Eq. 4-10}$$

The rates of discharge or charge of electricity cannot exceed the electrical storage discharge and charge limits defined by the battery manufacturer, in order to prevent excessive discharge/charge rates that would damage the battery or reduce its capacity:

$$\sum_j y_{jt} \le D^{E} \qquad \forall t \qquad \textbf{Eq. 4-11}$$

$$\sum_j z_{jt} \le C^{E} \qquad \forall t \qquad \textbf{Eq. 4-12}$$

Similarly, the smart building has a central thermal storage which can be taken as the sum of the sub-thermal storages from each home. Heat stored in the thermal storage at time t is equal to the amount stored at $t - 1$ plus the heat charged minus the heat discharged. The heat loss during the heat storage process is represented in the same way as shown for the

electrical storage. At each time interval, the thermal storage is the total storage amount over all sub-thermal storage in the building.

$$S_{jt}^{T} = S_{j,t-1}^{T} + \delta\eta^{T} g_{jt} - \delta f_{jt} / \eta^{T} \qquad \forall\ j,t \qquad \textbf{Eq. 4-13}$$

The discharged amount cannot exceed the storage amount from the previous time interval.

$$S_{j,t-1}^{T} \geq \delta f_{jt} / \eta^{T} \qquad \forall j,t \qquad \textbf{Eq. 4-14}$$

At each time interval, the thermal storage is the total storage amount over all sub-thermal storage in the building.

$$S_{t}^{TT} = \sum_{j} S_{jt}^{T} \qquad \forall t \qquad \textbf{Eq. 4-15}$$

Stored heat must return to the initial state at the end of the day so that no heat is accumulated over one day. The initial storage state value is also optimised through the model.

$$S_{0}^{TT} = S_{T}^{TT} = S^{IT} \qquad \textbf{Eq. 4-16}$$

The rates of discharge and charge of heat cannot exceed the thermal storage discharge and charge limits based on the type of storage medium, mass and latent heat of the material:

$$\sum_{j} f_{jt} \leq D^{T} \qquad \forall t \qquad \textbf{Eq. 4-17}$$

$$\sum_{j} g_{jt} \leq G^{T} \qquad \forall t \qquad \textbf{Eq. 4-18}$$

Charge and discharge of heat cannot happen at the same time for each home:

$$g_{jt} \leq M X_{jt}^{T} \qquad \forall j,t \qquad \textbf{Eq. 4-19}$$

$$f_{jt} \leq M(1 - X_{jt}^{T}) \qquad \forall j,t \qquad \textbf{Eq. 4-20}$$

4.3.4 Energy Balances

The electricity consumed during each time period is supplied by the CHP generator, electricity received from the electrical storage and grid, minus electricity sent to the electrical storage and grid. The power consumption capacity of some tasks varies over the operation time intervals, e.g. washing machine has different capacity profiles over washing and spinning processes. The electricity consumption is summed over the task operation periods θ.

$$\sum_{i}\sum_{\theta}^{P_{ji}-1} C_{i\theta}X_{ji,t-\theta} = w_{jt} + u_{jt} + y_{jt} + I_{jt} - z_{jt} - E_{jt} \qquad \forall j,t \qquad \textbf{Eq. 4-21}$$

Buying and selling of electricity from/to the grid cannot happen at the same time for each home:

$$I_{jt} \le MX_{jt}^{G} \qquad \forall j,t \qquad \textbf{Eq. 4-22}$$

$$E_{jt} \le M(1 - X_{jt}^{G}) \qquad \forall j,t \qquad \textbf{Eq. 4-23}$$

The heat consumed during each time period is equal to heat supplied by the CHP generator, boiler, heat received from the thermal storage, minus heat sent to the thermal storage.

$$H_{jt} = Qu_{jt} + x_{jt} + f_{jt} - g_{jt} \qquad \forall j,t \qquad \textbf{Eq. 4-24}$$

4.3.5 Starting Time and Finishing time

The operation time of each task must be within the given time window. The starting time of each task cannot be earlier than the given earliest starting time, and must finish before the latest finishing time. Each task of each home has to be started once.

$$H_{jt} = Qu_{jt} + x_{jt} + f_{jt} - g_{jt} \qquad \forall j,t \qquad \textbf{Eq. 4-25}$$

$$\sum_{T_{ji}^{S} \le t \le T_{ji}^{F} - P_{ji}} X_{jit} = 1 \qquad \forall j,i \qquad \textbf{Eq. 4-26}$$

4.3.6 Daily Cost

The total daily electricity cost includes: the operation and maintenance cost of the CHP generator, boiler, electrical storage and thermal storage; the cost of electricity purchased from the grid; the revenue from electricity sold to the grid. If the real-time pricing is applied, the total cost is calculated as in Eq. 4-27.

$$\begin{aligned}
\phi_j = & \sum_t \delta c^N u_{jt} / \alpha && \text{CHP operation cost} \\
& + \sum_t \delta c^N x_{jt} / \eta^B && \text{boiler operation cost} \\
& + \sum_t \delta c^E y_{jt} && \text{electrical storage maintenance cost} \qquad \forall j \qquad \textbf{Eq. 4-27} \\
& + \sum_t \delta c^T f_{jt} && \text{thermal storage maintenance cost} \\
& + \sum_t \delta c_t^I I_{jt} && \text{electricity buying cost from grid} \\
& - \sum_t \delta c^{Ex} E_{jt} && \text{revenue from electricity selling to grid}
\end{aligned}$$

4.4 Lexicographic Minimax Approach to Find a Fair Solution

In a smart building, each home has its own objective to minimise its own daily cost, and the objective of this problem is to minimise the total cost subject to fair cost distribution among homes. The lexicographic minimax approach is applied, which is described in this section.

When all the objectives are equally important, a fair solution tends to have close solution values among objective function values. Lexicographic minimax method is proposed to obtain such a solution. A lexicographic minimax problem is defined as follows:

$$\underset{x \in X}{lex\min} \{\Theta(\hat{\phi}_j(x))\} \qquad \textbf{Eq. 4-28}$$

where $\hat{\phi}_j(x)$ is vector of the objective value under fairness scenario for each home and $x \in X \subset R^n$ is a n-dimensional vector of decision variables, X is the decision space defined by Eq. (4-27) and $\Theta : R^J \to R^J$ maps orders of the component of vectors in a non-decreasing order. With a given vector $e = (e_1 ... e_J)$, $\Theta(e) = (\theta_1(e),...,\theta_J(e))$, where $\theta_j(e) \in \{e_1,...,e_J\}$ is the jth component in vector $\Theta(e)$ and $\theta_1(e) \geq ... \geq \theta_J(e)$. Then in the lexicographic minimax problem, the objective values are minimised in the decreasing order of the objective values, which means the highest objective value is minimised first, then the second and so on. Resulting from the principles of Pareto-optimality, we have:

Theorem 1. The optimal solution of the lexicographic minimax problem in Eq. 4-28, $x^* \in X$, is Pareto-optimal.

The lexicographic minimax problem in Eq. 4-28 is then transformed into a lexicographic minimisation problem in the following theorem in Erkut et al. [186].

Theorem 2. $x^* \in X$ is an optimal solution of problem Eq. 4-28 if and only if it is the optimal solution of the optimisation problem:

$$lex \min \{(\lambda_1 + \sum_{j=1}^{J} d_{1j}, \lambda_2 + \frac{1}{2}\sum_{j=1}^{J} d_{2j}, ..., \lambda_J + \frac{1}{J}\sum_{j=1}^{J} d_{Jj})$$

$$: x \in X, \lambda_n + d_{nj} \geq \hat{\phi}_j, d_{nj} \geq 0, n, j = 1,...,J\}. \qquad \textbf{Eq. 4-29}$$

The model in Eq. 4-29 is developed by optimising the weighted summation of the objectives iteratively and implementing the dual formulations of the models. Iterative algorithm [186] is applied to find the fair solution, let ψ_n^* be the optimal objective value obtained at iteration n. At iteration n, we solve the following MILP model:

$$\text{Min } \psi_n = \lambda_n + \frac{1}{n}\sum_{j=1}^{J} d_{nj}$$

$$\text{s.t. } \lambda_{n'} + d_{n'j} \geq \hat{\phi}_j \qquad \forall j, n' = 1,...,n$$

$$\lambda_{n'} + \frac{1}{n'}\sum_{j=1}^{J} d_{n'j} \leq \psi^*_{n'} \qquad \forall n' = 1,...,n-1 \qquad \textbf{Eq. 4-30}$$

$$d_{n'j} \geq 0 \qquad \forall j, n' = 1,...,n$$

Thus, the solution procedure of the iterative algorithm for the lexicographic minimisation problem is given as follows:

1. Initialise n=1
2. Solve model in Eq. 4-30 subject to Eq. 4-1 to 4-27
3. If n<J let n=n+1Go to step 2 ; If n=J stop

Fairness is defined as the relative cost based on the pre-determined cost boundaries from each home, maximum and minimum energy cost, $\phi_j^{\max}$ and $\phi_j^{\min}$:

$$\hat{\phi}_j = \frac{\phi_j - \phi_j^{\min}}{\phi_j^{\max} - \phi_j^{\min}} \qquad \textbf{Eq. 4-31}$$

where $\phi_j^{\max}$ and $\phi_j^{\min}$ are obtained by:

1. Without using any DERs, electricity is solely bought from grid, heat is generated only from boiler and all tasks start at the earliest starting time, energy cost from each smart home is taken as the maximum energy cost $\phi_j^{\max}$.
2. With DERs available, minimise ϕ_j in Eq. 4-27 for each home *j* to obtain the minimum energy cost from each smart home $\phi_j^{\min}$.

Based of the normalised fairness definition, each smart home wants to minimise its own cost and narrow the difference between the minimum cost $\phi_j^{\min}$. The solution is to be obtained by solving iterative minimisation problem Eq. 4-30 subject to constraints Eq. 4-1 to 4-27.

4.5 Illustrative Examples

The proposed MILP model for fair cost distribution among smart homes is applied for two numerical examples where a microgrid is available to provide energy locally. Example 1 has 10 smart homes while Example 2 has 50 smart homes.

4.5.1 Example 1: 10 Smart Homes

The common DERs shared by the 10 smart homes in Example 1 are given as following, where the capacities are obtained from the energy profiles while the technical parameters and costs are obtained from [65]:

- one CHP generator with a capacity of 4 kW_e and electrical efficiency of 35%. Heat to power ratio is assumed to be 1.3, and natural gas cost of 2.7 *p/kWh*;
- one boiler with capacity of 24 kW_{th} and natural gas cost of 2.7 *p/kWh*;
- one electrical storage unit with a capacity of 4 kW_eh, charge/discharge efficiency of 95%, both discharge limit and charge limit of 4 kW_e, and the maintenance cost of 0.5 p/kWh_e;
- one thermal storage unit with a capacity of 6 $kW_{th}h$; charge/discharge efficiency of 98%, both discharge limit and charge limit of 6 kW_{th}, and the maintenance cost of 0.1 p/kWh_{th};
- a grid connection (electricity import and export are available when operating parallel to grid); the real-time electricity price from half-hour time interval is collected from Balancing Mechanism Reporting System [181] as shown in Figure 3-2; when electricity is sold back to the grid, it is 1 p/kWh_e

The heat demand is generated from the Community's Heating Demand Profile Generator developed by the University of Strathclyde [192]. It is assumed the 10 smart homes are from a flat building built during 1998-2002 and there are 3 types of occupancy, which are listed in Table 4-1. Smart home 4,5,6 are top/ground flats while other homes are mid flats. The sample day is taken as a spring day, the heat demands of the 10 smart homes are shown in Figure 4-1.

Table 4-1 Household occupancy types [192]

	Type 1	**Type 2**	**Type 3**
Household type	A household that at lest one member has a part time job during the morning session.	A household that all members are working on a full time scheme	A household that there is one or more pensioners, disabled persons or unemployed
Unoccupied Period	9:00 - 13:00	9:00 - 18:00	N/A
Smart homes	1,4,7,10	2,5,8	3,6,9

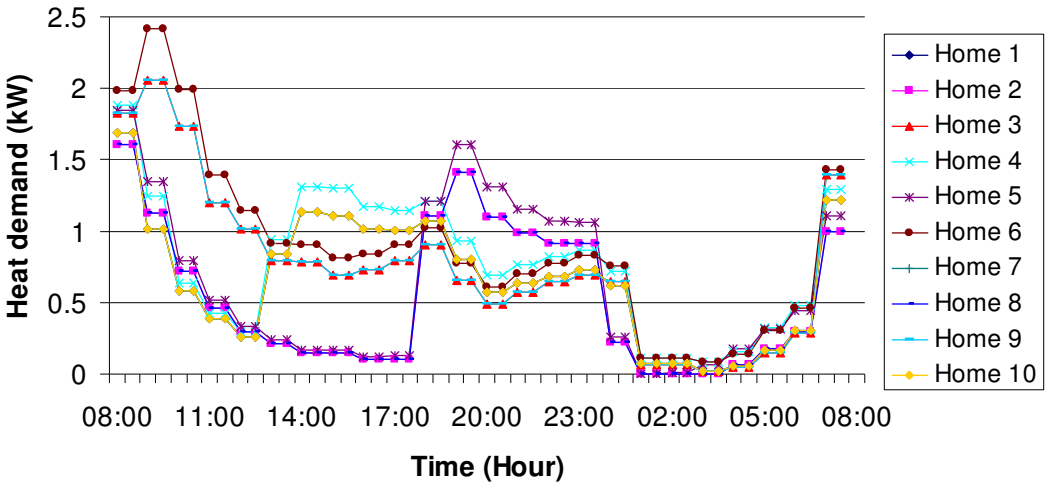

Figure 4-1 Heat demands of 10 smart homes in spring

There are 12 electrical appliances considered to be scheduled in smart homes, which are the same as in Chapter 3 shown in Table 3-1. All tasks, except the dishwasher and washing

machine, have constant power consumption rates during operation, while the electrical profiles for dish washer and washing machine are shown in Figure 3-3.

The earliest starting time for each task of each home is generated randomly based on the modified hourly operation probability distribution given in [183]. It should be noted that not all the tasks need to be operated for each home, so the tasks need to be implemented in Example 1 are assumed as shown in Table 2-1.

Table 4-2 Electrical task of each smart home

Home	Tasks
1	1-12
2	1-6
3	7-12
4	1-8
5	4-12
6	1-12
7	1-4, 9-12
8	1-4, 6-10
9	1-12
10	5-8, 10-12

The power demand of each smart home under earliest starting time baseline is presented in Figure 4-2.

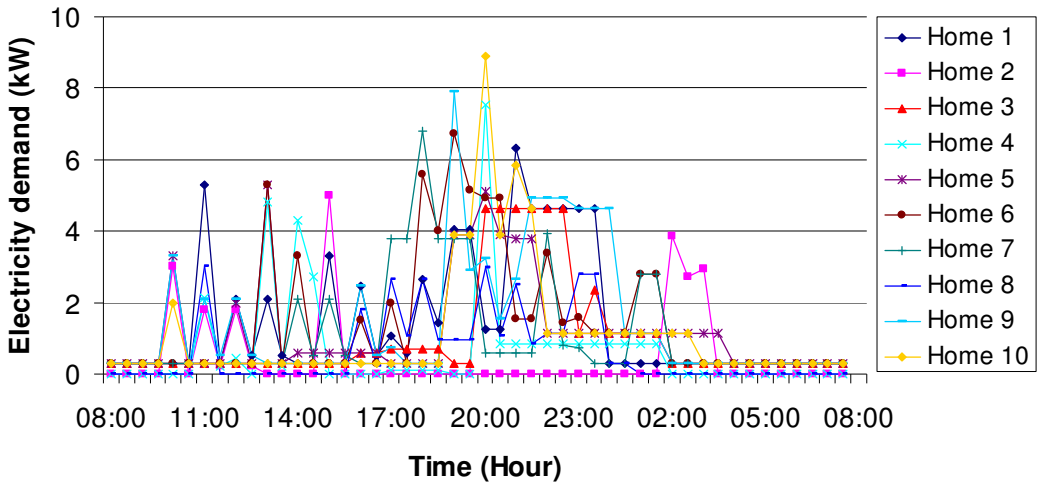

Figure 4-2 Electricity demand of 10 smart homes in spring under earliest starting time

The earliest starting time of each task from each smart home is given in Table 4-3 and the time window length is presented in Table 4-4.

Table 4-3 Electrical task earliest starting time in hour

	Home	1	2	3	4	5	6	7	8	9	10
1	Dishwasher	12	11	-	13	-	18	14	16	11	-
2	Washing machine	16	14	-	11	-	22	22	20	16	-
3	Spin dryer	19	17	-	14	-	25	25	23	19	-
4	Cooker hob	15	10	-	13	10	14	18	11	10	-
5	Cooker oven	11	15	-	20	13	13	-	-	19	20
6	Microwave	21	13	-	20	12	17	-	18	20	10
7	Interior lighting	18	-	20	20	22	19	-	17	20	21
8	Laptop	19	-	17	17	19	21	-	18	19	19
9	Desktop	17	-	16	-	14	19	20	22	20	-
10	Vacuum cleaner	18	-	19	-	20	16	22	21	21	21
11	Fridge	1	-	1	-	1	1	1	-	1	1
12	Electrical car	21	-	20	-	19	18	17	-	21	19

Table 4-4 Electrical task time window length in hour

	Home	1	2	3	4	5	6	7	8	9	10
1	Dishwasher	8	7.5	-	6.5	-	5.5	5	4.5	4	-
2	Washing machine	3	2.5	-	3	-	3	2.5	2.5	2.5	-
3	Spin dryer	5	4.5	-	3.5	-	2.5	2.5	2	1.5	-
4	Cooker hob	1	1.5	-	2.5	3	3.5	5.5	4.5	5	-
5	Cooker oven	1	1.5	-	2.5	3	3.5	-	4.5	5	5.5
6	Microwave	1	1.5	-	2.5	3	3	-	2	1.5	1
7	Interior lighting	6	-	6	6	6	6	-	6	6	6
8	Laptop	6	-	5.5	3.5	5	6	-	4.5	5	5.5
9	Desktop	6	-	4	-	5.5	6	5	3.5	4.5	-
10	Vacuum cleaner	8	-	4.5	-	5.5	6	6.5	7	7.5	8
11	Fridge	24	-	24	-	24	24	24	-	24	24
12	Electrical car	10	-	7	-	4	8	8.5	-	9.5	10

The total energy demand of the 10 smart homes under earliest starting time is given in Figure 4-3.

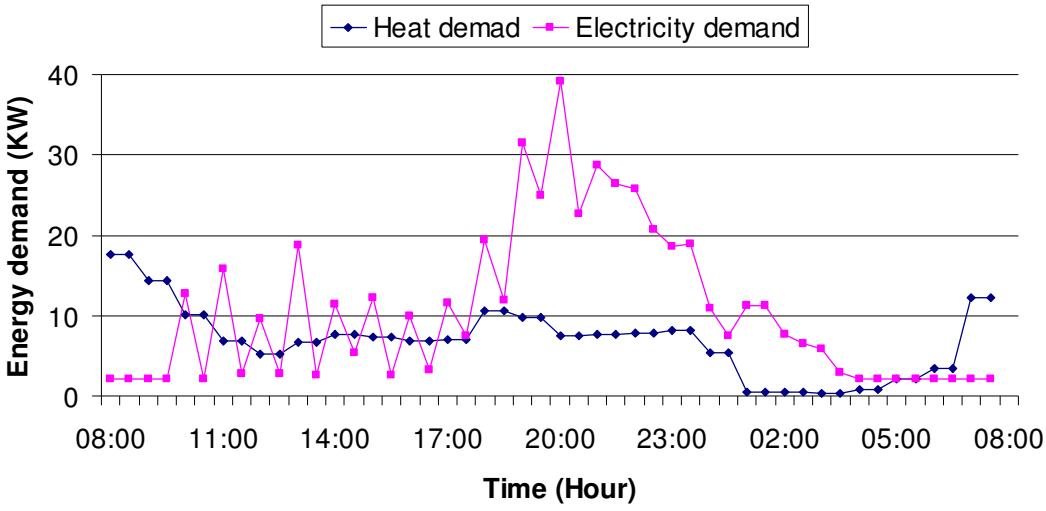

Figure 4-3 Total energy demand of 10 smart homes in spring under earliest starting time

4.5.2 Example 2: 50 Smart Homes with Different Types of Household

Example 2 has 50 smart homes in a smart building and has the same DERs as in Example 1 while the capacities are 5 times of those in Example 1. There are 9 homes as Top/Ground (TG) flats and 41 as Middle (M) flats. It is assumed that the 9 TG homes include 3 homes from each type of occupancy from Table 4-1, and the 41 M homes have 14 homes from type 1, 14 homes from type 2 and 13 homes from type 3. Typical heat demands in winter (Jan 1st –Apr 1st) for each type (T1, T2 and T3) of homes are given in Figure 4-4. The rest of homes have similar demand patterns while time windows have been shifted slightly or multiplied with numbers around 1.

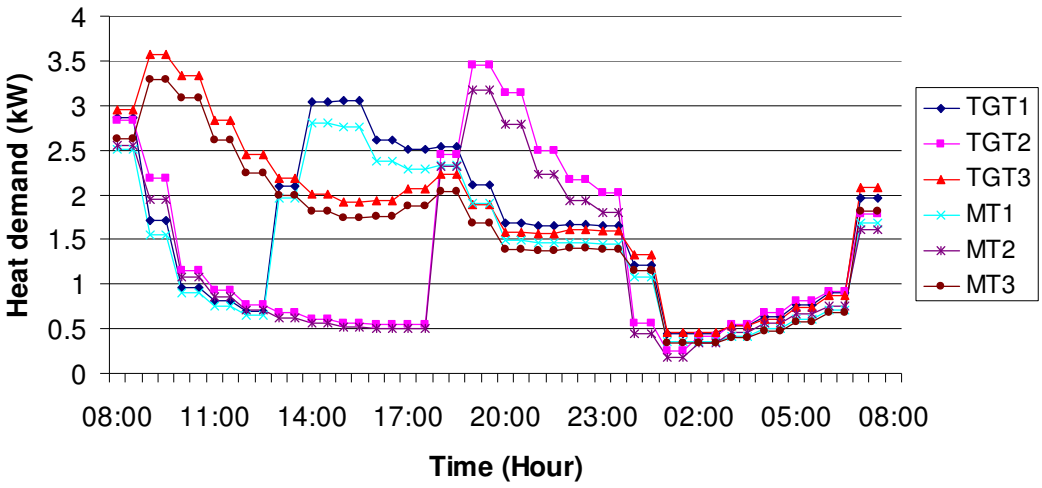

Figure 4-4 Heat demands of typical homes in winter

Households have been further classified into detail types by [192] as given in Table 4-5 for electricity demand generation, and the number of different types of household are listed. The national ownership of the electrical appliances is applied in this numerical example and the usage pattern and probability of occurrence vary among different detail types of household. And the ownership of electrical car is assumed to be 50% for the example building household. In Example 2, the occurrence of each task and the earliest starting time are generated randomly based on the given probabilities from different households. The operation time window length is generated randomly but the latest ending time is

guaranteed to be before the end of the time horizon. Total electricity and heat demands for a winter day are shown in Figure 4-5.

Table 4-5 Detail types of household

Detail type of household	No. of household
Single adult	12
Single Pensioner Adult	8
Two adults	10
Two adults with children	8
Two pensioners	2
Two adults and at least 1 pensioner	5
Three adults	5

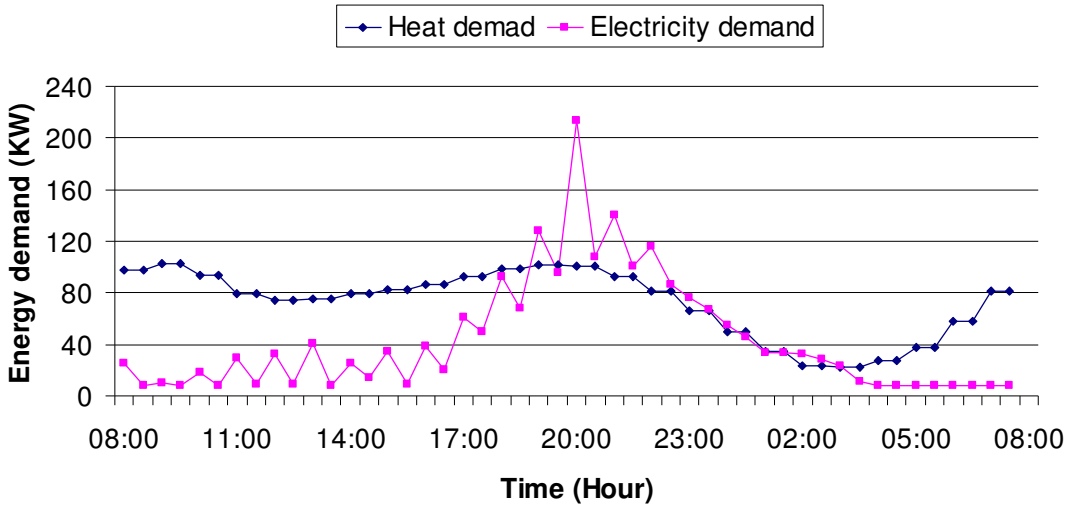

Figure 4-5 Total energy demand of 50 smart homes in winter under earliest starting time

4.6 Computational Results

Computational results are presented in this section, in which the computational environment is given first and the results from the two illustrative examples are presented. Detail optimal results of each smart home from Example 1 are provided in tables and

figures, while only total optimal cost and energy balances are presented for Example 2 because of the big number of smart homes involved.

4.6.1 Computational Environment

Lexicographic minimax method is applied for the fair cost distribution problem in the two numerical examples. The DER operation and electrical tasks starting time are both scheduled. The scheduling horizon for both examples is from 8 am in the morning until 8 am on the next day.

The developed MILP model is implemented using CPLEX 12.4.0.1 in GAMS 23.9 [128] on a PC with an Intel Core 2 Duo, 2.99 GHz CUP and 3.25GB of RAM. The model statistics of the two examples are presented in Table 4-6, where numbers of equations, continuous and discrete variables and average CPU time of each iterative run are presented. For the two examples, the optimality gap is 1%. It is evident that the proposed MILP model is able to provide fair cost distribution among smart homes in both numerical examples with modest computational difficulties.

Table 4-6 Model statistics

Example	Equations	Continuous variables	Discrete variables	Average CPU (s) per iteration	Min. CPU (s)	Max. CPU (s)
1	8,285	12,040	5,712	24	11	61
2	39,904	57,712	25,824	73	29	322

4.6.2 Example 1 Results

If only total cost of the 10 homes is minimised as the model presented in Chapter 3, the cost of each home is given in Table 4-7. The upper bound of the cost of each smart home is achieved based on the case when all heat is generated from boiler and electricity is solely bought from grid. Also all tasks start at their earliest starting time. The cost lower bound of each smart home is obtained from minimising energy cost of each single smart home where microgrid is available. Values of both the two bounds are listed in the table.

Table 4-7 Cost of each home from minimising total cost and fairness concern

Home	Max (£)	Min (£)	Cost (£)	Objective values	Fair cost(£)	Optimal objective values
1	2.95	1.95	2.07	0.12	2.08	0.1335
2	1.14	0.84	0.95	0.37	0.88	0.1335
3	2.06	1.55	1.60	0.10	1.62	0.1335
4	1.81	1.22	1.33	0.19	1.30	0.1335
5	2.53	1.73	1.91	0.23	1.84	0.1335
6	3.54	2.1	2.24	0.10	2.29	0.1337
7	2.81	1.56	1.62	0.05	1.73	0.1335
8	1.57	1.01	1.13	0.21	1.08	0.1335
9	2.92	1.98	2.15	0.18	2.11	0.1335
10	2.38	1.56	1.59	0.04	1.67	0.1335
Total	23.71	15.50	16.58	-	16.60	-

When only the total cost is minimised without considering the fair cost distribution, the minimum total cost is £16.58. Since cost from respective home is not considered, the cost is distributed without fairness concern as shown. The obtained cost from each home is compared under the proposed fairness concept, which is presented in the table. The total cost is distributed unfairly among homes, as the normalised objectives range from 0.04 to 0.37.

The optimal results from lexicographic minimax approach under the fairness concern are also presented in Table 4-7. The total cost is £16.60, which is very close to the minimum total value £16.58. The costs are fairly distributed according to the contribution from each home. The optimal objective values are the same as 0.1335 except minor difference from home 6. In total there is 30% savings for the whole smart building compared with the upper bound of total cost.

Figure 4-6 presents the optimal electricity demand of each home under task starting time scheduling. Compared with Figure 4-5, the electricity demands are shifted to the night time where the tariff is lower. The tasks are scheduled based on the real-time electricity pricing and given task operation time window.

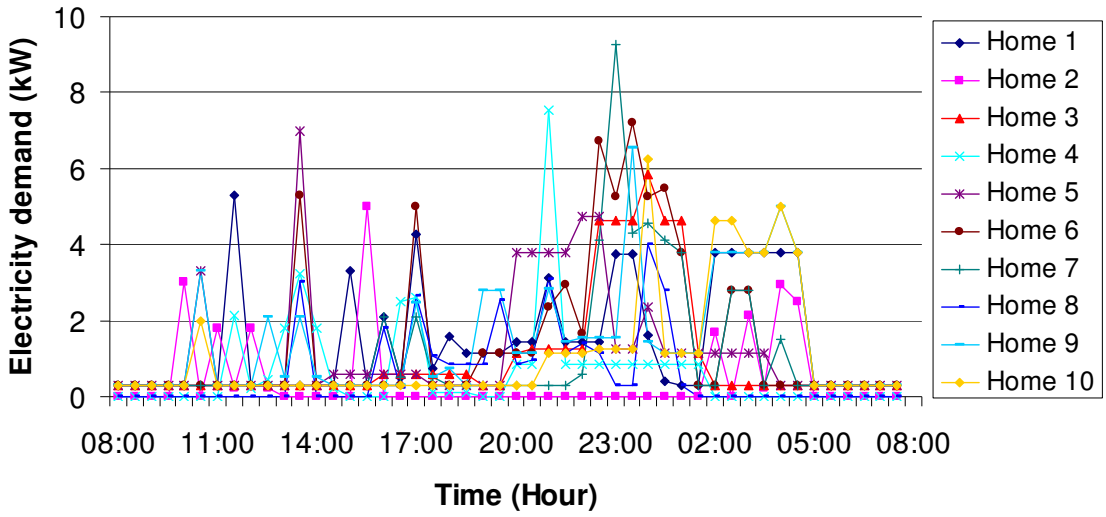

Figure 4-6 Optimal electricity demands of Example 1

The total electricity balance of the 10 homes is shown in Figure 4-7. CHP is providing constant maximum output 4 *kW* most of the time except during night time where heat demand is low, electrical storage is charged when tariff is low and discharged when it is high. Compared with the total electricity demand in Figure 4-3., the peaks of the total power demand have been moved to the night time instead of evening. Also the peak demand has been reduced from 39 *kW* to 32 *kW*. As defined in the model, each single home, electricity can not be charged and discharged at the same time. In this example, total electricity is charged and discharged at different time intervals here. However, based on the given assumption on how the electrical storage is used for homes, there is possibility that the total charge and discharge of electricity can occur simultaneously. The change and discharge from the electrical storage system for each home are not the same as the real total amount charge and discharge to the electrical storage in practice. Most likely, only the amount of usage is counted in the system as deposit money in a bank and then cost is calculated based on the total usage over the day. The electrical storage is shared in such way because of the different energy demand patterns among homes. Homes store the electricity obtained from CHP in the electrical storage when its electricity demand is low while heat demand is high. The stored electricity is discharged when the home has high

electricity demand. For the thermal storage, the charge and discharge follow similar behaviour. There is no electricity sold back to the grid in the example.

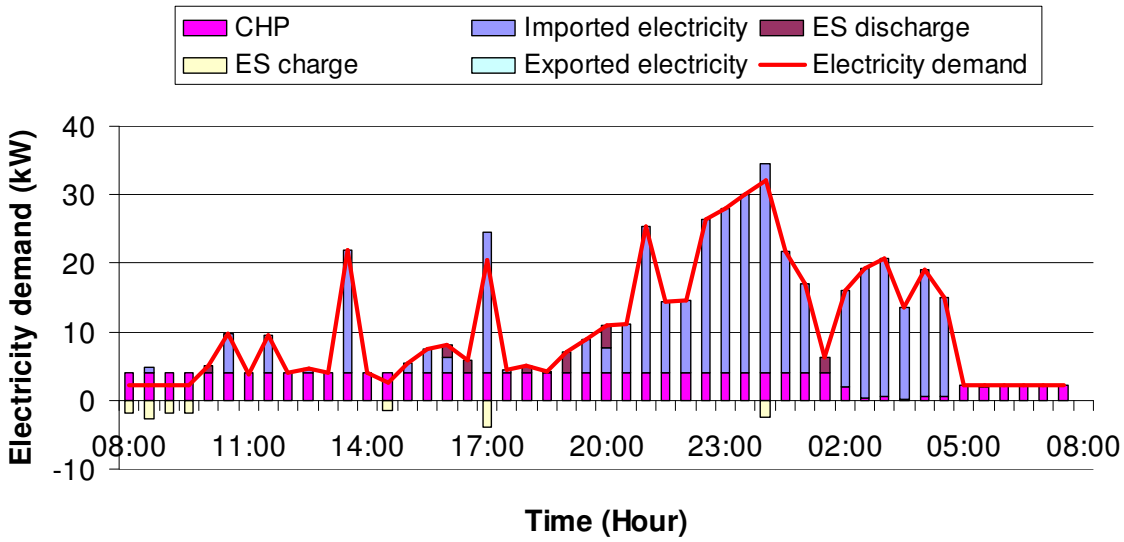

Figure 4-7 Electricity balance of Example 1 under fairness concern

Figure 4-8 presents the heat balances of the 10 homes under fairness concern. CHP becomes the main heat provider for the smart homes, while the remaining demand is supplied by the boiler. Thermal storage is used quite frequently in this example. As seen from the figure, for some hours thermal storage charge and discharge happens at the same time. It is because the thermal storage works as bank system for heat deposit for the 10 homes as discussed earlier for the electricity balance part.

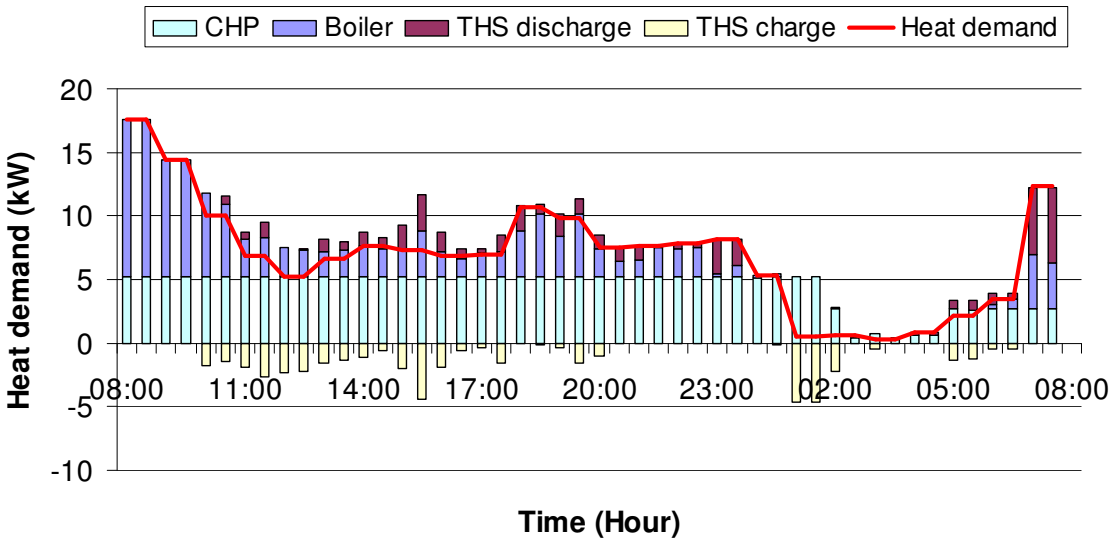

Figure 4-8 Heat balance of Example 1 under fairness concern

4.6.3 Example 2 Results

The optimal results of Example 2 are given in Table 4-8, where the total upper bound cost is £133.27 and total lower bound cost is £95.88. The minimum total cost without considering fair cost distribution is £101.06. In this example, the objective value of respective home varies within the range of 0.1388 to 0.1398 which is very narrow. The average of the objectives is 0.1394 and the standard deviation is 0.000228. In this work, lexicographic minimax approach is applied to find a fair solution under the condition that all the objectives are equally important. As expected, close solution values among objective function values are obtained in the two examples. The total cost is very close to the minimum total cost without fairness concern. The total savings is 24% which is obvious cost savings compared with the upper bound cost.

Table 4-8 Optimal results of Example 2

Objective value	0.1388 to 0.1398
Average of objective values	0.1394
Standard deviation of objective values	0.000228
Total cost (£)	101.10
Total savings (£)	32.17
Percentage	24%

Figure 4-9 and Figure 4-10 present the optimal energy balances of Example 2. As in Example 1, CHP is again providing energy constantly except several hours at the end of the time horizon. But based on the given tasks operation time window, Example 2 can only move the electricity peak hour from 20 o'clock to about midnight. Electrical tasks cannot be spread over night as done in Example 1. So, although heat demand ratio is high during winter time than spring time, CHP still does not generate energy at full capacity during the last few time periods. Fair cost distributions result from the electrical task operation time scheduling from each home as well as their competition for the cheap energy generated from CHP and usage of energy storages. No electricity is sold back to the grid again. Electrical storage is not used as much as thermal storage. As can be seen from the two examples, when CHP is utilised the heat to electricity ratio of the energy demand determines the equipment operation. The time window length results from living habits affect the task scheduling, equipment operation and final cost savings. Also if there are varieties of different living styles and more flexible tasks, the total savings can be further increased.

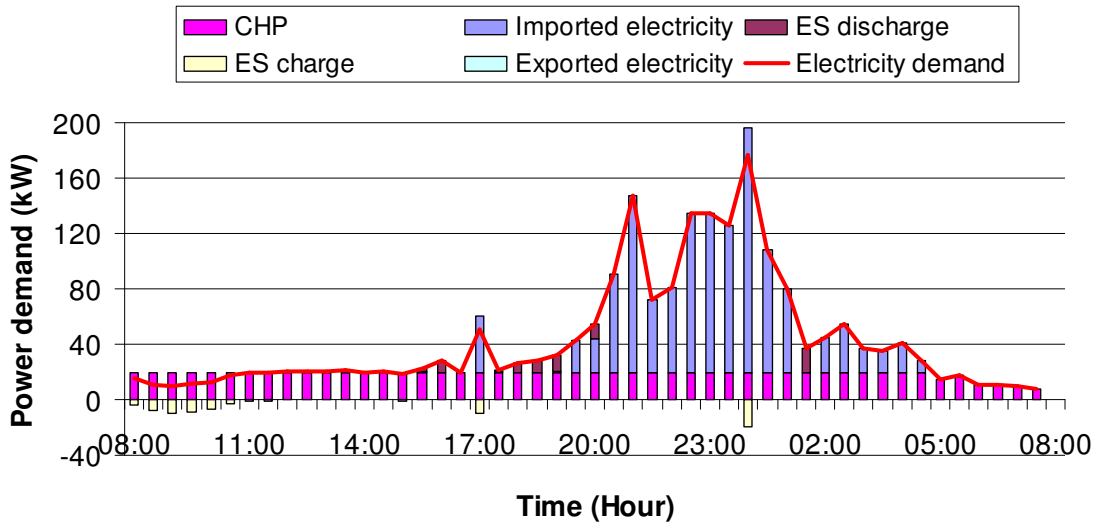

Figure 4-9 Electricity balance of Example 2 under fairness concern

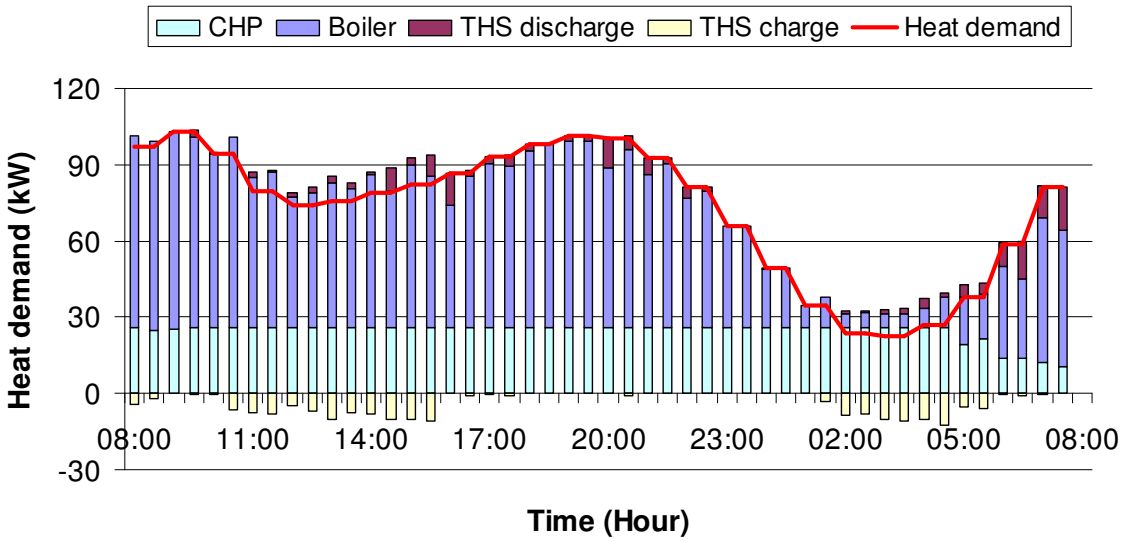

Figure 4-10 Heat balance of Example 2 under fairness concern

4.7 Concluding Remarks

An MILP model has been proposed for fair cost distribution among multiple smart homes in a building with a microgrid, using a lexicographic minimax optimisation approach. Two examples of 10 homes for a spring day and 50 homes for a winter day have been studied.

Twelve domestic electrical tasks and equipment operation have been scheduled based on given time window, real-time half-hourly grid electricity prices and given objective fairness. Significant cost savings have been obtained for the two numerical examples.

More importantly, this work focuses on the energy cost of each smart home as a cooperation participant in a building with a common microgrid. By applying lexicographic minimax approach, close solutions among objective functions have been obtained. However, the fair cost distribution depends heavily on the objective fairness definition. Different fairness criteria should be selected accordingly based on participants' preferences. Under certain circumstances, priorities should be assigned to some participants for particular reasons, such as poverty or location.

When the domestic task scheduling is implemented in real life, it could also affect people's behaviour and longer time windows are preferred to obtain more cost savings. CHP technology is generating cheap energy in the two examples and smart homes are competing with each other to obtain more energy from CHP rather than buying electricity from grid and getting heat from boiler. More DERs, such as wind generator, solar panel and heat pumps, can easily be added to the model to achieve higher cost savings or reduce gas emissions.

Chapter 5 Optimal Scheduling of Electric Vehicle Battery Usage with Degradation

In the previous two chapters, electric vehicles (EVs) are considered as household electricity consumption appliances and batteries can only be charged at home and discharged for transport utilisation. As energy storage devices, batteries of EV are suggested to be used for domestic utilisation and providing 'vehicle-to-grid' (V2G) service when applicable. However, the increase usage of battery results in increasing the battery degradation and decreasing the battery performance.

In this chapter, an MILP model is proposed to minimise the total electricity cost and battery degradation cost and try to maintain the demand under pre-specified threshold by scheduling the charge and discharge operations of EV battery while satisfying the electrical demands of EV and household power consumption.

5.1 Introduction and Literature Review

Plug-in hybrid electric vehicles (HEVs) and battery electric vehicles (BEVs) have been popular during the past decade due to the decrease in greenhouse gases and operation cost. They are potentially important to transform the transport sector towards sustainability by utilising a more diverse set of power sources from centralised electric power plants rather than petroleum [193]. Battery of electric EVs is suggested to be used for off-vehicle use, which provides V2G service. The benefits include peak load shifting and providing distributed grid-connected storage as a reserve against unexpected outages [194], as well as other ancillary services to the electricity network, where the peaks can be reduced and load can be levelled [195]. During peak power demand time, there is high potential of exporting electricity back to the grid and the distribution system needs to be upgraded for the bidirectional power flow [196]. Mean while, the broad usage of EVs results in a significant increase of load from grid which challenges the current power grid. They can impact the distribution grid through aspects of driving patterns, charging characteristics, charge timing and vehicle penetration [197]. EV faces two challenges: high cost from battery and battery charging to the utility grid interconnection [198]. Battery cost represent one-third of the EV

cost, although by reusing the partially worn out batteries shows a promising potential to promote EV economically [193], battery costs must drop significantly to obtain high market penetration [199].

Electric vehicle charging should be managed and coordinated to avoid power losses and lowering power quality and prolong the EV life time. The EV cycle life is defined as the number of complete charge-discharge cycles that the battery can perform before its nominal capacity falls below 80% of its initial rated capacity [200]. Huang et al. [201] integrate the realistic zoned characteristics with detailed residential model to anticipate the local distribution level effects of EVs on residential households. The work of [202] indicates EV charging can be added to planned demand side management schemes in the V2G concept. Binary PSO is applied for the scheduling of EV battery storage in a parking lot for V2G usage in [203], and the optimal scheduling of selling and buying times is provided to a fleet of vehicles. PHEVs are integrated into a smart building for energy and comfort management by Wang et al. [204], and the building become more economical and more reliable. In [205] a price-based demand response algorithm is proposed for EV charging schedules construction with day-ahead, given electricity price and trip schedule. Sheikhi et al. [206] optimise the start time of charging and the duration to obtain peak load shaving and minimum cost with a stochastic EV charging method. Ahn et al. [207] present an optimal decentralised charging control algorithm for EVs connected to smart grid to shift load with the objective of minimising electricity generation costs and emissions. Concept of real-time scheduling techniques for EV charging is proposed in [208] which minimises the impact of the power grid while guarantees the individual charging requirement. In [209], the authors examine how to implement demand side management to optimise the charging cycles of an EV and obtain the maximum financial savings with maximum renewable energy consumed and reduce both peak load demand and demand from thermal generation plants. The optimal EV battery charging scheduling is presented in [210] to achieve peak shaving and flat load profile for residential energy consumption. Sortomme and El-Sharkawi [211] develop a V2G algorithm to optimise energy and ancillary services, load regulation and spinning services, to maximise aggregator and customer profits and peak load reductions are also obtained. EV charging and discharging problem is addressed by He

et al. [212], and they formulate a globally optimal scheduling scheme and a locally optimal scheduling scheme to handle the problem of large population and random arrivals of EVs. A decentralised and a centralised charging strategies are both presented by Han et al. [213], and current state of charge (SOC), battery capacity, connecting time and electricity grid constraints are considered. Ota et al. [214] address smart charging control in an autonomous distributed V2G control scheme. Balancing control is applied to manage the battery SOC.

On the other hand, the increase of usage of battery results in increasing the battery degradation and decreasing the battery performance [215]. These effects should be considered to prolong the life-time of battery. Alan [216] proposes an aging model for lithium ion batteries in EVs based on theoretical models of crack propagation. Optimised partial EV charging method is presented in [217], which uses the next day vehicle usage prediction to charge the battery and it shows both battery energy capacity lifetime and power lifetime are prolonged. Cost of EV battery wear from V2G utilisation is analyzed by Zhou et al. [200], and the correlation between the number of charge cycles and EV battery wear is established. Authors of [218] present that the participation in V2G service influences the battery capacity degradation as a function of number of cycles, operation temperature, rates of charge and discharge, the depth of discharge (DOD) and total energy withdrawn. Guenther et al. [219] study the EV battery aging, calendar aging and cycle aging, under V2G scenario. Lyon et al. [220] investigate ‘smart charging’ policy for EV by shifting charging times. A genetic optimisation algorithm is applied in [221] to optimise the charging behaviour of a PHEV with battery aging concern based on cyclic and floating aging components. EV charge is optimised for simultaneous reduction of energy cost and battery degradation with a multi-objective GA over 24-hour drive cycle in the work of [222]. While in [223], the charging pattern for a fleet of PHEVs is optimised with the concern of both daily energy cost and battery degradation. Lunz et al. [224] show that intelligent charging algorithms can reduce electricity consumption costs and decrease battery depreciation for PHEV but demand peak is not considered. In the work of [225], EV charge is optimised with battery degradation concerns, in which energy capacity fade and power fade due to temperature, SOC and DOD are included.

In this chapter, an MILP model is proposed to minimise the total electricity expense of a residential area where EV battery is used as electricity storage when it arrives home as well as providing V2G service. EV battery operation is scheduled based on the real-time electricity (buying and selling) prices and electricity demand of each home in order to reduce the peak demand and avoid peak demand charge penalty from grid. Also battery degradation results from increased usage is considered, the battery degradation cost in included in the model as a function of SOC level. The charging time is selected based on the SOC besides electricity buying price from grid, to reduce the degradation cost which helps prolong the battery life time.

5.2 Problem Description

In this work, the EV battery can be used for domestic appliances rather than being used solely for transport. The battery can also provide V2G service when it benefits from buying electricity at low price while selling electricity back to the grid at a higher price. The charging time of EV batteries are scheduled to obtain minimum cost while limit the peak load. For a small community or parking area where a number of electric vehicles are located, batteries of electric vehicles are charged from the grid. It is assumed batteries can only be charged when they are in such area. Vehicle trip information is available and the battery storage status is provided to the model. The charging time is flexible over the given time period under given real-time electricity tariff. To minimise the total electricity cost, batteries are supposed to be charged during low tariff time periods. However, in that case, high total electricity demand outages could occur at those time periods which will affect the stability of the grids. In order to avoid such occasion, two demand boundaries from grid are applied, i) power ceiling which cannot be exceeded and ii) peak demand threshold, where high peak demand cost is charged over the electricity consumption above the agreed consumption threshold. Then the charging time of different electric vehicles will be scattered to maintain the demand under allowed charging rate and within given demand bounds. Considering the intensive use of battery in household and V2G, an MILP model is supposed to provide this charging scheduling for load shifting and cost minimisation together with minimising degradation cost.

The overall problem can be stated as follows:

Given are (a) a time horizon split into a number of equal intervals, (b) electricity demand of each home, (c) charge and discharge limit rates for EVs, (d) real-time electricity prices from grid and peak demand charge price to the over-threshold amount, (e) peak demand threshold from grid, (f) total power ceiling, (g) EV transport demand, (h) EV battery degradation cost based on SOC, (i) time intervals when EVs are home and away.

Determine (a) EV charge/discharge plan at home, (b) electricity bought from grid, (c) electricity sold to grid.

So as to minimise the total electricity and degradation costs.

5.3 Mathematical Formulation

The EVs charging problem is formulated as an MILP model. The aim of the work is to minimise the total electricity and degradation costs and try to maintain the demand under agreed thresholds by scheduling the charge and discharge operation of EV batteries while satisfying the electricity demands of EVs and household power consumption. The model determines the electricity buying and selling schedule and the battery charge/discharge schedule together with the rate at which they happen. Battery self-discharge and capacity loss are not considered in this work.

5.3.1 Nomenclature

Indices

i EV battery/home

j SOC level

t time interval

t_{it}^{c} time intervals t when EV i is away from home

t_{it}^{h} time intervals *t* when car *i* stays at home

Parameters

b_j battery charge cost of level *j (£/kWh*)

c_t^{Ex} electricity selling price to the grid at time t *(£/kWh*)

C_i nominal capacity of EV battery *i* (*kWh*)

D^E maximum EV battery discharge rate (*kW*)

G^E maximum EV battery charge rate (*kW*)

L_{it} electricity demand of home *i* at time interval *t* (*kW*)

p extra peak demand charge over the agreed threshold *(£/kWh*)

S_i^I initial state of EV battery *i* (*kWh*)

V_{it} driving electricity demand of EV *i* at time interval *t (kWh*)

$SOC^{\min}$ minimum SOC of EV battery (%)

$\overline{SOC_j}$ SOC at level *j* (%)

δ time interval duration (*hour*)

μ peak demand ceiling value (*kW*)

Variables

d_{it} degradation cost of EV battery *i* at time *t* (£)

E_{it} electricity exported to the grid for home i at time t (kW)

I_{it} electricity bought from grid for home i at time t (kW)

S_{it} electricity storage of EV battery i at time t (kWh)

y_{it} discharging rate of EV battery i at time t (kW)

z_{it} charging rate of EV battery i at time t (kW)

ξ_t extra electricity load from grid over the agreed threshold κ at time t (kWe)

ϕ total cost, objective value (£)

SOC_{it} state of charge of EV battery i at time t (%)

$SOCj_{itj}$ state of charge of EV battery i at time t from level j (%)

Binary Variables

W_{it} 1 if EV battery i is charged at time t, 0 otherwise

Y_{it} 1 if EV battery i is discharged at time t, 0 otherwise

Z_{itj} 1 if EV battery i at time t is at SOC status j level, 0 otherwise

5.3.2 Charge and Discharge Constraints

In order to protect the battery, the rate of discharge or charge should be under discharge or charge limit defined by the battery manufacture:

$$y_{it} \le D^E Y_{it} \qquad \forall i,t \qquad \textbf{Eq. 5-1}$$

$$z_{it} \le G^E W_{it} \qquad \forall i,t \qquad \textbf{Eq. 5-2}$$

Charging and discharging cannot happen at the same time for each EV battery:

$$Y_{it} + W_{it} \le 1 \qquad \forall i,t \qquad \textbf{Eq. 5-3}$$

5.3.3 EV Battery Storage Constraints

Electricity stored in the electrical storage at time *t* is equal to the amount stored at *t–1* plus the electricity charged minus the electricity discharged. No electricity loss is considered here.

$$S_{it} = S_{i,t-1} + \delta z_{it} - \delta y_{it} \qquad \forall i, t > 1 \qquad \textbf{Eq. 5-4}$$

$$S_{it} = S_i^I + \delta z_{it} - \delta y_{it} \qquad \forall i, t = 1 \qquad \textbf{Eq. 5-5}$$

At the end of the time horizon, the storage should be equal to the initial state in order to avoid net accumulation for the next time horizon.

$$S_{i0} = S_{iT} = S_i^I \qquad \forall i \qquad \textbf{Eq. 5-6}$$

5.3.4 Electricity Demand Constraints

Electrical car travel demand is provided by the EV battery:

$$\delta y_{it} = V_{it} \qquad \forall i, t \in t_{it}^c \qquad \textbf{Eq. 5-7}$$

When electrical car is at home, domestic electricity demand can be fulfilled by the EV battery and/or power grid. Electricity can be sold to the grid or stored in the battery:

$$y_{it} + I_{it} = L_{it} + z_{it} - E_{it} \qquad \forall i, t \in t_{it}^h \qquad \textbf{Eq. 5-8}$$

When EV is away from home, domestic demand can only be provided by the grid:

$$I_{it} = L_{it} \qquad \forall i,t \in t_{it}^{c} \qquad \textbf{Eq. 5-9}$$

When EV is away from home, there is no charging process:

$$z_{it} = 0 \qquad \forall i,t \in t_{it}^{c} \qquad \textbf{Eq. 5-10}$$

5.3.5 SOC Constraints

SOC calculation is based on the nominal battery capacity, it is assumed to be constant, although the capacity decreases with the battery aging. The electricity storage cannot exceed the battery capacity. And at any time period, SOC must be greater than the minimum SOC to protect the battery.

$$SOC_{it} = S_{it} / C_i \qquad \forall i,t \qquad \textbf{Eq. 5-11}$$

$$S_{it} \le C_i \qquad \forall i,t \qquad \textbf{Eq. 5-12}$$

$$SOC_{it} \ge SOC^{\min} \qquad \forall i,t \qquad \textbf{Eq. 5-13}$$

The SOC of battery can be classified to respective levels according to its value as shown in the Table 5-1, and the battery charge amount depends on the selected level. If any level is not selected, then no electricity is charged in that interval. Only one level can be selected.

Table 5-1 Battery cycle cost from different SOC

Level	SOC	Degradation cost per cycle (£)	Degradation cost per *kWh* charged (*p/kWh*)
1	20%-40%	0.61	3.2
2	40%-60%	0.41	2.8
3	60%-80%	0.24	2.5
4	80%-100%	0.14	3.0

$$\overline{SOC}_j Z_{itj} \le SOCj_{i,t-1,j} \le \overline{SOC}_{j+1} Z_{itj} \qquad \forall i,t,j \qquad \textbf{Eq. 5-14}$$

$$\sum_j SOCj_{itj} = SOC_{it} \qquad \forall i,t \qquad \textbf{Eq. 5-15}$$

$$\sum_j Z_{itj} = 1 \qquad \forall i,t \qquad \textbf{Eq. 5-16}$$

5.3.6 Electricity Demand Threshold Constraints

When the total electricity demand is over the agreed threshold, peak demand charge applies. Extra cost is charged over the amount that exceeds the threshold.

$$\xi_t \geq \sum_i I_{it} - \kappa \qquad \forall t \qquad \textbf{Eq. 5-17}$$

The electricity demand cannot exceed the maximum load of the household connection.

$$\sum_i I_{it} \leq \mu \qquad \forall t \qquad \textbf{Eq. 5-18}$$

5.3.7 Degradation Cost Constraints

When battery starts charging, degradation cost per cycle is counted based on the storage status of the previous time interval. If battery is charged continuously, degradation cost is only counted once at the beginning of the charging process.

$$d_{it} \geq \sum_j Z_{itj} b_j - (1 - W_{it} + W_{i,t-1}) \qquad \forall i,t \qquad \textbf{Eq. 5-19}$$

5.3.8 Objective Function

Objective function is to minimise the total cost, which includes the electricity cost from grid, peak demand charge cost and degradation cost minus the electricity revenue from selling electricity back to the grid.

$$\cos t = \sum_{it} \delta c_t^I I_{it} + \sum_t \xi_t p + \sum_{it} d_{it} - \sum_{it} \delta c_t^{Ex} E_{it} \qquad \textbf{Eq. 5-20}$$

5.4 Case Study

In this work, 20 households in a residential area are involved and each household is assumed to have an EV with a capacity of 24 kWh and which are full at the beginning of the time horizon. A laminated lithium-ion battery pack from Nissan Leaf is used. The basic information is provided in Table 5-2.

Table 5-2 Nissan Leaf battery pack specification [226]

Type	Laminated lithium-ion battery
Cost	$18,000
Life span	Estimate over 10 years or Life cycle is over 2000
Running range	160 *km*
Total capacity	24 *kWh*
Charging capacity	3.3 *kW*
Power output	Over 90 *kW*
Cathode material	$LiMn_2O_4$ with $LiNiO_2$
Anode material	Graphite

MATLAB code is applied to generate the EV travelling energy demands and car arrival times. The 20 car daily travelling demands are generated randomly from normal distribution within the range of 2-18 *kW*h per day, which is presented in Figure 5-1.

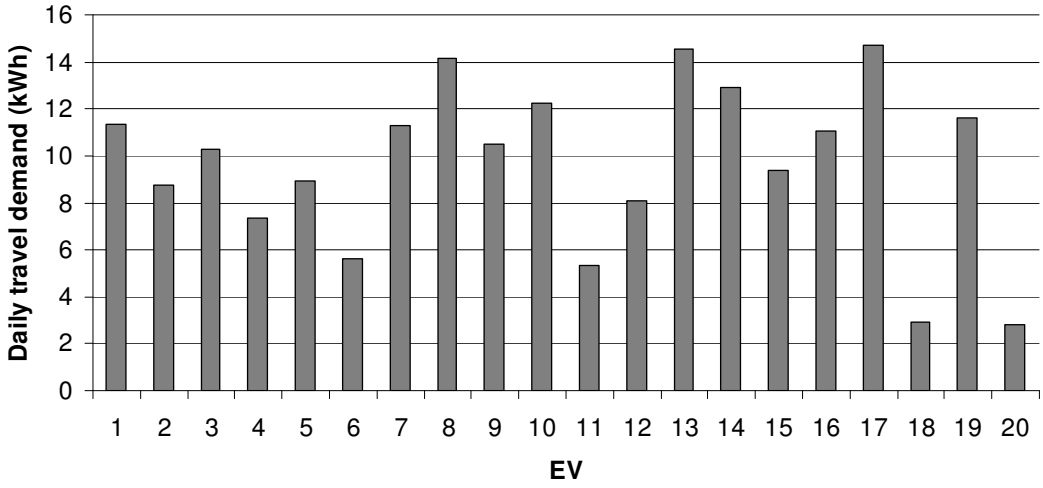

Figure 5-1 EV daily travel demand

Then, the hourly energy demand profile during EV travelling time is calculated by dividing the total daily demands with the total travelling hours. Although most probably the car travel only takes place during several separate time intervals within the total travelling time rather than being continuous, the EV travelling demands are assumed to be evenly distributed over the time horizon. The EV travelling demands distribution over travelling time does not affect the household usage and electricity charging from the grid. For all the houses, it is assumed that each of them has the same living habits during the five weekdays, which means they have the same EV travelling demand and domestic electricity demand over the five days. At the beginning of the 5 days, all batteries are assumed to be fully charged. To protect the battery, the SOC cannot drop below 20% at any time. The total travelling demand of the 20 EVs over the 5 days is 969 *kWh*.

It assumes all EVs start travelling from 8 am. In order to guarantee there is enough charging time, the arrival time has to be before 2 am which is 6 hours before the start of next travel. The car arrival times are generated based on the distribution of hourly probability for lighting in [183]. The number of car arrival times during each hour for the 20 EVs is given in Figure 5-2.

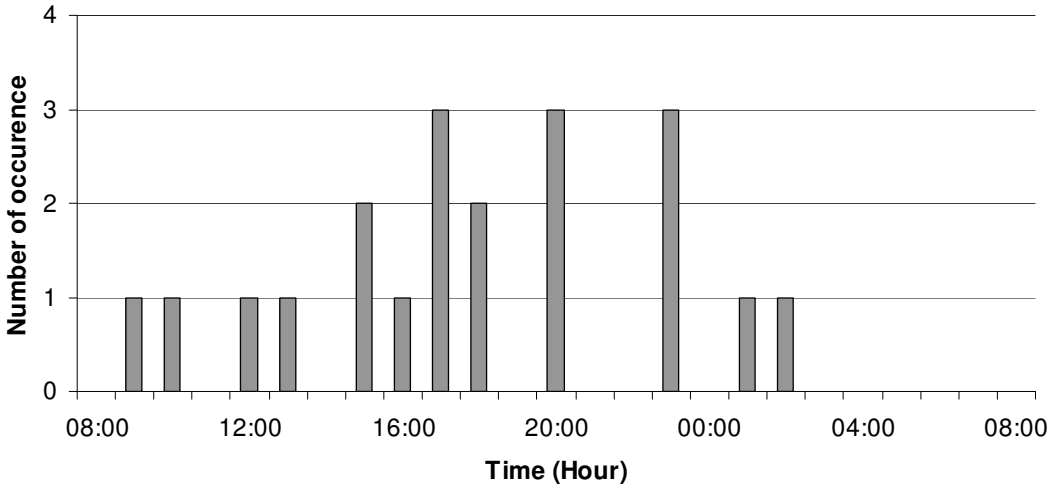

Figure 5-2 Number of occurrence of EV arriving

As soon as a car arrrives at home, it is assuemd to stay there until 8am net morning. Figure 5-3 shows the number of cars staying at home during each time interval for a single day, and all the five days have the same pattern.

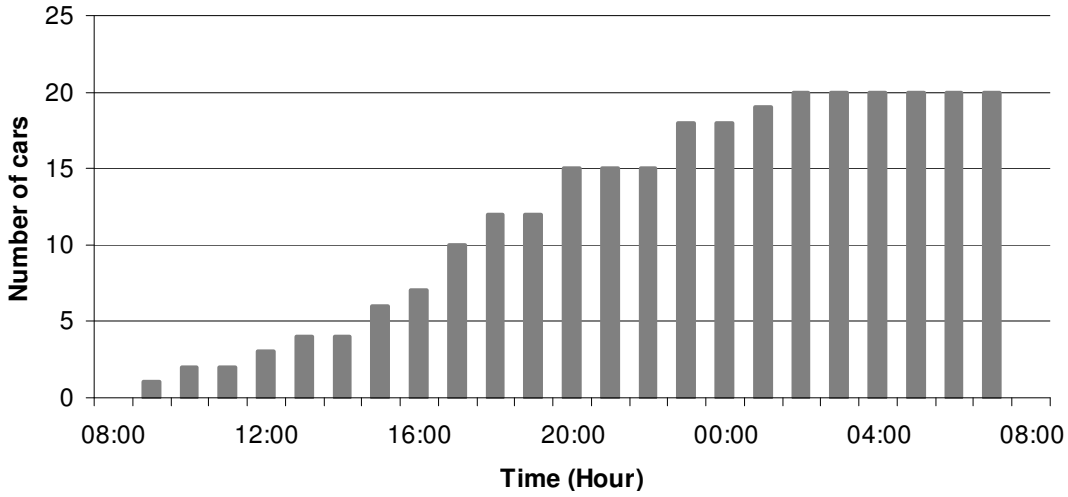

Figure 5-3 Number of EVs staying at home

The domestic electricity demand is assumed to be provided, which is obtained from UK Energy Research Centre [227] as unrestricted domestic electricity user demand for a winter weekday. Typical profile is given in Figure 5-4. Demand profile of each household is generated by shifting this profile between +/- 4 hours. The total domestic demand of the 20 households for 5 days is 2,459 *kWh*.

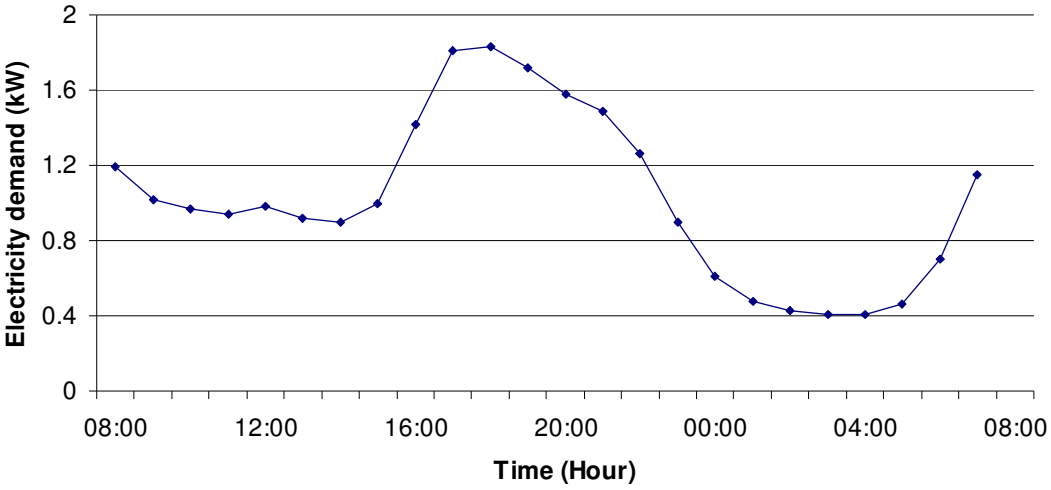

Figure 5-4 Unrestricted domestic electricity demand for winter weekday [227]

Real-time electricity prices for buying and selling are given in Figure 5-5, which are obtained from [181] and 10 *p/kWh* is added to represent the possible transmission cost and future tariff increase in 2020. Electricity tariff is higher during the day time and the peak electricity price appears in the evening. It is assumed that the 5 weekdays have the same daily electric tariff. If the demand from grid is over the agreed peak demand threshold, 10 *p/kWh* penalty applies and the total power ceiling is assigned as 100 *kW*.

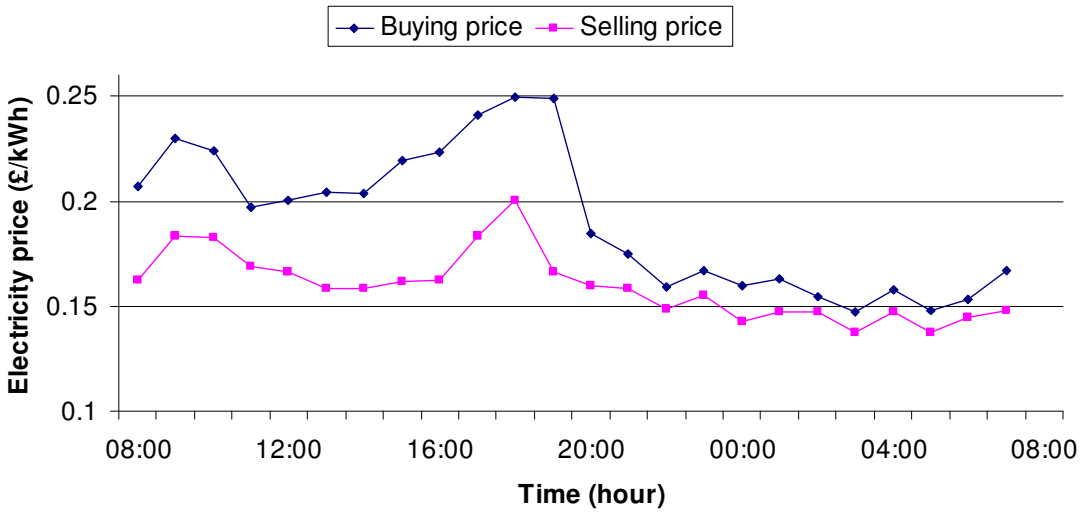

Figure 5-5 Electricity tariff (March 3rd , 2011) [181]

By convention, the end of life is defined as 80% of the original capacity remaining. Figure 5-6 shows an example of cost of a cycle based on a battery per *kWh* by Depth of Discharge (DOD) for Boston and Dallas [193]. The normalised cycle cost is higher in the hot region than in the cold region.

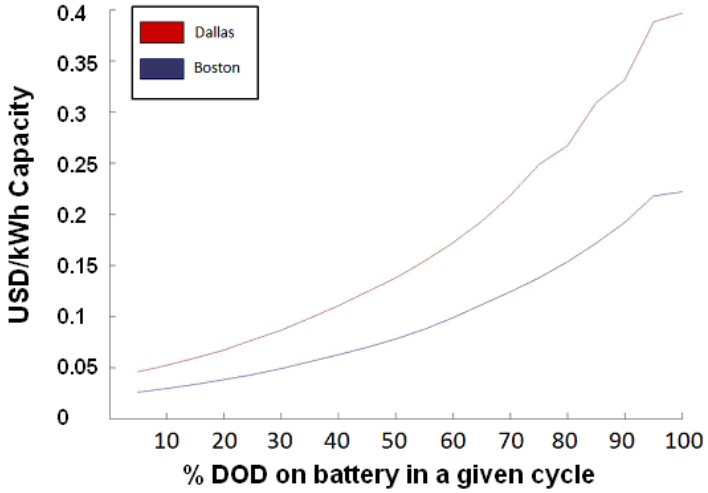

Figure 5-6 Normalised cost of cycling a battery to a given depth of discharge with a $750 capital cost [193]

Figure 5-7 provides the average degradation cost associated with the electricity charged into the battery which is converted based on the curve from Boston in Figure 5-6. It is assumed that for each life cycle, when battery is charged, it is fully charged from given DOD. It can be seen that the lowest average degradation cost appears at 60% SOC. Although smaller DOD (high SOC) has lower cycle cost, but when the battery is charged, the net electricity amount charged into the battery is also small.

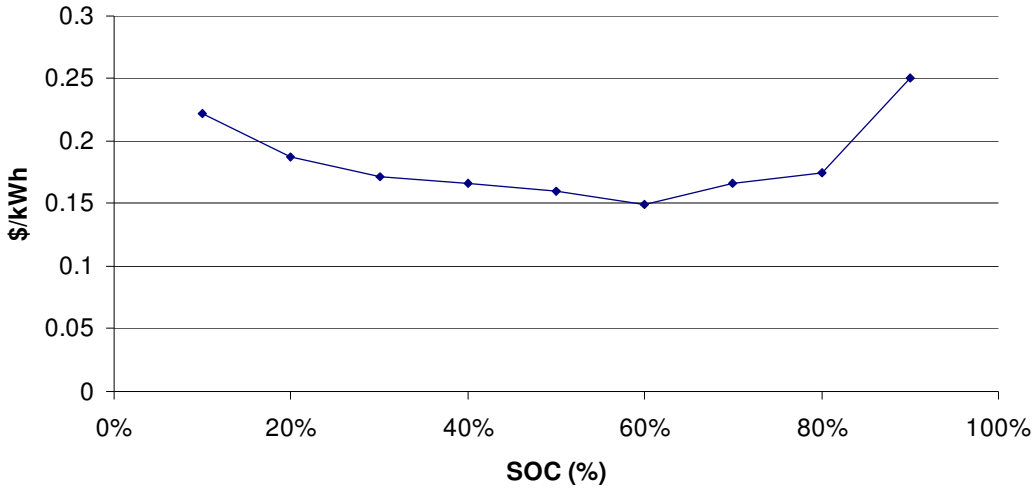

Figure 5-7 Degradation cost associated with the electricity charged

Battery replacement cost is estimated as \$200/*kWh* in 2020 according to cost forecasts found in [228]. So the degradation cost of a cycle based on different SOC levels is adjusted and given in Table 5-1.

5.5 Computational Results

5.5.1 Business-as-Usual Results

Figure 5-8 presents the electricity balance under the business-as-usual scenario (BAU), under which there is no intelligent charging and batteries from EVs are only used for travel and they are charged immediately when they arrive home. Batteries are charged at full charging rate, 3.3 *kW* and are fully charged by the end of each day. The total household electricity demand is 2,459 *kWh* while the total car electricity demand is 969 *kWh*. The total electricity cost is £715 and the peak demand from the grid occurs at 18 o'clock at 49 *kW*. The peak demands occur in the evening where electricity tariff is high. The total degradation cost is £34, which represents 4.5% of the total cost.

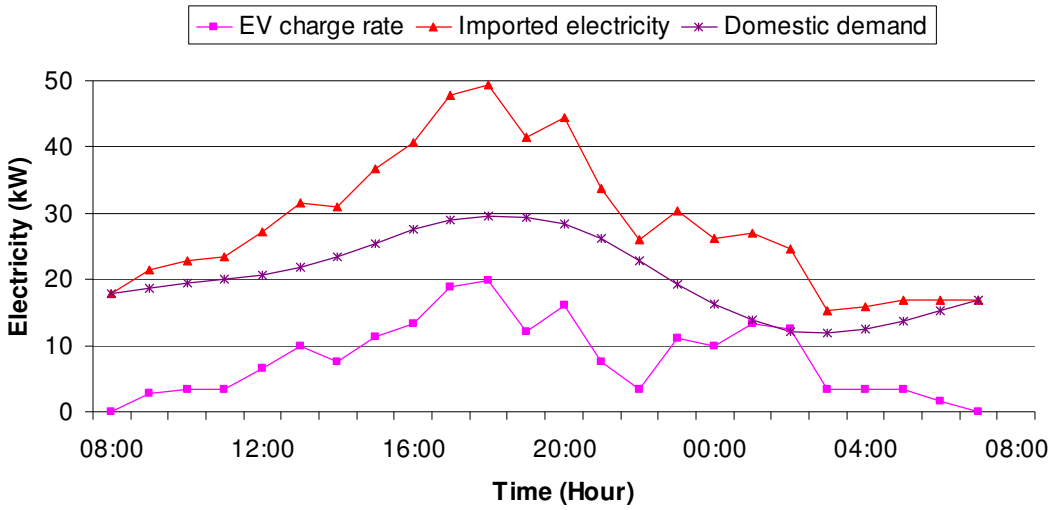

Figure 5-8 Electricity balance under BAU scenario

5.5.2 Optimal Results without Degradation Costs

If no degradation cost is considered and EV batteries are allowed to be used for household when they arrive home and can sell electricity back to the grid if it benefits, the optimal results under different thresholds are given in Table 5-3. The MILP model includes constraints Eq. 5-1 to 5-13, Eq. 5-17 and 5-18, while the objective function is Eq. 5-20 without the term of degradation cost. It is implemented using Gurobi 5.1.0 in GAMS 24.0 [128] on a PC with an Intel Core 2 Duo, 2.99 GHz CPU and 3.25GB of RAM. The model includes 15,646 equations, 19,441 continuous variables and 3,815 discrete variables. There is no optimal gap. Optimum charge and discharge schedule is provided for the EV batteries to minimise the total cost. Compared with BAU scenario, the cost saving is about 10% under different thresholds, and the peak demand from grid has been reduced for thresholds 40 *kW* and 35 *kW*. Electricity charge over threshold is reduced under all cases. Amount of electricity imported from grid is very similar, while exporting electricity to grid only happens when there is no threshold and 40 *kW* cases and the amount is relatively small. But EV batteries are used quite frequently to provide electricity for household application, over a quarter of the household demands is supplied by EV batteries under all thresholds. The computation time is quite fast under all conditions as shown in the table.

Table 5-3 Optimal results under different thresholds without degradation cost

Threshold (*kW*)	Without threshold	40	35	30
BAU cost	681	693	706	725
Optimal cost (£)	589	611	624	649
Cost savings (%)	14%	12%	12%	10%
Peak demand (*kW*)	81.3	40	35	77.9
Peak reduction (%)	39%	-23%	-41%	37%
BAU peak charge amount (*kWh*)	0	119	253	438
Peak charge amount (*kWh*)	0	0	0	156
Peak demand charge saving (%)	-	100%	100%	64%
Imported electricity (*kWh*)	3,739	3,473	3,427	3,427
Exported electricity (*kWh*)	311	46	0	0
Battery charge (*kWh*)	1,928	1,765	1,712	1,693
Household battery usage (*kWh*)	648	750	744	724
Household usage ratio (%)	26%	31%	30%	29%
Computation time (*s*)	0.3	0.7	0.7	0.7

5.5.3 Optimal Results with Degradation Costs

When degradation cost is considered to prolong the life time and improve the performance of the battery, the proposed MILP model will provide the optimum charge and discharge schedule for the batteries to minimise the total cost. All equations listed are involved. The model includes 41,886 equations, 41,041 continuous variables and 13,415 discrete variables. The optimality gap is 5%. Table 5-4 summarises the optimum results under different assigned peak demand thresholds. Because of the degradation cost, the total cost under any case is higher than that in Table 5-3.

Table 5-4 Optimal results under different thresholds with degradation cost

Threshold (*kW*)	Without threshold	40	35	30
BAU cost (£)	715	727	740	759
Optimal cost (£)	642	656	668	694
Cost savings (%)	10%	10%	10%	9%
Degradation cost (£)	50	41	38	40
Peak demand (*kW*)	78	40	35	58
Peak reduction (%)	58%	-19%	-29%	17%
BAU peak charge amount (*kWh*)	0	119	253	438
Peak charge amount (*kWh*)	0	0	0	103
Peak demand saving (%)	-	100%	100%	76%
Imported electricity (*kWh*)	3,644	3,491	3,445	3,457
Exported electricity (*kWh*)	217	64	18	30
Battery charge (*kWh*)	1,608	1,326	1,206	1,137
Household battery usage (*kWh*)	422	293	218	138
Household usage ratio (%)	17%	12%	9%	6%
Computation time (*s*)	2,225	890	99	70

When there is no threshold assigned, only total cost is to be minimised while peak demand effect is not considered. The total cost is £642 which is reduced by 10% compared with the BAU scenario, however, the peak demand has increased by about 58% to 78 *kW*. In total 15 *kWh* of electricity is sold back to the grid through electric vehicle batteries. As the threshold decreases from 40 *kW* to 30 *kW*, the total cost is slightly increased compared with the unlimited threshold scenario because of the penalty on the peak demand charge. The peak demands are within the assigned thresholds by shifting the charging time of the electric vehicle batteries where the thresholds are set as 40 *kW* and 35 *kW*. Under these thresholds, peak demands are below the BAU scenario. Compared with the BAU scenario, the cost savings are still 10% while the peak demand reductions are obvious. When 30 *kW* is applied, the peak demand is increased compared with the BAU scenario, however, the total amount of demand over threshold are still reduced by 76%. Because of the charging scheduling, batteries are charged mainly during periods with lower electricity tariff and the total cost is still lower than that from BAU scenario. Electricity is only exported at very low rate resulting from the low electricity selling price to the grid. Obviously when degradation

cost is considered, EV batteries are used less frequently and about 10% of household demand is provided by batteries in average. As the assigned peak demand threshold decreases, the household battery usage also decreases to lower the power demand from grid. If there is extra electricity provided by the battery, it is preferable to be supplied to the household. Only small amount of electricity is exported the grid over different thresholds, and the amount is expected to decrease along with thresholds decreasing. However, the optimal gap is 5%, the trend is not obtained in this case study. Under different peak demand thresholds, the computation time varies and decreases along with the threshold values. The charging time is less flexible when the peak demand threshold decreases.

Table 5-5 presents the occurrence of battery charging from different levels if degradation cost is ignored. Under the BAU scenarios, batteries are charged when it arrives home and do not discharge at home, so the charging levels are fixed rather than being selected. Since degradation cost is not considered, the charging process happens frequently during the 5 days, about 3 times per day for each battery. The charging occurs over the four given levels, batteries are charged whenever the electricity tariff is low without considering the degradation effect from SOC.

Table 5-5 Charging levels being selected without degradation cost

Charging level	BAU	Without threshold	40 kW	35 kW	30 kW
1	10	237	96	38	42
2	35	10	81	114	98
3	45	9	75	128	120
4	10	7	68	91	94
Total charging times	100	263	320	371	354

Table 5-6 presents the times of battery charging from different levels when degradation cost is considered. Under all thresholds, battery is charged less frequently than that if degradation cost is ignored. Each battery is charged about once per day. When there is no peak demand threshold constraint, battery is used as much as possible for homes and export electricity to grid. Batteries are charged most probably when it reaches the lower storage limit 20%, and are charged together when electricity tariff is low. The cost savings by using

batteries for household overcome the degradation cost. When thresholds are applied, the batteries are charged less and they are charged mostly from level 2 where the average degradation cost per *kWh* is relative low while still charge enough electricity for demand.

Table 5-6 Charging levels being selected with degradation cost

Charging level	BAU	Without threshold	40 *kW*	35 *kW*	30 *kW*
1	10	62	22	12	19
2	35	23	61	59	53
3	45	10	10	23	24
4	10	5	5	11	8
Total charging times	100	100	98	105	104

5.5.4 Electricity Balances under Different Thresholds

Figure 5-9 shows the electricity balance over 5 days under different thresholds. Since each home is assumed to have the same living habits over the 5 days, the demand patterns are cycled. However, the charge and discharge rates and exported electricity are slightly different from each other day. Because the batteries need to be fully charged at the end of the time period, there is an obvious battery charge peak at the end of the time horizon. Electricity is discharged for home use in the evening when electricity price is high. And it is sold back to grid only once in each day. If no threshold is applied, the peak demand cannot be guaranteed. When thresholds are applied, as threshold decreases, more night periods are used for charging to scatter the charging demand to avoid the peak demand penalty. Also less electricity is exported to the grid. Battery is mainly used for household to balance the electricity demand from grid. However, when the threshold goes down to 30 kW, peak demand over assigned threshold appears as shown in the figure. The charging scheduling tries to split demands over available time periods, but still has to break the threshold to obtain minimum cost while fulfilling the demand. Since most EVs are not available at homes, charge and discharge of batteries are limited in the morning.

(a) Without threshold

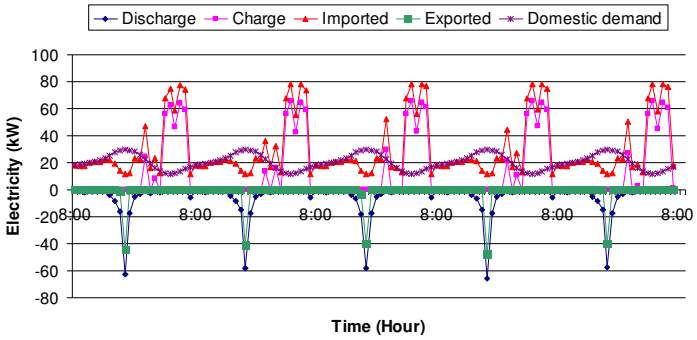

(b) 40 *kW*

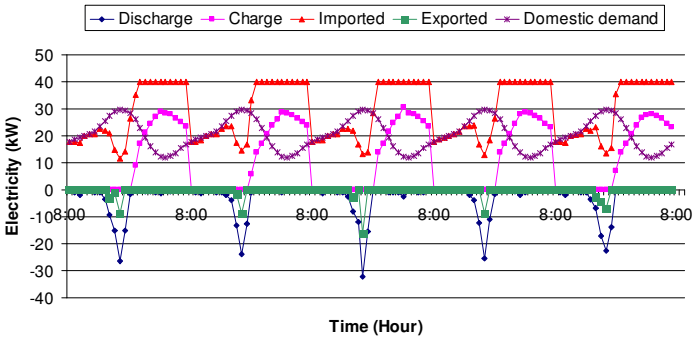

(c) 35 *kW*

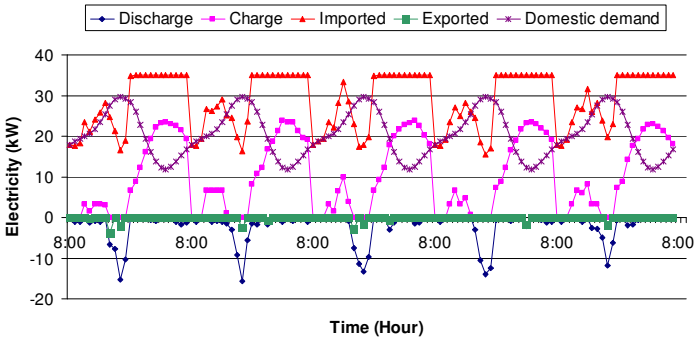

(d) 30 *kW*

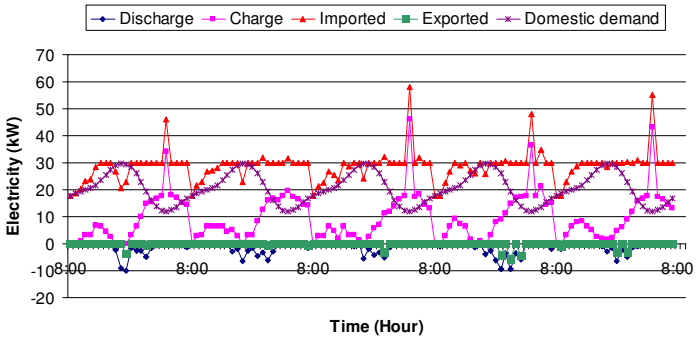

Figure 5-9 Optimum 5-day electricity balances

In order to have a closer look at the electricity balance, Figure 5-10 shows day 1 electricity balance under different thresholds. If no threshold is required, the highest peak demand from grid occurs at 4 o'clock when electricity price is the lowest. However, the peak demand is 78 *kW*, which is 58% increase from the BAU scenario. Batteries are discharged for household usage in the evening when electricity tariff are high and discharged during night when it is low. The batteries sell electricity back to the grid to achieve more benefits in the evening around 18 o'clock. Since some households have higher electricity demand or the cars have not arrived home yet, they still need to buy electricity from grid at these time periods. However, for other households, they can sell electricity back to the grid after reaching their own domestic electricity demand. That is why both imported electricity and exported electricity appear in Figure 5-10. When thresholds are applied, the optimum scheduling tries to limit the demand from grid within the threshold to avoid the penalty. Batteries are used for homes around 18 o'clock as well as the occurrence of electricity export. Even when the threshold goes down until 30 *kW*, the optimum results try to decrease the demand from grid at 18 and 19 o'clock where electricity tariff are high. Quite small amount of electricity is still exported to the grid.

(a) Without threshold

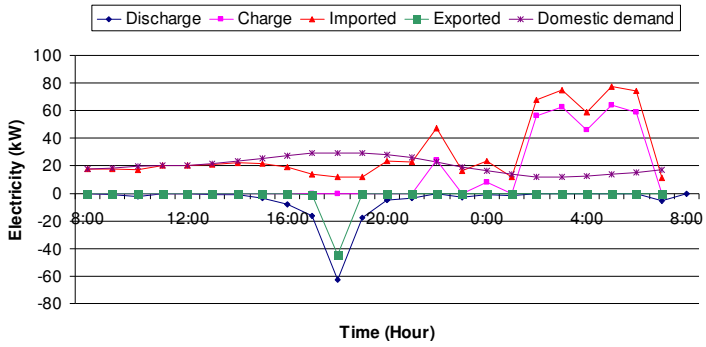

(b) 40 *kW*

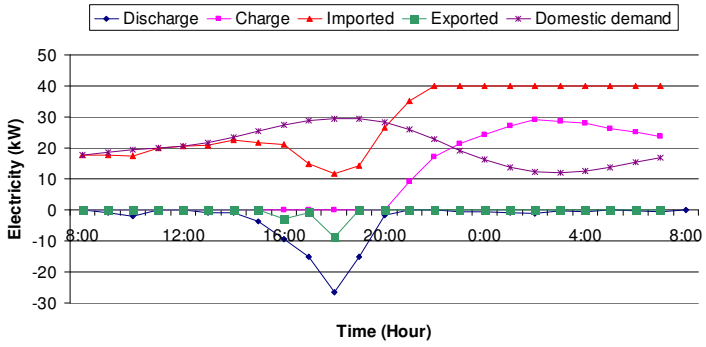

(c) 35 *kW*

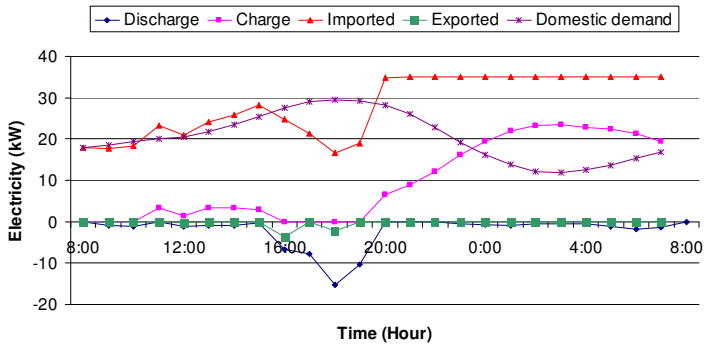

(d) 30 *kW*

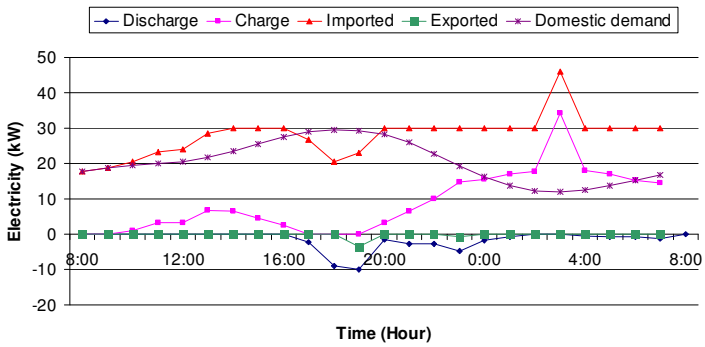

Figure 5-10 Optimum Day 1 electricity balances

5.6 Concluding Remarks

An MILP model has been proposed for optimum EV battery charge and discharge scheduling with degradation concern. Compared with BAU scenario, the optimum schedule results in lower total cost when no peak demand threshold is assigned. However, the peak demand increases since a battery tends to be charged at the time periods with low electricity tariff. By applying peak demand threshold, the peak demand from grid has been reduced accordingly by scheduling battery charge/discharge time. The demand is scattered and battery discharges for household consumption of some homes to reduce total demand from grid. Assigned thresholds facilitate the reduction of both total cost and peak demand. When degradation cost is considered, battery is used less frequently and is charged at the intervals where the average degradation cost per kWh is relative low. Although low battery cost forecast has been applied in this work, high capital cost is still an obstacle for the EV battery to be used in home and V2G service. The peak demand reduction and cost saving also depend on the living habits of the customers. If cars stay at home longer, or more cars are available in the morning, the total cost could be lower.

Chapter 6 Conclusions and Future Work

This thesis investigates several problems in the optimal design and scheduling of microgrid with the concern of the economic incentive for participants. Mathematical models have been developed and their results have been presented in the previous chapters. In this chapter, the work presented in this thesis is summarised and future work directions are provided.

6.1 Contributions of This Thesis

In this thesis, MILP-based models have been formulated for the design and scheduling problems of microgrid.

In Chapter 1, a general introduction related to microgrid has been provided, including the microgrid concept, optimal design and planning in microgrid, smart grid and microgrid together with the scope and outline of the thesis.

In Chapter 2, an MILP model has been proposed for the fair cost optimal distribution amongst participants in a general microgrid. The formulation is based on the Game-theory Nash bargaining solution approach for finding the optimal multi-partner cost levels subject to given upper bounds on the equivalent annual costs. The proposed model has been implemented on a case study of five local sites with different energy demand patterns, which provided the possibility for cooperation among participants. The results indicated the benefits of installing a microgrid are fairly distributed among participants.

In Chapter 3, the optimal scheduling of smart homes' energy consumption has been studied using an MILP approach. Both DER operation and household electricity consumption tasks have been scheduled. The model has been applied to two numerical examples for a winter day, 30 homes with the same living habits and 90 homes with different living habits. Cost savings and peak demand reduction were obtained through the energy consumption and DER operation managements.

In Chapter 4, the model in Chapter 3 has been extended to a multi-objective MILP model for respective cost optimisation in a smart building with multiple smart homes. Minimisation approach for lexicographic minimax method has been applied. The proposed model has considered two numerical examples with 10 smart homes and 50 smart homes respectively. The optimal results have presented significant cost savings for the two numerical examples with fair cost distribution among homes.

In Chapter 5, the scheduling of electric vehicle battery operation has been addressed with an MILP model. Instead of being used only as an electricity consumption appliance, EV battery is also utilised as energy storage system for home and can provide V2G service when it benefits from selling electricity back to grid. The model has been applied for a 20 households case to minimise 5 days electricity cost together with EV battery degradation cost. Cost savings and peak demand from grid have been investigated under different assigned peak demand thresholds.

MILP approaches have been applied in the work presented in this thesis. They deal with the optimal design and planning problems involving customer engagement in microgrid from the economic incentive. Cost minimisation, cost fair distribution and peak demand saving from grid are the main issues addressed here. The publications arisen from the work presented in this thesis are provided in Appendix E.

6.2 Future Work

This thesis investigates several problems for the design and planning in microgrid, and there are a number of possible directions for the future to extend the current study.

For the optimal design of microgrid provided in Chapter 2, the distances between sites are relatively small, so no electricity loss has been considered in the model. Also, it assumes that electricity can be sent to any other site, but in reality there might be constraints among sites due to microgrid connectivity, operation or management considerations. This model has the utility connection to the macrogrid so that the installed technologies meet heat demand locally and any excess electricity demand is met by the grid. If it is used for the islanded case, it may not be possible to satisfy electric demand without producing excess

heat. In such a case, the model needs to be modified to allow a certain amount of excess heat to be discarded. Deterministic prices have been assumed in the current work, while real prices are subject to uncertainty. Also, reliability measures should be incorporated given the variety characteristics of constituent microgrid components in this regard. Ultimately, multi-objective optimisation frameworks need to be developed to account for alternative competing performances measures related to economics, environment, risk, reliability etc. All these aspects affect the strategic decision-making among microgrid participants and could be investigated.

In Chapter 3 and 4, energy consumption and DER operation have been optimised under the available forecasted electricity price from the point of view of the customers. However, in the area of smart grids, it is considered that there is two-way communication between power supplier and customers. Traditional methods provide the customers only given electricity pricing while the smart grid could provide real-time electricity pricing. In the future, it might be possible to include this model as part of a full smart grid model where the electricity price is optimised along with the scheduling of tasks. Demand response programs can be included into the energy management system.

In Chapter 5, battery capacity loss and self discharge have not been considered. But their effects to the battery operation should be included in the model over long term. Also the effect of temperature increase during operation should be addressed as well to optimise the battery operation states and arrange the resting time for it to maximise its performance and guarantee the power output voltage. Electricity transfer among homes can be allowed to improve the interaction between homes and obtain better economic benefits and peak savings from grid.

In this thesis, planning and scheduling problems within microgrid are dealt with separately based on different time-scale concerns. An integrated framework can be built involving all proposed approaches. The long-time planning can be linked to the short-term scheduling, and the total cost reduction of all participants can accommodate the cost reduction of respective participants. Also EV batteries operation can cooperate with the domestic electricity consumption. Moreover, uncertainty can be considered in the future

developments. Uncertainties from energy tariffs, energy demand and climate change over time affect the design as well as the operation planning of microgrid. Also, if renewable energy resources are utilised, the uncertainties from weather raise the problem for the output forecast of non-dispatchable generators, such as wind turbine and solar panel. When microgrid is applied for residence, the living habits of customers play an important role in cost saving and peak demand reduction. On the other hand, if customers are involved in the decision making over their energy consumption, their living habits could be affected. Also their willingness to utilise renewable energy and preference to live with neighbours from different backgrounds are other issues to be investigated in analysis.

Appendix A Parameters of Chapter 2

Table A 1 Heat demand H_{tjs} in kW [134]

Day	Time period	School	hotel	Restaurant	Office	Residential building
day1	j1	30.9	65.6	0.0	2.8	67.4
day1	j2	42.1	17.5	2.5	2.4	11.8
day1	j3	42.1	22.2	2.3	2.4	22.3
day1	j4	42.1	17.5	1.9	2.4	11.8
day1	j5	18.0	60.2	2.3	2.0	35.8
day1	j6	9.3	8.4	0.8	0.0	0.0
day2	j1	15.4	56.6	0.0	1.4	60.0
day2	j2	29.8	11.1	1.5	1.4	5.9
day2	j3	29.8	15.9	1.6	1.4	16.4
day2	j4	29.8	11.1	1.2	1.4	5.9
day2	j5	13.3	53.8	1.6	1.0	28.4
day2	j6	4.6	7.5	0.4	0.4	0.0
day3	j1	0.0	47.5	0.0	0.0	52.6
day3	j2	17.4	4.7	0.5	0.5	0.0
day3	j3	17.4	9.5	0.9	0.5	10.5
day3	j4	17.4	4.7	0.5	0.5	0.0
day3	j5	8.7	47.5	0.9	0.0	21.1
day3	j6	0.0	4.7	0.0	0.0	0.0

Table A 2 Electricity demand L_{tjs} in kW [134]

Day	Time period	School	hotel	Restaurant	Office	Residential building
day1	j1	2.1	9.3	3.5	3.3	5.6
day1	j2	10.7	11.6	8.9	4.1	7.5
day1	j3	10.7	11.6	17.7	4.1	7.5
day1	j4	10.7	11.6	8.9	4.1	7.5
day1	j5	4.3	9.3	17.7	3.3	18.6
day1	j6	2.1	2.3	8.9	0.8	3.7
day2	j1	2.1	9.3	3.5	3.3	5.6
day2	j2	10.7	11.6	8.9	4.1	7.5
day2	j3	10.7	11.6	17.7	4.1	7.5
day2	j4	10.7	11.6	8.9	4.1	7.5
day2	j5	4.3	9.3	17.7	3.3	18.6
day2	j6	2.1	2.3	8.9	0.8	3.7
day3	j1	2.1	9.3	3.5	3.3	5.6
day3	j2	10.7	11.6	8.9	4.1	7.5
day3	j3	10.7	11.6	17.7	4.1	7.5
day3	j4	10.7	11.6	8.9	4.1	7.5
day3	j5	4.3	9.3	17.7	3.3	18.6
day3	j6	2.1	2.3	8.9	0.8	3.7

Table A 3 Time duration T_j in h [134]

T_{j1}	2
T_{j2}	3
T_{j3}	1
T_{j4}	5
T_{j5}	4
T_{j6}	9

Table A 4 Weighting factor W_t [134]

W_{t1}	120
W_{t2}	153
W_{t3}	92

Table A 5 μ_{sq} values from calculation

	School	**Hotel**	**Restaurant**	**Office**	**Residential building**
q1	0	0	0	0	0
q2	5.1	5.5	5.8	4.8	5.6
q3	5.8	6.2	6.4	5.5	6.3
q4	6.2	6.6	6.9	5.9	6.7
q5	6.5	6.9	7.1	6.2	7.0
q6	6.7	7.1	7.4	6.4	7.2
q7	6.9	7.3	7.5	6.6	7.4
q8	7.0	7.4	7.7	6.7	7.5
q9	7.2	7.5	7.8	6.9	7.7
q10	7.3	7.7	8.0	7.0	7.8
q11	7.4	7.8	8.1	7.1	7.9
q12	7.5	7.9	8.2	7.2	8.0
q13	7.6	7.9	8.2	7.3	8.1
q14	7.7	8.0	8.3	7.3	8.2
q15	7.7	8.1	8.4	7.4	8.2
q16	7.8	8.2	8.5	7.5	8.3

Table A 6 All other parameter values of Chapter 2

Parameter	Description	Unit	Location	Reference
a^B	lifetime of boiler	*Year*	15	[65]
a^C	lifetime of CHP	*Year*	15	[65]
a^T	lifetime of thermal storage	*Year*	25	[65]
c^{Ex}	price of exported electricity to the grid	*£/kWh*	0.01	[131]
c^I	price of electricity imported from the grid	*£/kWh*	0.13	[131]
c^{Ip}	peak price of electricity imported from the grid	*£/kWh*	0.20	[134] and defined
c^N	price of natural gas	*£/kWh*	0.027	[65]
c^T	cost per unit output for thermal storage unit	*£/kWh*	0.001	[65]
C_l^{CU}	CHP capacity upper limit at level l	*kW*	Table 2-3	[131] www.enviko.com
C_l^{CL}	CHP capacity lower limit at level l	*kW*	Table 2-3	[131] www.enviko.com
D^T	maximum discharge rate for thermal energy storage	*kW*	100	Self-defined
$\overline{e}_{ss'k}$	k available electricity transfer price levels from site s to site s'	*£/kWh*	0.03-0.10	Self-defined
F^B	capital recovery factor of the boiler	-	0.147	[65]
F^C	capital recovery factor of CHP	-	0.147	[65]
F^T	capital recovery factor of the thermal storage	-	0.128	[65]
G^T	maximum charge rate for thermal energy storage	*kW*	100	Self-defined
m	number of linearisation intervals of objective function	-	16	Break point
P_s	fixed cost for microgrid components, shared by site s	*£*	3400	[65]
Q_l	heat to power ratio for CHP generator at	-	Table 2-	[131] www.enviko.com

	capacity level l		3	
r	interest rate	-	12%	[65]
R_l	ramp limit for CHP generator from capacity level l	kW	20	Self-defined
$Y_{ss'}^U$	upper bound of electricity transferred from site s to site s'	kW	20	Self-defined
Y_s^U	upper bound of electricity sent to site s	kW	20	Self-defined
α_l	cost per kW_e installed for CHP generator of l level	£/kW_e	Table 2-3	[131] www.enviko.com
β	cost per kW_{th} installed for boiler	£/kW_{th}	40	[65]
γ	cost per $kW_{th}h$ installed for thermal energy storage	£/$kW_{th}h$	20	[65]
η	centralised electricity generation efficiency	-	35%	[133]
η_l^C	electrical efficiency of the CHP generator at level l	-	Table 2-3	[131] www.enviko.com
η^B	efficiency of boiler	-	80%	[65]
η^T	turn around efficiency of thermal energy storage	-	90%	[65]
κ_s	agreed electricity load limit from grid for site s	kW	5	Self-defined
ρ^G	CO_2 emission factor of grid electricity	$kgCO2/kWh$	0.422	[131]
ρ^N	CO_2 emission factor of natural gas	$kgCO2/kWh$	0.194	[131]
EAC_{sq}	linearised EAC values of site s at interval q	£	Table 2-8	From calculation
EAC_s^U	EAC upper bound value for site s	£	Table 2-8	From calculation

Appendix B Parameters of Chapter 3

Table B 1 Electricity price from grid c_t^I in £/kWh_e [181]

t	**Winter**	**Summer**	**t**	**Winter**	**Summer**
t1	0.050	0.059	t25	0.099	0.052
t2	0.047	0.077	t26	0.053	0.051
t3	0.050	0.135	t27	0.045	0.051
t4	0.101	0.149	t28	0.046	0.052
t5	0.096	0.144	t29	0.050	0.052
t6	0.067	0.143	t30	0.043	0.051
t7	0.080	0.144	t31	0.043	0.050
t8	0.070	0.142	t32	0.042	0.050
t9	0.081	0.118	t33	0.039	0.044
t10	0.074	0.102	t34	0.041	0.043
t11	0.073	0.131	t35	0.045	0.059
t12	0.068	0.106	t36	0.051	0.056
t13	0.075	0.083	t37	0.040	0.058
t14	0.084	0.082	t38	0.040	0.035
t15	0.080	0.059	t39	0.040	0.034
t16	0.075	0.060	t40	0.040	0.041
t17	0.082	0.060	t41	0.039	0.055
t18	0.092	0.064	t42	0.039	0.055
t19	0.051	0.068	t43	0.041	0.058
t20	0.100	0.067	t44	0.041	0.060
t21	0.165	0.063	t45	0.051	0.063
t22	0.123	0.059	t46	0.058	0.048
t23	0.111	0.052	t47	0.053	0.053
t24	0.092	0.052	t48	0.051	0.056

Table B 2 Power consumption capacity $C_{i\theta}$ in kW_e [177]

θ	**Washing machine**	**Dishwasher**
θ_1	2.15	1.80
θ_2	0.21	0.22
θ_3	0.45	1.80
θ_4		0.22

Table B 3 Heat demand H_t in kW_{th} [182]

t	**Winter**		**Summer**	
	Example 1	**Example2**	**Example 1**	**Example2**
t1	101.0	303.0	53.8	161.5
t2	101.0	303.0	53.8	161.5
t3	117.8	353.5	50.5	151.4
t4	117.8	353.5	50.5	151.4
t5	119.6	358.8	23.2	69.7
t6	119.6	358.8	23.2	69.7
t7	96.4	289.3	22.4	67.3
t8	96.4	289.3	22.4	67.3
t9	99.9	299.8	21.9	65.8
t10	99.9	299.8	21.9	65.8
t11	100.5	301.4	8.2	24.5
t12	100.5	301.4	8.2	24.5
t13	85.1	255.2	8.6	25.7
t14	85.1	255.2	8.6	25.7
t15	84.6	253.9	11.3	33.9
t16	84.6	253.9	11.3	33.9
t17	87.4	262.1	16.7	50.2
t18	87.4	262.1	16.7	50.2
t19	93.6	280.9	15.4	46.1
t20	93.6	280.9	15.4	46.1
t21	93.1	279.3	25.6	76.8
t22	93.1	279.3	25.6	76.8
t23	104.1	312.4	23.0	69.0

t24	104.1	312.4	23.0	69.0
t25	102.4	307.1	13.3	39.8
t26	102.4	307.1	13.3	39.8
t27	89.2	267.5	17.8	53.5
t28	89.2	267.5	17.8	53.5
t29	88.9	266.8	27.4	82.2
t30	88.9	266.8	27.4	82.2
t31	94.5	283.6	31.6	94.7
t32	94.5	283.6	31.6	94.7
t33	94.7	284.0	31.6	94.9
t34	94.7	284.0	31.6	94.9
t35	90.6	271.8	33.4	100.1
t36	90.6	271.8	33.4	100.1
t37	89.1	267.3	36.3	109.0
t38	89.1	267.3	36.3	109.0
t39	89.5	268.6	39.0	116.9
t40	89.5	268.6	39.0	116.9
t41	90.5	271.5	44.3	132.9
t42	90.5	271.5	44.3	132.9
t43	96.2	288.7	45.3	136.0
t44	96.2	288.7	45.3	136.0
t45	99.0	296.9	54.8	164.3
t46	99.0	296.9	54.8	164.3
t47	111.3	334.0	41.0	122.9
t48	111.3	334.0	41.0	122.9

Table B 4 Wind speed v_t in *m/s*, generated by MATLAB with Weibull distribution

t1	4.8	t13	10.8	t25	6.8	t37	11.8
t2	3.4	t14	9.9	t26	0.0	t38	0.5
t3	8.2	t15	7.7	t27	8.4	t39	1.9
t4	25.5	t16	9.8	t28	6.6	t40	10.5
t5	6.5	t17	7.9	t29	5.3	t41	8.8
t6	1.2	t18	0.0	t30	8.3	t42	28.1
t7	8.4	t19	27.2	t31	7.5	t43	3.2
t8	28.0	t20	3.9	t32	9.5	t44	10.7
t9	10.3	t21	6.4	t33	11.5	t45	4.6
t10	10.2	t22	8.7	t34	6.3	t46	30.1
t11	7.1	t23	4.7	t35	10.6	t47	7.9
t12	6.0	t24	10.1	t36	1.1	t48	2.1

Table B 5 Wind generator output w_t in kW_e

t	**Example 1**	**Example 2**	**t**	**Example 1**	**Example 2**	**t**	**Example 1**	**Example 2**
t1	2.6	7.7	t17	0.0	0.0	t33	2.9	8.7
t2	1.0	3.1	t18	1.5	4.5	t34	0.8	2.3
t3	0.0	0.0	t19	2.5	7.6	t35	9.6	28.8
t4	2.2	6.5	t20	9.6	28.8	t36	0.0	0.0
t5	0.0	0.0	t21	3.1	9.4	t37	1.4	4.1
t6	0.0	0.0	t22	3.0	8.9	t38	0.0	0.0
t7	1.5	4.4	t23	0.8	2.4	t39	5.2	15.6
t8	4.3	13.0	t24	1.9	5.8	t40	0.0	0.0
t9	2.3	6.8	t25	4.0	11.9	t41	2.3	7.0
t10	9.6	28.8	t26	0.0	0.0	t42	0.0	0.0
t11	9.6	28.8	t27	9.5	28.4	t43	0.0	0.0
t12	0.0	0.0	t28	7.4	22.3	t44	1.1	3.3
t13	0.0	0.0	t29	1.7	5.1	t45	0.8	2.5
t14	1.4	4.1	t30	0.0	0.0	t46	1.4	4.3
t15	0.0	0.0	t31	5.7	17.0	t47	1.8	5.4
t16	1.7	5.0	t32	1.2	3.5	t48	0.0	0.0

Table B 6 All other parameter values of Chapter 3 for the two examples

Parameter	Description	Unit	Value	Reference
A	wind generator blade area	m^2	20/60	Self-defined
c^E	cost per unit input (maintenance) for electrical storage unit	£/kWh_e	0.005	[65]
c^{Ex}	electricity selling price to grid	£/kWh_e	0.01	[131]
c^N	price of natural gas	£/kWh	0.027	[65]
c^T	cost per unit input (maintenance) for thermal storage unit	£/kWh_{th}	0.001	[65]
c^W	wind generator maintenance cost	£/$kWhe$	0.005	[65]
C_i	constant power consumption capacity of task i	kW_e	Table 3-1	[179]
C^B	boiler capacity	kW_{th}	120/360	Self-defined
C^C	CHP generator capacity	kW_e	20/60	Self-defined
C^E	electrical storage capacity	kWh_e	10/30	Self-defined
C^W	wind generator capacity	kW_e	10/30	Self-defined
C^T	thermal storage capacity	kWh_{th}	20/60	Self-defined
D^E	electrical storage discharge limit	kW_e	10/30	Self-defined
D^T	thermal storage discharge limit	kW_{th}	20/60	Self-defined
G^E	electrical storage charge limit	kW_e	10/30	Self-defined
G^T	thermal storage charge limit	kW_{th}	20/60	Self-defined
p	difference between peak and base electricity demand price from grid	£/ kWh_e	0.05	Self-defined
P_{ji}	processing time of task i of home j	-	Table 3-1	[179]
Q	CHP heat-to-power ratio	-	1.3	[65]
T_{ji}^F	latest finishing time of task i of home j	h	Table 3-1	[179]
T_{ji}^S	earliest starting time of task i of home j	h	Table 3-1	[179]
V^{nom}	nominal wind speed	m/s	12	[65]
V^{cut-in}	cut-in wind speed	m/s	5	[65]

$V^{cut-out}$	cut-out wind speed	*m/s*	25	[65]
δ	time interval duration	*h*	0.5	Self-defined
ρ	air density	*kg/m3*	1.23	[180]
η^B	boiler efficiency	-	80%	[65]
η^C	CHP generator electrical efficiency	-	35%	[65]
η^E	electrical storage charge/discharge efficiency	-	95%	[65]
η^T	thermal storage charge/discharge efficiency	-	98%	[65]
η^W	wind generator power coefficient	-	45%	[180]
κ	agreed electricity peak demand threshold from grid	kW_e	90	Self-defined

Appendix C Parameters of Chapter 4

Table C 1 Heat demand H_{jt} in kW_{th} in Example 1 [192]

	j1	**j2**	**j3**	**j4**	**j5**	**j6**	**j7**	**j8**	**j9**	**j10**
t1	1.7	1.6	1.8	1.9	1.8	2.0	1.7	1.6	1.8	1.7
t2	1.7	1.6	1.8	1.9	1.8	2.0	1.7	1.6	1.8	1.7
t3	1.0	1.1	2.1	1.2	1.3	2.4	1.0	1.1	2.1	1.0
t4	1.0	1.1	2.1	1.2	1.3	2.4	1.0	1.1	2.1	1.0
t5	0.6	0.7	1.7	0.6	0.8	2.0	0.6	0.7	1.7	0.6
t6	0.6	0.7	1.7	0.6	0.8	2.0	0.6	0.7	1.7	0.6
t7	0.4	0.5	1.2	0.4	0.5	1.4	0.4	0.5	1.2	0.4
t8	0.4	0.5	1.2	0.4	0.5	1.4	0.4	0.5	1.2	0.4
t9	0.3	0.3	1.0	0.3	0.3	1.1	0.3	0.3	1.0	0.3
t10	0.3	0.3	1.0	0.3	0.3	1.1	0.3	0.3	1.0	0.3
t11	0.8	0.2	0.8	0.9	0.2	0.9	0.8	0.2	0.8	0.8
t12	0.8	0.2	0.8	0.9	0.2	0.9	0.8	0.2	0.8	0.8
t13	1.1	0.1	0.8	1.3	0.2	0.9	1.1	0.1	0.8	1.1
t14	1.1	0.1	0.8	1.3	0.2	0.9	1.1	0.1	0.8	1.1
t15	1.1	0.1	0.7	1.3	0.2	0.8	1.1	0.1	0.7	1.1
t16	1.1	0.1	0.7	1.3	0.2	0.8	1.1	0.1	0.7	1.1
t17	1.0	0.1	0.7	1.2	0.1	0.8	1.0	0.1	0.7	1.0
t18	1.0	0.1	0.7	1.2	0.1	0.8	1.0	0.1	0.7	1.0
t19	1.0	0.1	0.8	1.1	0.1	0.9	1.0	0.1	0.8	1.0
t20	1.0	0.1	0.8	1.1	0.1	0.9	1.0	0.1	0.8	1.0
t21	1.1	1.1	0.9	1.2	1.2	1.0	1.1	1.1	0.9	1.1
t22	1.1	1.1	0.9	1.2	1.2	1.0	1.1	1.1	0.9	1.1
t23	0.8	1.4	0.7	0.9	1.6	0.8	0.8	1.4	0.7	0.8
t24	0.8	1.4	0.7	0.9	1.6	0.8	0.8	1.4	0.7	0.8
t25	0.6	1.1	0.5	0.7	1.3	0.6	0.6	1.1	0.5	0.6
t26	0.6	1.1	0.5	0.7	1.3	0.6	0.6	1.1	0.5	0.6
t27	0.6	1.0	0.6	0.8	1.2	0.7	0.6	1.0	0.6	0.6
t28	0.6	1.0	0.6	0.8	1.2	0.7	0.6	1.0	0.6	0.6
t29	0.7	0.9	0.6	0.8	1.1	0.8	0.7	0.9	0.6	0.7
t30	0.7	0.9	0.6	0.8	1.1	0.8	0.7	0.9	0.6	0.7
t31	0.7	0.9	0.7	0.9	1.1	0.8	0.7	0.9	0.7	0.7
t32	0.7	0.9	0.7	0.9	1.1	0.8	0.7	0.9	0.7	0.7
t33	0.6	0.2	0.6	0.7	0.3	0.8	0.6	0.2	0.6	0.6
t34	0.6	0.2	0.6	0.7	0.3	0.8	0.6	0.2	0.6	0.6
t35	0.1	0.0	0.1	0.1	0.0	0.1	0.1	0.0	0.1	0.1
t36	0.1	0.0	0.1	0.1	0.0	0.1	0.1	0.0	0.1	0.1
t37	0.1	0.0	0.1	0.1	0.0	0.1	0.1	0.0	0.1	0.1
t38	0.1	0.0	0.1	0.1	0.0	0.1	0.1	0.0	0.1	0.1
t39	0.0	0.0	0.0	0.1	0.1	0.1	0.0	0.0	0.0	0.0
t40	0.0	0.0	0.0	0.1	0.1	0.1	0.0	0.0	0.0	0.0
t41	0.1	0.1	0.0	0.2	0.2	0.1	0.1	0.1	0.0	0.1
t42	0.1	0.1	0.0	0.2	0.2	0.1	0.1	0.1	0.0	0.1
t43	0.2	0.2	0.2	0.3	0.3	0.3	0.2	0.2	0.2	0.2

t44	0.2	0.2	0.2	0.3	0.3	0.3	0.2	0.2	0.2	0.2
t45	0.3	0.3	0.3	0.5	0.4	0.5	0.3	0.3	0.3	0.3
t46	0.3	0.3	0.3	0.5	0.4	0.5	0.3	0.3	0.3	0.3
t47	1.2	1.0	1.4	1.3	1.1	1.4	1.2	1.0	1.4	1.2
t48	1.2	1.0	1.4	1.3	1.1	1.4	1.2	1.0	1.4	1.2

Table C 2 Heat demand H_{jt} in kW_{th} in Example 2 [192]

	j1	**j2**	**j3**	**j4**	**j5**	**j6**	**j7**	**j8**	**j9**	**j10**
t1	2.9	2.8	2.9	1.7	2.2	3.6	2.0	1.8	2.1	2.5
t2	2.9	2.8	2.9	1.7	2.2	3.6	2.0	1.8	2.1	2.5
t3	1.7	2.2	3.6	1.0	1.2	3.3	2.9	2.8	2.9	1.6
t4	1.7	2.2	3.6	1.0	1.2	3.3	2.9	2.8	2.9	1.6
t5	1.0	1.2	3.3	0.8	0.9	2.8	1.7	2.2	3.6	0.9
t6	1.0	1.2	3.3	0.8	0.9	2.8	1.7	2.2	3.6	0.9
t7	0.8	0.9	2.8	0.7	0.8	2.4	1.0	1.2	3.3	0.8
t8	0.8	0.9	2.8	0.7	0.8	2.4	1.0	1.2	3.3	0.8
t9	0.7	0.8	2.4	2.1	0.7	2.2	0.8	0.9	2.8	0.7
t10	0.7	0.8	2.4	2.1	0.7	2.2	0.8	0.9	2.8	0.7
t11	2.1	0.7	2.2	3.0	0.6	2.0	0.7	0.8	2.4	2.0
t12	2.1	0.7	2.2	3.0	0.6	2.0	0.7	0.8	2.4	2.0
t13	3.0	0.6	2.0	3.1	0.6	1.9	2.1	0.7	2.2	2.8
t14	3.0	0.6	2.0	3.1	0.6	1.9	2.1	0.7	2.2	2.8
t15	3.1	0.6	1.9	2.6	0.5	1.9	3.0	0.6	2.0	2.8
t16	3.1	0.6	1.9	2.6	0.5	1.9	3.0	0.6	2.0	2.8
t17	2.6	0.5	1.9	2.5	0.5	2.1	3.1	0.6	1.9	2.4
t18	2.6	0.5	1.9	2.5	0.5	2.1	3.1	0.6	1.9	2.4
t19	2.5	0.5	2.1	2.5	2.5	2.2	2.6	0.5	1.9	2.3
t20	2.5	0.5	2.1	2.5	2.5	2.2	2.6	0.5	1.9	2.3
t21	2.5	2.5	2.2	2.1	3.5	1.9	2.5	0.5	2.1	2.3
t22	2.5	2.5	2.2	2.1	3.5	1.9	2.5	0.5	2.1	2.3
t23	2.1	3.5	1.9	1.7	3.1	1.6	2.5	2.5	2.2	1.9
t24	2.1	3.5	1.9	1.7	3.1	1.6	2.5	2.5	2.2	1.9
t25	1.7	3.1	1.6	1.7	2.5	1.6	2.1	3.5	1.9	1.5
t26	1.7	3.1	1.6	1.7	2.5	1.6	2.1	3.5	1.9	1.5
t27	1.7	2.5	1.6	1.7	2.2	1.6	1.7	3.1	1.6	1.5
t28	1.7	2.5	1.6	1.7	2.2	1.6	1.7	3.1	1.6	1.5
t29	1.7	2.2	1.6	1.7	2.0	1.6	1.7	2.5	1.6	1.5
t30	1.7	2.2	1.6	1.7	2.0	1.6	1.7	2.5	1.6	1.5
t31	1.7	2.0	1.6	1.2	0.6	1.3	1.7	2.2	1.6	1.5
t32	1.7	2.0	1.6	1.2	0.6	1.3	1.7	2.2	1.6	1.5
t33	1.2	0.6	1.3	0.4	0.3	0.5	1.7	2.0	1.6	1.1
t34	1.2	0.6	1.3	0.4	0.3	0.5	1.7	2.0	1.6	1.1
t35	0.4	0.3	0.5	0.4	0.4	0.5	1.2	0.6	1.3	0.4
t36	0.4	0.3	0.5	0.4	0.4	0.5	1.2	0.6	1.3	0.4
t37	0.4	0.4	0.5	0.5	0.6	0.5	0.4	0.3	0.5	0.4
t38	0.4	0.4	0.5	0.5	0.6	0.5	0.4	0.3	0.5	0.4
t39	0.5	0.6	0.5	0.6	0.7	0.6	0.4	0.4	0.5	0.4
t40	0.5	0.6	0.5	0.6	0.7	0.6	0.4	0.4	0.5	0.4

t41	0.6	0.7	0.6	0.8	0.8	0.7	0.5	0.6	0.5	0.5
t42	0.6	0.7	0.6	0.8	0.8	0.7	0.5	0.6	0.5	0.5
t43	0.8	0.8	0.7	0.9	0.9	0.9	0.6	0.7	0.6	0.6
t44	0.8	0.8	0.7	0.9	0.9	0.9	0.6	0.7	0.6	0.6
t45	0.9	0.9	0.9	2.0	1.8	2.1	0.8	0.8	0.7	0.7
t46	0.9	0.9	0.9	2.0	1.8	2.1	0.8	0.8	0.7	0.7
t47	2.0	1.8	2.1	2.9	2.8	2.9	0.9	0.9	0.9	1.7
t48	2.0	1.8	2.1	2.9	2.8	2.9	0.9	0.9	0.9	1.7
	j11	**j12**	**j13**	**j14**	**j15**	**j16**	**j17**	**j18**	**j19**	**j20**
t1	2.6	2.6	1.6	2.0	3.3	1.7	1.6	1.8	0.7	0.7
t2	2.6	2.6	1.6	2.0	3.3	1.7	1.6	1.8	0.7	0.7
t3	2.0	3.3	0.9	1.1	3.1	2.5	2.6	2.6	1.7	1.6
t4	2.0	3.3	0.9	1.1	3.1	2.5	2.6	2.6	1.7	1.6
t5	1.1	3.1	0.8	0.9	2.6	1.6	2.0	3.3	2.5	2.6
t6	1.1	3.1	0.8	0.9	2.6	1.6	2.0	3.3	2.5	2.6
t7	0.9	2.6	0.7	0.7	2.2	0.9	1.1	3.1	1.6	2.0
t8	0.9	2.6	0.7	0.7	2.2	0.9	1.1	3.1	1.6	2.0
t9	0.7	2.2	2.0	0.6	2.0	0.8	0.9	2.6	0.9	1.1
t10	0.7	2.2	2.0	0.6	2.0	0.8	0.9	2.6	0.9	1.1
t11	0.6	2.0	2.8	0.6	1.8	0.7	0.7	2.2	0.8	0.9
t12	0.6	2.0	2.8	0.6	1.8	0.7	0.7	2.2	0.8	0.9
t13	0.6	1.8	2.8	0.5	1.7	2.0	0.6	2.0	0.7	0.7
t14	0.6	1.8	2.8	0.5	1.7	2.0	0.6	2.0	0.7	0.7
t15	0.5	1.7	2.4	0.5	1.8	2.8	0.6	1.8	2.0	0.6
t16	0.5	1.7	2.4	0.5	1.8	2.8	0.6	1.8	2.0	0.6
t17	0.5	1.8	2.3	0.5	1.9	2.8	0.5	1.7	2.8	0.6
t18	0.5	1.8	2.3	0.5	1.9	2.8	0.5	1.7	2.8	0.6
t19	0.5	1.9	2.3	2.3	2.0	2.4	0.5	1.8	2.8	0.5
t20	0.5	1.9	2.3	2.3	2.0	2.4	0.5	1.8	2.8	0.5
t21	2.3	2.0	1.9	3.2	1.7	2.3	0.5	1.9	2.4	0.5
t22	2.3	2.0	1.9	3.2	1.7	2.3	0.5	1.9	2.4	0.5
t23	3.2	1.7	1.5	2.8	1.4	2.3	2.3	2.0	2.3	0.5
t24	3.2	1.7	1.5	2.8	1.4	2.3	2.3	2.0	2.3	0.5
t25	2.8	1.4	1.5	2.2	1.4	1.9	3.2	1.7	2.3	2.3
t26	2.8	1.4	1.5	2.2	1.4	1.9	3.2	1.7	2.3	2.3
t27	2.2	1.4	1.5	1.9	1.4	1.5	2.8	1.4	1.9	3.2
t28	2.2	1.4	1.5	1.9	1.4	1.5	2.8	1.4	1.9	3.2
t29	1.9	1.4	1.5	1.8	1.4	1.5	2.2	1.4	1.5	2.8
t30	1.9	1.4	1.5	1.8	1.4	1.5	2.2	1.4	1.5	2.8
t31	1.8	1.4	1.1	0.4	1.2	1.5	1.9	1.4	1.5	2.2
t32	1.8	1.4	1.1	0.4	1.2	1.5	1.9	1.4	1.5	2.2
t33	0.4	1.2	0.4	0.2	0.3	1.5	1.8	1.4	1.5	1.9
t34	0.4	1.2	0.4	0.2	0.3	1.5	1.8	1.4	1.5	1.9
t35	0.2	0.3	0.4	0.3	0.3	1.1	0.4	1.2	1.5	1.8
t36	0.2	0.3	0.4	0.3	0.3	1.1	0.4	1.2	1.5	1.8
t37	0.3	0.3	0.4	0.5	0.4	0.4	0.2	0.3	1.1	0.4
t38	0.3	0.3	0.4	0.5	0.4	0.4	0.2	0.3	1.1	0.4
t39	0.5	0.4	0.5	0.6	0.5	0.4	0.3	0.3	0.4	0.2
t40	0.5	0.4	0.5	0.6	0.5	0.4	0.3	0.3	0.4	0.2
t41	0.6	0.5	0.6	0.7	0.6	0.4	0.5	0.4	0.4	0.3

t42	0.6	0.5	0.6	0.7	0.6	0.4	0.5	0.4	0.4	0.3
t43	0.7	0.6	0.7	0.7	0.7	0.5	0.6	0.5	0.4	0.5
t44	0.7	0.6	0.7	0.7	0.7	0.5	0.6	0.5	0.4	0.5
t45	0.7	0.7	1.7	1.6	1.8	0.6	0.7	0.6	0.5	0.6
t46	0.7	0.7	1.7	1.6	1.8	0.6	0.7	0.6	0.5	0.6
t47	1.6	1.8	2.5	2.6	2.6	0.7	0.7	0.7	0.6	0.7
t48	1.6	1.8	2.5	2.6	2.6	0.7	0.7	0.7	0.6	0.7
	j21	**j22**	**j23**	**j24**	**j25**	**j26**	**j27**	**j28**	**j29**	**j30**
t1	0.7	0.9	1.1	3.1	2.8	2.8	2.9	1.7	2.1	3.6
t2	0.7	0.9	1.1	3.1	2.8	2.8	2.9	1.7	2.1	3.6
t3	1.8	0.8	0.9	2.6	1.7	2.1	3.6	1.0	1.2	3.4
t4	1.8	0.8	0.9	2.6	1.7	2.1	3.6	1.0	1.2	3.4
t5	2.6	0.7	0.7	2.2	1.0	1.2	3.4	0.8	0.9	2.9
t6	2.6	0.7	0.7	2.2	1.0	1.2	3.4	0.8	0.9	2.9
t7	3.3	2.0	0.6	2.0	0.8	0.9	2.9	0.7	0.8	2.5
t8	3.3	2.0	0.6	2.0	0.8	0.9	2.9	0.7	0.8	2.5
t9	3.1	2.8	0.6	1.8	0.7	0.8	2.5	2.2	0.7	2.2
t10	3.1	2.8	0.6	1.8	0.7	0.8	2.5	2.2	0.7	2.2
t11	2.6	2.8	0.5	1.7	2.2	0.7	2.2	3.1	0.6	2.0
t12	2.6	2.8	0.5	1.7	2.2	0.7	2.2	3.1	0.6	2.0
t13	2.2	2.4	0.5	1.8	3.1	0.6	2.0	3.0	0.6	1.9
t14	2.2	2.4	0.5	1.8	3.1	0.6	2.0	3.0	0.6	1.9
t15	2.0	2.3	0.5	1.9	3.0	0.6	1.9	2.6	0.5	1.9
t16	2.0	2.3	0.5	1.9	3.0	0.6	1.9	2.6	0.5	1.9
t17	1.8	2.3	2.3	2.0	2.6	0.5	1.9	2.5	0.6	2.1
t18	1.8	2.3	2.3	2.0	2.6	0.5	1.9	2.5	0.6	2.1
t19	1.7	1.9	3.2	1.7	2.5	0.6	2.1	2.6	2.6	2.2
t20	1.7	1.9	3.2	1.7	2.5	0.6	2.1	2.6	2.6	2.2
t21	1.8	1.5	2.8	1.4	2.6	2.6	2.2	2.1	3.5	1.9
t22	1.8	1.5	2.8	1.4	2.6	2.6	2.2	2.1	3.5	1.9
t23	1.9	1.5	2.2	1.4	2.1	3.5	1.9	1.6	3.1	1.5
t24	1.9	1.5	2.2	1.4	2.1	3.5	1.9	1.6	3.1	1.5
t25	2.0	1.5	1.9	1.4	1.6	3.1	1.5	1.6	2.5	1.5
t26	2.0	1.5	1.9	1.4	1.6	3.1	1.5	1.6	2.5	1.5
t27	1.7	1.5	1.8	1.4	1.6	2.5	1.5	1.6	2.1	1.5
t28	1.7	1.5	1.8	1.4	1.6	2.5	1.5	1.6	2.1	1.5
t29	1.4	1.1	0.4	1.2	1.6	2.1	1.5	1.6	2.0	1.5
t30	1.4	1.1	0.4	1.2	1.6	2.1	1.5	1.6	2.0	1.5
t31	1.4	0.4	0.2	0.3	1.6	2.0	1.5	1.2	0.5	1.3
t32	1.4	0.4	0.2	0.3	1.6	2.0	1.5	1.2	0.5	1.3
t33	1.4	0.4	0.3	0.3	1.2	0.5	1.3	0.4	0.2	0.4
t34	1.4	0.4	0.3	0.3	1.2	0.5	1.3	0.4	0.2	0.4
t35	1.4	0.4	0.5	0.4	0.4	0.2	0.4	0.4	0.4	0.4
t36	1.4	0.4	0.5	0.4	0.4	0.2	0.4	0.4	0.4	0.4
t37	1.2	0.5	0.6	0.5	0.4	0.4	0.4	0.5	0.5	0.4
t38	1.2	0.5	0.6	0.5	0.4	0.4	0.4	0.5	0.5	0.4
t39	0.3	0.6	0.7	0.6	0.5	0.5	0.4	0.5	0.6	0.5
t40	0.3	0.6	0.7	0.6	0.5	0.5	0.4	0.5	0.6	0.5
t41	0.3	0.7	0.7	0.7	0.5	0.6	0.5	0.7	0.7	0.6
t42	0.3	0.7	0.7	0.7	0.5	0.6	0.5	0.7	0.7	0.6

t43	0.4	1.7	1.6	1.8	0.7	0.7	0.6	0.8	0.8	0.7
t44	0.4	1.7	1.6	1.8	0.7	0.7	0.6	0.8	0.8	0.7
t45	0.5	2.5	2.6	2.6	0.8	0.8	0.7	1.8	1.8	2.0
t46	0.5	2.5	2.6	2.6	0.8	0.8	0.7	1.8	1.8	2.0
t47	0.6	1.6	2.0	3.3	1.8	1.8	2.0	2.8	2.8	2.9
t48	0.6	1.6	2.0	3.3	1.8	1.8	2.0	2.8	2.8	2.9
	j31	**j32**	**j33**	**j34**	**j35**	**j36**	**j37**	**j38**	**j39**	**j40**
t1	1.8	1.8	2.0	0.8	0.8	0.7	1.0	1.2	3.4	2.3
t2	1.8	1.8	2.0	0.8	0.8	0.7	1.0	1.2	3.4	2.3
t3	2.8	2.8	2.9	1.8	1.8	2.0	0.8	0.9	2.9	1.4
t4	2.8	2.8	2.9	1.8	1.8	2.0	0.8	0.9	2.9	1.4
t5	1.7	2.1	3.6	2.8	2.8	2.9	0.7	0.8	2.5	0.8
t6	1.7	2.1	3.6	2.8	2.8	2.9	0.7	0.8	2.5	0.8
t7	1.0	1.2	3.4	1.7	2.1	3.6	2.2	0.7	2.2	0.7
t8	1.0	1.2	3.4	1.7	2.1	3.6	2.2	0.7	2.2	0.7
t9	0.8	0.9	2.9	1.0	1.2	3.4	3.1	0.6	2.0	0.6
t10	0.8	0.9	2.9	1.0	1.2	3.4	3.1	0.6	2.0	0.6
t11	0.7	0.8	2.5	0.8	0.9	2.9	3.0	0.6	1.9	1.8
t12	0.7	0.8	2.5	0.8	0.9	2.9	3.0	0.6	1.9	1.8
t13	2.2	0.7	2.2	0.7	0.8	2.5	2.6	0.5	1.9	2.5
t14	2.2	0.7	2.2	0.7	0.8	2.5	2.6	0.5	1.9	2.5
t15	3.1	0.6	2.0	2.2	0.7	2.2	2.5	0.6	2.1	2.5
t16	3.1	0.6	2.0	2.2	0.7	2.2	2.5	0.6	2.1	2.5
t17	3.0	0.6	1.9	3.1	0.6	2.0	2.6	2.6	2.2	2.1
t18	3.0	0.6	1.9	3.1	0.6	2.0	2.6	2.6	2.2	2.1
t19	2.6	0.5	1.9	3.0	0.6	1.9	2.1	3.5	1.9	2.1
t20	2.6	0.5	1.9	3.0	0.6	1.9	2.1	3.5	1.9	2.1
t21	2.5	0.6	2.1	2.6	0.5	1.9	1.6	3.1	1.5	2.1
t22	2.5	0.6	2.1	2.6	0.5	1.9	1.6	3.1	1.5	2.1
t23	2.6	2.6	2.2	2.5	0.6	2.1	1.6	2.5	1.5	1.7
t24	2.6	2.6	2.2	2.5	0.6	2.1	1.6	2.5	1.5	1.7
t25	2.1	3.5	1.9	2.6	2.6	2.2	1.6	2.1	1.5	1.3
t26	2.1	3.5	1.9	2.6	2.6	2.2	1.6	2.1	1.5	1.3
t27	1.6	3.1	1.5	2.1	3.5	1.9	1.6	2.0	1.5	1.3
t28	1.6	3.1	1.5	2.1	3.5	1.9	1.6	2.0	1.5	1.3
t29	1.6	2.5	1.5	1.6	3.1	1.5	1.2	0.5	1.3	1.3
t30	1.6	2.5	1.5	1.6	3.1	1.5	1.2	0.5	1.3	1.3
t31	1.6	2.1	1.5	1.6	2.5	1.5	0.4	0.2	0.4	1.3
t32	1.6	2.1	1.5	1.6	2.5	1.5	0.4	0.2	0.4	1.3
t33	1.6	2.0	1.5	1.6	2.1	1.5	0.4	0.4	0.4	1.0
t34	1.6	2.0	1.5	1.6	2.1	1.5	0.4	0.4	0.4	1.0
t35	1.2	0.5	1.3	1.6	2.0	1.5	0.5	0.5	0.4	0.3
t36	1.2	0.5	1.3	1.6	2.0	1.5	0.5	0.5	0.4	0.3
t37	0.4	0.2	0.4	1.2	0.5	1.3	0.5	0.6	0.5	0.3
t38	0.4	0.2	0.4	1.2	0.5	1.3	0.5	0.6	0.5	0.3
t39	0.4	0.4	0.4	0.4	0.2	0.4	0.7	0.7	0.6	0.4
t40	0.4	0.4	0.4	0.4	0.2	0.4	0.7	0.7	0.6	0.4
t41	0.5	0.5	0.4	0.4	0.4	0.4	0.8	0.8	0.7	0.4
t42	0.5	0.5	0.4	0.4	0.4	0.4	0.8	0.8	0.7	0.4
t43	0.5	0.6	0.5	0.5	0.5	0.4	1.8	1.8	2.0	0.5

t44	0.5	0.6	0.5	0.5	0.5	0.4	1.8	1.8	2.0	0.5
t45	0.7	0.7	0.6	0.5	0.6	0.5	2.8	2.8	2.9	0.6
t46	0.7	0.7	0.6	0.5	0.6	0.5	2.8	2.8	2.9	0.6
t47	0.8	0.8	0.7	0.7	0.7	0.6	1.7	2.1	3.6	1.5
t48	0.8	0.8	0.7	0.7	0.7	0.6	1.7	2.1	3.6	1.5
	j41	**j42**	**j43**	**j44**	**j45**	**j46**	**j47**	**j48**	**j49**	**j50**
t1	2.3	2.4	1.4	1.8	3.0	1.5	1.4	1.6	0.6	0.7
t2	2.3	2.4	1.4	1.8	3.0	1.5	1.4	1.6	0.6	0.7
t3	1.8	3.0	0.8	1.0	2.8	2.3	2.3	2.4	1.5	1.4
t4	1.8	3.0	0.8	1.0	2.8	2.3	2.3	2.4	1.5	1.4
t5	1.0	2.8	0.7	0.8	2.3	1.4	1.8	3.0	2.3	2.3
t6	1.0	2.8	0.7	0.8	2.3	1.4	1.8	3.0	2.3	2.3
t7	0.8	2.3	0.6	0.6	2.0	0.8	1.0	2.8	1.4	1.8
t8	0.8	2.3	0.6	0.6	2.0	0.8	1.0	2.8	1.4	1.8
t9	0.6	2.0	1.8	0.6	1.8	0.7	0.8	2.3	0.8	1.0
t10	0.6	2.0	1.8	0.6	1.8	0.7	0.8	2.3	0.8	1.0
t11	0.6	1.8	2.5	0.5	1.6	0.6	0.6	2.0	0.7	0.8
t12	0.6	1.8	2.5	0.5	1.6	0.6	0.6	2.0	0.7	0.8
t13	0.5	1.6	2.5	0.5	1.6	1.8	0.6	1.8	0.6	0.6
t14	0.5	1.6	2.5	0.5	1.6	1.8	0.6	1.8	0.6	0.6
t15	0.5	1.6	2.1	0.4	1.6	2.5	0.5	1.6	1.8	0.6
t16	0.5	1.6	2.1	0.4	1.6	2.5	0.5	1.6	1.8	0.6
t17	0.4	1.6	2.1	0.5	1.7	2.5	0.5	1.6	2.5	0.5
t18	0.4	1.6	2.1	0.5	1.7	2.5	0.5	1.6	2.5	0.5
t19	0.5	1.7	2.1	2.1	1.8	2.1	0.4	1.6	2.5	0.5
t20	0.5	1.7	2.1	2.1	1.8	2.1	0.4	1.6	2.5	0.5
t21	2.1	1.8	1.7	2.9	1.5	2.1	0.5	1.7	2.1	0.4
t22	2.1	1.8	1.7	2.9	1.5	2.1	0.5	1.7	2.1	0.4
t23	2.9	1.5	1.3	2.5	1.2	2.1	2.1	1.8	2.1	0.5
t24	2.9	1.5	1.3	2.5	1.2	2.1	2.1	1.8	2.1	0.5
t25	2.5	1.2	1.3	2.0	1.2	1.7	2.9	1.5	2.1	2.1
t26	2.5	1.2	1.3	2.0	1.2	1.7	2.9	1.5	2.1	2.1
t27	2.0	1.2	1.3	1.7	1.3	1.3	2.5	1.2	1.7	2.9
t28	2.0	1.2	1.3	1.7	1.3	1.3	2.5	1.2	1.7	2.9
t29	1.7	1.3	1.3	1.6	1.3	1.3	2.0	1.2	1.3	2.5
t30	1.7	1.3	1.3	1.6	1.3	1.3	2.0	1.2	1.3	2.5
t31	1.6	1.3	1.0	0.4	1.0	1.3	1.7	1.3	1.3	2.0
t32	1.6	1.3	1.0	0.4	1.0	1.3	1.7	1.3	1.3	2.0
t33	0.4	1.0	0.3	0.2	0.3	1.3	1.6	1.3	1.3	1.7
t34	0.4	1.0	0.3	0.2	0.3	1.3	1.6	1.3	1.3	1.7
t35	0.2	0.3	0.3	0.3	0.3	1.0	0.4	1.0	1.3	1.6
t36	0.2	0.3	0.3	0.3	0.3	1.0	0.4	1.0	1.3	1.6
t37	0.3	0.3	0.4	0.4	0.4	0.3	0.2	0.3	1.0	0.4
t38	0.3	0.3	0.4	0.4	0.4	0.3	0.2	0.3	1.0	0.4
t39	0.4	0.4	0.4	0.5	0.4	0.3	0.3	0.3	0.3	0.2
t40	0.4	0.4	0.4	0.5	0.4	0.3	0.3	0.3	0.3	0.2
t41	0.5	0.4	0.5	0.6	0.5	0.4	0.4	0.4	0.3	0.3
t42	0.5	0.4	0.5	0.6	0.5	0.4	0.4	0.4	0.3	0.3
t43	0.6	0.5	0.6	0.7	0.6	0.4	0.5	0.4	0.4	0.4
t44	0.6	0.5	0.6	0.7	0.6	0.4	0.5	0.4	0.4	0.4

t45	0.7	0.6	1.5	1.4	1.6	0.5	0.6	0.5	0.4	0.5
t46	0.7	0.6	1.5	1.4	1.6	0.5	0.6	0.5	0.4	0.5
t47	1.4	1.6	2.3	2.3	2.4	0.6	0.7	0.6	0.5	0.6
t48	1.4	1.6	2.3	2.3	2.4	0.6	0.7	0.6	0.5	0.6

Table C 3 Latest finishing time T_{ji}^{F} in Example 2 by self-defined

	i1	**i2**	**i3**	**i4**	**i5**	**i6**	**i7**	**i8**	**i9**	**i10**	**i11**	**i12**
j1	7	2	3	10	21	10	22	6	5	4	8	7
j2	19.5	18.5	23.5	16.5	12.5	22.5	24	23.5	20.5	22	8	5.5
j3	4	23	4	12	20	14	2	22.5	20	4	8	3
j4	5.5	5	6	10.5	22.5	4.5	3	0.5	4.5	24	8	0.5
j5	17	5	5.5	13	18	5	22	1	0.5	0.5	8	24
j6	17.5	19	21.5	18.5	14.5	24	24	1	23	24	8	5
j7	16	18.5	21.5	15.5	0.5	22.5	2	22	1	3.5	8	6
j8	16.5	18.5	21	19.5	15.5	23	24	23.5	20.5	1	8	6
j9	22	0.5	2.5	19	18	18.5	1	2	23.5	23.5	8	3.5
j10	1.5	2	0.5	13.5	0.5	22	22	2.5	6	7.5	8	6
j11	6	2	3	9	21	23	23	5	6	7	8	3.5
j12	20.5	13.5	18.5	14.5	21.5	21.5	2	21.5	22.5	24	8	2
j13	4	23	3	10	21	21	3	3.5	3	0.5	8	1
j14	4.5	3	2.5	0.5	22.5	10.5	23	0.5	1.5	3	8	1.5
j15	20	23	2	13	16	15	4	24	19.5	1.5	8	23
j16	5.5	22	0.5	0.5	0.5	11	24	4	4	5	8	6
j17	4	0.5	2.5	13.5	2.5	10.5	24	3	4	3.5	8	6.5
j18	22.5	0.5	3	18.5	17.5	19	1	1.5	22.5	23	8	3
j19	2	2.5	21.5	13	2	21.5	1	5	3.5	3.5	8	7
j20	1.5	21	21.5	14.5	0.5	9	1	3.5	2	5	8	2
j21	22	1	6	19	21	22	1	23	2	6	8	3
j22	19.5	18.5	23.5	16.5	12.5	22.5	24	23.5	20.5	22	8	5.5
j23	18	4	6.5	12	17	4	22	1.5	23	23.5	8	3
j24	22.5	23	2.5	13.5	14.5	20.5	23	21.5	2.5	2	8	2.5
j25	3	24	3	13	21	15	2	22	21.5	5	8	24
j26	18.5	14	16.5	16.5	23.5	23	2	23	1	2	8	1.5
j27	16	18.5	21.5	15.5	0.5	22.5	2	22	1	3.5	8	6
j28	18.5	22.5	1	14.5	17.5	14	4	23.5	17.5	3	8	4
j29	22	0.5	2.5	19	18	18.5	1	2	23.5	23.5	8	3.5
j30	1.5	19	21.5	22.5	1.5	11	3	0.5	2	5	8	5
j31	22	1	6	19	21	22	1	23	2	6	8	3
j32	23.5	22.5	3.5	12.5	13.5	19.5	23	22.5	1.5	1	8	5.5
j33	5	19	24	19	22	12	3	0.5	24	1.5	8	2
j34	17.5	19	22.5	12.5	21.5	22.5	2	22.5	0.5	2	8	3
j35	4	20	23	20	23	13	3	24	1.5	2.5	8	23
j36	16.5	5	5	13.5	18.5	5	22	2	1	1	8	4
j37	16	4.5	5	15.5	20.5	4.5	22	23	24	1.5	8	4.5
j38	1.5	23.5	2	14.5	22.5	14	2	21.5	19.5	6.5	8	5
j39	1	23.5	1.5	15	23	13.5	2	22	20.5	7	8	5.5
j40	16.5	13	15.5	18.5	1.5	21	2	22.5	1	4	8	3.5
j41	22	23	4	11	14	13	4	1	20	4	8	5

j42	20.5	13.5	18.5	14.5	21.5	21.5	2	21.5	22.5	24	8	2
j43	1	24	5	16	15	19	1	2.5	23	20.5	8	1
j44	20.5	1	4.5	20.5	22.5	23.5	1	20.5	0.5	3	8	22.5
j45	20	23	2	13	16	15	4	24	19.5	1.5	8	23
j46	21.5	23	1.5	14.5	15.5	21	23	24	4	3	8	5
j47	19	0.5	3.5	23.5	1.5	23.5	1	20	1	4.5	8	1.5
j48	20.5	22.5	1	15.5	16.5	20	23	22.5	1.5	4	8	6
j49	15	18.5	20.5	15	24	21.5	2	24	0.5	4.5	8	7
j50	1.5	19	21.5	22.5	1.5	11	3	0.5	2	5	8	5

Table C 4 Earliest starting time T_{ji}^{S} in Example 2 by self-defined

	i1	**i2**	**i3**	**i4**	**i5**	**i6**	**i7**	**i8**	**i9**	**i10**	**i11**	**i12**
j1	23	23	22	9	20	9	16	24	23	20	8	21
j2	12	16	19	15	11	21	18	19	17	18	8	21
j3	21	21	24	10	18	12	20	17	16	23.5	8	20
j4	23	2	2.5	8	20	2	21	21	24	19	8	19
j5	11	2	2.5	10	15	2	16	20	19	19	8	20
j6	12	16	19	15	11	21	18	19	17	18	8	21
j7	11	16	19	10	19	20	20	19	20	21	8	21.5
j8	12	16	19	15	11	21	18	19	17	18	8	21
j9	18	22	1	14	13	17	19	21	19	16	8	18
j10	22	24	23	8	19	21	16	21	24	23.5	8	20
j11	22	23	22	8	20	22	17	23	24	23	8	17.5
j12	13	11	14	13	20	20	20	17	19	20	8	17.5
j13	21	21	23	8	19	19	21	22	23	20	8	18
j14	22	24	23	22	20	8	17	21	21	22	8	20
j15	14	20	23	10	13	12	22	19	14	20	8	19
j16	24	19	22	21	21	8	18	22	22	23	8	22
j17	23	22	24	8	21	8	18	24	23	21	8	22
j18	18	22	1	14	13	17	19	21	19	16	8	18
j19	22	24	20	8	21	20	19	24	23	20	8	21.5
j20	22	19	20	9	19	8	19	22	20	21	8	16
j21	14	22	1	18	20	21	19	17	20	22	8	17
j22	12	16	19	15	11	21	18	19	17	18	8	21
j23	11	2	2.5	10	15	2	16	20	19	19	8	20
j24	16	20	23	11	12	18	17	18	22	21	8	21
j25	21	21	24	10	18	12	20	17	16	23.5	8	20
j26	13	11	14	13	20	20	20	17	19	20	8	17.5
j27	11	16	19	10	19	20	20	19	20	21	8	21.5
j28	14	20	23	10	13	12	22	19	14	20	8	19
j29	18	22	1	14	13	17	19	21	19	16	8	18
j30	22	17	20	17	20	10	21	19	20	21	8	19
j31	14	22	1	18	20	21	19	17	20	22	8	17
j32	16	20	23	11	12	18	17	18	22	21	8	21
j33	22	17	20	17	20	10	21	19	20	21	8	19
j34	11	16	19	10	19	20	20	19	20	21	8	21.5
j35	22	17	20	17	20	10	21	19	20	21	8	19
j36	11	2	2.5	10	15	2	16	20	19	19	8	20

j37	11	2	2.5	10	15	2	16	20	19	19	8	20
j38	21	21	24	10	18	12	20	17	16	23.5	8	20
j39	21	21	24	10	18	12	20	17	16	23.5	8	20
j40	13	11	14	13	20	20	20	17	19	20	8	17.5
j41	14	20	23	10	13	12	22	19	14	20	8	19
j42	13	11	14	13	20	20	20	17	19	20	8	17.5
j43	18	22	1	14	13	17	19	21	19	16	8	18
j44	14	22	1	18	20	21	19	17	20	22	8	17
j45	14	20	23	10	13	12	22	19	14	20	8	19
j46	16	20	23	11	12	18	17	18	22	21	8	21
j47	14	22	1	18	20	21	19	17	20	22	8	17
j48	16	20	23	11	12	18	17	18	22	21	8	21
j49	11	16	19	10	19	20	20	19	20	21	8	21.5
j50	22	17	20	17	20	10	21	19	20	21	8	19

Table C 5 All other parameter values of Chapter 4 in the two examples

Parameter	Description	Unit	Value	Reference
c^E	cost per unit input (maintenance) for electrical storage unit	£/kWh_e	0.005	[65]
c^{Ex}	electricity selling price to grid	£/kWh_e	0.01	[131]
c^N	price of natural gas	£/kWh	0.027	[65]
c^T	cost per unit input (maintenance) for thermal storage unit	£/kWh_{th}	0.001	[65]
C_i	constant power consumption capacity of task i	kW_e	Table 3-1	[179]
C^B	boiler capacity	kW_{th}	24/120	Self-defined
C^C	CHP generator capacity	kW_e	4/20	Self-defined
C^E	electrical storage capacity	kWh_e	4/20	Self-defined
C^T	thermal storage capacity	kWh_{th}	6/30	Self-defined
D^E	electrical storage discharge limit	kW_e	4/20	Self-defined
D^T	thermal storage discharge limit	kW_{th}	6/30	Self-defined
G^E	electrical storage charge limit	kW_e	4/20	Self-defined
G^T	thermal storage charge limit	kW_{th}	6/30	Self-defined
P_{ji}	processing time of task i of home j	-	Example 1 Table 3-1	[179]
Q	CHP heat-to-power ratio	-	1.3	[65]
T_{ji}^F	latest finishing time of task i of home j	h	Example 1 Table 4-4	Self-defined

T_{ji}^{S}	earliest starting time of task *i* of home *j*	*h*	Example 1 Table 4-3	Self-defined
δ	time interval duration	*h*	0.5	Self-defined
η^{B}	boiler efficiency	-	80%	[65]
η^{C}	CHP generator electrical efficiency	-	35%	[65]
η^{E}	electrical storage charge/discharge efficiency	-	95%	[65]
η^{T}	thermal storage charge/discharge efficiency	-	98%	[65]

Appendix D Parameters of Chapter 5

Table D 1 Electricity buying and selling prices, c_t^I and c_t^{Ex} in £/kWh_e [181]

t	c_t^I	c_t^{Ex}
t1	0.307	0.207
t2	0.330	0.230
t3	0.324	0.224
t4	0.297	0.197
t5	0.300	0.200
t6	0.304	0.204
t7	0.304	0.204
t8	0.320	0.220
t9	0.324	0.224
t10	0.341	0.241
t11	0.349	0.249
t12	0.349	0.249
t13	0.285	0.185
t14	0.275	0.175
t15	0.259	0.159
t16	0.267	0.167
t17	0.260	0.160
t18	0.263	0.163
t19	0.254	0.154
t20	0.247	0.147
t21	0.258	0.158
t22	0.248	0.148
t23	0.253	0.153
t24	0.267	0.167

Table D 2 Electricity demand L_{it} in kWh_e **[227]**

	i1	**i2**	**i3**	**i4**	**i5**	**i6**	**i7**	**i8**	**i9**	**i10**	**i11**	**i12**	**i13**	**i14**	**i15**	**i16**	**i17**	**i18**	**i19**	**i20**
t1	1.2	1.0	1.0	0.9	1.0	1.2	0.7	0.5	0.4	1.2	1.0	1.0	0.9	1.0	1.2	0.7	0.5	0.4	1.2	1.0
t2	1.0	1.0	0.9	1.0	0.9	1.2	1.2	0.7	0.5	1.0	1.0	0.9	1.0	0.9	1.2	1.2	0.7	0.5	1.0	1.0
t3	1.0	0.9	1.0	0.9	0.9	1.0	1.2	1.2	0.7	1.0	0.9	1.0	0.9	0.9	1.0	1.2	1.2	0.7	1.0	0.9
t4	0.9	1.0	0.9	0.9	1.0	1.0	1.0	1.2	1.2	0.9	1.0	0.9	0.9	1.0	1.0	1.0	1.2	1.2	0.9	1.0
t5	1.0	0.9	0.9	1.0	1.4	0.9	1.0	1.0	1.2	1.0	0.9	0.9	1.0	1.4	0.9	1.0	1.0	1.2	1.0	0.9
t6	0.9	0.9	1.0	1.4	1.8	1.0	0.9	1.0	1.0	0.9	0.9	1.0	1.4	1.8	1.0	0.9	1.0	1.0	0.9	0.9
t7	0.9	1.0	1.4	1.8	1.8	0.9	1.0	0.9	1.0	0.9	1.0	1.4	1.8	1.8	0.9	1.0	0.9	1.0	0.9	1.0
t8	1.0	1.4	1.8	1.8	1.7	0.9	0.9	1.0	0.9	1.0	1.4	1.8	1.8	1.7	0.9	0.9	1.0	0.9	1.0	1.4
t9	1.4	1.8	1.8	1.7	1.6	1.0	0.9	0.9	1.0	1.4	1.8	1.8	1.7	1.6	1.0	0.9	0.9	1.0	1.4	1.8
t10	1.8	1.8	1.7	1.6	1.5	1.4	1.0	0.9	0.9	1.8	1.8	1.7	1.6	1.5	1.4	1.0	0.9	0.9	1.8	1.8
t11	1.8	1.7	1.6	1.5	1.3	1.8	1.4	1.0	0.9	1.8	1.7	1.6	1.5	1.3	1.8	1.4	1.0	0.9	1.8	1.7
t12	1.7	1.6	1.5	1.3	0.9	1.8	1.8	1.4	1.0	1.7	1.6	1.5	1.3	0.9	1.8	1.8	1.4	1.0	1.7	1.6
t13	1.6	1.5	1.3	0.9	0.6	1.7	1.8	1.8	1.4	1.6	1.5	1.3	0.9	0.6	1.7	1.8	1.8	1.4	1.6	1.5
t14	1.5	1.3	0.9	0.6	0.5	1.6	1.7	1.8	1.8	1.5	1.3	0.9	0.6	0.5	1.6	1.7	1.8	1.8	1.5	1.3
t15	1.3	0.9	0.6	0.5	0.4	1.5	1.6	1.7	1.8	1.3	0.9	0.6	0.5	0.4	1.5	1.6	1.7	1.8	1.3	0.9
t16	0.9	0.6	0.5	0.4	0.4	1.3	1.5	1.6	1.7	0.9	0.6	0.5	0.4	0.4	1.3	1.5	1.6	1.7	0.9	0.6
t17	0.6	0.5	0.4	0.4	0.4	0.9	1.3	1.5	1.6	0.6	0.5	0.4	0.4	0.4	0.9	1.3	1.5	1.6	0.6	0.5
t18	0.5	0.4	0.4	0.4	0.5	0.6	0.9	1.3	1.5	0.5	0.4	0.4	0.4	0.5	0.6	0.9	1.3	1.5	0.5	0.4
t19	0.4	0.4	0.4	0.5	0.7	0.5	0.6	0.9	1.3	0.4	0.4	0.4	0.5	0.7	0.5	0.6	0.9	1.3	0.4	0.4
t20	0.4	0.4	0.5	0.7	1.2	0.4	0.5	0.6	0.9	0.4	0.4	0.5	0.7	1.2	0.4	0.5	0.6	0.9	0.4	0.4
t21	0.4	0.5	0.7	1.2	1.2	0.4	0.4	0.5	0.6	0.4	0.5	0.7	1.2	1.2	0.4	0.4	0.5	0.6	0.4	0.5
t22	0.5	0.7	1.2	1.2	1.0	0.4	0.4	0.4	0.5	0.5	0.7	1.2	1.2	1.0	0.4	0.4	0.4	0.5	0.5	0.7
t23	0.7	1.2	1.2	1.0	1.0	0.5	0.4	0.4	0.4	0.7	1.2	1.2	1.0	1.0	0.5	0.4	0.4	0.4	0.7	1.2
t24	1.2	1.2	1.0	1.0	0.9	0.7	0.5	0.4	0.4	1.2	1.2	1.0	1.0	0.9	0.7	0.5	0.4	0.4	1.2	1.2

Table D 3 Driving electricity demand V_{it} in kWh_e by self-defined

	i1	**i2**	**i3**	**i4**	**i5**	**i6**	**i7**	**i8**	**i9**	**i10**		**i11**	**i12**	**i13**	**i14**	**i15**	**i16**	**i17**	**i18**	**i19**	**i20**
t1	1.1	1.0	1.3	0.8	1.0	0.5	2.8	7.1	1.1	0.8	t1	0.3	1.2	2.9	0.9	1.3	0.9	0.8	0.3	0.8	2.8
t2	1.1	1.0	1.3	0.8	1.0	0.5	2.8	7.1	1.1	0.8	t2	0.3	1.2	2.9	0.9	1.3	0.9	0.8	0.3	0.8	0.0
t3	1.1	1.0	1.3	0.8	1.0	0.5	2.8	0.0	1.1	0.8	t3	0.3	1.2	2.9	0.9	1.3	0.9	0.8	0.3	0.8	0.0
t4	1.1	1.0	1.3	0.8	1.0	0.5	2.8	0.0	1.1	0.8	t4	0.3	1.2	2.9	0.9	1.3	0.9	0.8	0.3	0.8	0.0
t5	1.1	1.0	1.3	0.8	1.0	0.5	0.0	0.0	1.1	0.8	t5	0.3	1.2	2.9	0.9	1.3	0.9	0.8	0.3	0.8	0.0
t6	1.1	1.0	1.3	0.8	1.0	0.5	0.0	0.0	1.1	0.8	t6	0.3	1.2	0.0	0.9	1.3	0.9	0.8	0.3	0.8	0.0
t7	1.1	1.0	1.3	0.8	1.0	0.5	0.0	0.0	1.1	0.8	t7	0.3	1.2	0.0	0.9	1.3	0.9	0.8	0.3	0.8	0.0
t8	1.1	1.0	1.3	0.8	1.0	0.5	0.0	0.0	1.1	0.8	t8	0.3	0.0	0.0	0.9	0.0	0.9	0.8	0.3	0.8	0.0
t9	1.1	1.0	0.0	0.8	1.0	0.5	0.0	0.0	1.1	0.8	t9	0.3	0.0	0.0	0.9	0.0	0.9	0.8	0.3	0.8	0.0
t10	1.1	0.0	0.0	0.0	0.0	0.5	0.0	0.0	1.1	0.8	t10	0.3	0.0	0.0	0.9	0.0	0.9	0.8	0.3	0.8	0.0
t11	0.0	0.0	0.0	0.0	0.0	0.5	0.0	0.0	0.0	0.8	t11	0.3	0.0	0.0	0.9	0.0	0.9	0.8	0.3	0.8	0.0
t12	0.0	0.0	0.0	0.0	0.0	0.5	0.0	0.0	0.0	0.8	t12	0.3	0.0	0.0	0.9	0.0	0.9	0.8	0.3	0.8	0.0
t13	0.0	0.0	0.0	0.0	0.0	0.0	0.0	0.0	0.0	0.8	t13	0.3	0.0	0.0	0.9	0.0	0.0	0.8	0.0	0.8	0.0
t14	0.0	0.0	0.0	0.0	0.0	0.0	0.0	0.0	0.0	0.8	t14	0.3	0.0	0.0	0.9	0.0	0.0	0.8	0.0	0.8	0.0
t15	0.0	0.0	0.0	0.0	0.0	0.0	0.0	0.0	0.0	0.8	t15	0.3	0.0	0.0	0.9	0.0	0.0	0.8	0.0	0.8	0.0
t16	0.0	0.0	0.0	0.0	0.0	0.0	0.0	0.0	0.0	0.0	t16	0.3	0.0	0.0	0.0	0.0	0.0	0.8	0.0	0.0	0.0
t17	0.0	0.0	0.0	0.0	0.0	0.0	0.0	0.0	0.0	0.0	t17	0.3	0.0	0.0	0.0	0.0	0.0	0.8	0.0	0.0	0.0
t18	0.0	0.0	0.0	0.0	0.0	0.0	0.0	0.0	0.0	0.0	t18	0.0	0.0	0.0	0.0	0.0	0.0	0.8	0.0	0.0	0.0
t19	0.0	0.0	0.0	0.0	0.0	0.0	0.0	0.0	0.0	0.0	t19	0.0	0.0	0.0	0.0	0.0	0.0	0.0	0.0	0.0	0.0
t20	0.0	0.0	0.0	0.0	0.0	0.0	0.0	0.0	0.0	0.0	t20	0.0	0.0	0.0	0.0	0.0	0.0	0.0	0.0	0.0	0.0
t21	0.0	0.0	0.0	0.0	0.0	0.0	0.0	0.0	0.0	0.0	t21	0.0	0.0	0.0	0.0	0.0	0.0	0.0	0.0	0.0	0.0
t22	0.0	0.0	0.0	0.0	0.0	0.0	0.0	0.0	0.0	0.0	t22	0.0	0.0	0.0	0.0	0.0	0.0	0.0	0.0	0.0	0.0
t23	0.0	0.0	0.0	0.0	0.0	0.0	0.0	0.0	0.0	0.0	t23	0.0	0.0	0.0	0.0	0.0	0.0	0.0	0.0	0.0	0.0
t24	0.0	0.0	0.0	0.0	0.0	0.0	0.0	0.0	0.0	0.0	t24	0.0	0.0	0.0	0.0	0.0	0.0	0.0	0.0	0.0	0.0

Table D 4 All other parameter values of Chapter 5

Parameter	Description	Unit	Value	Reference
b_j	battery charge cost of level *j*	*£/kWh*	Table 5-1	Self-defined
C_i	nominal capacity of EV battery *i*	*kWh*	24	[226]
D^E	maximum EV battery discharge rate	*kW*	24	Self-defined
G^E	Maximum EV battery charge rate	*kW*	3.3	[226]
p	extra peak demand charge over the agreed threshold	*£/kWh*	0.10	Self-defined
S_i^I	initial state of EV battery *i*	*kWh*	24	Self-defined
$SOC^{\min}$	minimum SOC of EV battery	-	20%	Self-defined
$\overline{SOC_j}$	SOC at level *j*	-	Table 5-1	Self-defined
δ	time interval duration	*h*	1	Self-defined
μ	peak demand ceiling value	*kW*	100	Self-defined
κ	agreed electricity peak demand threshold from grid	*kW*	30/35/40	Self-defined

Appendix E Publications

The following is the list of the publications arising from the work in this thesis:

Articles in Refereed Journals

[1] D. Zhang, N. Shah and L.G. Papageorgiou. Efficient energy consumption and operation management in a smart building with microgrid. Energy Conversion and Management. 74 (2013) 209-22.

[2] D. Zhang, A. Hawkes, D. Brett, N. Shah and L.G. Papageorgiou (2013). Fair electricity transfer price and unit capacity selection for microgrids. Energy Economics. 36 (2013) 581–93.

Article in Refereed Conference Proceedings

[3] D. Zhang, N. Samsatli, A. Hawkes, D. Brett, N. Shah and L.G. Papageorgiou. Fair electricity transfer pricing and capacity planning in microgrid. International Conference on Sustainable Energy Technologies, Istanbul, Turkey, Sep 2011, page 1-6.

[4] D. Zhang, N. Samsatli, N. Shah and L.G. Papageorgiou. Optimal scheduling of smart homes energy consumption with microgrid. International Conference on Smart Grids, ENERGY 2011, Venice, Italy, May 2011, page 70-75.

References

[1] Colson CM, Nehrir MH. A review of challenges to real-time power management of microgrids. Power & Energy Society General Meeting. Calgary: IEEE; 2009. pp. 1-8.

[2] Mitra J, Suryanarayanan S. System analytics for smart microgrids. IEEE PES General Meeting: IEEE; 2010. pp. 1-4.

[3] Bossart S. DOE Perspective on Microgrids. Advanced microgrid concepts and technologies workshop. Sheraton Washington North in Beltsville, Maryland, 2012.

[4] Bhaskara SN, Chowdhury BH. Microgrids - A review of modeling, control, protection, simulation and future potential. Power and Energy Society General Meeting: IEEE; 2012. pp. 1-7.

[5] Ricketts C. How microgrids will change the way we get energy from A to B. Green Beat, 2010. URL *http://venturebeat.com/2010/07/06/microgrids-energy-transmission/*

[6] Tsikalakis AG, Hatziargyriou ND. Centralized control for optimizing microgrids Operation. IEEE Transactions on Energy Conversion. 2008;23:241-8.

[7] Marnay C, Venkataramanan G, Stadler M, Siddiqui A, Firestone R, Chandran B. Optimal Technology Selection and operation of microgrids in commercial buildings. Power Engineering Society General Meeting: IEEE; 2007. pp. 1-7.

[8] Hatziargyriou ND, Anastasiadis AG, Tsikalakis AG, Vasiljevska J. Quantification of economic, environmental and operational benefits due to significant penetration of Microgrids in a typical LV and MV Greek network. European Transactions on Electrical Power. 2011;21:1217-37.

[9] Ton DT, Smith MA. The U.S. Department of Energy's microgrid initiative. The Electricity Journal. 2012;25:84-94.

[10] Lasseter RH. MicroGrids. Power Engineering Society Winter Meeting Conference Proceedings: IEEE; 2002. pp. 305-8.

[11] Zamora R, Srivastava AK. Controls for microgrids with storage: Review, challenges, and research needs. Renewable and Sustainable Energy Reviews. 2010;14:2009-18.

[12] Lidula NWA, Rajapakse AD. Microgrids research: A review of experimental microgrids and test systems. Renewable and Sustainable Energy Reviews. 2011;15:186-202.

[13] Siddiqui AS, Marnay C, Edwards JL, Firestone R, Ghosh S, Stadler M. Effects of carbon tax on microgrid combined heat and power adoption. Journal of Energy Engineering. 2005;131:2.

[14] Piagi P, Lasseter RH. Autonomous control of microgrids. Power Engineering Society General Meeting: IEEE; 2006. pp. 1-8.

[15] Lasseter RH. Smart Distribution: Coupled Microgrids. Proceedings of the IEEE, 2011. pp. 1074-82.

[16] Hernandez-Aramburo CA, Green TC, Mugniot N. Fuel consumption minimization of a microgrid. IEEE Transactions on Industry Applications. 2005;41:673-81.

[17] Justo JJ, Mwasilu F, Lee J, Jung J-W. AC-microgrids versus DC-microgrids with distributed energy resources: A review. Renewable and Sustainable Energy Reviews. 2013;24:387-405.

[18] Ustun TS, Ozansoy C, Zayegh A. Recent developments in microgrids and example cases around the world—A review. Renewable and Sustainable Energy Reviews. 2011;15:4030-41.

[19] Lasseter RH, Akhil A, Marnay C, Stephens J, Dagle J, Guttromson R, et al. White paper on integration of distributed energy resources The CERTS MicroGrid Concept. Consortium for electric reliability technology solutions, 2002.
[20] DOE Microgrid Workshop Report. Microgrid workshop. San Diego, California, 2001.
[21] Abu-Sharkh S, Arnold R, J K, Li R, Markvart T, Ross J, et al. Can microgrids make a major contribution to UK energy supply? Renewable and Sustainable Energy Reviews. 2006;10:78-127.
[22] Zhang Z, Huang X, Jiang J, Wu B. A load-sharing control scheme for a microgrid with a fixed frequency inverter. Electric Power Systems Research. 2010;80:311-7.
[23] Funabashi T, Yokoyama R. Microgrid field test experiences in Japan. Power Engineering Society General Meeting: IEEE; 2006. pp. 1-2.
[24] Sun Z, Zhang X-y. Advances on distributed generation technology. Energy Procedia. 2012;17:32-8.
[25] Mu SJ, Huang M, Yang JJ, Yu J, Li TH, Hu JS. Overview of communication and control techniques in the microgrid. Applied Mechanics and Materials. 2011;71-78:2382-8.
[26] Zadeh MRD, Hajimiragha A, Adamiak M, Palizban A, Allan S. Design and implementation of a microgrid controller. 64th Annual Conference for Protective Relay Engineers, 2011. pp. 137-45.
[27] Salomonsson D, Soder L, Sannino A. An Adaptive control System for a DC microgrid for data centers. IEEE Transactions on Industry Applications, 2008. pp. 1910-7.
[28] Rui B, Ming D, Ting Ting X. Design of common communication platform of microgrid. 2nd IEEE International Symposium on Power Electronics for Distributed Generation Systems (PEDG), 2010. pp. 735-8.
[29] Rua D, Pereira LFM, Gil N, Lopes JAP. Impact of multi-microgrid communication systems in islanded operation. Innovative Smart Grid Technologies (ISGT Europe), 2nd IEEE PES International Conference and Exhibition: IEEE;2011. pp. 1-6.
[30] Logenthiran T, Srinivasan D, Khambadkone AM, Htay Nwe A. Multiagent system for real-time operation of a microgrid in real-time digital simulator. IEEE Transactions on Smart Grid. 2012;3:925-33.
[31] Lu D, Francois B. Strategic framework of an energy management of a microgrid with a photovoltaic-based active generator. 8th International Symposium on Advanced Electromechanical Motion Systems & Electric Drives Joint Symposium: IEEE; 2009. pp. 1-6.
[32] Su W, Wang J. Energy management systems in microgrid operations. The Electricity Journal. 2012;25:60-45.
[33] Suryanarayanan S, Rietz RK, Mitra J. A framework for energy management in customer-driven microgrids. PES General Meeting: IEEE; 2010. pp. 1-4.
[34] Gangale F, Mengolini A, Onyeji I. Consumer engagement: An insight from smart grid projects in Europe. Energy Policy. 2013;60:621-8..
[35] Alvial-Palavicino C, Garrido-Echeverría N, Jiménez-Estévez G, Reyes L, Palma-Behnke R. A methodology for community engagement in the introduction of renewable based smart microgrid. Energy for Sustainable Development. 2011;15:314-23.

[36] Geelen D, Reinders A, Keyson D. Empowering the end-user in smart grids: Recommendations for the design of products and services. Energy Policy. 2013;12:2472-83.
[37] Huang J, Jiang C, Xu R. A review on distributed energy resources and MicroGrid. Renewable and Sustainable Energy Reviews. 2008;12:2472-83.
[38] Sudtharalingam S, Leach M, Brett DJL, Staffell I, Bergman N, Barton JP, et al. UK microgeneration. Part II: technology overviews. Proceedings of the ICE - Energy. 2010;163:143-65.
[39] Salomonsson D, Soder L, Sannino A. An adaptive control system for a DC microgrid for data Centers. 42nd IAS Annual Meeting Conference Record on Industry Applications Conference: IEEE; 2007. pp. 2414-21.
[40] Carley S. Distributed generation: an empirical analysis of primary motivators. Energy Policy. 2009;37:1648-59.
[41] Ismail MS, Moghavvemi M, Mahlia TMI. Current utilization of microturbines as a part of a hybrid system in distributed generation technology. Renewable and Sustainable Energy Reviews. 2013;21:142-52.
[42] Rabiee A, Khorramdel H, Aghaei J. A review of energy storage systems in microgrids with wind turbines. Renewable and Sustainable Energy Reviews. 2013;18:316-26.
[43] Gabbar HA, Islam R, Isham MU, Trivedi V. Risk-based performance analysis of microgrid topology with distributed energy generation. International Journal of Electrical Power & Energy Systems. 2012;43:1363-75.
[44] Divya KC, Østergaard J. Battery energy storage technology for power systems—an overview. Electric Power Systems Research. 2009;79:511-20.
[45] Tan X, Li Q, Wang H. Advances and trends of energy storage technology in microgrid. International Journal of Electrical Power & Energy Systems. 2013;44:179-91.
[46] Passey R, Spooner T, MacGill I, Watt M, Syngellakis K. The potential impacts of grid-connected distributed generation and how to address them: A review of technical and non-technical factors. Energy Policy. 2011;39:6280-90.
[47] Chen SX, Gooi HB, Wang MQ. Sizing of energy storage for microgrids. IEEE Transactions on Smart Grid. 2012;3:142-51.
[48] Krishnamurthy S, Jahns TM, Lasseter RH. The operation of diesel gensets in a CERTS microgrid. Power and Energy Society General Meeting - Conversion and Delivery of Electrical Energy in the 21st Century: IEEE; 2008. pp. 1-8.
[49] Bracco S, Delfino F, Pampararo F, Robba M, Rossi M. The University of Genoa smart polygeneration microgrid test-bed facility: The overall system, the technologies and the research challenges. Renewable and Sustainable Energy Reviews. 2013;18:442-59.
[50] Katiraei F, Abbey C, Tang S, Gauthier M. Planned islanding on rural feeders - utility perspective. Power and Energy Society General Meeting - Conversion and Delivery of Electrical Energy in the 21st Century: IEEE; 2008. pp. 1-6.
[51] Loix T. The first micro grid in The Netherlands: Bronsbergen | Leonardo ENERGY. Leonardo Energy. 2009. URL *http://www.leonardo-energy.org/sites/leonardo-energy/files/root/pdf/2009/article2.pdf*
[52] Barnes M, Dimeas A, Engler A, Fitzer C, Hatziargyriou N, Jones C, et al. Microgrid laboratory facilities, International Conference on Future Power Systems, 2005. pp. 1-6

[53] Njogu M. Distributed generation and microgrids for small island electrification in developing countries: A review. Solar Energy society of India. 2008;18:6-20.
[54] Jayawarna N, Barnes M, Jones C, Jenkins N. Operating microgrid energy storage control during network faults. International Conference on System of Systems Engineering: IEEE; 2007. pp. 1-7.
[55] Araki I, Tatsunokuchi M, Nakahara H, Tomita T. Bifacial PV system in Aichi airport-site demonstrative research plant for new energy power generation. Solar Energy Materials and Solar Cells. 2009;93:911-6.
[56] Morozumi S, Nakama H, Inoue N. Demonstration projects for grid-connection issues in Japan. e & i Elektrotechnik und Informationstechnik. 2008;125:426-31.
[57] Hiroyuki Hatta HK. A study of centralized voltage control method for distribution system with distributed generation, 19th International Conference on Electricity Distribution, 2007. pp.1-4.
[58] Hirose K, Takeda T, Muroyama S. Study on field demonstration of multiple power quality levels system in Sendai. 28th Annual International Telecommunications Energy Conference, 2006. pp. 1-6.
[59] Mao M, Ding M, Su J, Liuchen C, Sun M, Zhang G. Testbed for microgrid with multi-energy Generators. Canadian Conference on Electrical and Computer Engineering, 2008. pp. 637-40.
[60] Jong-Yul K, Jin-Hong J, Seul-Ki K, Soon-Man K. Test result of microgrid management function in KERI pilot plant. 8th International Conference on Power Electronics and ECCE Asia (ICPE & ECCE): IEEE; 2011. pp. 825-32.
[61] Choi S, Park S, Kang D-J, Han S-j, Kim H-M. A microgrid energy management system for inducing optimal demand response. International Conference on Smart Grid Communications (SmartGridComm): IEEE; 2011. pp. 19-24.
[62] Zhang Y, Gatsis N, Giannakis GB. Robust energy management for microgrids with high-penetration renewables. IEEE Transactions on Sustainable Energy, 2013. pp:1-10.
[63] Logenthiran T, Srinivasan D, Khambadkone AM, Sundar Raj T. Optimal sizing of distributed energy resources for integrated microgrids using evolutionary strategy. Congress on Evolutionary Computation (CEC): IEEE; 2012. pp. 1-8.
[64] Lin N, Zhou B, Wang X. Optimal placement of distributed generators in micro-grid. Consumer Electronics, International Conference on Communications and Networks (CECNet), 2011. pp. 4239-42.
[65] Hawkes AD, Leach MA. Modelling high level system design and unit commitment for a microgrid. Applied Energy. 2009;86:1253-65.
[66] Marnay C, Venkataramanan G, Stadler M, Siddiqui AS, Firestone R, Chandran B. Optimal technology selection and operation of commercial-building microgrids. IEEE Transactions on Power Systems. 2008;23:975-82.
[67] Stluka P, Godbole D, Samad T. Energy management for buildings and microgrids. Conference on Decision and Control and European Control: IEEE; 2011. pp. 5150-7.
[68] Logenthiran T, Srinivasan D, Khambadkone AM, Aung HN. Multi-agent system (MAS) for short-term generation scheduling of a microgrid. International Conference on Sustainable Energy Technologies (ICSET): IEEE; 2010. p. 1-6.
[69] Meidani H, Ghanem R. Multiscale Markov models with random transitions for energy demand management. Energy and Buildings. 2013;61:267-74.

[70] Arteconi A, Hewitt NJ, Polonara F. Domestic demand-side management (DSM): Role of heat pumps and thermal energy storage (TES) systems. Applied Thermal Engineering. 2013;51:155-65.
[71] Hooshmand A, Malki HA, Mohammadpour J. Power flow management of microgrid networks using model predictive control. Computers & Mathematics with Applications. 2012;64:869-76.
[72] Clastres C. Smart grids: Another step towards competition, energy security and climate change objectives. Energy Policy. 2011;39:5399-408.
[73] Larsen K. Smart grids - a smart idea? Renewable energy focus 2009. URL *http://www.renewableenergyfocus.com/view/5030/smart-grids-a-smart-idea/*
[74] Sun Q, Wu J, Zhang Y, Jenkins N, Ekanayake J. Comparison of the development of smart grids in China and the United Kingdom. PES Innovative Smart Grid Technologies Conference Europe (ISGT Europe): IEEE; 2010. pp. 1-6.
[75] Zhang R, Du Y. New challenges to power system planning and operation of smart grid development in China. International Conference on Power System Technology: IEEE; 2010. pp. 1-8.
[76] Sarker MAR, Nagasaka K. Web enabled smart microgrid model with renewable energy resources in Bangladesh power system. International Conference on Advanced Mechatronic Systems (ICAMechS), 2012. pp. 345-50.
[77] Lien C-H, Bai Y-W, Lin M-B. Remote-controllable power outlet system for home power management. IEEE Transactions on Consumer Electronics. 2007;53:1634-41.
[78] Jin X, He Z, Liu Z. Multi-agent-based cloud architecture of smart grid. Energy Procedia. 2011;12:60-6.
[79] Erol-Kantarci M, Kantarci B, Mouftah HT. Cost-aware smart microgrid network design for a sustainable smart grid. GLOBECOM Workshops (GC Wkshps): IEEE; 2011. pp. 1178-82.
[80] Wolsink M. The research agenda on social acceptance of distributed generation in smart grids: Renewable as common pool resources. Renewable and Sustainable Energy Reviews. 2012;16:822-35.
[81] Wang B, Sechilariu M, Locment F. Intelligent DC microgrid with smart grid communications: control strategy consideration and design. IEEE Transactions on Smart Grid, 2012. pp. 2148-56.
[82] Asano H, Bando S, Watanabe H. Methodology to design the capacity of a microgrid. International Conference on System of Systems Engineering: IEEE; 2007. pp. 1-6.
[83] Zhang Y, Mao M, Ding M, Chang L. Study of energy management system for distributed generation systems. Third International Conference on Electric Utility Deregulation and Restructuring and Power Technologies: IEEE; 2008. pp. 2465-9.
[84] Obara S. Equipment arrangement planning of a fuel cell energy network optimized for cost minimization. Renewable Energy. 2007;32:382-406.
[85] Arefifar SA, Mohamed YAI, EL-Fouly THM. Supply-adequacy-based optimal construction of microgrids in smart distribution systems. IEEE Transactions on Smart Grid, 2012. pp. 1491-502.
[86] Kumar M, Singh SN, Srivastava SC. Design and control of smart DC microgrid for integration of renewable energy sources. Power and Energy Society General Meeting: IEEE; 2012. pp. 1-7.

[87] Liu S, Wu Z, Dou X, Zhao B, Zhao S, Sun C. Optimal configuration of hybrid solar-wind distributed generation capacity in a grid-connected microgrid. Innovative Smart Grid Technologies (ISGT): IEEE; 2013. pp. 1-6.
[88] Fu Q, Montoya LF, Solanki A, Nasiri A, Bhavaraju V, Abdallah T, et al. Microgrid generation capacity design with renewables and energy storage addressing power quality and surety. IEEE Transactions on Smart Grid, 2012. pp. 2019-27.
[89] Fu Q, Solanki A, Montoya LF, Nasiri A, Bhavaraju V, Abdallah T, et al. Generation capacity design for a microgrid for measurable power quality indexes. Innovative Smart Grid Technologies (ISGT): IEEE; 2012. pp. 1-6.
[90] Mizani S, Yazdani A. Optimal design and operation of a grid-connected microgrid. Electrical Power & Energy Conference (EPEC): IEEE; 2009. pp. 1-6.
[91] Basu AK, Chowdhury S, Chowdhury SP. Strategic deployment of CHP-based distributed energy resources in microgrids. Power & Energy Society General Meeting: IEEE; 2009. pp. 1-6.
[92] Bando S, Asano H, Sasajima K, Odajima N, Sei M, Ogata T. Optimal configuration of energy supply system in a microgrid with steam supply from a municipal waste incinerator. 8th International Conference on Power Electronics and ECCE Asia (ICPE & ECCE): IEEE; 2011. pP. 557-64.
[93] Mohammadi M, Hosseinian SH, Gharehpetian GB. GA-based optimal sizing of microgrid and DG units under pool and hybrid electricity markets. International Journal of Electrical Power & Energy Systems. 2012;35:83-92.
[94] Sheikhi A, Ranjbar AM, Oraee H. Financial analysis and optimal size and operation for a multicarrier energy system. Energy and Buildings. 2012;48:71-8.
[95] Bhumkittipich K, Phuangpornpitak W. Optimal placement and sizing of distributed generation for power loss reduction using particle swarm optimization. Energy Procedia. 2013;34:307-17.
[96] Alonso M, Amaris H, Alvarez-Ortega C. Integration of renewable energy sources in smart grids by means of evolutionary optimization algorithms. Expert Systems with Applications. 2012;39:5513-22.
[97] Obara S., Watanabe S. Optimization of equipment capacity and an operational method based on cost analysis of a fuel cell microgrid. International Journal of Hydrogen Energy. 2012;37:7814-30.
[98] King DE, Morgan MG. Customer-focused assessment of electric power microgrids. Journal of Energy Engineering. 2007;133:150-64.
[99] Mehleri ED, Sarimveis H, Markatos NC, Papageorgiou LG. A mathematical programming approach for optimal design of distributed energy systems at the neighbourhood level. Energy. 2012;44:96-104.
[100] Logenthiran T, Srinivasan D, Khambadkone AM, Sundar Raj T. Optimal sizing of distributed energy resources for integrated microgrids using evolutionary strategy. Congress on Evolutionary Computation (CEC): IEEE; 2012. pp. 1-8.
[101] Basu AK. Microgrids: Planning of fuel energy management by strategic deployment of CHP-based DERs – An evolutionary algorithm approach. International Journal of Electrical Power & Energy Systems. 2013;44:326-36.
[102] Stadtler H. A framework for collaborative planning and state-of-the-art. OR Spectrum. 2007;31:5-30.
[103] Fudenberg D, Tirole J. Game Theory. Cambridge1991.

[104] John F. Nash J. The bargaining problem. Econometrica. 1950;18:155-62.

[105] Yang Z, Sirianni P. Balancing contemporary fairness and historical justice: A 'quasi-equitable' proposal for GHG mitigations. Energy Economics. 2010;32:1121-30.

[106] Carpio LGT, Pereira Jr. AO. Economical efficiency of coordinating the generation by subsystems with the capacity of transmission in the Brazilian market of electricity. Energy Economics. 2007;29:454-66.

[107] Sueyoshi T. An agent-based approach equipped with game theory: Strategic collaboration among learning agents during a dynamic market change in the California electricity crisis. Energy Economics. 2010;32:1009-24.

[108] Aplak HS, Sogut MZ. Game theory approach in decisional process of energy management for industrial sector. Energy Conversion and Management. 2013;74:70-80.

[109] Xiaotong L, Yimei L, Xiaoli Z, Ming Z. Generation and transmission expansion planning based on game theory in power engineering. Systems Engineering Procedia. 2012;4:79-86.

[110] Mei S, Wang Y, Liu F, Zhang X, Sun Z. Game approaches for hybrid power system planning. IEEE Transactions on Sustainable Energy,2012. pp. 506-17.

[111] Leng M, Parlar M. Game-theoretic analyses of decentralized assembly supply chains: Non-cooperative equilibria vs. coordination with cost-sharing contracts. European Journal of Operational Research. 2010;204:96-104.

[112] Ohnson MP, Norman B. Game theory in supply chian analysis. Handbook of Quantitative Supply Chain Analysis: Modelling in the E-Business Era. D.Simchi-L ed. Boston: Kluwer; 2004. pp. 13-66.

[113] Nagarajan M, Sosic G. Game-theoretic analysis of cooperation among supply chain agents: Review and extensions. European Journal of Operational Research. 2008;187:719-45.

[114] Min CG, Kim MK, Park JK, Yoon YT. Game-theory-based generation maintenance scheduling in electricity markets. Energy. 2013;55:310-8.

[115] Oliveira FS, Ruiz C, Conejo AJ. Contract design and supply chain coordination in the electricity industry. European Journal of Operational Research. 2013;227:527-37.

[116] Zamarripa MA, Aguirre AM, Méndez CA, Espuña A. Mathematical programming and game theory optimization-based tool for supply chain planning in cooperative/competitive environments. Chemical Engineering Research and Design. 2013; 91:1588-600.

[117] Zhao Y, Wang S, Cheng TCE, Yang X, Huang Z. Coordination of supply chains by option contracts: A cooperative game theory approach. European Journal of Operational Research. 2010;207:668-75.

[118] Li X, Gao L, Li W. Application of game theory based hybrid algorithm for multi-objective integrated process planning and scheduling. Expert Systems with Applications. 2012;39:288-97.

[119] Mathies C, Gudergan SP. The role of fairness in modelling customer choice. Australasian Marketing Journal. 2011;19:22-9.

[120] Salles RM, Barria JA. Lexicographic maximin optimisation for fair bandwidth allocation in computer networks. European Journal of Operational Research. 2008;185:778-94.

[121] Leng M, Zhu A. Side-payment contracts in two-person nonzero-sum supply chain games: Review, discussion and applications. European Journal of Operational Research. 2009;196:600-18.
[122] Rosenhal E. A game-theoretic approach to transfer pricing in a vertically integrated supply chain. International Journal of Production Economics. 2008;115:542-52.
[123] Ertogral K, Wu SD. Auction-theoretic coordination of production planning in the supply chain. IIE Transactions. 2000;32:931-40-40.
[124] Yaiche H, Mazumdar RR, Rosenberg C. A game theoretic framework for bandwidth allocation and pricing in broadband networks. IEEE/ACM Transactions on Networking. 2000;8:667-78.
[125] Ganji A, Khalili D, Karamouz M. Development of stochastic dynamic Nash game model for reservoir operation. I. The symmetric stochastic model with perfect information. Advances in Water Resources. 2007;30:528-42.
[126] Gjerdrum J, Shah N, Papageorgiou LG. Fair transfer price and inventory holding policies in two-enterprise supply chains. European Journal of Operational Research. 2002;143:582-99.
[127] Gjerdrum J, Shah N, Papageorgiou LG. Transfer prices for multienterprise supply chain optimization. Industrial & Engineering Chemistry Research. 2001;40:1650-60.
[128] Brooke A, Kendrick D, Meeraus A, Raman R. GAMS - A User's Guide. 2008.
[129] Hawkes AD, Brett DJL, Brandon NP. Fuel cell micro-CHP techno-economics: Part 1 - model concept and formulation. International Journal of Hydrogen Energy. 2009;34:9545-57.
[130] Hawkes AD, Brett DJL, Brandon NP. Fuel cell micro-CHP techno-economics: Part 2 - Model application to consider the economic and environmental impact of stack degradation. International Journal of Hydrogen Energy. 2009;34:9558-69.
[131] Weber C, Shah N. Optimisation based design of a district energy system for an eco-town in the United Kingdom. Energy. 2011;36:1292-308.
[132] Streckienė G, Martinaitis V, Andersen AN, Katz J. Feasibility of CHP-plants with thermal stores in the German spot market. Applied Energy. 2009;86:2308-16.
[133] Centralised Electricity Generation. Department of Energy and Climate change 2011. URL *http://chp.decc.gov.uk/cms/centralised-electricity-generation/*
[134] Electricity Prices. Ontario Energy Board 2012. *http://www.ontarioenergyboard.ca/OEB/Consumers/Electricity/Electricity+Prices#rpp*
[135] Shaneb OA, Coates G, Taylor PC. Sizing of residential μCHP systems. Energy and Buildings. 2011;43:1991-2001.
[136] Bagherian A, Tafreshi SMM. A developed energy management system for a microgrid in the competitive electricity market. Bucharest PowerTech: IEEE; 2009. pp. 1-6.
[137] Mohamed FA, Koivo HN. System modelling and online optimal management of microGrid using mesh adaptive direct search. International Journal of Electrical Power & Energy Systems. 2010;32:398-407.
[138] Morais H, Kádár P, Faria P, Vale ZA, Khodr HM. Optimal scheduling of a renewable micro-grid in an isolated load area using mixed-integer linear programming. Renewable Energy. 2010;35:151-6.

[139] Silva M, Morais H, Vale Z. An integrated approach for distributed energy resource short-term scheduling in smart grids considering realistic power system simulation. Energy Conversion and Management. 2012;64:273-88.
[140] Obara S., Kawai M, Kawae O, Morizane Y. Operational planning of an independent microgrid containing tidal power generators, SOFCs, and photovoltaics. Applied Energy. 2012; 102:1343-57.
[141] Mohammadi S, Mozafari B, Solimani S, Niknam T. An adaptive modified firefly optimisation algorithm based on Hong's point estimate method to optimal operation management in a microgrid with consideration of uncertainties. Energy. 2013;51:339-48.
[142] Motevasel M, Seifi AR, Niknam T. Multi-objective energy management of CHP (combined heat and power)-based micro-grid. Energy. 2013;51:123-36.
[143] Sechilariu M, Wang B, Locment F. Building-integrated microgrid: Advanced local energy management for forthcoming smart power grid communication. Energy and Buildings. 2013;59:236-43.
[144] Aghaei J, Alizadeh M-I. Multi-objective self-scheduling of CHP (combined heat and power)-based microgrids considering demand response programs and ESSs (energy storage systems). Energy. 2013; 55:1044-54.
[145] Baziar A, Kavousi-Fard A. Considering uncertainty in the optimal energy management of renewable micro-grids including storage devices. Renewable Energy. 2013;59:158-66.
[146] Marzband M, Sumper A, Ruiz-Álvarez A, Domínguez-García JL, Tomoiagă B. Experimental evaluation of a real time energy management system for stand-alone microgrids in day-ahead markets. Applied Energy. 2013;106:365-76.
[147] Liao G-C. Solve environmental economic dispatch of smart microgrid containing distributed generation system – Using chaotic quantum genetic algorithm. International Journal of Electrical Power & Energy Systems. 2012;43:779-87.
[148] Kopanos GM, Georgiadis MC, Pistikopoulos EN. Energy production planning of a network of micro combined heat and power generators. Applied Energy. 2012; 102:1522-34.
[149] Lior N. Sustainable energy development: The present (2009) situation and possible paths to the future. Energy. 2010;35:3976-94.
[150] Nguyen TA, Aiello M. Energy intelligent buildings based on sser activity: A survey. Energy and Buildings. 2012; 56:244-57.
[151] Escrivá-Escrivá G. Basic actions to improve energy efficiency in commercial buildings in operation. Energy and Buildings. 2011;43:3106-11.
[152] Yohanis Y, Mondol J, Wright A, Norton B. Real-life energy use in the UK: How occupancy and dwelling characteristics affect domestic electricity use. Energy and Buildings. 2008;40:1053-9.
[153] Hu W, Chen Z, Bak-Jensen B. Optimal operation strategy of battery energy storage system to real-time electricity price in Denmark. IEEE PES General Meeting: IEEE; 2010. pp. 1-7.
[154] Pedrasa MAA, Spooner TD, MacGill IF. Coordinated scheduling of residential distributed energy resources to optimize smart home energy services. IEEE Transactions on Smart Grid. 2010;1:134-43.

[155] Wissner M. The smart grid – A saucerful of secrets? Applied Energy. 2011;88:2509-18.
[156] Zoka Y, Sugimoto A, Yorina N, Kawahara K, Kubokawa J. An economic evaluation for an autonomous independent network of distributed energy resources. Electric Power Systems Research. 2007;77:831-8.
[157] Logenthiran T, Srinivasan D, Khambadkone AM. Multi-agent system for energy resource scheduling of integrated microgrids in a distributed system. Electric Power Systems Research. 2011;81:138-48.
[158] Dagdougui H, Minciardi R, Ouammi A, Robba M, Sacile R. Modeling and optimization of a hybrid system for the energy supply of a "Green" building. Energy Conversion and Management. 2012;64:351-63.
[159] Rojchaya S, Konghirun M. Development of energy management and warning system for resident: An energy saving solution. 6th International Conference on Electrical Engineering/Electronics, Computer, Telecommunications and Information Technology: IEEE; 2009. pp. 426-9.
[160] Naraharisetti PK, Karimi IA, Anand A, Lee D-Y. A linear diversity constraint – Application to scheduling in microgrids. Energy. 2011;36:4235-43.
[161] Chen C-Y, Tsoul Y-P, Liao S-C, Lin C-T. Implementing the design of smart home and achieving energy conservation. 7th IEEE International Conference on Industrial Informatics: IEEE; 2009. pp. 273-6.
[162] Mohamed FA, Koivo HN. Online management genetic algorithms of microgrid for residential application. Energy Conversion and Management. 2012;64:562-8.
[163] Pinto J, Grossmann I. Assignment and sequencing models for the scheduling of process systems. Annals of Operations Research. 1998;81:433-66.
[164] Shaik MA, Floudas CA, Kallrath J, Pitz H-J. Production scheduling of a large-scale industrial continuous plant: Short-term and medium-term scheduling. Computers & Chemical Engineering. 2009;33:670-86.
[165] Shah N, Pantelides CC, Sargent RWH. A general algorithm for short-term scheduling of batch operations—II. Computational issues. Computers & Chemical Engineering. 1993;17:229-44.
[166] Sun H-C, Huang Y-C. Optimization of Power Scheduling for Energy Management in Smart Homes. Procedia Engineering. 2012;38:1822-7.
[167] Sou KC, Weimer J, Sandberg H, Johansson KH. Scheduling smart home appliances using mixed integer linear programming. Conference on Decision and Control and European Control: IEEE; 2011. pp. 5144-9.
[168] Nistor S, Wu J, Sooriyabandara M, Ekanayake J. Cost optimization of smart appliances. 2nd IEEE PES International Conference and Exhibition on Innovative Smart Grid Technologies: IEEE; 2011. pp. 1-5.
[169] Costanzo GT, Kheir J, Zhu G. Peak-load shaving in smart homes via online scheduling. International Symposium on Industrial Electronics: IEEE; 2011. pp. 1347-52.
[170] Castillo-Cagigal M, Gutiérrez A, Monasterio-Huelin F, Caamaño-Martín E, Masa D, Jiménez-Leube J. A semi-distributed electric demand-side management system with PV generation for self-consumption enhancement. Energy Conversion and Management. 2011;52:2659-66.

[171] Kriett PO, Salani M. Optimal control of a residential microgrid. Energy. 2012;42:321-30.
[172] Keyson DV, Mahmud AA, de Hoogh M, Luxen R. Designing a portable and low cost home energy management toolkit. Procedia Computer Science. 2013;19:646-53.
[173] Fuselli D, De Angelis F, Boaro M, Squartini S, Wei Q, Liu D, et al. Action dependent heuristic dynamic programming for home energy resource scheduling. International Journal of Electrical Power & Energy Systems. 2013;48:148-60.
[174] Muratori M, Roberts MC, Sioshansi R, Marano V, Rizzoni G. A highly resolved modeling technique to simulate residential power demand. Applied Energy. 2013;107:465-73.
[175] Chen Z, Wu L, Fu Y. Real-time price-based demand response management for residential appliances via stochastic optimization and robust optimization. IEEE Transactions on Smart Grid, 2012. pp. 1-9.
[176] Rastegar M, Fotuhi-Firuzabad M, Aminifar F. Load commitment in a smart home. Applied Energy. 2012;96:45-54.
[177] Derin O, Ferrante A. Scheduling energy consumption with local renewable micro-generation and dynamic electricity prices. Proceedings of the First Workshop on Green and Smart Embedded System Technology: Infrastructures, Methods and Tools, Stockholm, Sweden. 2010. pp. 1-6.
[178] Finn P, O'Connell M, Fitzpatrick C. Demand side management of a domestic dishwasher: Wind energy gains, financial savings and peak-time load reduction. Applied Energy. 2013;101:678-85.
[179] Domestic Electrical Energy Usage. Electropaedia2010. URL *http://www.mpoweruk.com/electricity_demand.htm*
[180] Villanueva D, Feijóo A. Wind power distributions: A review of their applications. Renewable and Sustainable Energy Reviews. 2010;14:1490-5.
[181] Balancing Mechnism Reporting System. The new electricity trading arrangements 2010. URL *http://www.bmreports.com/*
[182] Energy A. CHP Sizer Version 2. AEA Technology plc; 2004.
[183] Paatero JV, Lund PD. A model for generating household electricity load profiles. International Journal of Energy Research. 2006;30:273-90.
[184] Zhou N, Marnay C, Firestone R, Gao W, Nishida M. An analysis of the DER adoption climate in Japan using optimization results for prototype buildings with U.S. comparisons. Energy and Buildings. 2006;38:1423-33.
[185] Abidin HZ, Din NM. Sensor node placement based on lexicographic minimax. International Symposium on Telecommunication Technologies (ISTT), 2012. pp. 82-7.
[186] Erkut E, Karagiannidis A, Perkoulidis G, Tjandra SA. A multicriteria facility location model for municipal solid waste management in North Greece. European Journal of Operational Research. 2008;187:1402-21.
[187] Klein RS, Luss H, Smith DR. A lexicographic minimax algorithm for multiperiod resource allocation. Mathematical Programming. 1992;55:213-34.
[188] Ogryczak W. On the lexicographic minimax approach to location problems. European Journal of Operational Research. 1997;100:566-85.

[189] Wang L, Fang L, Hipel KW. Cooperative water resource allocation based on equitable water rights. International Conference on Systems, Man and Cybernetics: IEEE; 2003. pp. 4425-30.
[190] Wang L, Fang L, Hipel KW. Mathematical programming approaches for modeling water rights allocation. Journal of Water Resources Planning and Management. 2007;133:50-9.
[191] Liu S, Papageorgiou LG. Multiobjective optimisation of production, distribution and capacity planning of global supply chains in the process industry. Omega. 2013;41:369-82.
[192] Strathclyde Domestic Energy Modeling tool. University of Strathclyde. 2013. http://www.esru.strath.ac.uk/EandE/Web_sites/06-07/Carbon_neutral/tools%20folder/S.D.E.M.%20modelling.htm
[193] Hinkle C, Millner A, Ross W. Bi-directional power architectures for electric vehicles. 2011 8th International Conference & Expo on Emerging Technologies for a Smarter World: IEEE; 2011. pp. 1-6.
[194] Peterson SB, Whitacre JF, Apt J. The economics of using plug-in hybrid electric vehicle battery packs for grid storage. Journal of Power Sources. 2010;195:2377-84.
[195] Guille C, Gross G. A conceptual framework for the vehicle-to-grid (V2G) implementation. Energy Policy. 2009;37:4379-90.
[196] Srivastava AK, Annabathina B, Kamalasadan S. The challenges and policy options for integrating plug-in hybrid electric vehicle into the electric grid. The Electricity Journal. 2010;23:83-91.
[197] Green RC, Wang L, Alam M. The impact of plug-in hybrid electric vehicles on distribution networks: A review and outlook. Renewable and Sustainable Energy Reviews. 2011;15:544-53.
[198] Tie SF, Tan CW. A review of energy sources and energy management system in electric vehicles. Renewable and Sustainable Energy Reviews. 2013;20:82-102.
[199] Hedegaard K, Ravn H, Juul N, Meibom P. Effects of electric vehicles on power systems in Northern Europe. Energy. 2012; 48:356-68.
[200] Zhou C, Qian K, Allan M, Zhou W. Modeling of the cost of EV battery wear due to V2G application in power systems. IEEE Transactions on Energy Conversion. 2011;26:1041-50.
[201] Huang S, Safiullah H, Xiao J, Hodge B-MS, Hoffman R, Soller J, et al. The effects of electric vehicles on residential households in the city of Indianapolis. Energy Policy. 2012;49:442-55.
[202] Mullan J, Harries D, Bräunl T, Whitely S. The technical, economic and commercial viability of the vehicle-to-grid concept. Energy Policy. 2012;48:394-406.
[203] Hutson C, Venayagamoorthy GK, Corzine KA. Intelligent scheduling of hybrid and electric vehicle storage capacity in a parking lot for profit maximization in grid power transactions. Energy 2030 Conference: IEEE; 2008. pp. 1-8.
[204] Wang Z, Wang L, Dounis AI, Yang R. Integration of plug-in hybrid electric vehicles into energy and comfort management for smart building. Energy and Buildings. 2012;47:260-6.
[205] De Ridder F, D'Hulst R, Knapen L, Janssens D. Applying an activity based model to explore the potential of electrical vehicles in the smart grid. Procedia Computer Science. 2013;19:847-53.

[206] Sheikhi A, Bahrami S, Ranjbar AM, Oraee H. Strategic charging method for plugged in hybrid electric vehicles in smart grids; a game theoretic approach. International Journal of Electrical Power & Energy Systems. 2013;53:499-506.
[207] Ahn C, Li C-T, Peng H. Optimal decentralized charging control algorithm for electrified vehicles connected to smart grid. Journal of Power Sources. 2011;196:10369-79.
[208] Kang J, Duncan SJ, Mavris DN. Real-time scheduling techniques for electric vehicle charging in support of frequency regulation. Procedia Computer Science. 2013;16:767-75.
[209] Finn P, Fitzpatrick C, Connolly D. Demand side management of electric car charging: Benefits for consumer and grid. Energy. 2012;42:358-63.
[210] Mets K, Verschueren T, De Turck F, Develder C. Exploiting V2G to optimize residential energy consumption with electrical vehicle (dis)charging. First International Workshop on Smart Grid Modeling and Simulation (SGMS): IEEE; 2011. pp. 7-12.
[211] Sortomme E, El-Sharkawi MA. Optimal scheduling of vehicle-to-grid energy and ancillary services. IEEE Transactions on Smart Grid, 2012. pp. 351-9.
[212] He Y, Venkatesh B, Guan L. Optimal scheduling for charging and discharging of electric vehicles. IEEE Transactions on Smart Grid, 2012. p. 1095-105.
[213] Han H, Xu H, Yuan Z, Zhao Y. Interactive charging strategy of electric vehicles connected in Smart Grids. 7th International Power Electronics and Motion Control Conference (IPEMC), 2012. pp. 2099-103.
[214] Ota Y, Taniguchi H, Nakajima T, Liyanage KM, Baba J, Yokoyama A. Autonomous distributed V2G (Vehicle-to-Grid) satisfying scheduled charging. IEEE Transactions on Smart Grid, 2012. pp. 559-64.
[215] Peterson SB, Apt J, Whitacre JF. Lithium-ion battery cell degradation resulting from realistic vehicle and vehicle-to-grid utilization. Journal of Power Sources. 2010;195:2385-92.
[216] Millner A. Modeling Lithium Ion battery degradation in electric vehicles. Conference on Innovative Technologies for an Efficient and Reliable Electricity Supply: IEEE; 2010. pp. 349-56.
[217] Hoke A, Brissette A, Maksimovic D, Kelly D, Pratt A, Boundy D. Maximizing lithium ion vehicle battery life through optimized partial charging. Innovative Smart Grid Technologies (ISGT): IEEE; 2013. pp. 1-5.
[218] Bishop JDK, Axon CJ, Bonilla D, Tran M, Banister D, McCulloch MD. Evaluating the impact of V2G services on the degradation of batteries in PHEV and EV. Applied Energy. 2013;111:206-18.
[219] Guenther C, Schott B, Hennings W, Waldowski P, Danzer MA. Model-based investigation of electric vehicle battery aging by means of vehicle-to-grid scenario simulations. Journal of Power Sources. 2013; 239:604-10 .
[220] Lyon TP, Michelin M, Jongejan A, Leahy T. Is “smart charging” policy for electric vehicles worthwhile? Energy Policy. 2012;41:259-68.
[221] Lunz B, Walz H, Sauer DU. Optimizing vehicle-to-grid charging strategies using genetic algorithms under the consideration of battery aging. Vehicle Power and Propulsion Conference: IEEE; 2011. pp. 1-7.

[222] Bashash S, Moura SJ, Fathy HK. Charge trajectory optimization of plug-in hybrid electric vehicles for energy cost reduction and battery health enhancement. American Control Conference. 2010. pp. 5824-31.

[223] Bashash S, Moura SJ, Fathy HK. On the aggregate grid load imposed by battery health-conscious charging of plug-in hybrid electric vehicles. Journal of Power Sources. 2011;196:8754-47.

[224] Lunz B, Yan Z, Gerschler JB, Sauer DU. Influence of plug-in hybrid electric vehicle charging strategies on charging and battery degradation costs. Energy Policy. 2012;46:511-9.

[225] Hoke A, Brissette A, Maksimovic D, Pratt A, Smith K. Electric vehicle charge optimization including effects of lithium-ion battery degradation. Vehicle Power and Propulsion Conference (VPPC): IEEE; 2011. pp. 1-8.

[226] Nissan Leaf Wiki 2012. URL *http://nissanleafwiki.com/index.php?title=Battery,_Charging_System*

[227] Electricity load profile UK Energy Research Centre; 2013.
URL *http://data.ukedc.rl.ac.uk/browse/edc/Electricity/LoadProfile/data.*

[228] Miller JF. Analysis of current and projected battery manufacturing costs for electric, hybrid, and plug-in hybrid electric vehicles. World Electric Vehicle Journal. 2010;4:347-350.